Rubor, calor, tumor, dolor: objective assessments of inflammation

Voorde, W. ten

RUBOR CALOR TUMOR DOLOR

Objective assessments of inflammation

WOUTER TEN VOORDE

RUBOR, CALOR, TUMOR, DOLOR

OBJECTIVE ASSESSMENTS OF INFLAMMATION

DESIGN Caroline de Lint, Den Haag (caro@delint.nl)

Publication of this thesis was financially supported by the Centre for Human Drug Research (CHDR) foundation in Leiden, the Netherlands

RUBOR, CALOR, TUMOR, DOLOR

OBJECTIVE ASSESSMENTS OF INFLAMMATION

Proefschrift

ter verkrijging van
de graad van doctor aan de Universiteit Leiden
op gezag van rector magnificus prof.dr.ir. H. Bijl
volgens besluit van het college voor promoties
te verdedigen op dinsdag 17 december 2024
klokke 13:00 uur

door
Wouter ten Voorde
geboren te Leiderdorp
in 1995

Promotores
Prof. dr. J. Burggraaf
Prof. dr. R. Rißmann

Co-promotor
Dr. T. Niemeyer-Van der Kolk

Promotiecommissie
Prof. dr. M.H. Vermeer
Prof. dr. C.A.J. Knibbe
Prof. dr. E. Middelkoop (Amsterdam UMC)
Dr. K. van der Maaden

CHAPTER I

INTRODUCTION

Early-stage drug development in the field of dermatology has its challenges. The human skin, functioning as the body's largest organ, orchestrates a complex interplay of cellular interactions to regulate crucial processes such as inflammation, immune responses, wound healing, and angiogenesis.[1] This subtle interplay is disturbed in many inflammatory and autoimmune skin diseases and the development of novel dermatological agents focusses mainly on compounds modulating this disturbance.[2] In the early exploratory stage of clinical drug development, trials are conducted in the absence of clinical information about the drug. Uncertainty about its active dose, regimen and pharmacological activity contribute to a relatively low probability of success, amounting to 13.8% from phase I to market registration across all therapeutic areas. For drugs targeting immunosuppressive and anti-inflammatory processes, the likelihood of success is even lower at 6.3%.[3]

In an effort to increase the probability of success from early phases to market registration, an alternative, more rational approach was proposed, wherein pharmacodynamic properties are evaluated at the earliest clinical stage of drug development.[4] The European Medicines Agency (EMA) underscores the importance of assessing these pharmacodynamic properties, i.e., all possible effects of a drug in the body, including therapeutic effects, adverse effects, and side effects of drugs in the early exploratory stage of clinical drug development.[5] How does this paradigm shift impact early-stage drug development in clinical pharmaco-dermatology? From our perspective, exploring pharmacodynamic properties at such an early stage of drug development raises a few challenges: how to evaluate pharmacodynamic endpoints in early-stage dermatology trials and which specific pharmacodynamic endpoints should be considered for evaluation.

HOW TO EVALUATE PHARMACODYNAMIC ENDPOINTS IN EARLY-STAGE DRUG DEVELOPMENT

Using pharmacodynamic endpoints in early-stage clinical drug development is not new. With the increasing complexity of drugs and poor success rates, even more focus is put on gaining comprehensive insight into the mechanism of action at an early stage. This necessitates the understanding of downstream signalling events in proteins and cells. In the field of immuno-oncology, a notable 74% of phase I studies have integrated pharmacodynamic markers, with 94% of these being blood-based.[6] This trend is also observed in clinical trials focusing on immunological indications, driven by the availability of blood-based assays, a pathway-oriented development, and the wealth of experience gained in the oncology domain.

At the Centre for Human Drug Research (CHDR), a non-profit clinical research institute at the interface between academia and the pharmaceutical industry, objective pharmacodynamic endpoints have extensively been used over the past decade, either in studies in patients or by using pharmacological challenge models. Both pharmacokinetic and quantitative pharmacodynamic endpoints have supported critical decisions in drug development, also in the field of dermatological drug development. For example, antimicrobial peptides have been shown not to improve clinical symptoms of atopic dermatitis as quantified using objective pharmacodynamics.[7]

SKIN CHALLENGE MODELS

One essential issue when evaluating the pharmacodynamic properties of (novel) dermatological agents in an early-stage dermatology trial in healthy volunteers is the absence of a disorder, which can impede the exploration of key aspects of drug development. Inflammation, for example, is a significant factor in various dermatological conditions. Skin inflammation represents an immune response to invading pathogens, skin injuries, and exposure to xenobiotics, microbes, and parasites. Inflammation manifests itself clinically through features such as erythema, pain, heat, and swelling.[8] A range of immune cells from the innate and adaptive systems collaborate to eliminate the invading pathogens. Imbalance among these immune cells can contribute to the development of chronic skin conditions like psoriasis vulgaris, atopic dermatitis, and acne vulgaris.[9–11] Evaluating potential anti-inflammatory agents in healthy volunteers is complicated and necessitates a challenge model capable of mimicking the physiological and pathophysiological processes associated with an inflammatory skin disease. In that case, pharmacological challenge tests are needed to provide unequivocal proof of pharmacological activity.

A range of pharmacological challenge models and tests have been validated in the past years.[12] Except for the UV exposure model, most skin challenge models in dermatology trials share a commonality in the administration of a pharmacological agent to provoke an immune response. An example of intervention using a pharmacological agent is used within the KLH challenge model where researchers have been able to detect dose-dependent responses of a novel monoclonal antibody against OX40 ligand, developed for atopic dermatitis by using a KLH challenge model.[13] However, physical interventions on the skin could also provoke an immunologic and inflammatory response and mimic a dermatological disease, which is illustrated by the UVB exposure model in pain studies and more recently in cutaneous lupus erythematosus.[14] Another

trauma-based challenge model is the wound healing model, which finds application in both preclinical and clinical research.[15,16] Various wound healing models are utilized in humans, including techniques based on tape stripping, induction of blisters or abrasion, laser-induced wounds, split-thickness, and biopsies.[16] In general, techniques in wound healing models can be categorized into two classes: partial thickness (e.g., tape stripping, blister, abrasion, laser-induced wounds, split thickness) and full thickness (e.g., full thickness biopsy techniques). The choice of method depends on the specific research question. Full thickness biopsies necessitate comprehensive dermal, epithelization, and subcutaneous procedures for healing, whereas studies employing partial thickness or blister wounds predominantly focuses on epidermal healing and processes influenced within the epidermis or dermis.

The demonstrated success of skin challenge models in early drug development trials in general is evident. However, CHDR has limited experience with wound healing models, including both partial thickness and full thickness models. Additive to the development of pharmacological skin challenge models, new trauma-based derma-immunological challenges, such as the partial and full thickness wound models, hold substantial promise not only for advancing our understanding of human (patho)physiology, but also increasing our knowledge about pharmacodynamics early in the drug development process.

A BLUEPRINT FOR CONDUCTING EARLY-STAGE DERMATOLOGY TRIALS

There was only limited guidance on how to execute early-stage clinical trials involving innovative topical or systemic drugs situated at the intersection of dermatology and clinical pharmacology. In 2020, a blueprint was proposed outlining the methodology for conducting early-stage clinical pharmacology studies within the field of clinical pharmaco-dermatology.[17] In short, this blueprint highlights five cornerstones capturing the essential facets of an early-stage clinical pharmacology study (Figure 1). These cornerstones entail the exploration of pharmacokinetic and pharmacodynamic properties of a new drug, the inclusion of sensitive and objective endpoints, a multidisciplinary setup, and integrating data from different domains. Rissmann underscores the significance of adopting a multidisciplinary framework, necessitating collaborations with fellow researchers on a global scale. Adhering to the principles outlined in these five cornerstones may enhance the likelihood of early detection of undesirable drug features, whether related to safety, pharmacokinetics, or pharmacodynamics, thereby mitigating the risk of drug failure during pivotal trials.

Figure 1 Blueprint for conducting early-stage clinical pharmacology studies in the field of clinical pharmaco-dermatology.

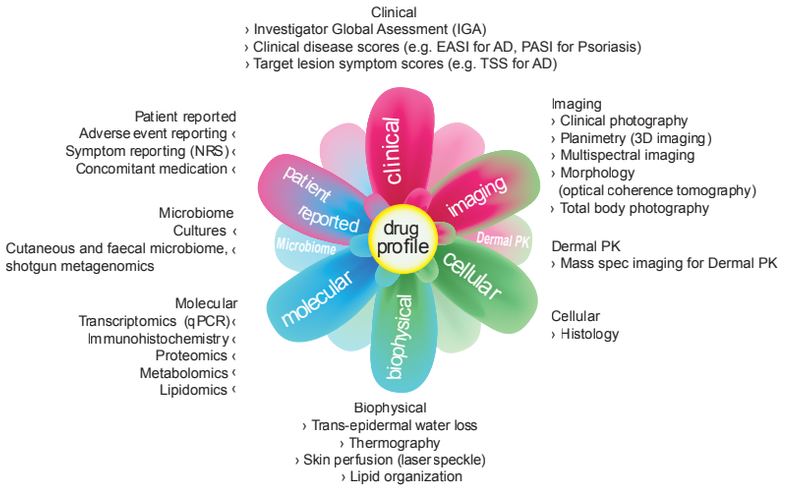

WHICH PHARMACODYNAMIC ENDPOINTS TO CONSIDER

Although the number of novel techniques to assess the pharmacodynamic properties of a (novel) dermatological agent has expanded in the field of dermatology, pivotal dermatology trials are dominated by physician-evaluated scores. Clinical efficacy scales, such as the Eczema Area and Severity Index (EASI) for atopic dermatitis (AD), Psoriasis Area and Severity Index for psoriasis vulgaris (PV) and inflammatory lesion count for acne vulgaris (AV) or investigator global assessments, play a vital role in the assessment of drug efficacy in early-stage dermatology trials. Irrespective of the specific dermatological disease, clinical efficacy scales are based on the number of lesions, the area affected, and the severity of the disease, often classified based on color. Most of these scores use discrete numbers from 0-3 (e.g., EASI). Despite efforts towards objectivity, most clinical scores necessitate a clinical judgment from the physician. The subjective nature of clinical scores, influenced by factors such as clinical training, color perception, and even ambient lighting conditions, can impact the physician's judgment. Their limited objectivity, potential inter-rater variability and lack of sensitivity might compromise unbiased conclusions, while assessments to evaluate the pharmacodynamic properties of a (novel) compound ought to be as valid, consistent, accurate, reproducible, and error-free as possible.

Typically, clinical efficacy scales find application in pivotal phase 3 trials involving large patient cohorts. These outcomes are often associated with the prevention or decrease in symptoms, such as erythema, scaling, or itch. Detecting significant effects on such endpoints necessitates trials with large sample sizes and prolonged follow-up periods. Incorporating clinical scores into phase I research might lead to trials with inadequate sample size and short follow-up periods, precluding robust statistical analyses. Consequently, phase I studies are often underpowered to decisively approve or reject a compound for further development.

To gain more rigorous insight into the pharmacodynamic effects of a novel dermatological agent, objective outcome measures are needed. For example, monitoring microcirculation can provide insights into the severity, progression, and response to treatment of various skin diseases.[18] Microcirculation is just one aspect of skin health; the comprehensive evaluation of skin responses to dermatological therapeutics may involve multiple biomarkers. Lack of insight into the mechanisms and processes of wound healing, for example, has hindered the development of new interventions and therapies so far.[19,20]

A biomarker refers to a broad subcategory of medical signs of clinically significant patient outcomes that can be accurately and reproducibly measured.[21] Ideally, a parametric and accurate biomarker of the pharmacological influence of a critical pathophysiological process is available to reflect the pharmacodynamic effect of a therapeutic agent. Given the intricate interplay of physiological processes in human skin, including inflammation, immune responses, wound healing, and angiogenesis, these processes offer valuable insights into assessing the pharmacodynamic impact of therapeutic treatments. Physiological processes, exemplified by erythema, wound healing, barrier function, and skin surface biomarkers, present opportunities to identify readily applicable biomarkers in early-stage dermatology trials. However, the challenge remains in identifying biomarkers accurate enough to reflect the pharmacological influence of critical pathophysiological processes and determining the tools capable of precise measurement.

OBJECTIVE MEASURES OF PHARMACODYNAMIC ENDPOINTS IN DERMATOLOGICAL DRUG TRIALS

The selection of an appropriate pharmacodynamic endpoint is of paramount significance in the context of early-stage drug trials. Recent advancements in the development and application of digital tools, imaging techniques and combinations of serum biomarkers have substantially advanced the realm of objective measures as pharmacodynamic endpoints in dermatology trials.

A rapidly growing list of tools is currently available for the comprehensive characterization of drug effects in the individual patient. The earlier-introduced blueprint on how to perform early-stage dermatological drug trials also offers guidance on how to include different sensitive and objective endpoints and integrate data from different domains, assessed by multiple techniques. The so-called 'DermaToolbox' encompasses innovative methodologies applicable in early-stage drug development trials, introducing a multidimensional approach spanning clinical, imaging, biophysical, molecular, cellular, microbiome, and physician- and patient-reported biomarkers. Digital indices, for instance, demonstrated by the digital Psoriasis Area and Severity Index (PASI) widely used in psoriasis trials, and the digital Eczema Area and Severity Index (EASIdig) in atopic dermatitis trials, have succeeded their non-digital counterparts.[22]

Transepidermal water loss (TEWL) quantifies the amount of evaporated water moving through a fixed area of the stratum corneum to the skin surface within a given time frame. TEWL has become the most widely used objective measurement for evaluating the barrier function of skin in healthy individuals and in patients with skin diseases linked to skin barrier dysfunction, such as atopic dermatitis.[23]

In addition, the spectrum of imaging techniques has expanded considerably over the years.[24] Examples are stereophotogrammetry, Optical Coherence Tomography (OCT) and Laser Speckle Contrast Imaging (LSCI). Stereophotogrammetry, also known as 3D photography, involves the simultaneous acquisition of two images of the lesion from slightly varied angles, allowing creation of a three-dimensional reconstruction. From this, a range of measurements can be obtained, including lesion dimensions, properties, and surface features.[25] OCT is applied for high-resolution, *in vivo* imaging of skin structure and vasculature to quantify and monitor inflammation in conditions like psoriasis and atopic dermatitis,[26] while measurements performed via LSCI are based on the dynamic change in backscattered light because of interaction with red blood cells; LSCI is used to objectively quantify perfusion in inflammatory skin lesions.[27] It is evident that non-contact and reliable imaging modalities hold promise in detecting slight changes that may often go unnoticed by the naked human eye.

PROBLEM STATEMENT

In summary, evaluating the pharmacodynamic properties of a dermatological agent seems indisputable for well-informed decision-making in the early stage of drug development. Despite the multitude of early-stage drug trials incorporating pharmacodynamical endpoints, there seems to be a lack of understanding how to integrate pharmacodynamic outcomes into early-stage dermatological

drug trials. Success stories from investigations employing objective pharmacodynamic endpoints in both disease and challenge models underscore the feasibility of integrating such endpoints during the initial clinical stages of drug development. The predominant focus of studies in the earlier stages of drug development remains on healthy volunteers, with challenge models being unequivocally endorsed in most cases. The introduction of novel trauma-based derma-immunological skin challenges, including partial and full-thickness wound models, holds promise for enhancing our comprehension of dermatological physiological processes and advancing early-stage pharmacodynamic knowledge.

Considering the presumed limitations in the objectivity of clinical efficacy scores, we advocate a more objective approach that incorporates imaging techniques and precise biomarkers as pharmacodynamic endpoints in early-stage dermatology trials. While outcomes reported by physicians and patients offer clinically relevant information and can be integrated into routine dermatologic practice and pivotal phase 3 dermatology trials, their applicability in early-stage trials is limited. There is a great need for more reliable and objective outcome measures, given the increasing development of compounds for dermatological-immunological disorders.

AIMS AND OUTLINE OF THIS THESIS

This thesis describes how pharmacological and trauma-based derma-immunological challenges are developed and how objective pharmacodynamic endpoints are evaluated in early-stage trials in the field of clinical pharmaco-dermatology. **Section I** of this thesis discusses the development of trauma-based derma-immunological challenges and how these models support the characterization of different immunological pharmacodynamic processes. **Chapter 2** covers the characterization of a cutaneous wound model to objectively test novel wound healing treatments. In this chapter, three- and four-mm full thickness punch biopsies were taken on the lower back of healthy volunteers and left to heal without intervention. In **chapter 3**, a suction blister model is developed to characterize epidermal wound healing. By using negative pressure, skin blisters were induced over approximately two hours. After removal of the epidermal sheet blisters were left untreated in the observational study and treated with a novel topical cream. The characterization of pharmacodynamic endpoints after the development of pharmacological challenge models is discussed in **section II**. **Chapter 4** describes the study of an intradermal challenge with substance P in healthy participants to understand and distinguish between wheal and flare responses following various substance P doses. In **chapter 5**, the pharmacodynamic activity of IRAK4 inhibitors is evaluated and characterized after inducing an inflammatory response via the topical application of imiquimod and systemic application of lipopolysaccharide. **Section III** illustrates how pharmacodynamic endpoints can be incorporated in a classical phase I feasibility and dosing study about microneedles. In **chapter 6**, we pre-explored the nature and extent of impact of repeated methotrexate injections via microneedles in children. In **chapter 7**, we investigated the feasibility of intradermal administration of adalimumab via hollow microneedles and conventional needles and evaluated the effects on percutaneous perfusion in a classical phase I feasibility and dosing trial. **Chapter 8** summarizes the results of all chapters and highlights future avenues for early-stage drug development in dermatology.

REFERENCES

1. Bigby JA. Goodman and Gillman's The Pharmacological Basis of Therapeutics. Arch Dermatol. 1992;128(1):132. doi:10.1001/ARCHDERM.1992.01680110146030
2. Diotallevi F, Offidani A. Skin, Autoimmunity and Inflammation: A Comprehensive Exploration through Scientific Research. Int J Mol Sci. 2023;24(21):24. doi:10.3390/IJMS242115857
3. Wong CH, Siah KW, Lo AW. Estimation of clinical trial success rates and related parameters. Biostatistics. 2019;20(2):273-286. doi:10.1093/BIOSTATISTICS/KXX069
4. Cohen AF, Burggraaf J, Van Gerven JMA, Moerland M, Groeneveld GJ. The use of biomarkers in human pharmacology (Phase I) studies. Annu Rev Pharmacol Toxicol. 2015;55:55-74. doi:10.1146/ANNUREV-PHARMTOX-011613-135918
5. EMEA/CHMP/SWP. Guideline on Strategies to Identify and Mitigate Risks for First-in-human and Early Clinical Trials with Investigational Medicinal Products.
6. Salawu A, Hernando-Calvo A, Chen RY, et al. Impact of pharmacodynamic biomarkers in immuno-oncology phase 1 clinical trials. Eur J Cancer. 2022;173:167-177. doi:10.1016/J.EJCA.2022.06.045
7. Niemeyer–van der Kolk T, Buters TP, Krouwels L, et al. Topical antimicrobial peptide omiganan recovers cutaneous dysbiosis but does not improve clinical symptoms in patients with mild to moderate atopic dermatitis in a phase 2 randomized controlled trial. J Am Acad Dermatol. 2022;86(4):854-862. doi:10.1016/J.JAAD.2020.08.132
8. Tracy RP. The five cardinal signs of inflammation: Calor, Dolor, Rubor, Tumor ... and Penuria (Apologies to Aulus Cornelius Celsus, De medicina, c. A.D. 25). J Gerontol A Biol Sci Med Sci. 2006;61(10):1051-1052. doi:10.1093/GERONA/61.10.1051
9. Bieber T. Atopic Dermatitis. https://doi.org/101056/NEJMra074081. 2008;358(14):1483-1494. doi:10.1056/NEJMRA074081
10. Leung DYM, Soter NA. Cellular and immunologic mechanisms in atopic dermatitis. J Am Acad Dermatol. 2001;44(1 Suppl):S1. doi:10.1067/MJD.2001.109815
11. Schön MP, Detmar M, Parker CM. Murine psoriasis-like disorder induced by naive CD4+ T cells. Nat Med. 1997;3(2):183-188. doi:10.1038/NM0297-183
12. Assil S, Rissmann R, Doorn MBA van, Assil S, Rissmann R, Doorn MBA van. Pharmacological Challenge Models in Clinical Drug Developmental Programs. Transl Stud Inflamm. Published online April 3, 2019. doi:10.5772/INTECHOPEN.85352
13. Saghari M, Gal P, Gilbert S, et al. OX40L Inhibition Suppresses KLH-driven Immune Responses in Healthy Volunteers: A Randomized Controlled Trial Demonstrating Proof-of-Pharmacology for KY1005. Clin Pharmacol Ther. 2022;111(5):1121-1132. doi:10.1002/cpt.2539
14. Siebenga PS, van Amerongen G, Klaassen ES, de Kam ML, Rissmann R, Groeneveld GJ. The ultraviolet B inflammation model: Postinflammatory hyperpigmentation and validation of a reduced UVB exposure paradigm for inducing hyperalgesia in healthy subjects. Eur J Pain. 2019;23(5):874-883. doi:10.1002/EJP.1353
15. Masson-Meyers DS, Andrade TAM, Caetano GF, et al. Experimental models and methods for cutaneous wound healing assessment. Int J Exp Pathol. 2020;101(1-2):21-37. doi:10.1111/iep.12346
16. Wilhelm KP, Wilhelm D, Bielfeldt S. Models of wound healing: an emphasis on clinical studies. Ski Res Technol. 2017;23(1):3-12. doi:10.1111/SRT.12317
17. Rissmann R, Moerland M, van Doorn MBA. Blueprint for mechanistic, data-rich early phase clinical pharmacology studies in dermatology. Br J Clin Pharmacol. 2020;86(6):1011-1014. doi:10.1111/bcp.14293
18. Roustit M, Cracowski JL. Non-invasive assessment of skin microvascular function in humans: an insight into methods. Microcirculation. 2012;19(1):47-64. doi:10.1111/J.1549-8719.2011.00129.X
19. Öhnstedt E, Lofton Tomenius H, Vågesjö E, Phillipson M. The discovery and development of topical medicines for wound healing. Expert Opin Drug Discov. 2019;14(5):485-497. doi:10.1080/17460441.2019.1588879
20. Zielins ER, Brett EA, Luan A, et al. Emerging drugs for the treatment of wound healing. Expert Opin Emerg Drugs. 2015;20(2):235-246. doi:10.1517/14728214.2015.1018176
21. Strimbu K, Tavel JA. What are biomarkers? Curr Opin HIV AIDS. 2010;5(6):463-466. doi:10.1097/COH.0B013E32833ED177
22. Modasia KH, Kaliyadan F. Digital Tools for Assessing Disease Severity in Dermatology. Indian Dermatol Online J. 2022;13(2):190. doi:10.4103/IDOJ.IDOJ_636_21
23. Alexander H, Brown S, Danby S, Flohr C. Research Techniques Made Simple: Transepidermal Water Loss Measurement as a Research Tool. J Invest Dermatol. 2018;138(11):2295-2300.e1. doi:10.1016/J.JID.2018.09.001
24. Jartarkar SR, Patil A, Wollina U, et al. New diagnostic and imaging technologies in dermatology. J Cosmet Dermatol. 2021;20(12):3782-3787. doi:10.1111/JOCD.14499
25. Lumenta DB, Kitzinger HB, Selig H, Kamolz LP. Objective quantification of subjective parameters in scars by use of a portable stereophotographic system. Ann Plast Surg. 2011;67(6):641-645. doi:10.1097/SAP.0B013E3182380877
26. Katkar RA, Tadinada SA, Amaechi BT, Fried D. Optical Coherence Tomography. Dent Clin North Am. 2018;62(3):421-434. doi:10.1016/J.CDEN.2018.03.004
27. Heeman W, Steenbergen W, van Dam GM, Boerma EC. Clinical applications of laser speckle contrast imaging: a review. J Biomed Opt. 2019;24(8):1. doi:10.1117/1.JBO.24.8.080901

SECTION I

PHARMACODYNAMICS AND TRAUMA-BASED DERMA-IMMUNOLOGICAL CHALLENGES

CHAPTER II

A MULTIMODAL, COMPREHENSIVE CHARACTERIZATION OF A CUTANEOUS FULL-THICKNESS WOUND MODEL IN HEALTHY VOLUNTEERS

Published in the Journal of Experimental Dermatology, 2023

Wouter ten Voorde[1,2], Mahdi Saghari[1,2], Jiry Boltjes[1], Marieke L de Kam[1], Ahnjili Zhuparris[1], Gary Feiss[3], Thomas P Buters[1,2], Errol P Prens[4], Jeffrey Damman[5], Tessa Niemeyer-van der Kolk[1], Matthijs Moerland[1], Jacobus Burggraaf[1,2,6], Martijn B A van Doorn[4], Robert Rissmann[1,2,6]

1 Centre for Human Drug Research, Leiden, NL
2 Leiden University Medical Centre, Leiden, NL
3 Cutanea Life Sciences, Wayne, Pennsylvania, USA.
4 Department of Dermatology Erasmus Medical Centre, Rotterdam, NL
5 Department of Pathology Erasmus Medical Centre, Rotterdam, NL
6 Leiden Academic Centre for Drug Research, Leiden University, Leiden, NL

ABSTRACT

Development of pharmacological interventions for wound treatment is challenging due to both poorly understood wound healing mechanisms and heterogeneous patient populations. A standardized and well-characterized wound healing model in healthy volunteers is needed to aid in-depth pharmacodynamic and efficacy assessments of novel compounds. The current study aims to objectively and comprehensively characterize skin punch biopsy-induced wounds in healthy volunteers with an integrated, multimodal test battery. Eighteen (18) healthy male and female volunteers received three biopsies on the lower back which were left to heal without intervention. The wound healing process was characterized using a battery of multimodal, non-invasive methods as well as histology and qPCR analysis in re-excised skin punch biopsies. Biophysical and clinical imaging readouts returned to baseline values in 28 days. Optical coherence tomography detected cutaneous differences throughout the wound healing progression. qPCR analysis showed involvement of proteins, quantified as mRNA fold increase, in one or more healing phases. All modalities used in the study were able to detect differences over time. Using multidimensional data visualization, we were able to create a distinction between wound healing phases. Clinical and histopathological scoring were concordant with non-invasive imaging read-outs. This well-characterized wound healing model in healthy volunteers will be a valuable tool for the standardized testing of novel wound healing treatments.

INTRODUCTION

Cutaneous trauma as induced by a cut or burn of the skin initiates a cascade of phasic events to restore the skin's function. Classically, the phases of wound healing are referred to as haemostasis, inflammation, proliferation, and remodelling (Figure 1A), where each phase elicits a peak activity at a certain time in the wound healing cascade (arbitrarily depicted in Figure 1A).[1,2,3,4] The phases are marked by signalling pathways mediated by numerous cell types, growth factors, and cytokines under normal conditions.[5,6] After haemostasis each subsequent phase is characterised by changes in the microenvironment including the secretion of cytokines and chemokines, and the attraction, migration, and activation of various cell types.[7] In addition, the microbiome is thought to play an important role in wound healing.[8] In delayed wound healing and chronic wounds, the typical cascade is impaired, mainly in the inflammation phase.[9] For these situations, an intervention for improved and accelerated wound healing is desirable.

Currently no clear consensus has been reached regarding the most important factors resulting in delayed healing in humans and how to improve or accelerate wound healing.[10] Lack of insight into the mechanisms and processes of wound healing which has hindered the development of new interventions and therapies.[11,12] The heterogenicity of wounds related to complex comorbidities and differences in wound induction (i.e., acute wound, burn wound, cut wound, chronic wound) creates challenges. The need to find effective treatment options for acute and chronic wounds is unmet. The financial burden to treat chronic wounds is estimated to be approximately $ 15-22 billion by the end of 2024.[13,14] In the last five years, only a limited number of clinical trials have been performed focusing on a novel treatment for wounds using an evidence-based approach. One contributing factor may be the lack of a robust human wound healing model for early phase clinical studies.[15,16] The current standard endpoint to evaluate wound healing (also used by regulators) is based on time to complete healing, and focusses on the wound visible with the naked eye.[17] A more in depth human wound healing model using healthy volunteers had been introduced earlier.[18,19]However, while the model had shown that optical coherence tomography (OCT) is capable of distinguishing cutaneous structural changes and that the measurement was comparable to histology the focus rested on the non-invasive nature of this device alone. A full integration of modalities to changes in the skin's structure, function, and micro-environment could aid in wound healing drug development.

To address these challenges, a study was designed with the aim to comprehensively characterize the mechanisms and processes of physiological wound

healing. A standardized 3 mm full-thickness skin punch biopsy on the back of healthy volunteers was made and measured with a standardized, multimodal test battery yielding a multidimensional approach.[20,21] All healing phases after haemostasis were extensively, (non)-invasively characterized in different domains, i.e., biophysical, cellular, molecular, clinical aspects, and clinical imaging. Methods with objective and biomarker-based readout were deployed as depicted in Figure 1A and 1C. Finally, the data were integrated using advanced data visualisation techniques to fully exploit this high-temporal and high-spatial resolution data set.

MATERIALS AND METHODS

This was a prospective single-arm, biopsy-location randomized, observational study in healthy volunteers performed at the Centre for Human Drug Research, Leiden, The Netherlands (NL63280.056.17). The trial was executed in accordance with the declaration of Helsinki. The independent Medical Review and Ethics Committee 'Medisch Ethische Toetsingscommissie van de Stichting Beoordeling Ethiek Biomedisch Onderzoek' (Assen, the Netherlands) approved the study prior to clinical study activities. All subjects received oral and written information and gave written informed consent before participation. The study lasted from November 2017 till March 2018. The trial was registered on ClinicalTrials.gov (NCT03433820).

SUBJECTS, STUDY DESIGN AND RANDOMIZATION

In total, 18 non-smoking healthy male and female volunteers (Fitzpatrick skin type I-II), aged 18-30 years with a body mass index (BMI) between 18-30 kg/m² were included. Main exclusion criteria were history of pathological scar formation, smoking, clinically relevant skin conditions, and diseases associated with immunosuppressive or immunomodulatory medication. Overall health status was assessed by physical examination, electrocardiogram (ECG), blood pressure measurements and blood analysis.

An overview of the wound healing phases used to classify the data and the trial design are depicted in Figure 1A and 1B. All subjects underwent three full-thickness skin punch biopsies (3 mm) on the lower back on the first study day, which were randomly performed on the right or left side of the lower back. After the biopsy procedure, the wounds were covered with gauze dressing until haemostasis was completed. After haemostasis the wounds were left untreated and uncovered. Subjects were randomized to receive two repeated biopsies on day 7, 14 or 21 and on day 28, 42, or 56 (n=6 per repeated biopsy day), respectively. For all imaging, clinical, and biophysical parameters eighteen 3 mm were

Figure 1 (A) Schematic representation of wound healing phases. Phase separation into set days is arbitrary and can differ dependent on the wound. (B) Clinical study design. Three-times 3 mm biopsies were taken on day 0 either on the right or left side of the lower back and were left to heal without intervention. *Subjects were randomized to receive the first 4 mm re-biopsy on day 7, day 14 or day 21. **Subjects were randomized to receive the second 4 mm re-biopsy on day 28, day 42 or day 56. (C) Blueprint for mechanistic and clinical pharmacology studies. Adapted from Rissmann et al. (2020). All assessments are reported in this article.

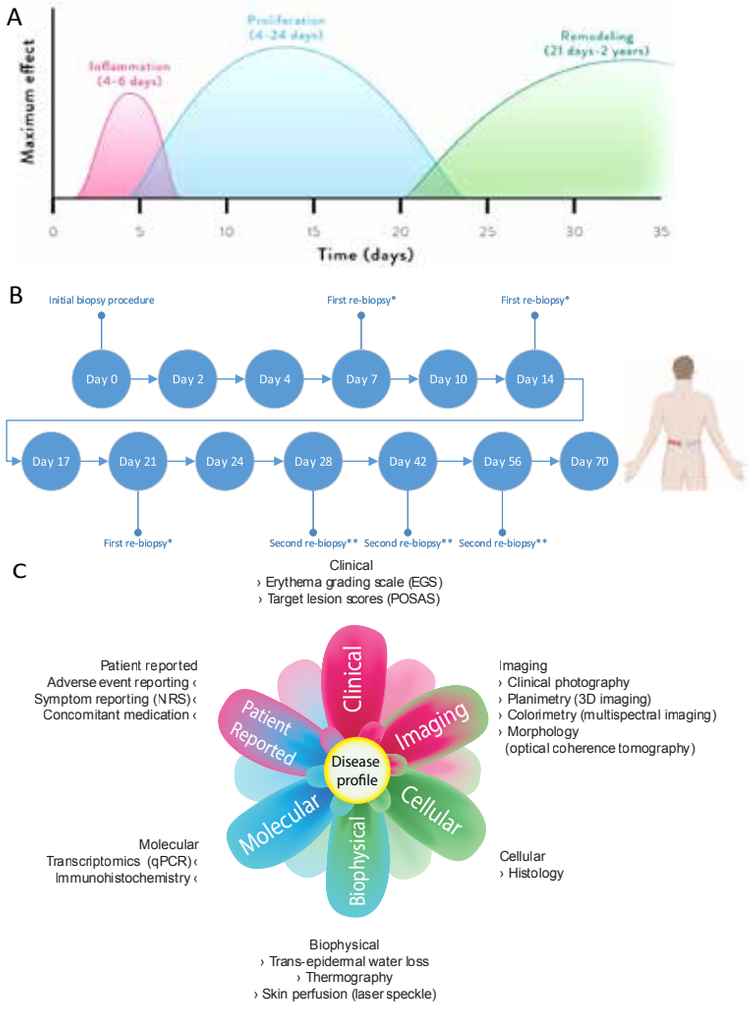

followed over time. For all molecular and cellular parameters eighteen 3 mm biopsies were measured on day 0, and six 4 mm biopsies were measured on subsequent timepoints.

BIOPHYSICAL: SKIN BLOOD PERFUSION AND SKIN BARRIER FUNCTION

Skin blood perfusion was quantified using Dynamic-Optical Coherence Tomography (D-OCT; VivoSight OCT, Michelson diagnostics, Kent, United Kingdom) at baseline and on each study day visit as described before.[22,23] Subjects were acclimatized to a temperature-controlled room and lighting was kept constant for the entire duration of the trial. D-OCT recordings were captured using a 6 mm probe placed directly over the wound creating a closed environment between skin and laser. 120 consecutive scans with a depth of up to 1.5 mm were taken of the wounds in approximately 20 seconds. Cutaneous microcirculation was quantified by calculating the average speckle signal returning from a depth of 0.1 mm up to 0.35 mm to reduce artefacts and noise signal.[24]

Skin barrier function was measured using transepidermal water loss measurements (TEWL; Aquaflux AF200, Biox Systems, London, United Kingdom). Subjects were acclimatized to the room for 15 minutes before the start of a measurement. A probe was placed on the wound creating a closed chamber of 3 mm, after which a measurement was started. Humidity differences between the TEWL chamber and the skin results in movement of water particles. Sensors in the chamber detect the water particles over time. A measurement lasted for 90 seconds or until steady-state flux was reached.

CLINICAL IMAGING: ERYTHEMA, PLANIMETRY, AND MORPHOLOGY

Skin erythema was quantified using multispectral imaging (Antera 3D®, Miravex, Dublin, Ireland), as described in detail before.[22,23,25] The multispectral camera creates a closed chamber of 25 cm^2 for image capture with standardized lighting and distance. A region of interest of 4 mm in diameter was defined and kept analogous with all analyzed images. Skin erythema was defined as the a* value (AU) using the CIELab color classification system.[26]

Planimetry (volume, surface, depth) of the induced wounds was measured using stereophotogrammetry (LifeViz 3D®, Quantificare, Biot, France).[27] Two 2D images were created simultaneously using a parallel lensing system. Standardized lighting and distance were established by flash, a light-controlled room, and guidance lasers. Standardized pictures were taken on all study day visits. Images were analyzed using accompanying software (DermaPix®, Quantificare, Biot, France). The inner wounds (wounds without perilesional elevation/depression of skin included) were traced by a single experienced analyst. Analysis was performed only when a wound was present. Depth, surface, and volume were reported in mm, mm^2 and mm^3, respectively. Volume was calculated using an algorithm based on volume calculations for a cone.

Qualitative assessment of the skin's morphology was performed using Optical Coherence Tomography (OCT; VivoSight, Michelson Diagnostics Ltd, Maidstone, United Kingdom). A 6 mm probe was placed directly over the wound and recorded 120 consecutive images in approximately 20 seconds. Recordings were up to 1.5 mm in depth and reached a lateral and spatial resolution of 7.5 µm and 5 µm, respectively. Qualitative inspection of the images was performed by two experienced observers and quantitative analysis comprised automated epidermal thickness measurements. Epidermal thickness was calculated by subtracting the signal corresponding to the change from epidermis to dermis (dermo-epidermal junction) from the signal corresponding to the transition from air to skin.

MOLECULAR & CELLULAR: SKIN PUNCH BIOPSIES

Three- and four-millimeter skin punch biopsies were snap frozen in liquid nitrogen directly after harvest. Biopsies were stored at ≤ -80°C until shipment and analyzed at the Immunology Laboratory of Erasmus Medical Center, Rotterdam, The Netherlands. mRNA extraction was performed using GenElute™ Mammalian Total RNA Miniprep kit (Sigma Aldrich™, RTN350-1KT) and expression was determined for CTGF, EGF, FGF1, FGF2, GM-CSF, IL-6, IL-10, IL-33, IL-1β, MMP1, MMP3, MMP9, PDGFA, PDGFB, PGF, TGF-β1, TGF-β3, TNF, VEGF-A relative to the housekeeping gene ABL using quantitative reverse transcriptase polymerase chain reaction (RT-qPCR, ViiA™ 7 Real-Time PCR system). Furthermore, biopsies were hematoxylin-eosin stained to compare with time matched OCT recordings and clinical images. Histopathological scores were graded by an independent histopathologist. Histopathology scores were given to 5 healing parameters (wound re-epithelization, granulation tissue, inflammation, neoangiogenesis, and connective tissue formation) with corresponding assessment parameters, and were graded from 0-3 corresponding to absent, scant, moderate, and profound, respectively. To evaluate the wound healing over time, re-biopsies were used in the histopathologist scoring, as reported earlier.[28]

CLINICAL: RED-YELLOW-BLACK, ERYTHEMA GRADING SCALE, AND PATIENT OBSERVER SCAR ASSESSMENT SCORES

Clinical scores of the wounds were performed using the red yellow black (RYB) score, erythema grading scale (EGS), and Patient Observer Scar Assessment Scores (POSAS) as described before.[29,30,31] All scores were performed by a single trained physician. The RYB score consisted of three wound parameters: wound presence, wound color, and wound humidity. RYB scores were only completed on

days that a wound was present. EGS scores were graded absent, mild, moderate, or severe and were performed on all study day visits. POSAS scores were only performed when the wound was closed. Since the wounds were created on the lower back only the observer scores of the POSAS were performed.

DATA VISUALIZATION

An exploratory data analysis and visualization of the wound healing data was performed to identify distinct wound healing phases. To visualize if the different wound healing phases could be clustered based on the objective wound healing parameters, the data was projected into a t-distributed Stochastic Neighbor Embedding (t-SNE) space using the Python (Python Software Foundation) package scikit-learn version 1.0.2. t-SNE is an effective non-linear dimensionality reduction technique used to create a two-dimensional representation of a high dimensional dataset to visualize and identify potential clusters.[32] Data from all timepoints were arbitrarily divided over three phases based on literature.[33–36] The inflammation phase lasted from day 2 to day 7, the proliferation phase from day 10 to day 24, and the remodeling phase from day 28 to day 70. Data from day 0 was used as healthy pre-challenged skin.

For further visual comparison of categorical groups across multiple quantitative parameters a radar chart was developed. The magnitude of the parameter for each data point in relation to the maximum magnitude of the parameter across all the data points was calculated using Python (Python Software Foundation) and classified using the wound healing phases depicted in Figure 1A.[37]

STATISTICS

All statistical and randomization programming was performed by a study-independent statistician and created using SAS 9.4 software (SAS Institute Inc., Cary, NC, USA). Biopsies were randomly performed using a randomization list with order of biopsy codes. The randomization code was only made available after study completion. For all physical, imaging, and clinical parameters data are summarized and displayed and reported descriptively (mean ±, SD).

RESULTS

A total of thirty-two (32) volunteers were screened for participation in the study. Fourteen (14) volunteers were excluded based on in/exclusion criteria. Nine (50%) male and nine (50%) female Caucasian subjects participated in this trial (Table 1). No serious adverse events (SAEs) or discontinuation due to AEs occurred. All AEs were of mild severity and self-limiting.

Table 1 Subject demographics and baseline characteristics

Age (years)	
n	18
Mean (SD)	21.9 (2.0)
Median	22.0
Min, Max	18, 25
Height (cm)	
n	18
Mean (SD)	176.8 (8.2)
Median	176.9
Min, Max	164.1, 193.5
Weight (kg)	
n	18
Mean (SD)	70.2 (10.2)
Median	70.1
Min, Max	55.3, 91.95
BMI (kg/m²)	
n	18
Mean (SD)	22.4 (2.6)
Median	21.8
Min, Max	18.3, 27.9
Sex	
Female	9 (50.0%)
Male	9 (50.0%)
Race	
White	18 (100.0%)
Fitzpatrick Skin Type	
1 (always burns and never tans)	1 (5.6%)
2 (always burns and tans min)	17 (94.4%)

SKIN BLOOD PERFUSION AND SKIN BARRIER FUNCTION RESTORED WITHIN 28 DAYS AFTER THE INITIAL BIOPSY

An increased cutaneous microcirculation (Figure 2A) was observed after the skin punch biopsy procedure as quantified with OCT indicating the start of the inflammation phase (Figure 2B). The average blood flow peaked at day 2 (mean 0.11 ± 0.03 AU, Phase II) and was elevated up to day 7 (mean 0.11 ± 0.03 AU, Phase II). From day 7 onwards a return to baseline was observed, which completed at day 17 showing the transition from the inflammation to the proliferation phase (mean 0.05 ± 0.01 AU, Phase III).

The skin barrier function represented by TEWL flux levels was highly impaired directly after the skin punch biopsy on day 0 (Figure 2C). A maximum mean flux of 61.0 g/m²h was observed on day 2 (Phase II), which decreased over time returning to the baseline value at day 28 (mean 13.8 ± 4.1 g/m²h, Phase IV).

Figure 2 Biophysical response after 3 mm skin punch biopsies over time. (A) representative images of D-OCT skin blood perfusion parameter at a measuring depth of 0.35 mm on the indicated study days. (B) Skin blood perfusion, displayed in change from baseline (day 0) [mm/s] up to day 70, is increased after wounding and gradually decreases over time (n = 18). (C) Transepidermal water loss, displayed in change from baseline [g/m2h] over time, is increased after wound induction and decreases steeply over time (n = 18). All data are expressed as change from baseline, means ± standard deviation.

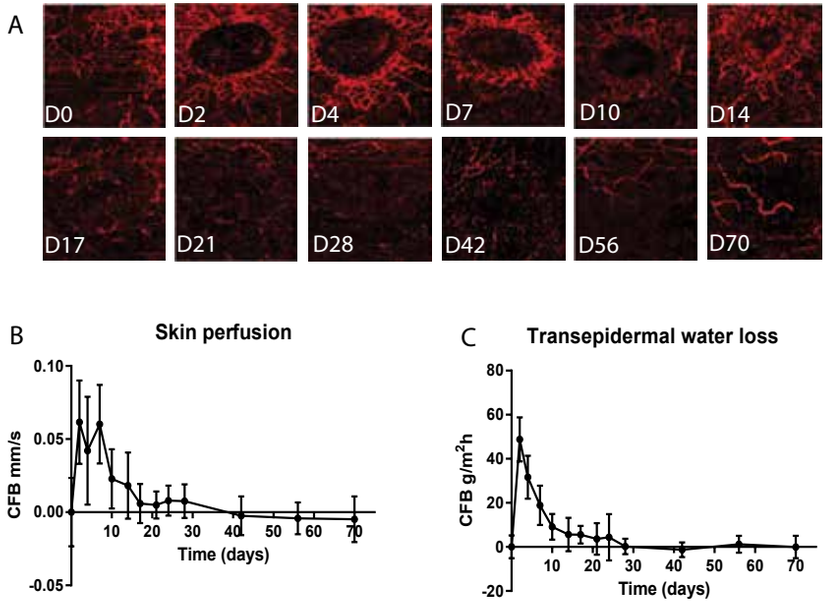

NOVEL CLINICAL IMAGING TOOL CAN OBJECTIVELY IDENTIFY DIFFERENCES IN SIZE, COLOR AND CUTANEOUS STRUCTURES OF THE INDUCED WOUNDS

Erythema of the skin as quantified by multispectral clinical imaging was visible in all wound healing phases starting two days after biopsy procedure (mean 27.44 ± 4.16 AU, Phase II) and remained variably present up to day 70 (mean 25.39 ± 2.34 AU, Phase IV), not returning to the baseline value at end of study (Figure 3A–B).

Stereophotogrammetric parameters (volume, surface, depth) are displayed in Figure 3C–E. Two days after biopsy procedure there was a negative wound volume (mean −1.32 ± 0.95 mm^3, Phase II), indicating a concave planimetry. From day 2 up to day 10. During the inflammation and proliferation phases (Phase II/III) the wound volume became positive (mean 0.58 ± 0.39 mm^3), followed by a decrease and return to the pre-biopsy conditions on day 28 (Phase IV). Although no wound was visible anymore after day 28 in the remodeling phase (and no analysis could be performed) a small elevation of the skin was observed upon visual inspection on day 28 and during the following visits.

The initial wounds had a mean surface of 7.55 ± 1.24 mm^2 at day 2 (Phase II). A gradual wound closure was observed from day 2 up to day 24 (mean 0.11 ± 0.39 mm^2, Phase II/III), with full closure of the wound on day 28 (Phase IV). The mean maximum inner wound depth quantified 2 days after the biopsy procedure (Phase II) was −0.41 ± 0.15 mm, which returned to a flat and normalized state at day 28 (Phase IV).

Automatically calculated epidermal thickness measurements calculated by OCT showed an increase in epidermal thickness in the remodeling phase 4 weeks after wounding followed by a gradual decrease over time up to day 70 (Figure 3F). Epidermal thickness did not return to baseline values in 70 days. Epidermal thickness measurements could not be performed on day 7, 10 and 14 due to crust interference and lack of epidermis.

MRNA EXPRESSION LEVELS OF WOUND RELATED PROTEINS CLEARLY FOLLOW THE WOUND HEALING PHASES

The molecular response to skin wounding was studied by quantifying mRNA expression in snap frozen 3- and 4-mm biopsies using qPCR (Figure 4). In general, day 0 data consist of 18 skin punch biopsies, whilst the remaining time points consist of 6 skin punch biopsies due to the randomized procedure for repeated biopsies. The inflammation phase (Phase II) was characterized by the upregulation of several pro-inflammatory cytokines between day 0 and 7 (i.e. IL-1β IL-10, IL-33, TNF, GM-CSF, VEGF-A) followed by a decrease and stabilization at day 28 (Figure 4A–E). mRNA expression levels of proteins that are thought to be involved in the proliferation (Phase III) and remodeling phase (Phase IV) of wound healing (i.e. PGF, TGFβ1, TGFβ3, MMP1, MMP3, MMP9) were already upregulated at day 7. Interestingly, TGF-β3 remained increased up to day 70. All other parameters showed a gradual decrease over time or a plateau at the end of the observational period, Figure 4.

HISTOLOGY SCORES ALIGNED TO WOUND HEALING PHASES

Histopathology scoring was performed for each biopsy. Only in case the biopsy was fragmented and/or scoring was not applicable no score was given. Figures S1–S5 display all histology scores. Complete re-epithelialization (Phase III, Figure S1) was achieved on day 14 for all biopsies. As of day 28, all epithelization parameters returned to pre-wounded skin.

Figure 3 Wound planimetry and clinical imaging. (A) Representative images of wound healing progression over time (photos taken at indicated days). (B) Skin erythema, displayed as change from baseline arbitrary units over time (n=18). (C–E) Volume, surface and depth displayed in change from baseline mm³, mm² and mm, respectively (n=18). (F) Automatically calculated epidermal thickness displayed in mm over time (n=18). Data on day 0 is epidermal thickness calculated pre-biopsy procedure. Figures A–E are expressed as change from baseline, means ± standard deviation. Figure F is expressed as means ± standard deviation.

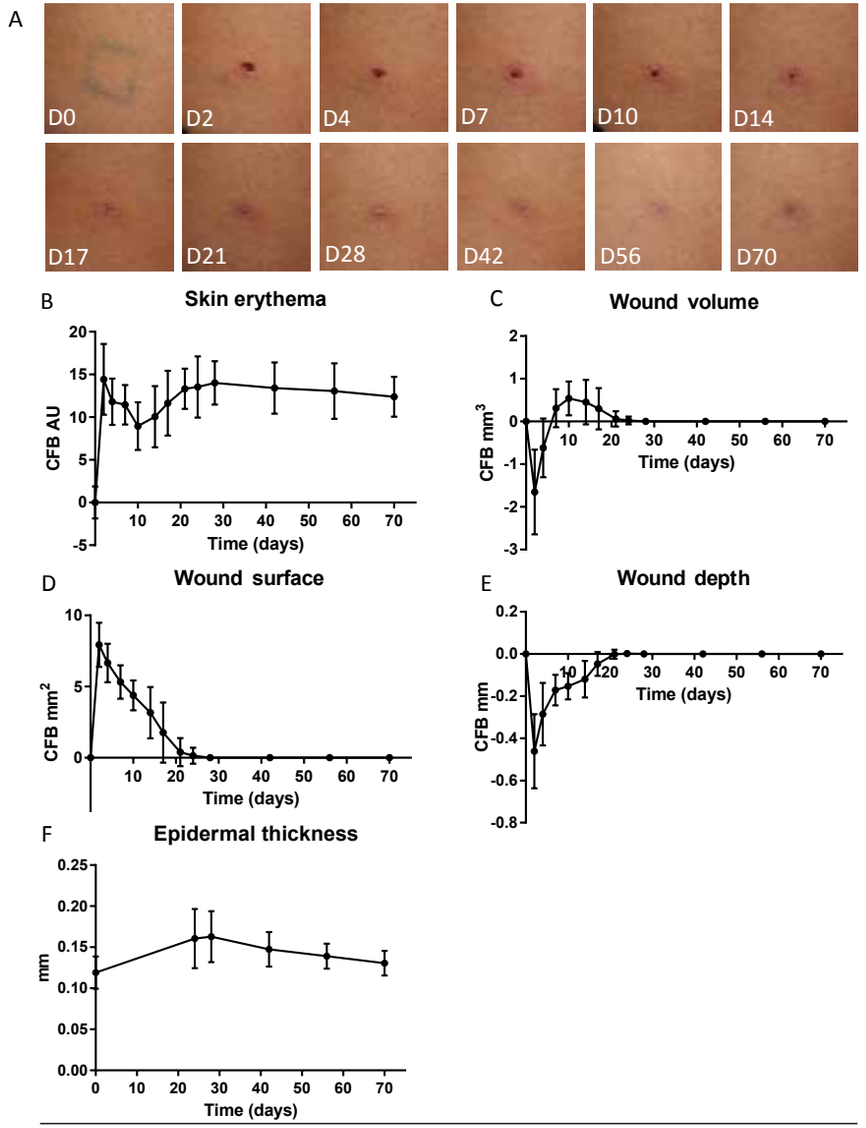

Figure 4 mRNA expressing quantified using qPCR. Data is expressed as individual data points with means, relative to housekeeping gene ABL (n=18 for day 0, n=6 for all other timepoints). Colour coding corresponds to wound healing phases depicted in Figure 1A. Black=pre-challenged skin, pink=inflammation phase, blue=proliferation phase, green=remodeling phase. Data are expressed as means.

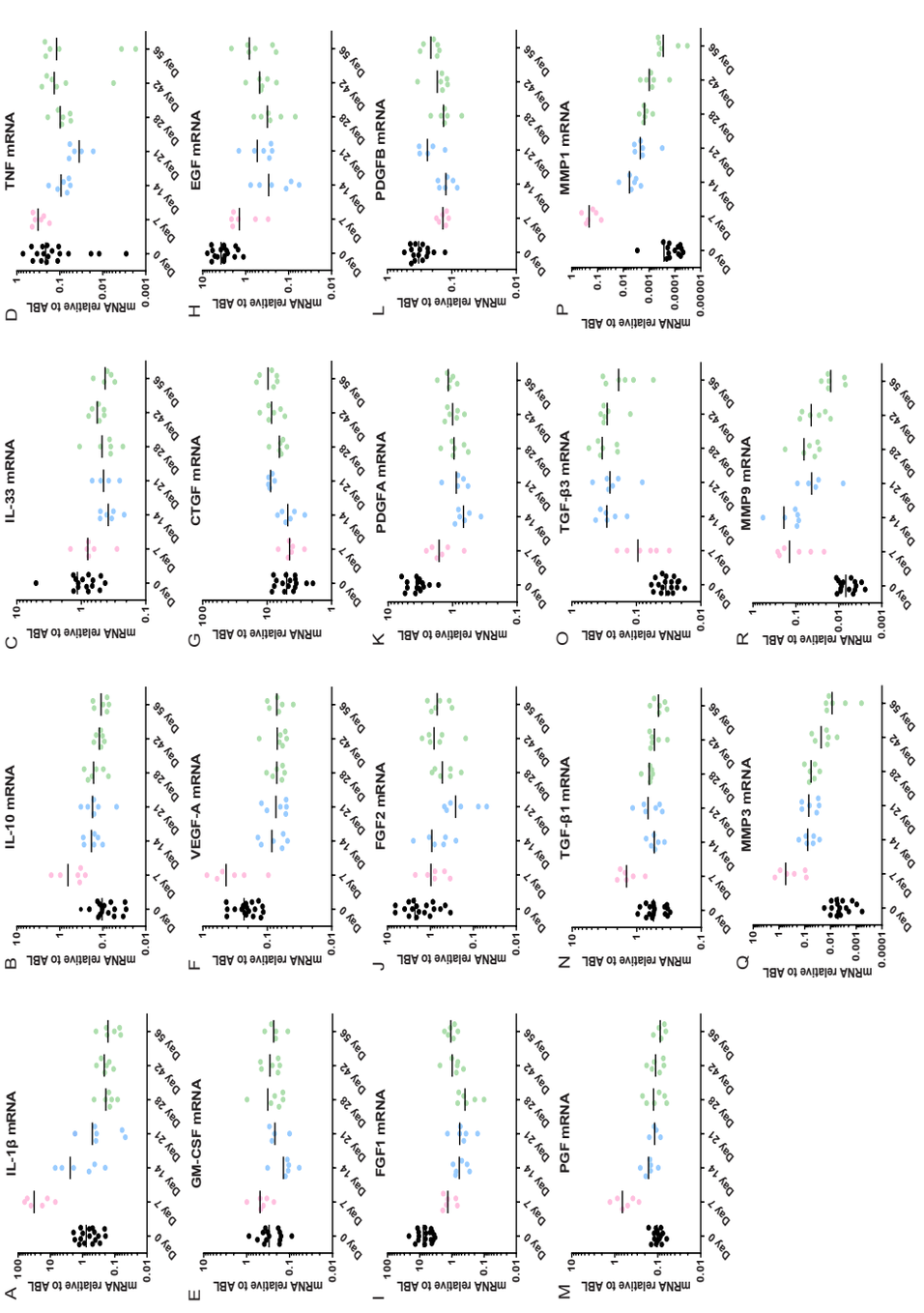

Inflammation scores (Phase II, Figure S2) were divided in three categories (neutrophils, histiocytes, lymphocytes) and an overarching parameter 'total inflammation'. For two biopsies, signs of inflammation were already observed on day 0. On day 7, all biopsies that could be assessed showed scant signs of inflammation, which changed to moderate inflammation in some biopsies and returned to scant after 42 days in most of the biopsies.

Neoangionesis (sign of Phase II/III, Figure S3) was scored using two characteristics: vessel proliferation and orientation. Vessel proliferation was visible on day 7 in all biopsies and remained mild to moderately present up to day 70. Vessel orientation was primarily vertical on day 14 (4 biopsies). On all other days, vessel orientation was primarily mixed (vertical and horizontal).

Granulation tissue (sign of Phase III/IV, Figure S4) was scored using the characteristics: area affected by granulation tissue in % and fibrin deposition. Scant, moderate, profound and excessive correspond to 0%–25%, 25%–50%, 50%–75%, 75%–100% affected, respectively. On day 7, fibrin disposition was profoundly visible and decreased over time up to clearance at day 21. The percentage of area affected was the highest on day 21 and day 28. On day 56 the percentage of area affected differed greatly (2 biopsies scored absent, 4 biopsies scored profound).

Characteristics associated with connective tissue formation (sign of Phase IV) are shown in Figure S5. Proteoglycan/mucin deposition was affected 7 days after wounding. From day 14 onwards, the deposition returned to normal. Elastin deposition remained unchanged throughout the study. With advancement in time, the amount of collagen deposition fluctuated but was eventually profoundly expressed on day 70. Interestingly, the collagen orientation changed over time from horizontal orientated to mixed orientated. On day 70, 4 biopsies showed horizontal orientation, whereas 2 biopsies showed mixed orientation.

DATA VISUALIZATION

A complete data visualization using all data described in the preceding sections except epidermal thickness measurements is displayed in Figure 5. The radar chart (Figure 5A) shows involvement of most parameters for the distinction of phases. The magnitude of pro/anti-inflammatory proteins in the inflammation phase is higher compared to all other phases. In addition, all multidimensional data has been compressed to a one-dimensional t-SNE graph (Figure 5B). The t-SNE plot shows distinct pre-challenged, inflammation, proliferation and remodeling clusters. The figure also illustrates some overlap between the proliferation and remodeling phase. Data points collected from pre-challenged skin and datapoints collected in the inflammation phase shows close clustering and no clear overlap with other phases.

Figure 5 Data visualization using radar chart and t-SNE.

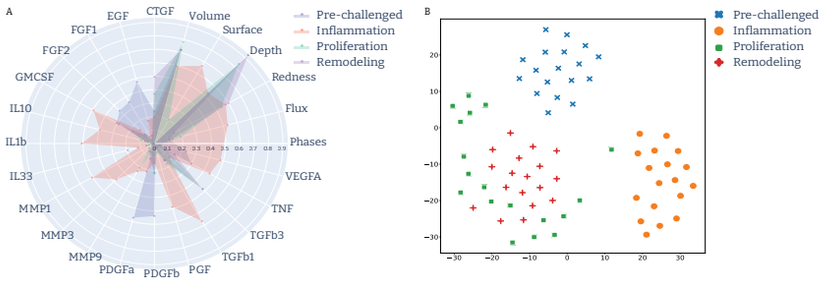

NON-INVASIVE OCT IMAGES VS INVASIVE HISTOLOGY

Figure S6 depicts the progression of wound healing over time as measured by OCT. For comparison, histology slides from day 0, 7, 14, 21, 28, 42, 56 were added to Figure S6, illustrating the different wound healing processes over time (excluding the haemostasis phase, phase I) measured invasively vs non-invasively.

In intact skin (Figure S6A), skin characteristics such as the stratum corneum, epidermis, dermis, dermo-epidermal junction and blood vessels could easily be discriminated in the OCT image.

Phase II (day 2–7): 7 days after wound induction, the first signs of restoration became apparent by a clear haemostatic crust in both the OCT and histology recordings (Figure S6B). In addition, the migrating epidermal tongue originating from the epidermal bulge directly adjacent to the wound and the several dilated perilesional blood vessels were also present as signs of this phase.

Phase III (day 10–24): Complete restoration of the epidermis occurred after 14 days (Figure S6C). In histology, this was shown by an epidermal bulge originating from both perilesional sides of the wound accompanied by a cellular infiltrate. For OCT, the restored epidermis was visualized by a bright white band next to the epidermal bulge caused by the inflammatory infiltrate. Other processes related to the proliferation phase of wound healing were observed 21 days after wounding in both the histology and OCT images (Figure S6D). The epithelium layers were thickened and granulation tissue at the base of the wound was formed.

Phase IV (day 28–70): 28 days after wounding the first processes involved in the remodeling phase of wound healing were seen (Figure S6E). A mixed extracellular matrix orientation was observed in both histological and OCT recordings. In addition, a further flattening of the epidermis was seen. This flattening of the epidermis continued up to day 42 after wounding (Figure S6F). The epidermis was thickened compared to unwounded skin and no rete ridges

were visible. Furthermore, a thickening in the upper epithelium layers was seen in the histology recording. The orientation of blood vessels was mixed (horizontal and vertical) but less in density compared to unwounded skin. 56 (Figure S6G) and 70 (Figure S6H) days after wounding, the skin showed increased roughness (on OCT recordings) indicating a less dense extracellular matrix compared to 42 days post wounding. 70 days after wounding, the epidermis was still thickened compared to unwounded skin (Figure S6A, OCT graph) and showed clear signs of fibrosis (hyperreflective dermis).

CLINICAL SCORES ARE CONSISTENT WITH CLINICAL IMAGING

EGS and RYB scores were performed on all study day visits. POSAS scores were performed from the day that the wound was closed (day 14). Data on the scores in frequency over time are displayed in Figure S7. A shift from severe (day 2–10, phase II/III) to moderate (day 14–28, phase III/IV) to mild (day 42–70, phase IV) erythema was observed in the EGS scores. The RYB scores shifted from black to no wound (wound closure) from day 14 onwards. POSAS scorings showed a steep decrease from day 14 up to day 28. A plateau was formed from day 28 to day 70. The scores did not return to the minimal scores of a POSAS score.

DISCUSSION

In this study, we aimed to characterize physiological wound healing with a multimodal test battery consisting mainly of non-invasive methodologies in a healthy volunteer challenge model. We demonstrate for the first time that a test battery of non-invasive techniques can objectively monitor quantifiable changes over time of the distinct wound healing phases, that is phase II inflammation, phase III proliferation and phase IV remodeling, while excluding the haemostasis phase. Additionally, multiple parameters were integrated and visualized in a radar chart highlighting the most important parameters and most suitable biomarkers per phase. Lastly, data integration of all parameters by means of t-SNE showed clear clusters per phase. Remarkably pre-challenged skin and the inflammation phase were the most pronounced clusters.

CLINICAL IMAGING AS OBJECTIVE READ-OUT FOR WOUND HEALING ASSESSMENT

Clinical imaging of cutaneous disorders in dermatology is often performed for treatment efficacy evaluation over time.[38] Recent advancements in imaging techniques allows for quantitative and objective measurements to be performed over time without the need for subjective clinical scoring.[39] Using clinical (3D)-imaging we were able to collect objective data on differences over time for 5 characteristics, that is erythema, volume, surface, depth, epidermal thickness. In the observational period, of this study, skin erythema never returned to baseline indicating that the remodeling phase continues for much longer than 70 days.[40] Changes observed in stereophotogrammetric parameters (volume, surface and depth) were in line with known literature on wound closure times. Despite the haemostatic crust covering the wound, the 3D camera used in this study was still able to detect differences in wound surface and depth. For wound volume, an arbitrary elevation was observed. This was partly accounted for the period a haemostatic crust was present and partly due to skin elevation due to fibrosis.

To summarize, all imaging techniques were able to objectively characterize the phases of wound healing and offer many advantages for both the clinic and in clinical research. One of the biggest advantages is that with these techniques serial non-invasive measurements can be performed on lesions providing objective data over time. Invasive biopsies can only be taken on a limited basis, whilst non-invasive techniques can be used any time. These techniques also have some limitations. 3D photography requires a trained operator to draw wound circumference, thereby introducing potential inter-operator variability. In addition, the effect of crust formation on imaging values is unclear and requires caution with interpretation of data.

SKIN BARRIER FUNCTION MEASUREMENTS ARE USEFUL WHEN ASSESSING WOUND HEALING

TEWL is a technique often used in pre-clinical and clinical research as an objective measurement for assessing the barrier function. One of the limitations often reported is the variability of the technique due to fluctuations in humidity, temperature, anatomical site and sweat.[41] In this study, TEWL values decreased over time, that is representing the progression of healing, while maintaining a constant and low variability between subjects. Potential reasons why TEWL values in this study were more robust compared to literature are the use of a temperature-controlled room, standardized measurement setup, a fixed operator, acclimatation time and routine calibration of equipment. TEWL values were increased up to 3 weeks after wounding, which is fully aligned with the time needed for keratinocytes to migrate the epidermis as seen in autoradiographic analysis of unaffected epidermal skin from psoriasis, mycosis fungoides and basal cell carcinoma patients.[42,43] In the current study no dressing was applied after haemostasis was achieved. The question remains whether the TEWL profile over time will remain the same with occlusive dressing in place. It is known from literature that dressing plays a vital role in wound management and future research should include skin barrier measurements using multiple wound dressing protocols.[44]

FREQUENT, IN-DEPTH MOLECULAR PROFILING OF WOUND HEALING PHASES

qPCR analysis performed in this study provided a comprehensible mechanistic insight into the molecular processes at play during wound healing. IL-10, IL-1β, IL-33, TNF, GM-CSF were all upregulated in the first days biopsies were taken (day 0, day 7) indicating on a role in the haemostasis and inflammation phase, which is in line with literature.[45,46] Interestingly, differences over time were observed between TGF-β1 and TGF-β3. This group of growth factors is known to be involved in both inflammation and proliferation phases and are believed to activate similar intracellular signaling pathways.[47] However, we found that TGF-β1 was only elevated up until 7 days after wounding, whilst TGF-β3 was increased up to day 56 (reaching a plateau on day 14). Wang et al. showed that hypertrophic derived fibroblasts and scar tissue produced more TGF-β1 compared to normal wound healing, indicating that prolonged elevation of TGF-β1 leads to more scarring.[48] Ferguson et al. discovered that skin wounds in mammalian embryos heal without scarring. Notably, TGF-β3 is elevated in these embryos, implying that TGF- β3 has anti scarring properties.[49] Another interesting find was the decrease in several growth factor genes (EGF, FGF1, FGF2, PDGFA, PDGFB) after wounding. For PDGF it is known from literature that it is upregulated early after wounding.[50] However, in the current study we observed a decrease in these growth factors 7 days after wounding and no return to baseline within 70 days. The first timepoint that post-biopsy samples were taken was after 7 days, which might be after an elevation in growth factors in the early days (2–6 days). In the literature a short and steep elevation of PDGF has been reported.[6,50] After the decrease at day 7 a slight elevation over time occurred, which was insufficient to return to baseline within the 70 days study period. For the MMPS, and in particular MMP-1, we observe a steep increase 7 days after wounding and a slow return to baseline. This is consistent with literature suggesting high levels of MMP-1 one day after wounding followed by a slow return to baseline.[51]

Furthermore, we observed that growth factor levels increase slightly over time but that the time course of the study was insufficient to capture a return to baseline of these genes. Even though the goal of this study was to characterize normal wound healing without intervention and no unexpected findings were anticipated, we did not foresee IL-6 to only yield zero values in the qPCR analysis (data not shown). A potential explanation for this could be an analytical assay issue given that all other tested proteins yielded quantifiable levels and no other explanation could be found. IL-6 is known to play a vital part in inflammation and activates both innate and the adaptive immune system.[52] In addition, it is known from literature that IL-6 gene expression is elevated in reepithelization of human skin wounds.[53] Therefore, it was expected that IL-6 would be elevated following the biopsy procedure.

INTEGRATED, MULTIDIMENSIONAL DATA VISUALIZATION SHOWS DISTINCT WOUND HEALING PHASES

We also assessed if integration of all the objective measures could function as a tool to distinguish healing phases and indicate the most important parameters in a certain phase, indicating the most suitable biomarkers per healing phase. Based on a radar plot, it can be concluded that important distinguishing biomarkers in all phases were wound depth, wound volume and mRNA expression of TGFβ3 in the skin punch biopsy. Most of the biomarkers were primarily affected in the inflammation phase indicating that the modalities used in the study are well capable of detecting differences in this phase. Interestingly, some biomarkers (i.e. IL-33, FGF1, PGF) were only affected in one of the phases showing good distinguishing power of this biomarker. Due to the non-linearity of the data the decision was made to visualize the integration of data using t-SNE. From this t-SNE plot a clear clustering of phases was seen. Pre-challenged skin showed the clearest demarcation compared to the other phases. This is consistent with expectations since all the data used for the integration model showed the biggest differences from day 0 to day 2. Interestingly, data points associated with the proliferation and maturation phases were closest to each other, indicating that there is a partial overlay of processes in the proliferation phase and remodeling phase. Although this visualization of the data suggests that the modalities can be used to distinguish in what phase a certain wound is, it should be interpreted with caution. The time points assignment to the different phases are based on literature and visual assessment of the investigators creating a selection bias.

OCT AS NOVEL TOOL FOR NON-INVASIVE WOUND CHARACTERIZATION

OCT has previously been used to visualize and quantify the microcirculation of the skin.[54-56] Vessel density in blister wounds using OCT has been quantified by Larsen et al. and this research group has been able to correlate (albeit weakly) the vessel density measurements with the inflammatory reaction scored using histology.[57] The visualization by OCT in this study showed distinct vasodilatation in the first days after wounding followed by an inwards perfusion on day 14 hinting towards neoangiogenesis inside the wound bed, therewith confirming the applicability of OCT measurements for characterization of the inflammatory status of the skin. OCT has not been frequently used in the field of dermatology for the evaluation of skin morphology. The majority of studies that have been performed were in small populations, focused on few endpoints or were performed in animal models.[58-60] In this study, we confirm applicability of the OCT not only for inflammatory characteristics but also morphological characteristics, allowing a full non-invasive characterization of the wound healing process. OCT images matched the histology recordings regarding the detectability of

distinct cutaneous shapes. Restoration of the epidermis, dilatation of blood vessels, granulation tissue and thickening and flattening of the epidermis could all be clearly characterized using OCT. However, despite being able to distinguish cutaneous structures and changes in the microenvironment, OCT also has some limitations. It does not have the diagnostic power and resolution needed to detect all wound healing processes and small microenvironmental changes without the need for histology comparison. In addition, the technique requires trained operators to reduce the number of artefacts in scans. Despite all these limitations the future of the technique looks promising. With recent advancements in resolution, measuring depth, image analysis and standardization of measurement the technique holds promise to replace the need for invasive skin biopsies and become a standard diagnosis tool.[61]

Our study is a first step towards a complete model for adequate drug and device testing in wound healing. These results contribute to a better understanding of the inflammatory responses in the skin's microenvironment. Although the results appear promising, some aspects could be optimized to increase sensitivity and improve the distinguishing power of the non-invasive imaging modalities. The first days of acute wound healing are vital in predicting time to closure and to monitor the first processes in the inflammation phase. Due to the bleeding period in the haemostasis phase, it is difficult to image the wounds shortly after wounding. In hindsight an extra visit 1 day after wounding would have been useful in determining the maximum response (i.e. skin blood perfusion, TEWL). Another addition that could be useful in evaluating wound healing would be the clinical scoring of re-epithelialization and contraction, to explicitly compare with objective endpoints. The wounds induced in this study were small, acute and self-resolving punch biopsies, which reflects the normal wound healing of acute sterile wounds and comparability with chronic, slow healing wounds should be further explored. In addition, the size and location of the wounds are important factors influencing wound healing and should be considered when extrapolating results to a different setting. Lastly, future research should be focused on including intervention as positive and negative controls to better assess the usability of the model in drug and device testing.

CONCLUSION

We successfully developed a rapid, quantitative human wound healing model by using a multimodal approach. Clinical imaging, biophysical and non-invasive morphological read-outs were fully concordant with histology and clinical scoring. Future use of the model together with test battery will enable early proof-of-concept of novel wound healing treatments using a homogeneous healthy study population.

REFERENCES

1 Singer AJ, Clark RAF. Cutaneous Wound Healing. N Engl J Med. 1999;341(10):738-746. doi:10.1056/NEJM199909023411006
2 Akbik D, Ghadiri M, Chrzanowski W, Rohanizadeh R. Curcumin as a wound healing agent. Life Sci. 2014;116(1):1-7. doi:10.1016/J.LFS.2014.08.016
3 Agren MS, Karlsmark T, Hansen JB, Rygaard J. Occlusion versus air exposure on full-thickness biopsy wounds. J Wound Care. 2001;10(8):301-304. doi:10.12968/JOWC.2001.10.8.26109
4 Theoret C, Schumacher J. Physiology of Wound Healing. Equine Wound Manag Third Ed. Published online November 9, 2016:1-13. doi:10.1002/9781118999219.CH1
5 Apfel SC. Nerve growth factor for the treatment of diabetic neuropathy: What went wrong, what went right, and what does the future hold? Int Rev Neurobiol. 2002;50:393-413. doi:10.1016/s0074-7742(02)50083-0
6 Werner S, Grose R. Regulation of Wound Healing by Growth Factors and Cytokines. Physiol Rev. 2003;83(3):835-870. doi:10.1152/physrev.2003.83.3.835
7 Sorg H, Tilkorn DJ, Hager S, Hauser J, Mirastschijski U. Skin Wound Healing: An Update on the Current Knowledge and Concepts. Eur Surg Res. 2017;58(1-2):81-94. doi:10.1159/000454919
8 Ashrafi M, Xu Y, Muhamadali H, et al. A microbiome and metabolomic signature of phases of cutaneous healing identified by profiling sequential acute wounds of human skin: An exploratory study. PLoS One. 2020;15(2). doi:10.1371/JOURNAL.PONE.0229545
9 Landén NX, Li D, Ståhle M. Transition from inflammation to proliferation: a critical step during wound healing. Cell Mol Life Sci. 2016;73(20):3861-3885. doi:10.1007/s00018-016-2268-0
10 Demidova-Rice TN, Hamblin MR, Herman IM. Acute and Impaired Wound Healing: Pathophysiology and Current Methods for Drug Delivery, Part 1: Normal and Chronic Wounds: Biology, Causes, and Approaches to Care. Adv Skin Wound Care. 2012;25(7):304. doi:10.1097/01.ASW.0000416006.55218.D0
11 Öhnstedt E, Lofton Tomenius H, Vågesjö E, Phillipson M. The discovery and development of topical medicines for wound healing. Expert Opin Drug Discov. 2019;14(5):485-497. doi:10.1080/17460441.2019.1588879
12 Zielins ER, Brett EA, Luan A, et al. Emerging drugs for the treatment of wound healing. Expert Opin Emerg Drugs. 2015;20(2):235-246. doi:10.1517/14728214.2015.1018176
13 A Robust Market Rich with Opportunities: Advanced Wound Dressings. https://www.pm360online.com/. Accessed January 10, 2022. https://www.pm360online.com/a-robust-market-rich-with-opportunities-advanced-wound-dressings/
14 Sen CK. Human Wounds and Its Burden: An Updated Compendium of Estimates. Adv Wound Care. 2019;8(2):39. doi:10.1089/WOUND.2019.0946
15 Pastar I, Wong LL, Egger AN, Tomic-Canic M. Descriptive vs mechanistic scientific approach to study wound healing and its inhibition: Is there a value of translational research involving human subjects? Exp Dermatol. 2018;27(5):551. doi:10.1111/EXD.13663
16 Brölmann FE, Eskes AM, Sumpio BE, et al. Fundamentals of randomized clinical trials in wound care: Reporting standards. Wound Repair Regen. 2013;21(5):641-647. doi:10.1111/WRR.12087
17 Kirsner RS, Margolis DJ, Baldursson BT, et al. Fish skin grafts compared to human amnion/chorion membrane allografts: A double-blind, prospective, randomized clinical trial of acute wound healing. Wound Repair Regen. 2020;28(1):75. doi:10.1111/WRR.12761
18 Greaves NS, Benatar B, Whiteside S, Alonso-Rasgado T, Baguneid M, Bayat A. Optical coherence tomography: A reliable alternative to invasive histological assessment of acute wound healing in human skin? Br J Dermatol. 2014;170(4):840-850. doi:10.1111/bjd.12786
19 Greaves NS, Iqbal SA, Hodgkinson T, et al. Skin substitute-assisted repair shows reduced dermal fibrosis in acute human wounds validated simultaneously by histology and optical coherence tomography. Wound Repair Regen. 2015;23(4):483-494. doi:10.1111/wrr.12308
20 Rissmann R, Moerland M, van Doorn MBA. Blueprint for mechanistic, data-rich early phase clinical pharmacology studies in dermatology. Br J Clin Pharmacol. 2020;86(6):1011-1014. doi:10.1111/bcp.14293
21 Ud-Din S, Bayat A. Non-invasive objective devices for monitoring the inflammatory, proliferative and remodelling phases of cutaneous wound healing and skin scarring. Exp Dermatol. 2016;25(8):579-585. doi:10.1111/exd.13027
22 Jacobse J, ten Voorde W, Tandon A, et al. Comprehensive evaluation of microneedle-based intradermal adalimumab delivery vs. subcutaneous administration: results of a randomized controlled clinical trial. Br J Clin Pharmacol. 2021;87(8):3162-3176. doi:10.1111/BCP.14729
23 Saghari M, Gal P, Ziagkos D, et al. A randomized controlled trial with a delayed-type hypersensitivity model using keyhole limpet haemocyanin to evaluate adaptive immune responses in man. Br J Clin Pharmacol. 2021;87(4):1953-1962. doi:10.1111/BCP.14588
24 Themstrup L, Ciardo S, Manfredi M, et al. *In vivo* , micro-morphological vascular changes induced by topical brimonidine studied by Dynamic optical coherence tomography. J Eur Acad Dermatology Venereol. 2016;30(6):974-979. doi:10.1111/jdv.13596
25 Buters TP, Hameeteman PW, Jansen IME, et al. Intradermal lipopolysaccharide challenge as an acute *in vivo* inflammatory model in healthy volunteers. Br J Clin Pharmacol. Published online 2021. doi:10.1111/BCP.14999
26 Ly BCK, Dyer EB, Feig JL, Chien AL, Del Bino S. Research Techniques Made Simple: Cutaneous Colorimetry:

A Reliable Technique for Objective Skin Color Measurement. J Invest Dermatol. 2020;140(1):3-12.e1. doi:10.1016/j.jid.2019.11.003
27 Rijsbergen M, Pagan L, Niemeyer-van der Kolk T, et al. Stereophotogrammetric three-dimensional photography is an accurate and precise planimetric method for the clinical visualization and quantification of human papilloma virus-induced skin lesions. J Eur Acad Dermatology Venereol. 2019;33(8):1506-1512. doi:10.1111/JDV.15474
28 van der Kolk T, Assil S, Rijneveld R, et al. Comprehensive, Multimodal Characterization of an Imiquimod-Induced Human Skin Inflammation Model for Drug Development. Clin Transl Sci. 2018;11(6):607-615. doi:10.1111/CTS.12563
29 Cuzzell JZ. The new RYB color code. Am J Nurs. 1988;88(10):1342—1346. doi:10.2307/3470923
30 Tan J, Liu H, Leyden JJ, Leoni MJ. Reliability of Clinician Erythema Assessment grading scale. J Am Acad Dermatol. 2014;71(4):760-763. doi:10.1016/j.jaad.2014.05.044
31 Chae JK, Kim JH, Kim EJ, Park K. Values of a Patient and Observer Scar Assessment Scale to Evaluate the Facial Skin Graft Scar. Ann Dermatol. 2016;28(5):615. doi:10.5021/AD.2016.28.5.615
32 Van Der Maaten L, Hinton G. Visualizing Data using t-SNE. J Mach Learn Res. 2008;9:2579-2605.
33 Rasche H. Haemostasis and thrombosis: an overview. Eur Hear J Suppl. 2001;3(suppl_Q):Q3-Q7. doi:10.1016/S1520-765X(01)90034-3
34 Versteeg HH, Heemskerk JWM, Levi M, Reitsma PH. New fundamentals in hemostasis. undefined. 2013;93(1):327-358. doi:10.1152/PHYSREV.00016.2011
35 Midwood KS, Williams LV, Schwarzbauer JE. Tissue repair and the dynamics of the extracellular matrix. Int J Biochem Cell Biol. 2004;36(6):1031-1037. doi:10.1016/J.BIOCEL.2003.12.003
36 Chang HY, Sneddon JB, Alizadeh AA, et al. Gene Expression Signature of Fibroblast Serum Response Predicts Human Cancer Progression: Similarities between Tumors and Wounds. PLoS Biol. 2004;2(2). doi:10.1371/JOURNAL.PBIO.0020007
37 Pedregosa Fabianpedregosa F, Michel V, Grisel Oliviergrisel O, et al. Scikit-learn: Machine Learning in Python Gaël Varoquaux Bertrand Thirion Vincent Dubourg Alexandre Passos PEDREGOSA, VAROQUAUX, GRAMFORT ET AL. Matthieu Perrot. J Mach Learn Res. 2011;12:2825-2830. Accessed January 5, 2022. http://scikit-learn.sourceforge.net.
38 Kaliyadan F, Manoj J, Venkitakrishnan S, Dharmaratnam A. Basic digital photography in dermatology. Indian J Dermatol Venereol Leprol. 2008;74(5):532-536. doi:10.4103/0378-6323.44334
39 Hibler B, Qi Q, Rossi A. Current state of imaging in dermatology. Semin Cutan Med Surg. 2016;35(1):2-8. doi:10.12788/j.sder.2016.001
40 Gonzalez ACDO, Andrade ZDA, Costa TF, Medrado ARAP. Wound healing - A literature review. An Bras Dermatol. 2016;91(5):614-620. doi:10.1590/abd1806-4841.20164741
41 Alexander H, Brown S, Danby S, Flohr C. Research Techniques Made Simple: Transepidermal Water Loss Measurement as a Research Tool. J Invest Dermatol. 2018;138(11):2295-2300.e1. doi:10.1016/J.JID.2018.09.001
42 Silverman RA, Lender J, Elmets CA. Effects of occlusive and semiocclusive dressings on the return of barrier function to transepidermal water loss in standardized human wounds. J Am Acad Dermatol. 1989;20(5):755-760. doi:10.1016/S0190-9622(89)70086-4
43 Weinstein GD, Van Scott EJ. Autoradiographic Analysis of Turnover Times of Normal and Psoriatic Epidermis. J Invest Dermatol. 1965;45(4):257-262. doi:10.1038/JID.1965.126
44 Bishop A. Wound assessment and dressing selection: an overview. Br J Nurs. 2021;30(5):S12-S20. doi:10.12968/BJON.2021.30.5.S12
45 Dinarello CA. Overview of the IL-1 family in innate inflammation and acquired immunity. Immunol Rev. 2018;281(1):8. doi:10.1111/IMR.12621
46 Lim JY, Choi BH, Lee S, Jang YH, Choi JS, Kim YM. Regulation of wound healing by granulocyte-macrophage colony-stimulating factor after vocal fold injury. PLoS One. 2013;8(1). doi:10.1371/JOURNAL.PONE.0054256
47 Roberts AB, Sporn MB. Differential expression of the TGF-beta isoforms in embryogenesis suggests specific roles in developing and adult tissues. Mol Reprod Dev. 1992;32(2):91-98. doi:10.1002/MRD.1080320203
48 Wang R, Ghahary A, Shen Q, Scott PG, Roy K, Tredget EE. Hypertrophic scar tissues and fibroblasts produce more transforming growth factor-beta1 mRNA and protein than normal skin and cells. Wound Repair Regen. 2000;8(2):128-137. doi:10.1046/J.1524-475X.2000.00128.X
49 Ferguson MW, Duncan J, Bond J, et al. Prophylactic administration of avotermin for improvement of skin scarring: three double-blind, placebo-controlled, phase I/II studies. Lancet. 2009;373(9671):1264-1274. doi:10.1016/S0140-6736(09)60322-6
50 Breuing K, Andree C, Helo G, Slama J, Liu PY, Eriksson E. Growth Factors in the Repair of Partial Thickness Porcine Skin Wounds. Plast Reconstr Surg. 1997;100(3):657-664. doi:10.1097/00006534-199709000-00018
51 Caley MP, Martins VLC, O'Toole EA. Metalloproteinases and Wound Healing. Adv Wound Care. 2015;4(4):225. doi:10.1089/WOUND.2014.0581
52 Johnson BZ, Stevenson AW, Prêle CM, Fear MW, Wood FM. The Role of IL-6 in Skin Fibrosis and Cutaneous Wound Healing. Biomedicines. 2020;8(5). doi:10.3390/BIOMEDICINES8050101
53 Ågren MS, Litman T, Eriksen JO, Schjerling P, Bzorek M, Gjerdrum LMR. Gene Expression Linked to Reepithelialization of Human Skin Wounds. Int J Mol Sci. 2022;23(24). doi:10.3390/IJMS232415746/S1
54 Glinos GD, Verne SH, Aldahan AS, et al. Optical coherence tomography for assessment of epithelialization in a human *ex vivo* wound model. Wound Repair Regen. 2017;25(6):1017-1026. doi:10.1111/WRR.12600
55 Yuan Z, Zakhaleva J, Ren H, Liu J, Chen W, Pan Y. Noninvasive and high-resolution optical monitoring of healing of diabetic dermal excisional wounds implanted with biodegradable in situ gelable hydrogels. Tissue Eng Part C Methods. 2010;16(2):237-247. doi:10.1089/ten.TEC.2009.0152
56 Holmes J, Schuh S, Bowling FL, Mani R, Welzel J. Dynamic Optical Coherence Tomography Is a New Technique for Imaging Skin Around Lower Extremity Wounds. Int J Low Extrem Wounds. 2019;18(1):65-74. doi:10.1177/1534734618821015
57 Larsen HF, Ahlström MG, Gjerdrum LMR, et al. Noninvasive measurement of reepithelialization and microvascularity of suction-blister wounds with benchmarking to histology. Wound Repair Regen. 2017;25(6):984-993. doi:10.1111/WRR.12605
58 Cobb MJ, Chen Y, Underwood RA, Usui ML, Olerud J, Li X. Noninvasive assessment of cutaneous wound healing using ultrahigh-resolution optical coherence tomography. J Biomed Opt. 2006;11(6):064002. doi:10.1117/1.2388152
59 Wang Z, Pan H, Yuan Z, Liu J, Chen W, Pan Y. Assessment of Dermal Wound Repair after Collagen Implantation with Optical Coherence Tomography. Tissue Eng Part C Methods. 2008;14(1):35-45. doi:10.1089/tec.2007.0285
60 Welzel J, Lankenau E, Birngruber R, Engelhardt R. Optical coherence tomography of the human skin. J Am Acad Dermatol. 1997;37(6):958-963. doi:10.1016/S0190-9622(97)70072-0
61 Ogien J, Levecq O, Cazalas M, et al. Handheld line-field confocal optical coherence tomography for dermatology. https://doi.org/101117/122545546. 2020;11211:44-53. doi:10.1117/12.2545546

Supplementary Figure 1 Histopathology score on wound re-epithelialization (n=18 for day 0, n=6 for all other timepoints)

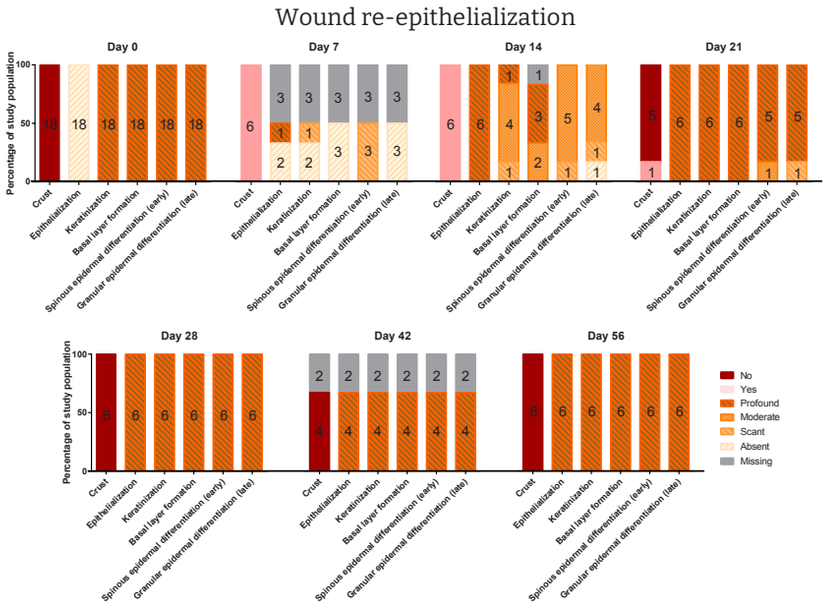

Supplementary Figure 2 Histopathology score on inflammation status (n=18 for day 0, n=6 for all other timepoints)

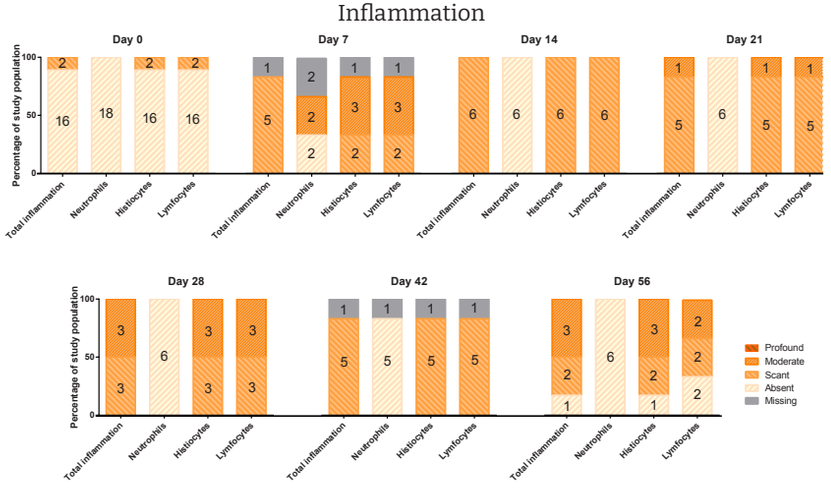

Supplementary Figure 3 Histopathology score on neoangionesis (n=18 for day 0, n=6 for all other timepoints)

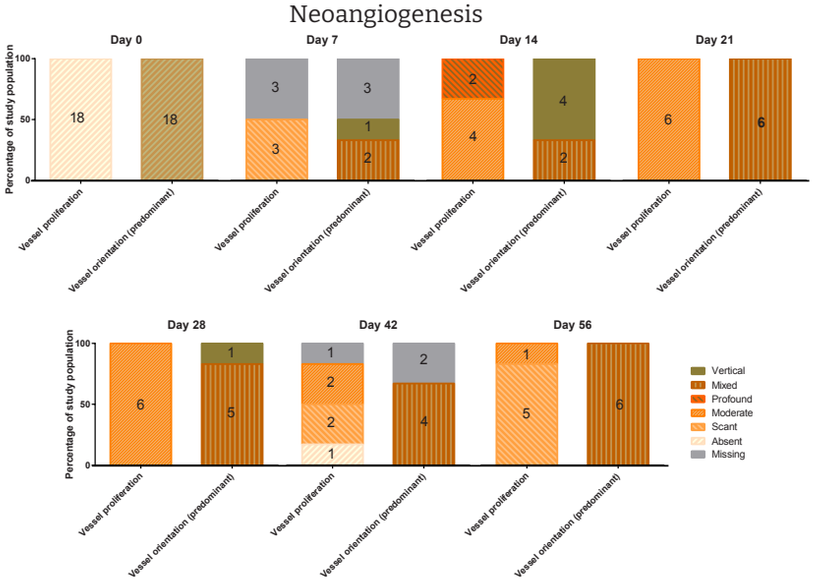

Supplementary Figure 4 Histopathology score on granulation tissue (n=18 for day 0, n=6 for all other timepoints)

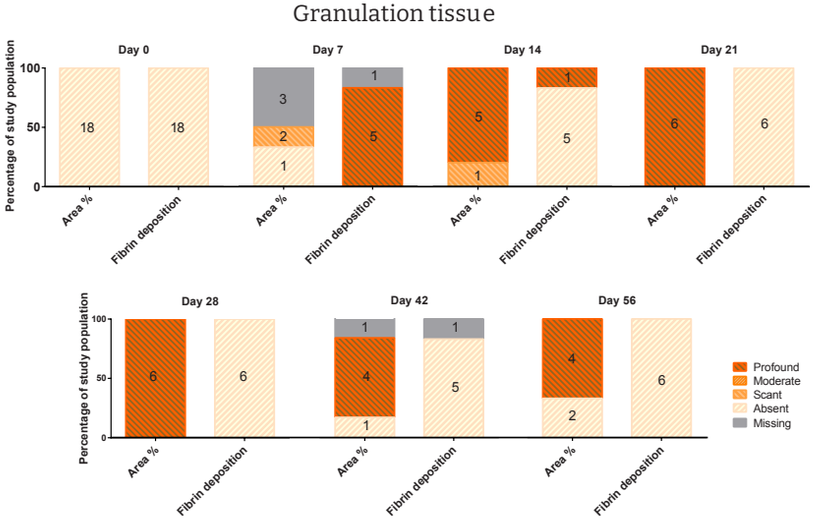

Supplementary Figure 5 Histopathology score on connective tissue formation (n=18 for day 0, n=6 for all other timepoints

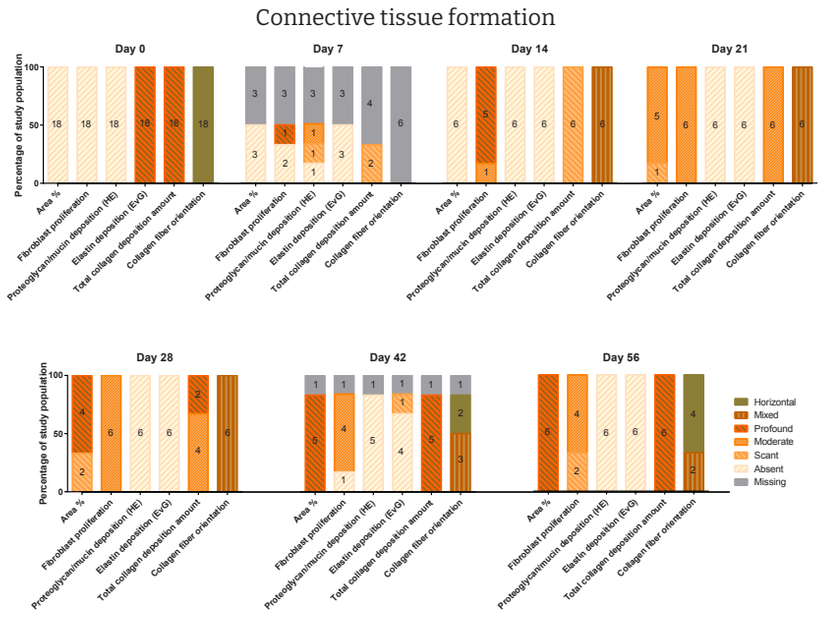

Supplementary Figure 6 Representative OCT images time-matched with histology

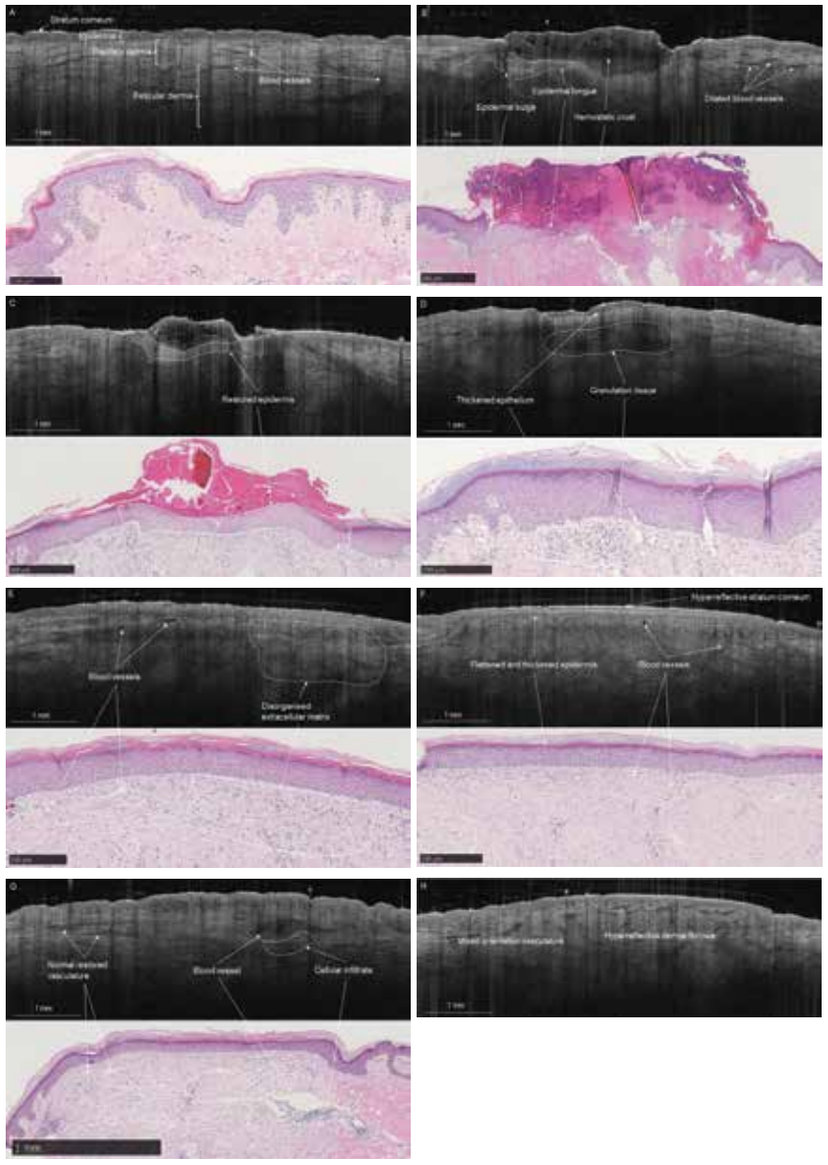

Supplementary Figure 7 Clinical scores

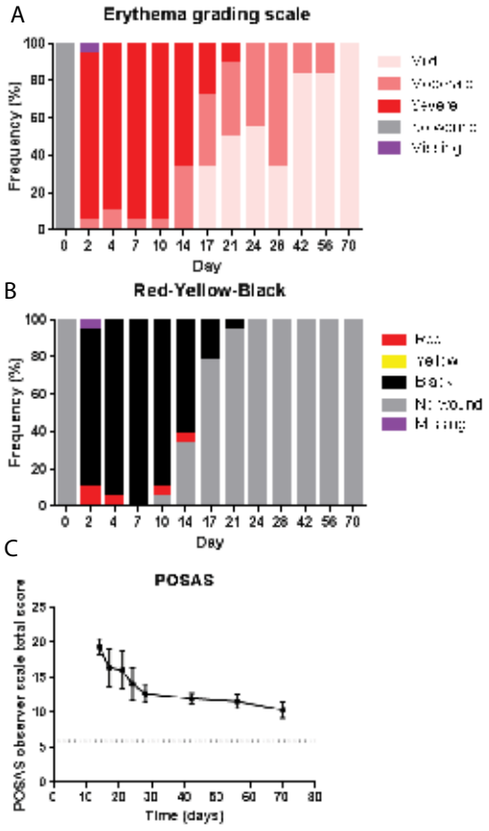

CHAPTER III

A SUCTION BLISTER MODEL TO CHARACTERIZE EPIDERMAL WOUND HEALING AND EVALUATE THE EFFICACY OF THE TOPICAL WOUND HEALING AGENT INM-755 IN HEALTHY VOLUNTEERS

Published in the European Journal of Pharmaceutical Science (special issue: An Industrial Perspective on the Challenges and Opportunities in Topical and Transdermal New Drug and Generic Product Development), 2024

Wouter ten Voorde[1,2], Selinde Wind[1,2], Ismahaan Abdisalaam[1,5], Alexandra Mancini[4], Erica Klaassen[1], Feeke Linders[1], Manon A.A Jansen[1], Tessa Niemeyer-van der Kolk[1], Jacobus Burggraaf[1,2], Robert Rissmann[1,2,3]

1 Centre for Human Drug Research, Leiden, NL
2 Leiden University Medical Centre, Leiden, NL
3 Leiden Academic Center for Drug Research, Leiden University, Leiden, NL
4 InMed Pharmaceuticals Inc. Vancouver, CA
5 Department of Dermatology, Erasmus Medical Center, Rotterdam, NL

ABSTRACT

Non-healing wounds represent a substantial medical burden with few effective treatments available. To address this challenge, we developed a novel epidermal wound healing model using suction blisters in healthy volunteers. This model allowed for the comprehensive assessment of wound healing dynamics and the evaluation of INM-755, a topical cream containing cannabinol, as a potential therapeutic agent.

Two clinical studies were conducted: an observational study and an interventional study. In both studies, healthy volunteers underwent a suction blister procedure on their lower back, creating open epidermal wounds. Wound healing parameters were assessed using advanced imaging systems. Skin barrier function and perfusion were evaluated through trans epidermal water loss (TEWL) and dynamic optical coherence tomography (D-OCT), respectively.

The observational study demonstrated the successful and reproducible Induction of blisters and the removal of epidermal sheet, enabling quantifiable measurements of wound healing parameters over time. Re-epithelialization was observed, revealing recovery of skin barrier function and perfusion. In the interventional study, differences of treatments over time were quantified using the above-described techniques.

Despite differences from disease-specific blistering, our developed model provides a valuable platform for studying wound healing mechanisms and assessing novel therapeutic interventions. The sensitivity to treatment effects demonstrated in our study underscores the potential utility of this model in early-phase clinical drug development programs targeting wound healing disorders.

INTRODUCTION

Cutaneous wound healing is a complex process divided into four main phases: hemostasis, inflammation, proliferation, and remodeling.[1] In chronic, non-healing wounds, one or more of the four phases of wound healing is delayed or disturbed. Most commonly this impairment is present in the inflammation phase, in which persistent inflammatory activity induced by infection or re-injury interferes with healing of the wound.[2,3]

Current treatment options for chronic non-healing wounds are limited and mainly focused on wound care and patient-reported symptoms, e.g. itch, highlighting the high medical need in the field of chronic non-healing wounds.[4,5] However, developing novel therapies for non-healing chronic wounds is challenging, from both a discovery and a clinical development perspective. Current treatment strategies focus on gene and cell therapies albeit still in early stage.[6,7,8] Wounds can be highly heterogeneous with a high variability in severity and symptoms among patients, and research on pathophysiology shows that many interconnected pathways are involved.

Testing new treatment strategies is challenging due to the lack of sensitive objective biomarkers that can I) quantify the characteristics of wounds and II) are able to detect changes after treatment. Both aspects are needed for clinical trials. The absence of a robust human wound healing model suitable for early-phase clinical studies is one reason for the restricted number of clinical trials addressing an evidence-based approach for treating wounds.[9,10] Most wound models are transferred from pre-clinical mouse models to humans and primarily focus on excisional, scratch, or burn wounds.[11] However, the process of epidermal wound healing most likely differs from wound healing of deeper and/or differently induced wounds, making the previously developed models likely unsuitable for clinical trials. Previously, we studied normal wound healing in healthy volunteers and established a key set of biomarkers for clinical trials. We developed a model in which normal wound healing of a full-thickness skin biopsy was extensively characterized using objective imaging techniques combined with molecular readouts in re-excised biopsies. The results of this study showed that with these techniques, it is possible to thoroughly follow the process of normal wound healing, making it a suitable model for early-phase clinical drug development programs targeting wound healing.[12] To date, no epidermal wound healing model exists with full separation of the epidermis. Despite the use of suction blistering in several clinical studies to investigate various components of wound healing, these suction blister models only included one or two fragmented objective readouts, e.g. isolated transepidermal water loss assessment, but never employed a full comprehensive characterization looking at perfusion, wound parameters, barrier function, and immunological readouts.[13]

A suction blister model to characterize wound healing would be beneficial for therapeutic agents addressing bullous diseases, such as epidermolysis bullosa (EB). INM-755 represents such a novel therapeutic agent – a topical cream containing cannabinol (CBN). Pre-clinical studies demonstrated the capacity of INM-755 to reduce the expression of matrix metalloproteinase-9 (MMP-9) and interleukin-8 (IL-8), factors that are typically elevated in blisters of EB patients and are believed to play a role in blister formation in this patient population.[14,15]

In the current studies, we aimed to develop a novel epidermal wound healing model suitable for the full characterization of epidermal wound healing and for testing the efficacy of novel therapeutics in healthy volunteers. Specifically, the objectives were I) to develop an epidermal wound healing model based on suction blisters; II) to extensively characterize epidermal wound healing using the developed model in healthy volunteers, and III) to test the effects of INM-755, a novel therapeutic agent for epidermal wounds, using the developed model in healthy volunteers.

MATERIALS AND METHODS

Two clinical studies were performed. The first study was a prospective observational study in healthy volunteers to characterize time-dependent epidermal wound healing after a suction blister-induced wound (NL71806.056.19). The second study was a randomized, double-blind, vehicle-controlled interventional Phase I study in healthy volunteers to study the effects of INM-755 on epidermal wound healing in the model as developed in the first study (NL72831.056.20). Both studies were performed at the Centre for Human Drug Research, Leiden, The Netherlands and lasted from February 2020 to March 2020 and from July 2020 to September 2020, respectively, with the Declaration of Helsinki as the guiding principle. Ethical study approval was received from the independent Medical Review and Ethics Committee 'Medische Ethische Toetsingscommissie van de Stichting Beoordeling Ethiek Biomedisch Onderzoek' (Assen, the Netherlands) prior to the start of the clinical phase for each study. Subjects gave written informed consent before participation in the study after receiving oral and written information.

SUBJECTS AND STUDY DESIGN

Twelve (observational study) and eight (intervention study) healthy non-smoking male or female volunteers were included, aged between 18 and 45, with a Fitzpatrick skin type of I-III, and a BMI ranging from 18-30 kg/m^2. Individuals were excluded from the study if they had a history of pathological scar formation or clinically significant skin conditions requiring immunosuppressive/immunomodulatory medication. Participants' overall health status was evaluated through physical examination, ECG, vital signs, and blood analysis.

In the observational study, subjects underwent the suction blister procedure on Day 0. One blister was created on each subject's lower back. The blister roof, i.e. epidermal sheet, was harvested after blister formation to create an open, non-bleeding epidermal wound. Initially, the wound was covered with non-adhesive gauze dressing which was renewed daily. After Day 6, the wound was left uncovered.

In the interventional study, at baseline four blisters were created on each subject's lower back, spaced at least 5 cm apart. The blister roof was harvested after blister formation to create an open epidermal wound. Each subject received four treatments randomly assigned to the four blister locations: high concentration INM-755 cream (HD), low concentration INM-755 cream (LD), a matching vehicle, or no treatment. Assignment was blinded for treated blisters (INM-755 and vehicle). The assigned treatment per blister was applied in excess (approximately 75 mg/cm^2) by a dedicated blinded physician for 14 consecutive days and the treated wounds were afterwards covered with a semi-adhesive Mepitel® dressing. To ensure optimal condition for drug uptake, a non-adhesive gauze dressing was applied over the Mepitel® dressing. The untreated blister, as a control for wound healing, was covered with the same type of non-adhesive gauze dressing.

Pharmacodynamic assessments comprised clinical imaging, biophysical assessments, clinical scores, and molecular readouts, and were performed on days 0, 1, 3, 6, 9, and 12 for the observational study and daily from Day 0 up to Day 21 for the interventional study.

TREATMENT

INM-755 is a topical cream containing CBN, a weak agonist for the Cannabinoid-1 and Cannabinoid-2 receptors. Pre-clinical studies with INM-755 showed reduced expression of MMP-9 and IL-8 after challenging incubated cells with TNFα and IFNɣ. MMP-9 and IL-8 are known to be upregulated in blisters of EB patients and are suspected to contribute to blister formation. Additionally, after treatment with INM-755, an upregulation in basal keratin 15 (K15) was observed. K15 might substitute basal keratin 14 (K14) in forming a construct with keratin 5, which could lead to strengthening of the skin in EB patients with a K14 mutation (data on file). In addition to the high concentration INM-755 cream, low concentration INM-755 cream, a matching vehicle, or no treatment were assigned to the blister locations.

SKIN SUCTION BLISTER PROCEDURE

Suction blisters were induced using the NP-4 suction blister device (Electric Diversities in Maryland, USA) following Standard Operating Procedures. The device generated an approximately 10 mm diameter blister in 79 to 154 minutes by applying under pressure (up to 8 INHG). After the blister was formed, the roof was punctured with a needle to aspirate the fluid. The blister roof, or epidermal sheet, was removed with scissors. The wound diameter was measured using a standardized calliper.

OUTCOME ASSESSMENTS

CHARACTERISATION OF EPIDERMAL WOUND HEALING

Clinical images to evaluate dimensional wound healing parameters (e.g. wound surface, diameter, volume) were taken of the suction blister-induced wound study using a 3D stereo camera system (LifeViz® QuantifiCare, Valbonne, France). Analysis of the data was performed according to the CHDR standard procedure.[16] Additionally, epidermal wound healing was qualitatively evaluated using dynamic-optical coherence tomography (D-OCT) from Michelson diagnostics (VivoSight OCT, Kent, UK).

SKIN BARRIER FUNCTION

Trans epidermal water loss (TEWL) was used to determine the barrier function of the skin. Before the measurement began, the subjects underwent a 15-minute acclimatization process to the room. Subsequently, a probe was affixed to the wound to establish a 7 mm closed chamber, after which the measurement procedure was initiated as described previously.[12] The disparities in humidity between the TEWL chamber and the skin causes the movement of water molecules, which are detected by the sensors within the chamber over time. The measurement was sustained for either 90 seconds or until the steady-state flux was attained.

SKIN PERFUSION

Cutaneous microcirculation was measured using D-OCT from Michelson diagnostics (VivoSight OCT, Kent, UK). The procedure was performed at baseline and during each visit throughout the trial, following the protocols described previously.[17] A 6 mm probe was placed directly over the inner wound. 120 consecutive scans were taken, each with a depth of up to 1.5 mm, in about 20 seconds. The cutaneous microcirculation was calculated by determining the average speckle signal that returned from a depth of 0.1 mm to 0.35 mm to reduce artifacts and noise signals.

EVALUATION OF INM-755 EFFECTS

SKIN ERYTHEMA

Multispectral imaging (Antera 3D, Miravex, Dublin, Ireland, was used to quantify skin's erythema in the interventional study as described previously.[18] By creating a closed chamber environment, standardized images were taken at all study visits. A region of interest of 12 mm was selected and kept analogous throughout. Skin erythema is expressed as CIELab a* value in arbitrary units.

WOUND HEALING PARAMETERS

In the observational study, dimensional wound healing parameters (e.g. wound surface, diameter, volume) were explored using the 3D stereo camera system (LifeViz QuantifiCare, Valbonne, France). In the interventional study, 3D image analysis could not be performed due to a technical malfunction. In both studies, clinical images were taken of the suction blister-induced wound.

SKIN BARRIER FUNCTION

Skin barrier function was measured using TEWL as described above in the method section 'characterization of wound healing model'.

SKIN PERFUSION

Skin perfusion was measured using D-OCT as described above in the method section 'characterization of wound healing model'.

SKIN SURFACE BIOMARKERS

In the interventional study, skin surface biomarkers interleukin-8 (IL-8), matrix metalloproteinase-9 (MMP-9), interleukin-1 receptor antagonist (IL-1RA), vascular endothelial growth factor (VEGF), tissue inhibitor of metalloproteinases (TIMP-1, and TIMP-2) were measured exploratively using FibroTx patches (FibroTx, Estonia). A patch comprises a multiplexed capture-antibody micro-array that is fastened to the skin via a dermal adhesive bandage. Upon application to the skin for 15 minutes, the antibodies imprinted on the micro-array selectively capture skin biomarkers via immunological recognition. The captured biomarkers were then subjected to a quantitative analysis through the utilization of a spot- ELISA (enzyme-linked immunosorbent assay).

SAFETY AND TOLERABILITY

Safety and tolerability of INM-755 was frequently monitored in the interventional study by tracking adverse events, taking vital signs, and conducting standard blood analysis. In addition, local application site reactions were monitored

by scoring erythema, oedema, scaling, and asking subjects about a stinging/burning sensation using well-defined criteria. The results are displayed as local tolerability assessments (LTA) and reported as a percentage from total. Physician-reported LTAS (erythema, oedema, scaling) were scored by the same blinded physician throughout the study and consisted of categorical scores ranging from 0-3. Scoring was performed directly after blister induction and on each subsequent study day. Red-yellow-black (RYB) scores were given to assess the color and humidity of the blister wounds. RYB was scored after bandage removal and before drug application on each study day.

STATISTICS

No formal statistical significance analysis was performed for the observational study considering the lack of treatment groups and the focus on feasibility of the techniques. All data displayed for the observational study is summarized in descriptive statistics and reported as means over time. For the interventional study, a statistical model was applied to analyze repeated wound healing parameters. A mixed model ANCOVA with fixed factors of treatment, wound number, time, and treatment-by-time interaction, and random factors of subject, subject-by-treatment interaction, and subject-by-time interaction was used. It also included the baseline value, taken immediately after blister formation, as a covariate. The following contrasts were calculated within the model: LD INM-755 vs. vehicle, HD INM-755 vs. vehicle, HD INM-755 vs. LD INM-755, LD INM-755 vs. untreated, HD INM-755 vs. untreated, vehicle vs. untreated. Categorical LTA parameters were summarized by frequencies and treatment. For OCT skin perfusion and IL-1RA measurements the data was log-transformed because of log-normal distribution.

RESULTS

Twenty subjects (12 in the observational study, 8 in the interventional study) were enrolled in the studies and all completed the trial according to the protocol. All study subjects were Caucasian and had a mean age of 26.2 (19-37) years in the observational study and 23.4 (18-32) years in the interventional study. INM-755 in all dose levels was safe and well tolerated. The most frequent reported treatment-related adverse event was application site erythema, which was present in 8 (100%) of the epidermal wounds that received vehicle and LD INM-755, and in 7 (87.5%) of the epidermal wounds that received HD INM-755. No dose relationship in adverse events was detected.

Table 1 Subject demographics

Study	Observational	Interventional
Age (years)		
n	12	8
Mean (SD)	26.2 (4.3)	23.4 (5.0)
Median	26.0	22
Min, Max	19, 37	18, 32
Height (cm)		
n	12	8
Mean (SD)	176.6 (10.1)	177.4 (5.8)
Median	177.6	177.1
Min, Max	162.3, 198.5	169.5, 185.4
Weight (kg)		
n	12	8
Mean (SD)	70.0 (11.7)	67.9 (5.8)
Median	68.2	68.2
Min, Max	52.9, 92.3	60.7, 74.6
BMI (kg/m^2)		
n	12	8
Mean (SD)	22.4 (2.39)	21.5 (1.6)
Median	22.4	21.3
Min, Max	18.2, 27.4	18.8, 24.5
Sex		
Female	6 (50.0%)	4 (50.0%)
Male	6 (50.0%)	4 (50.0%)
Race		
White	12 (100.0%)	8 (100.0%)
Fitzpatrick Skin Type		
1 (always burns and never tans)	1 (8.3%)	1 (12.5%)
2 (often burns and tans lightly)	7 (58.3%)	2 (25.0%)
3 (burns moderate and tans gradually)	4 (33.3%)	5 (62.5%)

CHARACTERISATION OF EPIDERMAL WOUND HEALING

In all 12 subjects included in the observational study, a complete suction blister developed within 154 minutes following the start of the suction procedure. In each case, the epidermal layer was effectively detached using a combination of tweezers and scissors.

Clinical imaging of induced blisters showed gradual restoration of the skin barrier over time (Figure 1A). As part of the feasibility process, quantifying the variability among subjects before and after undergoing the blister procedure for the three parameters tested (surface, TEWL, perfusion) was crucial. Figures 1B, C, and D illustrate the coefficient of variation for blister surface, TEWL, and perfusion, respectively. Following the induction of epidermal wounds, variability remained within acceptable limits (CV < 30%) for all parameters.[19]

In terms of wound healing, re-epithelialization of the epidermis measured with 3D photo analysis started within 3 days and was complete within 9-11 days (Figure 1E). After induction of the epidermal wound, TEWL immediately increased and gradually decreased during the observation period over time (Figure 1F). TEWL did not return to the baseline status within the study duration. This pattern was also present for skin perfusion as measured with D-OCT. The timing of return to a normal perfusion of the skin was longer than 12 days (Figure 1G).

Skin morphology before and after the blister procedure was visualized using OCT. Figure 2A depicts normal skin, while Figure 2B shows skin post-epidermal sheet removal. Notably, Figure 2B shows visible rupture marks on the dermo-epidermal junction. No variation in intensity is observed, signifying complete epidermal removal. Additionally, the hyperreflective bands in Figure 2B denote blister fluid seeping from the newly formed wound.

EFFECTS OF INM-755

Clinical images of epidermal blisters are displayed in Figure 3A. Skin erythema quantified using multispectral imaging is displayed in Figure 3B. Immediately after the blister procedure, all treatment groups (pre-dose versus post-dose) demonstrated a noticeable increase in skin erythema. During the first five days after wounding a trend towards separation between treatment arms can be observed. Following the initial increase in erythema, there was no longer a noticeable pattern, as the erythema in the untreated wound returned to baseline as rapidly the treated wounds.

A steep increase was noted in TEWL from pre-blister (baseline) flux measurements (approximately 10 g/m²/h) to post-blister measurements (approximately 100 g/m²/h) after the removal of the epidermis (Figure 3C). From Day 2 to Day 7, a steep decrease in the flux measurements was observed. After Day 7, the TEWL generally gradually decreased to a mean of about 15 g/m²/h on Day 21, close to baseline TEWL flux of about 10 g/m²/h. TEWL of epidermal wounds treated with INM-755 in both concentrations and the vehicle recovered slightly quicker than the TEWL of untreated wounds (contrast LD INM-755 – untreated p=0.0518, difference 4.2, (95%CI: -0.036, -8.409). Contrast HD INM-755 – untreated p=0.0512, difference 4.1, (95%CI: -0.023, -8.194). Contrast vehicle – untreated p=0.0335, difference 4.4, (95%CI: 0.0392, -8.405)).

Figure 1 A) Representative images of epidermal wound healing over time. B-D) Variability within subjects measured before and after blister induction displayed as individual data points. Coefficient of variation is displayed for all parameters before and after induction, except for blister surface where no blisters were present. E-G) All data are displayed as mean +- SD, n=12

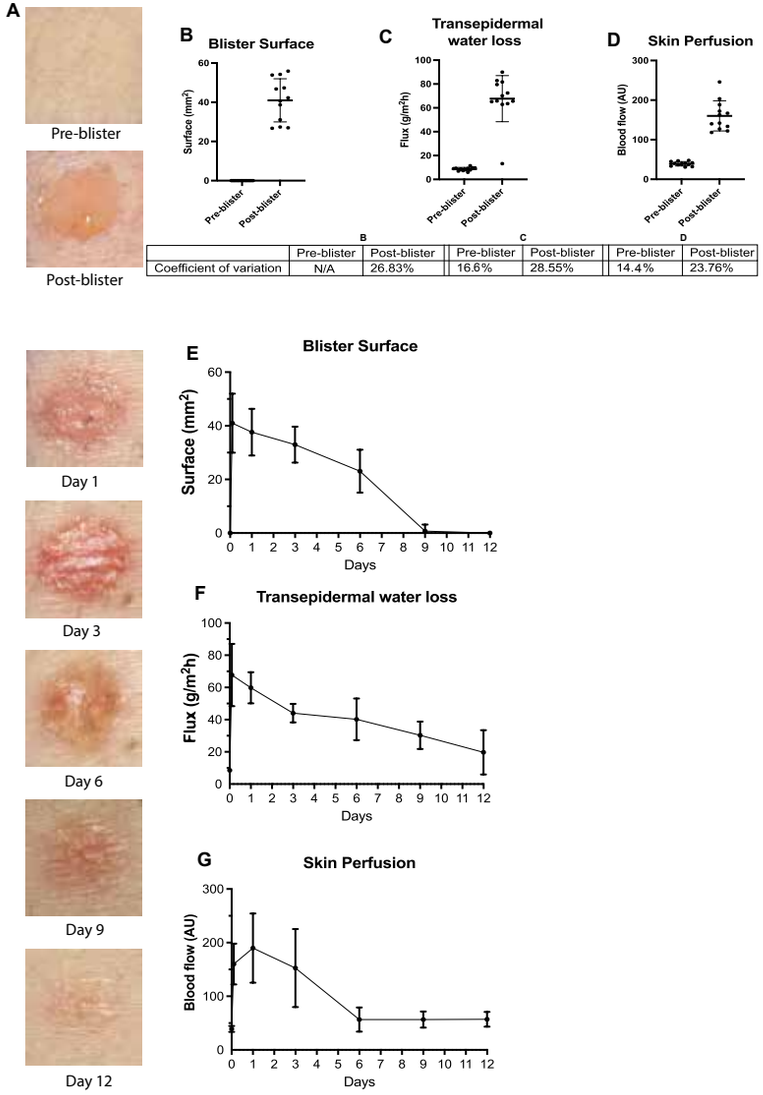

Figure 2 Cross sectional images as measured WITH D-OCT. A) Representative image of skin before blister induction. B) Representative image of skin after blister induction. Distinct anatomical structures are displayed in the image.

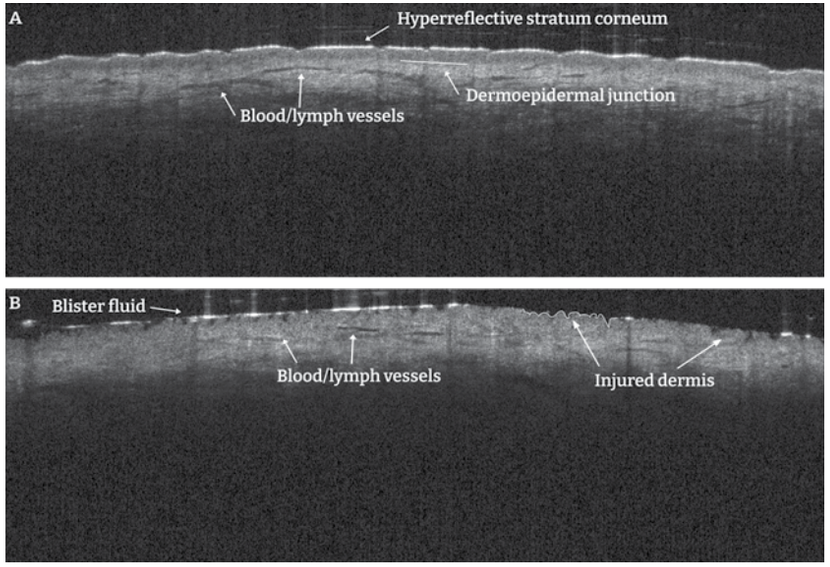

Skin perfusion as measured with D-OCT is displayed in Figure 3D. An increase in blood flow (AU) was observed directly after blister induction from approximately 25 AU to 90-115 AU. Perfusion of the skin returned to the baseline status within 5 days of treatment for all treatment arms. It recovered significantly faster after treatment with HD INM-755 (contrast HD INM-755 versus vehicle (p=0.0139, difference: -15.3%, (95%CI: -25.5%, -3.8%)), contrast HD INM-755 versus untreated (p=0.0437, difference: -12.6%, (95%CI: -23.2%, -0.4%)).

Figure 4 depicts the quantity (ng/mL) of all six biomarkers collected over time. In the statistical model, time was a significant (p<0.05) predictor for all tested cytokines except IL-1RA. VEGF was not analyzed statistically because of too many samples below level of quantification (BLOQ). Data BLOQ has been set at ½ of LLOQ value for the graph. No significant treatment effects were observed for IL-1RA, IL-8, MMP-9, and TIMP-2. However, a significant difference was found for TIMP-1 between the untreated blister wounds and the blisters treated with LD INM-755 (p=0.0085, difference -0.121, 95%CI: -0.207, -0.035). Throughout the healing process, the untreated wounds contained higher levels of TIMP-1.

Figure 3 A) Wound healing progression displayed per treatment arm over time. Images shown are from a single subject B-D) Erythema, TEWL, and Skin perfusion displayed over time, respectively. All data displayed are mean +- SD, n=8.

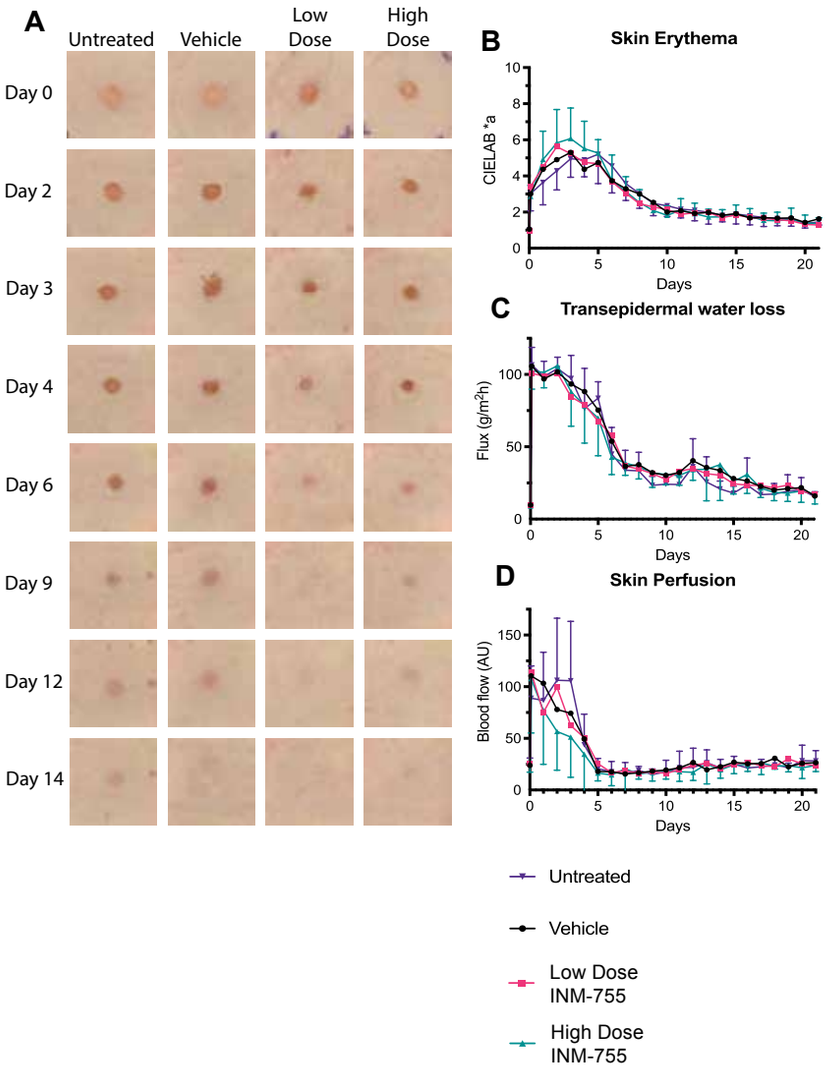

LTA scores for all four parameters tested are presented in Figure 5A-D. Of the four potential local reactions (erythema, oedema, scaling, stinging/burning) scored in the LTA, erythema was the most reported in the study. Oedema and stinging/burning were only reported sporadically. Scaling of the skin occurred throughout the study without a relationship to drug doses. No clear difference between treatments was observed in the LTA scoring.

RYB scores (Figure 5E) show that only red wounds were present, and that wound disappearance took longer for untreated blister wounds. Humidity scores ranged from dry to wet with an emphasis on dry wounds 8-9 days after wounding for treated wounds (LD INM-755, HD INM-755, and vehicle) and 11 days for untreated wounds.

Figure 4 Concentration of exploratory biomarkers displayed over time in days. All data are displayed in mean +- SD. Data plotted in Figure 4F (VEGF) included data points set at ½ LLOQ.

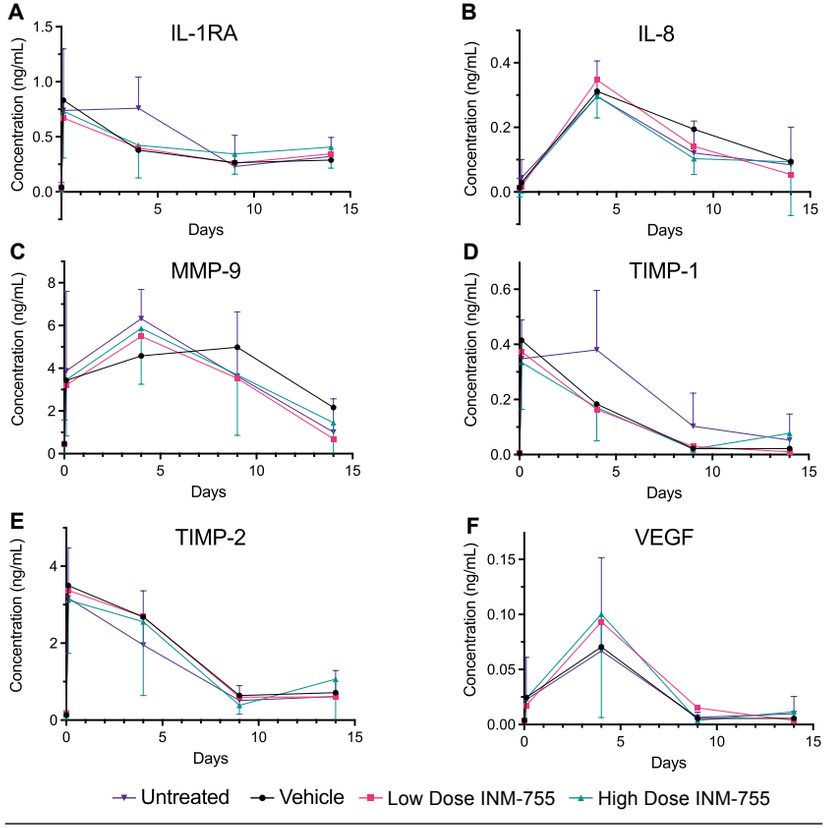

Figure 5 A-D) Local Tolerability Assessment plotted per parameter over time. E) Red-Yellow-Black score displayed per treatment arm over time. All data are displayed in percentages of total, n=8.

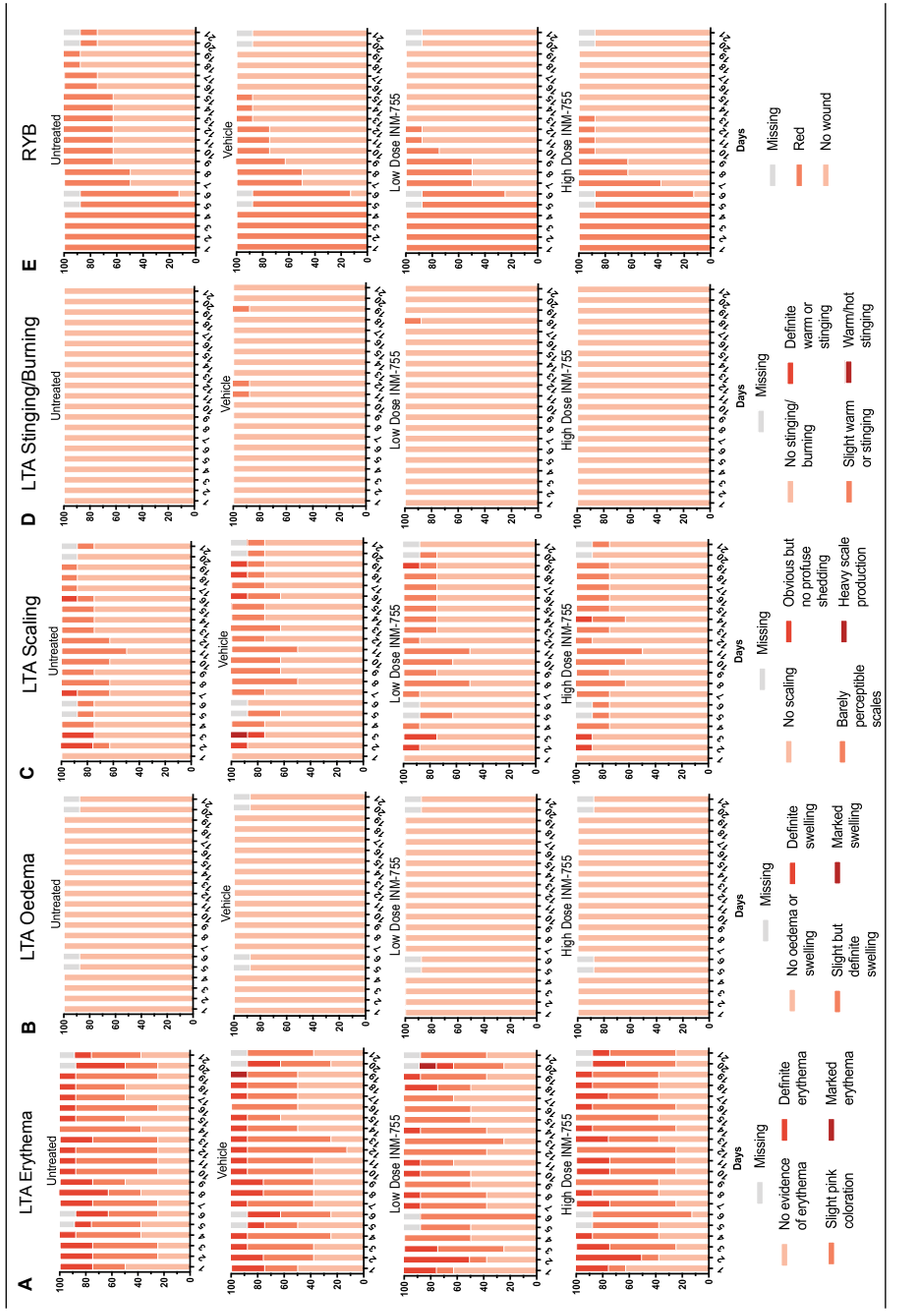

DISCUSSION

In these studies, we aimed to develop a novel epidermal wound healing model suitable for the comprehensive characterization of epidermal wound healing and testing of the efficacy of novel therapeutics in healthy volunteers. We successfully created an epidermal wound healing model based on suction blisters. The findings of the observational study indicate that the creation of blisters using under pressure devices was achievable in all subjects, and we demonstrated that the epidermal sheet could successfully be removed. With an acceptable coefficient of variation in all tested methodologies and detectable differences over time, the model was considered feasible to be used for the extensive characterization of wound healing and to test the effects of INM-755 in healthy volunteers.

In the first, i.e. observational, study we showed that a combination of several state-of-the art imaging techniques allows for better and quantitative assessment over time with high specificity to detect small physiological differences, compared to visual assessments of wound closure often used as pharmacodynamic endpoint in later phase clinical trials and in clinical practice.[20] By using D-OCT, TEWL, and 3D photography, we were able to follow normal epidermal wound healing and quantify skin perfusion, barrier function, and wound closure. Interestingly, wound closure was complete within the follow-up period based on 3D imaging and visual inspection. TEWL and skin perfusion, however, did not return to baseline within the observational period indicating that skin restoration was not entirely complete at the end of the study (Day 12). This is in line with previous research showing that skin barrier function requires approximately 4 weeks to return to baseline.[12,21] This finding indicates that when relying on visual examination and clinical imaging, there is a tendency to suggest that the wound has completely healed, despite other wound healing parameters not having fully returned to their baseline levels.

By using the suction blister model, we were able to investigate the effects of INM-755 in healthy volunteers and found differences in erythema for treated (including vehicle treatment) versus untreated blister wounds. Treated wounds seemed to be more erythematous than untreated wounds, as quantified with multispectral imaging (high standard deviation). Notably, the untreated blister exhibited higher perfusion levels in the initial post-wounding days when compared to treated blisters. However, this pattern is reversed for skin erythema. Given the strong correlation between erythema and perfusion in biological processes, it is implausible that the difference is attributed to treatment effects and could potentially be caused by artefacts. One possible explanation is that differences can be explained by interference of the creams, given that both devices employ different methods of detection (color versus laser). Back reflectance or absorption of the light coming from the multispectral camera might have caused differences in detection.

Although 3D imaging proved to be a valuable tool in wound assessment, it also has its limitations. In the interventional study, a technical malfunction resulted in faulty analysis and thus data was not included in this article. In combination with the need for trained operators and analysts, the technique is not easily implemented in standard clinical care.

In the interventional study the skin barrier of all treated (including vehicle treatment) blisters recovered faster than those of untreated blisters, as determined by TEWL. The difference in moistness, i.e. a higher water content of the wounds, due to application of the cream, could have contributed to this finding. Furthermore, it is known from literature that moist wounds close and return to baseline status quicker, which is in line with the results of earlier studies.[22–24] Although some literature suggests that TEWL is not a useful tool in wound healing studies due to wound secretion, our previous study and the current study showed that TEWL can detect changes in water loss even when crust or skin debris is present.[12,25] Especially in bullous diseases, this is useful considering the moist and disrupted environment.

Biomarkers were successfully captured through the exploratory FibroTx biomarker analysis in our wound healing model. Of all tested biomarkers, IL-8, MMP-9, TIMP-1, and TIMP-2 showed significant differences over time, demonstrating a link with wound healing. MMP-9 was directly elevated after wounding in all treatment arms without difference between treatments. The elevation of MMP-9 directly after wounding is in line with literature suggesting a role in cell migration early in the inflammation phase.[26] Interestingly, TIMPs were also increased directly after wounding but returned to baseline quicker than MMP-9, which even continued to increase up to Day 4. Considering the function of TIMPs, it is interesting to see MMP-9 continuing to rise over time, even with elevated TIMP levels. IL-8 was not elevated directly after wounding but showed a maximum response on Day 4. Elevated IL-8 after wounding was expected, considering the strong chemoattractant for leucocytes.[27] VEGF is known to be involved in stimulating vascular permeability, resulting in recruitment of inflammatory cells,[28] aligning with our observations: we noticed a tendency for VEGF levels to rise in all treatment groups during the initial inflammation phase and then return to normal within two weeks post-injury. However, it's crucial to note that the reliability of our VEGF data was limited due to numerous values being below the limit of quantification (BLOQ), preventing us from conducting statistical analyses. Although IL-1RA did not significantly change over time using the statistical model, visual inspection of the figure shows separation between

treated blisters and untreated blisters on Day 4. From literature it is known that IL-1RA has a predominant role in the early phase of wounding and it could be that IL-1RA levels were even more increased in the initial 3 days, and that the increase observed on Day 4 is already a decline in elevation.[29]

One constraint in this study involves using diverse imaging techniques at varying time points in both the observational and interventional study. This precludes a direct comparison of findings between the two studies, even though such a comparison was not the main objective of our research. With the interventional study, we generated proof-of-concept for the developed wound healing model enabling us to explore the impact of INM-755 by assessing wound healing parameters.

Considering quantitative endpoints in early-phase clinical drug development, local tolerability assessments scored the progression of wound healing with little specificity. Although the assessment was included in the study as a safety measure for treatment with INM-755 and not a pharmacodynamic endpoint, it did give insight into erythema of blister wounds. The discrete nature of the scoring system does not allow for advanced statistics or nuances between wounds and no statistical differences were found. Based on LTA alone, no erythema differences in treatment arms could be identified, whereas with clinical imaging we were able to quantitatively describe differences in wound erythema over time as well as detect a small trend towards separation between treatment arms.

Although these two studies are a first step toward an epidermal wound model in healthy volunteers, the question remains whether the blisters in the model sufficiently mimic EB blisters. From literature, blisters are created at the dermal-epidermal junction, in line with the most prevalent types of EB.[30] However, these blisters are formed using force and trauma, whereas EB blisters are formed because of lack of cell adhesion. This difference in creation plus the different expression of keratin and MMP, might cause differences in the inflammation profile as well as the anatomical outlook. Furthermore, in this study, we removed the blister roof to administer INM-755 on open wounds, whereas in EB treatment, the epidermal sheet is not always removed because of the risk of infection. Lastly, anatomical location of wounds contributes to the time to healing and chance of infection.[31–33] Next to that, the disposition of immune cells differ across body locations and thereby influence the healing process. Lastly, the selected location of the wound in combination with practical challenges with the under-pressure blister device and application on the skin impacts the blister formation process dependent on location. The epidermal wound healing model used in this research was conducted on the lower back, so caution should be taken when extrapolating these findings to other anatomical sites.

Over the years, several techniques have been developed to induce partial thickness wounds,[34] and the development of imaging methodologies to measure skin responses has been progressing in parallel.[35] Compared to other partial thickness models (e.g. tape stripping, abrasion, laser-induced wounds, split thickness) skin blister methodology as used in this study is time consuming and requires a complete seal and constant under-pressure. The procedural challenges make it difficult to draw blisters on certain body areas and movement of a subject can cancel under-pressure. In general, the selection of a partial thickness wound healing model should be based on the goal of the study and be as representative of the disease as possible.

Although there are limitations to the model regarding comparability to EB and differences among anatomical sites, the setup of these models can help in development of therapies targeting chronic and epidermal wound diseases. Bullous diseases are known to be rare and inclusion of patients in a clinical study is therefore difficult. By using a wound healing model in healthy volunteers, an early signal of efficacy can be found without the need for big multicentre clinical trials including a hand-full of patients.

Altogether, this study demonstrates the effective establishment of an epidermal wound healing model, providing robust groundwork for subsequent explorations into the wound healing process. With its capacity to monitor changes over time and discern variations between treatments, this model serves as a dynamic tool for assessing the effectiveness of novel treatments within the realm of wound healing.

REFERENCES

1 Guo S, Dipietro LA. Factors affecting wound healing. J Dent Res. 2010;89(3):219-229. doi:10.1177/0022034509359125

2 Gonzalez ACDO, Andrade ZDA, Costa TF, Medrado ARAP. Wound healing - A literature review. An Bras Dermatol. 2016;91(5):614-620. doi:10.1590/abd1806-4841.20164741

3 Velnar T, Bailey T, Smrkolj V. The wound healing process: An overview of the cellular and molecular mechanisms. J Int Med Res. 2009;37(5):1528-1542. doi:10.1177/147323000903700531

4 Hou PC, Wang HT, Abhee S, Tu WT, McGrath JA, Hsu CK. Investigational Treatments for Epidermolysis Bullosa. Am J Clin Dermatol. 2021;22(6):801-817. doi:10.1007/S40257-021-00626-3

5 Han G, Ceilley R. Chronic Wound Healing: A Review of Current Management and Treatments. Adv Ther. 2017;34(3):599. doi:10.1007/S12325-017-0478-Y

6 Shaabani E, Sharifiaghdam M, Faridi-Majidi R, De Smedt SC, Braeckmans K, Fraire JC. Gene therapy to enhance angiogenesis in chronic wounds. Mol Ther Nucleic Acids. 2022;29:871. doi:10.1016/J.OMTN.2022.08.020

7 Eming SA, Krieg T, Davidson JM. Gene Therapy and Wound Healing. Clin Dermatol. 2007;25(1):79. doi:10.1016/J.Clindermatol.2006.09.011

8 Prodinger C, Reichelt J, Bauer JW, Laimer M. Epidermolysis bullosa: Advances in research and treatment. Exp Dermatol. 2019;28(10):1176-1189. doi:10.1111/EXD.13979

9 Pastar I, Wong LL, Egger AN, Tomic-Canic M. Descriptive vs mechanistic scientific approach to study wound healing and its inhibition: Is there a value of translational research involving human subjects? Exp Dermatol. 2018;27(5):551. doi:10.1111/EXD.13663

10 Brölmann FE, Eskes AM, Sumpio BE, et al. Fundamentals of randomized clinical trials in wound care: Reporting standards. Wound Repair Regen. 2013;21(5):641-647. doi:10.1111/WRR.12087

11 Masson-Meyers DS, Andrade TAM, Caetano GF, et al. Experimental models and methods for cutaneous wound healing assessment. Int J Exp Pathol. 2020;101(1-2):21-37. doi:10.1111/iep.12346

12 Ten Voorde W, Saghari M, Boltjes J, et al. A multimodal, comprehensive characterization of a cutaneous wound model in healthy volunteers. Exp Dermatol. 2023;32(7):1028-1041. doi:10.1111/exd.14808

13 Wilhelm KP, Wilhelm D, Bielfeldt S. Models of wound healing: an emphasis on clinical studies. Ski Res Technol. 2017;23(1):3-12. doi:10.1111/SRT.12317

14 Prodinger C, Reichelt J, Bauer JW, Laimer M. Epidermolysis bullosa: Advances in research and treatment. Exp Dermatol. 2019;28(10):1176-1189. doi:10.1111/exd.13979

15 Lettner T, Lang R, Klausegger A, Hainzl S, Bauer JW, Wally V. MMP-9 and CXCL8/IL-8 Are Potential Therapeutic Targets in Epidermolysis Bullosa Simplex. PLoS One. 2013;8(7):e70123. doi:10.1371/Journal.pone.0070123

16 Rijsbergen M, Pagan L, Niemeyer-van der Kolk T, et al. Stereophotogrammetric three-dimensional photography is an accurate and precise planimetric method for the clinical visualization and quantification of human papilloma virus-induced skin lesions. J Eur Acad Dermatology Venereol. 2019;33(8):1506-1512. doi:10.1111/JDV.15474

17 Jacobse J, ten Voorde W, Tandon A, et al. Comprehensive evaluation of microneedle-based intradermal adalimumab delivery vs. subcutaneous administration: results of a randomized controlled clinical trial. Br J Clin Pharmacol. 2021;87(8):3162-3176. doi:10.1111/BCP.14729

18 Saghari M, Gal P, Ziagkos D, et al. A randomized controlled trial with a delayed-type hypersensitivity model using keyhole limpet haemocyanin to evaluate adaptive immune responses in man. Br J Clin Pharmacol. 2021;87(4):1953-1962. doi:10.1111/BCP.14588

19 Shechtman O. The Coefficient of Variation as an Index of Measurement Reliability. Published online 2013:39-49. doi:10.1007/978-3-642-37131-8_4

20 Wei EX, Kirsner RS, Eaglstein WH. End points in dermatologic clinical trials: A review for clinicians. J Am Acad Dermatol. 2016;75(1):203-209. doi:10.1016/j.jaad.2016.01.052

21 Kottner J, Hillmann K, Fimmel S, Seité S, Blume-Peytavi U. Characterisation of epidermal regeneration *in vivo*: a 60-day follow-up study. J Wound Care. 2013;22(8):395-400. doi:10.12968/JOWC.2013.22.8.395

22 Dyson M, Young S, Pendle CL, Webster DF, Lang SM. Comparison of the effects of moist and dry conditions on dermal repair. J Invest Dermatol. 1988;91(5):434-439. doi:10.1111/1523-1747.EP12476467

23 Oudshoorn MHM, Rissmann R, van der Coelen D, Hennink WE, Ponec M, Bouwstra JA. Effect of synthetic vernix biofilms on barrier recovery of damaged mouse skin. Exp Dermatol. 2009;18(8):695-703. doi:10.1111/J.1600-0625.2009.00858.X

24 Oudshoorn MHM, Rissmann R, Van Der Coelen D, Hennink WE, Ponec M, Bouwstra JA. Development of a murine model to evaluate the effect of vernix caseosa on skin barrier recovery. Exp Dermatol. 2009;18(2):178-184. doi:10.1111/J.1600-0625.2008.00780.X

25 Alborova A, Lademann J, Kramer A, et al. *In vivo* analysis of wound healing by optical methods. GMS Krankenhhyg Interdiszip. 2008;3(1):Doc10. Accessed February 14, 2024. /pmc/articles/PMC2831523/

26 Kandhwal M, Behl T, Singh S, et al. Role of matrix metalloproteinase in wound healing. Am J Transl Res. 2022;14(7):4391. doi:10.31838/ijpr/2020.SP2.087

27 Rennekampff HO, Hansbrough JF, Kiessig V, Doré C, Sticherling M, Schröder JM. Bioactive Interleukin-8 Is Expressed in Wounds and Enhances Wound Healing. J Surg Res. 2000;93(1):41-54. doi:10.1006/JSRE.2000.5892

28 Johnson KE, Wilgus TA. Vascular Endothelial Growth Factor and Angiogenesis in the Regulation of Cutaneous Wound Repair. Adv Wound Care. 2014;3(10):647. doi:10.1089/WOUND.2013.0517

29 Macleod T, Berekmeri A, Bridgewood C, Stacey M, McGonagle D, Wittmann M. The Immunological Impact of IL-1 Family Cytokines on the Epidermal Barrier. Front Immunol. 2021;12. doi:10.3389/FIMMU.2021.808012

30 Vukmanovic-Stejic M, Agius E, Booth N, et al. The kinetics of CD4+Foxp3+ T cell accumulation during a human cutaneous antigen-specific memory response *in vivo*. J Clin Invest. 2008;118(11):3639. doi:10.1172/JCI35834

31 Bischoff M, Kinzl L, Schmelz A. The complicated wound. Unfallchirurg. 1999;102(10):797-804. doi:10.1007/S001130050483

32 Degreef HJ. How to heal a wound fast. Dermatol Clin. 1998;16(2):365-375. doi:10.1016/S0733-8635(05)70019-X

33 Tahir Mahmood D, Kareem Qadir H, Mohammed Hussein M. Relationship between Characteristics of the Wound and Healing Duration among Patients Treated during Home-Visits. Arch Razi Inst. 2023;78(4):1323-1332. doi:10.32592/ARI.2023.78.4.1323

34 Wilhelm KP, Wilhelm D, Bielfeldt S. Models of wound healing: an emphasis on clinical studies. Ski Res Technol. 2017;23(1):3-12. doi:10.1111/SRT.12317

35 Gaurav V, Agrawal S, Najeeb A, Ahuja R, Saurabh S, Gupta S. Advancements in Dermatological Imaging Modalities. Indian Dermatol Online J. 2024;15(2):278. doi:10.4103/IDOJ.IDOJ_852_23

SECTION II

PHARMACODYNAMICS AND PHARMACOLOGICAL CHALLENGES

CHAPTER IV

INTRADERMAL SUBSTANCE P AS A CHALLENGE AGENT IN HEALTHY INDIVIDUALS

Published in the Journal of Clinical and Translational Science, 2023

Wouter ten Voorde[1,2,*], Chika Akinseye[3,*], Ismahaan Abdisalaam[1,4], Selinde Wind[1,2], Naomi Klarenbeek[1], Menthe Bergmans[1,4], Martijn van Doorn[1,4], Robert Rissmann[1,2,5], Rejbinder Kaur[3], Sarah Hotee[3], Katie Foster[3], Arati Nair[6], Lea Fortunato[3], Colin Macphee[3], Sarah Mole[3], Katrine Baumann[7], Richard Brigandi[8] **Shared first authorship*

1 Centre for Human Drug Research, Leiden, NL
2 Leiden University Medical Center, Leiden, NL
3 GSK, Stevenage, UK
4 Department of Dermatology, Erasmus Medical Center, Rotterdam, NL
5 Leiden Academic Centre for Drug Research, Leiden, NL
6 GSK, Karnataka, India
7 RefLab ApS, Copenhagen, DENMARK
8 GSK, Philadelphia, Pennsylvania, USA

ABSTRACT

Pharmacological challenge models are deployed to evaluate drug effects during clinical development. Intradermal injection of Substance P (SP) neuropeptide, a potential challenge agent for investigating local mediators, is associated with wheal and flare response mediated by the MRGPRX2 receptor. Although dose-dependent data on SP effects exist, full characterization and information on potential carryover effect after repeated challenge are lacking. This open-label, two-part, prospective enabling study of SP intradermal challenge in healthy participants aimed to understand and distinguish between wheal and flare responses following various SP doses. Part 1 included one challenge visit to determine optimum SP dose range for evaluation in part 2, which determined variability in 20 participants and used intradermal microdialysis (IDM) for SP-challenged skin sampling. At 5, 15, 50, and 150 PMOL doses, respectively, posterior median area under the curve (AUC; AUC_{0-2h}) was 4090.4, 5881.2, 8846.8, and 9212.8 mm^2/min, for wheal response, and 12020.9, 38154.3, 65470.6, and 67404.4 mm^2/min for flare response (SP-challenge visit 2). When the challenge was repeated 2 weeks later, no carryover effect was observed. IDM histamine levels were relatively low, resulting in low confidence in the data to define temporal characteristics for histamine release following SP challenge. No safety concerns were identified using SP. Wheal and flare responses following intradermal SP challenge were dose-dependent and different. The results indicate that this challenge model is fit-for-purpose in future first-in-human studies and further assessment of novel drugs targeting dermal inflammatory disease responses, such as chronic spontaneous urticaria, chronic inducible urticaria, and pseudo-allergic reactions.

INTRODUCTION

Substance P (SP) is a neuropeptide that acts on mast cells in the skin, resulting in neurogenic inflammation[1] primarily through activation of mast cells via the Mas-related G-protein coupled receptor X2 (MRGPRX2) and neurokinin 1 receptor on endothelial cells.[2,3,4,5] Mast cell degranulation is the key pathophysiological event in diseases, including chronic spontaneous urticaria, chronic inducible urticaria, and pseudo-allergic reactions.[6,7,8] Although there are several other challenges available that are associated with MRGPRX2 signalling, such as somatostatin, proteases such as cathepsin S, and antimicrobial peptide insulin-like growth factor-binding protein 5 (AMP-IBP5), previous studies have demonstrated that SP plays a role in neurogenic inflammation and pain associated with wound healing.[8,9,10,11] A high-affinity MRGPRX2 antagonist has yet to be developed.[12]

SP is upstream in the inflammatory response signalling cascade and may be a useful challenge agent for the investigation of locally acting mediators in some settings.[3,13] Challenge models mimic pharmacologically induced conditions, providing a valuable tool to assess an inflammatory response in healthy human volunteers and analyse the potential efficacy of drugs in development before going to patient populations.[5,14,15,16] Increasing doses of SP via intradermal injection are associated with an increased wheal and flare response,[9,10,11] as well as intradermal release of several inflammatory mediators, such as histamine and tryptase. Histamine can be used as an active control versus SP, as histamine is an agent known to produce wheal and flare responses.[5] Although dermal challenges with SP are available and date back to the 1970s,[17] a detailed understanding of the effect of increasing SP dose on wheal and flare, characterization of doses over multiple timepoints, and histamine response, are lacking. There are no published results of pharmaceutical agents tested with this model as of yet.[10] Optimizing the intradermal challenge model will facilitate future clinical and pharmacological evaluation of antagonists to block or decrease the induced wheal and flare response. Novel compounds targeting MRGPRX2 would be one potential application. In addition, to our knowledge, the test–retest variability as well as potential for carryover of effect following repeated SP challenge has not previously been reported.

The aim of the current study was to elucidate the robustness of SP response by evaluating the effect of various SP doses on wheal and flare as end points related to MRGPRX2 receptor-mediated mast cell degranulation. MRGPRX2 is exclusively expressed on mast cells, is responsible for non-IGE-mediated mast cell activation, and has affinity for many molecules, including SP and various drugs.[8,18] As such, an SP challenge model may be used to evaluate drugs for inhibition of the MRGPRX2 pathway, which are designed to treat non-IGE-mediated diseases.

The study was conducted in two parts: the objective of part 1 was to select the correct SP doses suitable for further investigation in part 2. In this paper, the results of part 2 of the study will be explored in detail, with part 1 data outlined in the Supplement. In part 2, the effect of the SP dose on wheal and flare response was evaluated at two consecutive challenge visits. Intradermal microdialysis (IDM) was also performed in part 2 of the study. IDM involves the insertion of dialysis membranes into the dermis, which is then perfused at a low speed with the perfusate. Endogenous or exogenous molecules soluble in the extracellular fluid diffuse into the membrane and are then collected in small vials for analysis. By means of this technique, continuous sampling of interstitial fluid from SP-challenged skin is possible and allows for evaluation of an effect-time relationship.[17] Overall, this study aimed to develop an SP challenge model that is fit-for-purpose for future studies and to understand the mechanistic pathways downstream of SP activation.

MATERIALS AND METHODS

STUDY DESIGN

This was a single-center, two-part, prospective enabling study of SP intradermal challenge in healthy participants conducted between February and March 2021. An open-label design was chosen for operational considerations and because the main read-outs of wheal and flare were determined by the calliper method. The study was registered at ClinicalTrials.gov with the identifier NCT04676763; the study protocol was approved by the Ethics Committee of the Stichting Beoordeling Ethiek Biomedisch Onderzoek.

Parts 1 and 2 were conducted sequentially. In part 1 (Figure 1A), participants attended one challenge visit as outpatients, and in part 2 (Figure 1B), participants attended two challenge visits as outpatients and had one follow-up phone call. From screening to last follow-up visit, the duration of part 1 was up to 4 weeks, and the duration of part 2 was up to 7 weeks.

The intradermal SP challenge was administered sequentially from the lowest to the highest dose, as 5, 15, 50, and 150 PMOL SP, respectively, at a volume of 50 µL. The SP doses were in line with previously published research;[10] we aimed to establish a dose–response relationship, therefore a 30-fold difference was selected for this study.

At each challenge visit, participants first received saline by intradermal injection, and histamine by skin prick, as negative and positive controls, respectively. The participant received SP if the wheal response met the acceptable saline and histamine response criteria, 20 min after each control challenge. The standardized interval of 20 min ensured that delayed responders could still participate, given that the effects of histamine are short-lived.[19,20] The acceptable responses were defined as saline wheal less than or equal to 1 mm or histamine wheal greater than or equal to 3 mm, primarily measured using the longest diameter of the wheal by callipers, which were readily available to clinical study sites for standard use. Following confirmation of acceptable saline and histamine control responses, participants received up to four intradermal injections of SP at different doses.

Figure 1 Study design. IDM, intradermal microdialysis; SP, substance P. *Asterisks refer to the positive histamine control that were performed at the back for the thigh. Figure was created using BioRender.com.

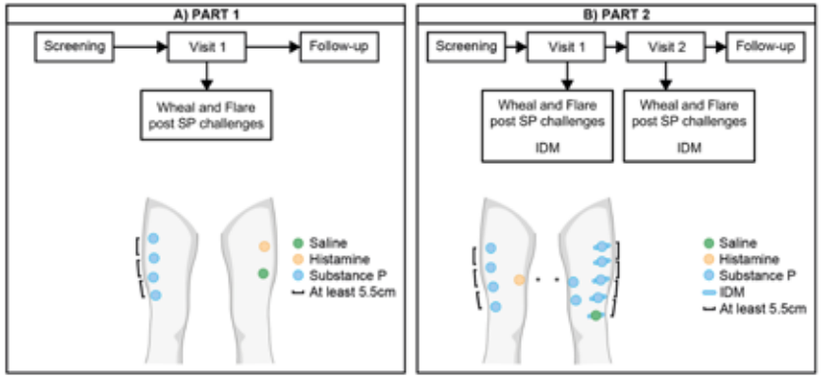

During part 2 of the study, participants also underwent IDM, which comprised an additional single injection of saline and four increasing doses of SP like those used in the flare and wheal challenges. IDM probes were inserted intradermally in the skin of the upper leg of participants (Figure 1B). In total, ~450 µL of dialysate was collected from each probe to measure histamine content in each participant. The IDM probes were inserted at least 2 h before the baseline sampling to reduce IDM procedure-induced wheal and/or flare. IDM samples were taken at the challenge site, before and after each challenge. The samples were taken up to 120 min post-SP challenge, however, an interim analysis on the first eight participants determined that samples taken past 30 min reached below the lower limit of quantification (LLOQ) values, and it was therefore decided to only analyse samples up to 40 min post-challenge for the remainder of the participants.

The histamine assay was validated on a fit-for-purpose principle: validation of the exploratory relative quantification of histamine concentration in IDM samples was performed as an extension of previous validation by RefLab ApS

(Copenhagen, Denmark) of their in-house basophil histamine release assay. Extension of the validation for the context of use described here covered the IDM perfusate, IDM probes, and sample stability upon storage conditions required in this study. The LLOQ and upper limit of quantification of the assay were determined during the method validation extension. Data were included in the analysis only if they met predefined acceptance criteria based on variability between replicates and if they measured within the validated range of the assay.

STUDY POPULATION

Participants were recruited via advertisements on social media and a healthy volunteer database at the Centre for Human Drug Research, Leiden, The Netherlands. Eligible participants were men and non-pregnant women, 18–64 years of age, with Fitzpatrick skin type I–II, body weight greater than or equal to 50 kg, and a body mass index within the range of 19.7–29.4 kg/m^2. Participants were required to have a positive response to the histamine skin prick and a negative response to the saline injection at screening. Participants were excluded from the study if they had significant skin-related disorders, skin damage, or other disfiguration (tattoos, body piercings, and branding) on or near the site of application, which could interfere with assessments. Additional exclusion criteria included use of any form of H1 or H2 antihistamines, tricyclic antidepressants, beta-2 agonists, dopamine, or beta-blocking agents within 14 days of the first challenge, and individuals who were at risk or had previously experienced complications from a skin biopsy (including excess bleeding, infection, or scarring/keloid formation). Participants were also ineligible if they used topical medications and were unable to refrain from the use of topical medications from the first to the last challenge visit. Written informed consent was obtained from each participant prior to the performance of any study-specific procedures.

STUDY OUTCOMES

The primary outcome measure was wheal response, which is the area in millimetres squared (mm^2) and was calculated using the formula for an area of ellipse with the longest and orthogonal diameters measured with callipers. The response was summarized in various secondary outcomes: area under the curve (AUC; mm^2/min) during the 2-h post-challenge period at each dose of SP,[21] maximum area of wheal, time taken to observe the maximum wheal area, and time to complete disappearance of wheal. The same secondary outcomes were investigated for flare response during the 2-h post-challenge period. Other secondary outcomes included incidence of adverse events (AEs) and incidence of laboratory or physical findings of clinical importance (including electrocardiogram assessment at screening, baseline, and post-challenge).

STATISTICAL ANALYSIS

Descriptive summaries were calculated for the wheal and flares responses.

The statistical analysis of the SP-induced wheal/flare AUCs was conducted using the SAS software version 9.4 (SAS Institute, USA), using a Bayesian repeated measures model. Point estimates and associated variability were reported as posterior medians and 95% credible intervals.

To assess the dose-dependent response, we calculated the ratio of the SP-induced wheal/flare AUC between two consecutive doses of SP. A ratio exceeding one indicates an increase in the AUC between the two consecutive doses of SP. The confidence associated with this ratio was assessed by calculating the probability of that ratio being above one.

RESULTS

BASELINE CHARACTERISTICS

Overall, 32 participants were enrolled, and 29 participants completed the study: nine participants in part 1 and 20 in part 2. Of the three participants who did not complete the study, two were excluded due to a coronavirus disease 2019 (COVID-19) infection, and one voluntarily chose to withdraw. In total, 20 of 32 (62.5%) participants were women, and the median age (range) of participants was 22 (18–49) years. Additional details of the participant characteristics are presented in Table S1.

WHEAL RESPONSE

SP produced a dose-dependent wheal response in both parts of the study (Table 1), with the posterior median for SP-induced wheal AUC demonstrating a clear distinction between the different doses of SP (Figure 2). Please see Figure S1 and Table S2 for mean wheal AUC following skin challenges for part 1 of the study. In part 2 of the study, during visit one, the range in response was pronounced, with a posterior median that ranged between 4036.7 and 10011.0 mm^2/min, for 5 and 150 PMOL of SP, respectively. A dose-dependent ratio of 1.5 was obtained between SP 15 and 5 PMOL, signifying that the wheal AUC at SP 15 PMOL was 1.5 times higher than the wheal AUC response at SP 5 PMOL (Table 1). At visit two, the range in response was similar to the one observed at visit one: the posterior median ranged between 4090.4 and 9212.8 mm^2/min for SP 5 and 150 PMOL, respectively (Table 1). At both visits, an SP-dependent wheal response was observed with most of the ratios greater than one. Please see Figure S2 for mean wheal AUC following skin challenges with IDM intervention.

Figure 2 Mean wheal AUC following skin challenges (Part 2, non-IDM). AUC, area under the curve; IDM, intradermal microdialysis; min, minutes; SP, substance P.

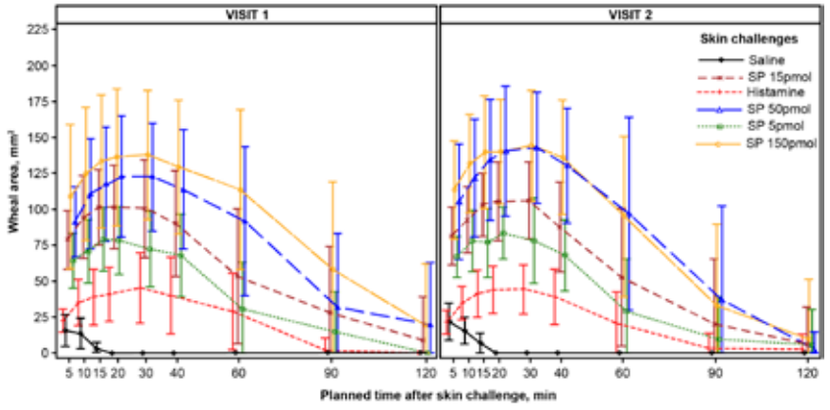

The mean maximum wheal response increased with SP doses in both parts of the study (Figure 2). A summary of wheal responses following skin challenges is provided in Table S3. During part 2, 5 PMOL of SP produced a mean maximum wheal response of 85.8 mm² and 92.2 mm² at visits one and two (at 20 min), respectively; this increased to 148.9 mm² and 153.0 mm², respectively. The mean time taken to achieve maximum wheal area was similar across all SP doses in both parts of the study and ranged from 20.4 to 31.7 min during visit one of part 2 (Table S3). The maximal effect (E_{max}) at 50 PMOL of SP, with a median max area of 141.1 mm², was first observed at visit one during part 2 of the study (Table S3).

The mean time to maximum response during part 2 was similar across visits, ranging from 20.4 to 31.7 min for visit one and 20.9 to 28.3 min for visit two. When time to complete resolution of the wheal was evaluated, it was observed that the wheal area lasted longer with the highest dose of SP (90 min at 150 PMOL). In part 2, at visit one, wheal area in four participants lasted longer than 2 h at SP doses of 50 and 150 PMOL, whereas all wheal responses resolved within 2 h at the lower dosages; a similar trend was observed in part 1 (Table S2). In part 2, the SP-induced wheal responses were similar with and without IDM interventions (Figure 2 and Figure S2).

FLARE RESPONSE

SP produced a dose-dependent flare response, with the posterior median for SP-induced flare AUC demonstrating a distinction between the different doses of SP (Figure 3 and Table 1). See Figure S3 and Table S2 for mean flare AUC following skin challenges for part 1 of the study. In part 2 of the study, during visit one, the variability in response had a posterior median that ranged between 9070.7 and 67260.8 mm²/min, for 5 and 150 PMOL of SP, respectively. At visit two, the variability in response was more pronounced, with a posterior median ranging between 12020.9 and 67494.4 mm²/min, for 5 and 150 PMOL of SP, respectively (Table 1). A dose-dependent AUC ratio of 3.9 and 3.2 was obtained for SP 15 and SP 5 PMOL at visit one and visit two, respectively (Table 1).

Figure 3 Mean flare AUC following skin challenges (Part 2, non-IDM). AUC, area under the curve; IDM, intradermal microdialysis; min, minutes; SP, substance P.

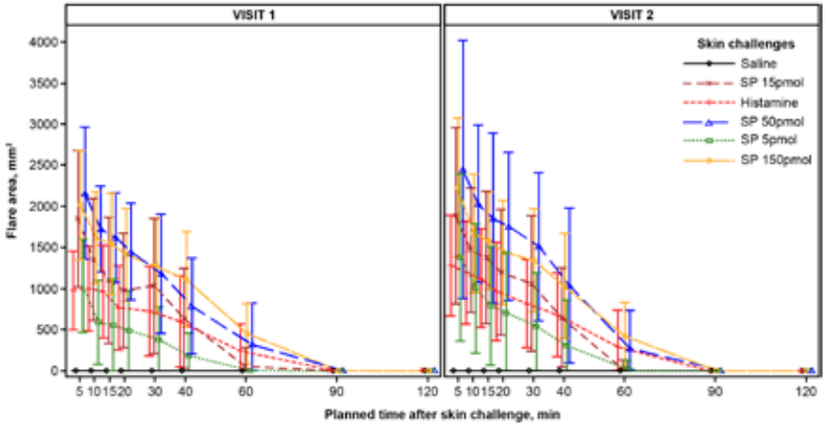

Please see Figure S4 for mean flare AUC following skin challenges with IDM intervention.

SP challenges were associated with a rapid onset of flare response within 5 min after SP administration (Figure 3). For both parts of the study, a dose-dependent flare response was observed between the 5-min and 20-min timepoints with a peak time to maximum response observed between 5 and 10 min (Figure 3 and Table 1). Intra-participant variability in flare response was observed between visits one and two of part 2 of the study, resulting in a difference in mean flare areas being observed between the two visits (Table 1). In both parts of the study, there was a saturation effect at 50 PMOL of SP (E_{max} effect). The IDM interventions did not change SP-induced flare responses, and all flare responses were resolved at the same timepoint of 90 min (Figure 3).

IDM HISTAMINE ANALYSIS

Mean histamine concentrations measured in part 2 IDM samples were detectable 0–30 min following an SP challenge of at least 15 PMOL, with a peak response at 10 min (Figure S5). Histamine concentrations were increased in a dose-dependent manner to SP challenges of 15, 50, and 150 PMOL, although there was variability in response. Histamine levels were not detectable (values below LLOQ, 10 ng/mL) 0–30 min following saline and 5 PMOL of SP. Histamine concentrations were also less than the LLOQ at all timepoints after 30 min for all challenges tested. For the first eight participants included in the interim analysis, there was no measurable histamine following saline and 5 PMOL of SP challenge. At 50 PMOL of SP, there was a relatively small histamine response at 10 and 20 min for a subset of participants at visit two only. A higher proportion of subjects had detectable histamine levels with 150 PMOL of SP challenge in comparison to 50 PMOL (Figure S5).

SAFETY

AEs of mild intensity were experienced by one participant (11%) in part 1 (pruritus) and two participants (10%) in part 2 (headache). The pruritus AE in part 1 was considered SP-related, whereas the AEs in part 2 were considered unrelated to SP administration. No moderate or serious AEs were experienced by any of the participants, and no major safety concerns were observed within the clinical laboratory parameters. In addition, no clinically significant electrocardiogram abnormalities were observed.

DISCUSSION

The time profile of the challenge for wheal and flare responses provides greater insight and characterization of the effect of multiple doses of SP over multiple timepoints, in addition to determining the potential carryover effect following repeated challenge. In this study, lower doses of SP produced dose-dependent wheal and flare responses over the 2-h post-challenge period, as measured by the AUC in both parts of the study with low test–retest variability. The safety and tolerability of the challenge agent was acceptable, with only a small number of mild AEs occurring. These findings are consistent with a previous study, which looked at the effect of SP on wheal and flare on human skin.[2] The large maximum wheal response of 153 mm^2 increased with increasing doses of SP, and wheal response lasted only 90 min with the highest SP dose.

Wheal and flare reactions can be induced by SP through intradermal injection or skin prick testing. Antihistamines can suppress these reactions, suggesting SP activates skin mast cells to release histamine.[22] In a study by Fujisawa et al. using skin-derived cultured mast cells, the MRGPRX2 receptor was found to be responsible for histamine release induced by SP instead of the traditional SP receptor NK-1R.[23] The present study sought to determine the dose–response and the robustness of the SP challenge model, by assessing the effect of ascending dose of intradermal SP on wheal and flare responses in healthy participants. This study also aimed to establish and validate an SP intradermal challenge model to allow the future clinical evaluation of the pharmacological ability of MRGPRX2 receptor antagonists to block or decrease the induced wheal and flare response; in a single- or multiple-ascending-dose trial, the challenge would be used to demonstrate functional target engagement in humans.[24]

The study was designed to determine the potential carryover of effect and the outcome. Wheal and flare responses following intradermal challenge with increasing doses of SP were found to differ, and limited carryover of effect was observed following repeated challenge: baseline visits were comparable between visit one and visit two and no differences were observed before dosing. The SP challenge model does not represent a disease model, but a pharmacological model that can establish engagement and proof-of-pharmacology in a first-in-human setting. This supports the potential use of the challenge model in future clinical assessment of novel pharmacological agents that antagonize the induced wheal and flare response, for example, during future clinical assessments of novel agents in healthy volunteers before evaluation in patients with diseases such as chronic spontaneous urticaria, rosacea, and atopic dermatitis, caused by activation of MRGPRX2 receptor.[25] Other examples of pharmacological intradermal challenge models include the histamine challenge model, the imiquimod model and the lipopolysaccharide model of inflammation.[15,26,27] In the current study, the SP challenge model was characterized and the results can be assessed as fit-for-purpose validation of this method.[28]

Our study also evaluated flare responses and demonstrated that SP challenges produced a dose-dependent flare response; flare response lasted longest (between 5 and 10 min) with the highest dose of SP. The results are supported by previous findings, in which SP was observed to induce a dose-dependent wheal and flare for the lower doses.[2,10,29,30]

Notably, our findings show an E_{max} at SP 50 PMOL in the first challenge visit. Further, we found that there was variability in both the wheal and the flare AUCs observed with different doses. A dose-dependent flare response was observed between the 5- and 20-min timepoints, which coincided with findings from the published literature: response during the first 5 min was reported to be the most reproducible period to assess the inflammatory response.[31]

For the majority of participants, responses disappeared within 2 h following SP administration. Only a few lasted longer, and individuals with longer-lasting

responses were excluded from the analysis. However, it must be noted that this analysis was conducted with a small number of participants, and it is unclear if similar trends would manifest in larger studies. Nonetheless, the relatively small sample size in the present study was similar to that utilized in a prior challenge study,[31] and suggests that the skin challenge is suitable for small cohorts in the early phases of clinical development. One could argue that this study may have been limited by its open-label design; however, controlling for the risk of bias was not required for this type of design and appropriate within-subject controls were used.

Our study showed that IDM interventions did not change SP-induced wheal and flare responses, and this further supports the use of the SP model. The concentration of histamine in the clinical samples, released in response to SP challenge, was lower than expected based on previous findings.[32] These relatively low concentrations of histamine may have been due to a rapid local clearance of histamine in the skin after the mediator was released from the skin mast cells. This hypothesis was consistent with the often rapid decline in histamine concentrations observed when two consecutive samples from the same probe were positive, that is, above the LLOQ. This rapid clearance of histamine following SP challenge in skin has previously been reported,[32] similarly with a peak response measured up to 10 min.

In conclusion, we demonstrate that a pharmacological model with SP in healthy participants should be considered for proof-of-pharmacology analyses in first-in-human studies. The use of SP in a challenge study could enable researchers to investigate the release of locally acting mediators, in addition to immune cell markers.

REFERENCES

1 Mashaghi A, Marmalidou A, Tehrani M, Grace PM, Pothoulakis C, Dana R. Neuropeptide substance P and the immune response. Cell Mol Life Sci. 2016;73:4249-4264. doi: 10.1007/s00018-016-2293-z

2 Foreman JC, Jordan CC, Oehme P, Renner H. Structure-activity relationships for some substance P-related peptides that cause wheal and flare reactions in human skin. J Physiol. 1983;335:449-465. doi: 10.1113/jphysiol.1983.sp014543

3 Chompunud Na Ayudhya C, Amponnawarat A, Ali H. Substance P serves as a balanced agonist for MRGPRX2 and a single tyrosine residue is required for β-arrestin recruitment and receptor internalization. Int J Mol Sci. 2021;22:5318. doi: 10.3390/ijms22105318

4 Siiskonen H, Harvima I. Mast cells and sensory nerves contribute to neurogenic inflammation and pruritus in chronic skin inflammation. Front Cell Neurosci. 2019;13:422. doi: 10.3389/fncel.2019.00422

5 Andersen HH, Elberling J, Arendt-Nielsen L. Human surrogate models of histaminergic and non-histaminergic itch. Acta Derm Venereol. 2015;95:771-777. doi: 10.2340/00015555-2146

6 Dobrican C-T, Muntean IA, Pintea I, Petricău C, Deleanu DM, Filip GA. Immunological signature of chronic spontaneous urticaria. Exp Ther Med. 2022;23:1-7. doi: 10.3892/etm.2022

7 Terhorst-Molawi D, Hawro T, Grekowitz E, et al. Anti-KIT antibody, barzolvolimab, reduces skin mast cells and disease activity in chronic inducible urticaria. Allergy. 2022;78:1269-1279. doi: 10.1111/all.15585

8 Kumar M, Duraisamy K, Chow B-K. Unlocking the non-IgE-mediated pseudo-allergic reaction puzzle with mas-related G-protein coupled receptor member X2 (MRGPRX2). Cells. 2021;10:1033. doi: 10.3390/cells10051033

9 Borici-Mazi R, Kouridakis S, Kontou-Fili K. Cutaneous responses to substance P and calcitonin gene-related peptide in chronic urticaria: the effect of cetirizine and dimethindene. Allergy. 1999;54:46-56. doi: 10.1034/j.1398-9995.1999.00726.x

10 Grouzmann E, Bigliardi P, Appenzeller M, Pannatier A, Buclin T. Substance P-induced skin inflammation is not modulated by a single dose of sitagliptin in human volunteers. Biol Chem. 2011;392:217-221. doi: 10.1515/bc.2011.003

11 Zirbs M, Reindel U, Hermann K, et al. Reduced skin reactivity to vasoconstrictor and vasodilator substances in atopic eczema. Eur J Dermatol. 2013;23:812-819. doi: 10.1684/ejd.2013.2191

12 Ogasawara H, Noguchi M. Therapeutic potential of MRGPRX2 inhibitors on mast cells. Cell. 2021;10:2906. doi: 10.3390/cells10112906

13 Gupta K, Harvima IT. Mast cell-neural interactions contribute to pain and itch. Immunol Rev. 2018;282:168-187. doi: 10.1111/imr.12622

14 Assil S, Rissmann R, van Doorn MBA. Chapter 3: Pharmacological challenge models in clinical drug developmental programs. In: Ane CFN, ed. Translational Studies on Inflammation. IntechOpen; 2019. doi: 10.5772/intechopen.85352

15 Buters TP, Hameeteman PW, Jansen IME, et al. Intradermal lipopolysaccharide challenge as an acute *in vivo* inflammatory model in healthy volunteers. Br J Clin Pharmacol. 2022;88:680-690. doi: 10.1111/bcp.14999

16 Rissmann R, Moerland M, van Doorn MBA. Blueprint for mechanistic, data-rich early phase clinical pharmacology studies in dermatology. Br J Clin Pharmacol. 2020;86:1011-1014. doi: 10.1111/bcp.14293

17 Weidner C, Klede M, Rukwied R, et al. Acute effects of substance P and calcitonin gene-related peptide in human skin – a microdialysis study. J Invest Dermatol. 2000;115:1015-1020. doi: 10.1046/j.1523-1747.2000.00142.x

18 Babina MJI. The pseudo-allergic/neurogenic route of mast cell activation via MRGPRX2: discovery, functional programs, regulation, relevance to disease, and relation with allergic stimulation. Itch. 2020;5:e32. doi: 10.1097/itx.0000000000000032

19 Evilevitch V, Wu TT, Lindgren L, Greiff L, Norrgren K, Wollmer P. Time course of the inflammatory response to histamine and allergen skin prick test in guinea-pigs. Acta Physiol Scand. 1999;165:409-414. doi: 10.1046/j.1365-201x.1999.00526.x

20 Lehmann S, Deuring E, Weller K, et al. Flare size but not intensity reflects histamine-induced itch. Skin Pharmacol Physiol. 2020;33:244-252. doi: 10.1159/000508795

21 Grant JA, Riethuisen J-M, Moulaert B, DeVos C. A double-blind, randomized, single-dose, crossover comparison of levocetirizine with ebastine, fexofenadine, loratadine, mizolastine, and placebo: suppression of histamine-induced wheal-and-flare response during 24 hours in healthy male subjects. Ann Allergy Asthma Immunol. 2002;88:190-197. doi: 10.1016/S1081-1206(10)61995-3

22 Kaplan A, Lebwohl M, Giménez-Arnau AM, Hide M, Armstrong AW, Maurer M. Chronic spontaneous urticaria: focus on pathophysiology to unlock treatment advances. Allergy. 2023;78:389-401. doi: 10.1111/all.15603

23 Fujisawa D, Kashiwakura JI, Kita H, et al. Expression of Mas-related gene X2 on mast cells is upregulated in the skin of patients with severe chronic urticaria. J Allergy Clin Immunol. 2014;134:622-633.e9. doi: 10.1016/j.jaci.2014.05.004

24 Saghari M, Gal P, Gilbert S, et al. OX40L inhibition suppresses KLH-driven immune responses in healthy volunteers: a randomized controlled trial demonstrating proof-of-pharmacology for KY1005. Clin Pharmacol Ther. 2022;111:1121-1132. doi: 10.1002/cpt.2539

25 Shtessel M, Limjunyawong N, Oliver ET, et al. MRGPRX2 activation causes increased skin reactivity in patients with chronic spontaneous urticaria. J Invest Dermatol. 2021;141:678-681.e2. doi: 10.1016/j.jid.2020.06.030

26 van der Kolk T, Assil S, Rijneveld R, et al.

Comprehensive, multimodal characterization of an imiquimod-induced human skin inflammation model for drug development. Clin Transl Sci. 2018;11:607-615. doi: 10.1111/cts.12563
27 Maddox D, Reed C. Clinical pharmacodynamics of antihistamines. Ann Allergy. 1987;59:43-48.
28 Kruizinga M, Stuurman FE, Exadaktylos V, et al. Development of novel, value-based, digital endpoints for clinical trials: a structured approach toward fit-for-purpose validation. Pharmacol Rev. 2020;72:899-909. doi: 10.1124/pr.120.000028
29 Wallengren J, Håkanson R, Andrén-Sandberg Å. Physiological factors influence the substance P-evoked flare in human skin. Pain versus Man. Raven Press; 1992:63-69.
30 Yano H, Wershil BK, Arizono N, Galli SJ. Substance P-induced augmentation of cutaneous vascular permeability and granulocyte infiltration in mice is mast cell dependent. J Clin Invest. 1989;84:1276-1286. doi: 10.1172/jci114295
31 Joseph V, Yang X, Gao SS, et al. Development of AITC-induced dermal blood flow as a translational *in vivo* biomarker of TRPA1 activity in human and rodent skin. Br J Clin Pharmacol. 2021;87:129-139. doi: 10.1111/bcp.14370
32 Church MK, Bewley AP, Clough GF, Burrows LJ, Ferdinand SI, Petersen LJ. Studies into the mechanisms of dermal inflammation using cutaneous microdialysis. Int Arch Allergy Immunol. 1997;113:131-133. doi: 10.1159/000237526

Supplementary Figure 1 Mean wheal AUC following skin challenges (Part 1). AUC, area under the curve; min, minutes; SP, substance P.

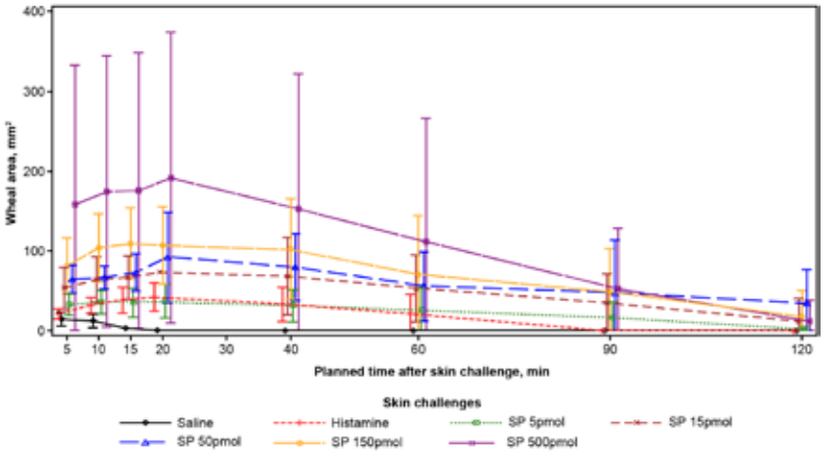

Supplementary Figure 2 Mean wheal AUC following skin challenges (Part 2, with IDM intervention). AUC, area under the curve; IDM, intradermal microdialysis; min, minutes; SP, substance P.

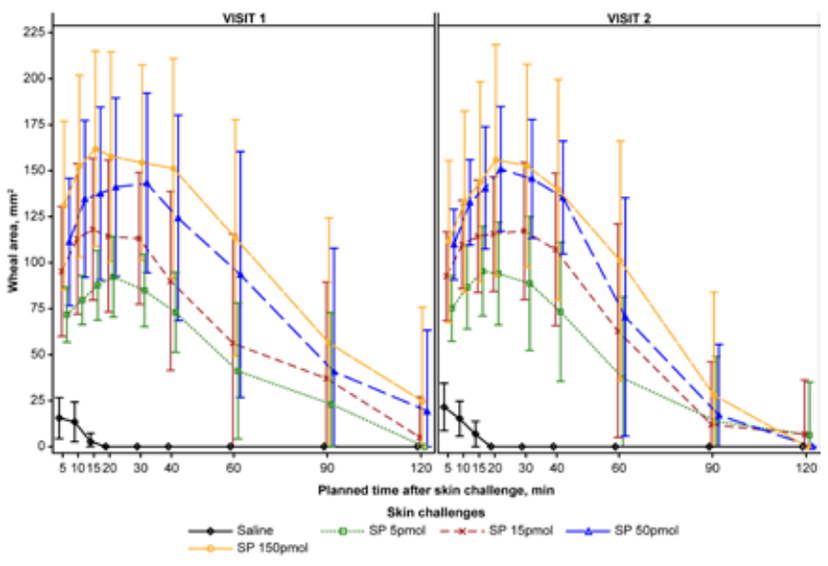

Supplementary Figure 3 Mean flare AUC following skin challenges (Part 1). AUC, area under the curve; min, minutes; SP, substance P.

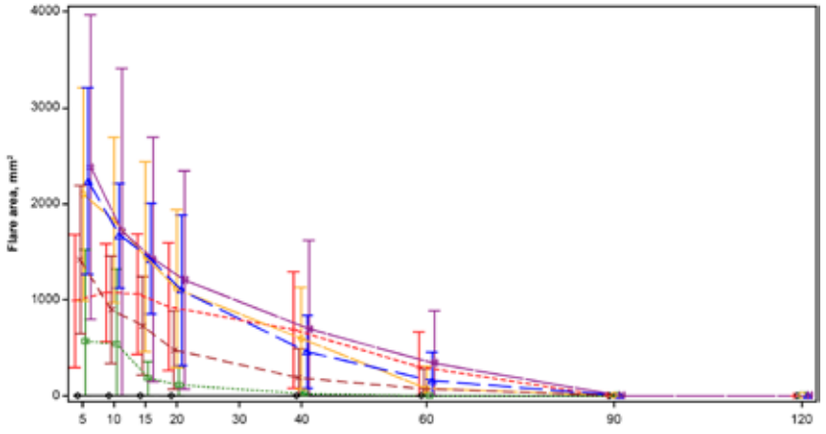

Supplementary Figure 4 Mean flare AUC following skin challenges (Part 2, with IDM intervention). AUC, area under the curve; IDM, intradermal microdialysis; min, minutes; SP, substance P.

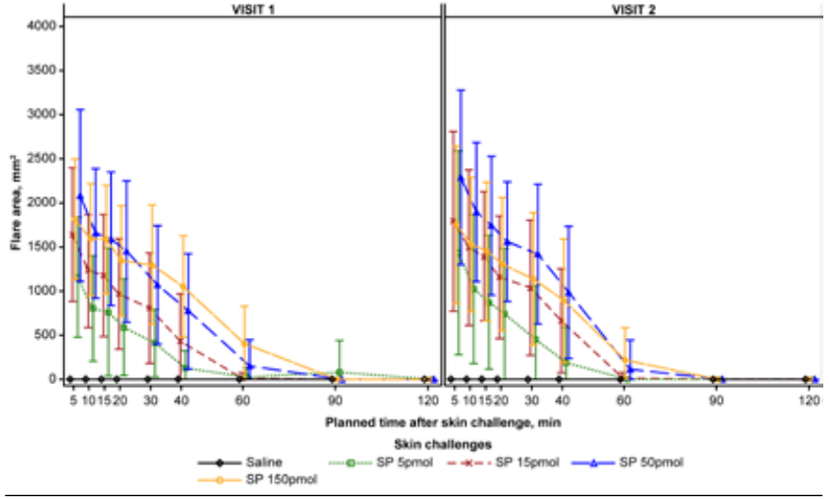

Supplementary Figure 5 Subject profile panel plot by individual histamine concentrations (IDM) following skin challenges. AUC, area under the curve; IDM, intradermal microdialysis; min, minutes; SP, substance P.

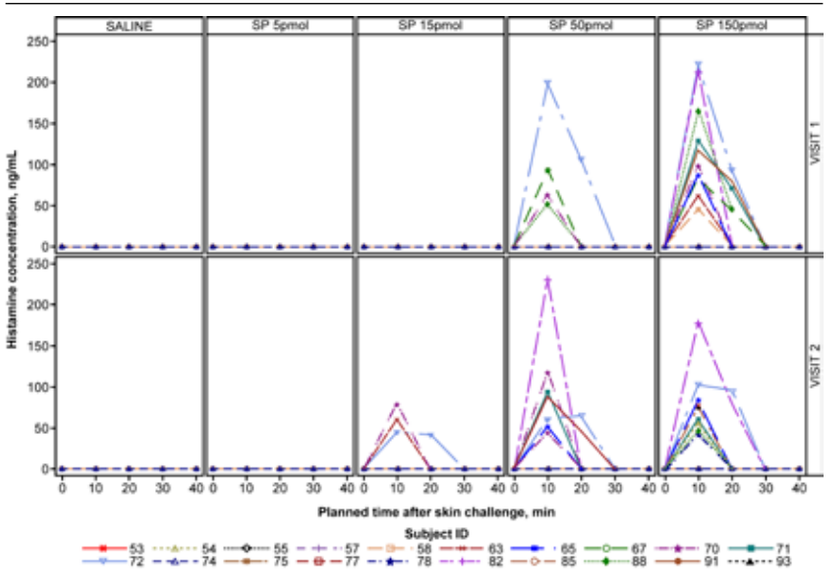

Supplementary Table 1 Participant demographics

	Included in skin challenge evaluations		Enrolled
	Part 1 (*n* = 9)	Part 2 (*n* = 20)	Total (*n* = 32*)
Sex, n (%)			
Female	6 (67)	13 (65)	20 (63)
Male	3 (33)	7 (35)	12 (38)
Age (years)*			
Median (min, max)	22 (21, 32)	22 (18, 49)	22 (18, 49)
Age group (years)*, n (%)			
≤18	0	1 (5)	2 (6)
19–64	9 (100)	19 (95)	30 (94)
Ethnicity, n (%)			
Not Hispanic or Latino	9 (100)	20 (100)	32 (100)
Race, n (%)			
White (Arabic/North African Heritage)	0	2 (10)	2 (6)
White (White/European Heritage	9 (100)	18 (90)	30 (94)
Height (cm)			
Median (min, max)	178.0 (166, 190)	174.5 (161, 198)	175.5 (161, 198)
Weight (kg)			
Median (min, max)	72.1 (60.3, 94.5)	71.6 (56.2, 93.7)	71.9 (56.2, 104.8)
Body mass index (kg/m²)			
Median (min, max)	21.9 (20.5, 27.3)	22.4 (19.7, 29.4)	22.4 (19.7, 29.4)
Concomitant medications, n (%)			
Any medication	5 (56)	14 (70)	-

**Of the 32 participants, 3 were excluded from the study due to COVID-19 infection (n = 2) and voluntary exclusion (n = 1).*

Supplementary Table 2 Summary of wheal and flare AUC following skin challenge with ascending Substance P doses (Part 1)

Challenge visit	SP challenge (dose, number of participants)	Posterior median (mm²/min)	95% CrI (lower, upper)	Probability (ratio >1)*
PART I – Wheal AUC_{0-2h}				
Visit I	SP 5 pmol, n = 9	1887.2	(904.8, 3919.7)	
	SP 15 pmol, n = 9	4333.1	(2075.7, 9027.1)	
	SP 50 pmol, n = 4	4473.3	(1473.6, 13695.1)	
	SP 150 pmol, n = 9	5631.5	(2717.1, 11790.2)	
	SP 500 pmol, n = 5	6579.5	(2448.2, 17609.7)	
	SP 15 pmol/SP 5 pmol	2.3	(0.8, 6.5)	0.9
	SP 50 pmol/SP 15 pmol	1.0	(0.3, 3.9)	0.5
	SP 150 pmol/SP 50 pmol	1.3	(0.3, 4.7)	0.6
	SP 500 pmol/SP 150 pmol	1.2	(0.3, 4.0)	0.6
PART I – Flare AUC_{0-2h}				
Visit I	SP 5 pmol, n-9	3967.8	(1439.6, 10788.2)	
	SP 15 pmol, n-9	18733.4	(6859.4, 51068.5)	
	SP 50 pmol, n-4	47333.9	(10337.0, 213649.4)	
	SP 150 pmol, n-9	31904.4	(11687.0, 87191.80)	
	SP 500 pmol, n-5	24530.4	(6267.2, 96405.6)	1.0
	SP 15 pmol/SP 5 pmol	4.7	(1.2, 19.7)	1.0
	SP 50 pmol/SP 15 pmol	2.5	(0.4, 15.5)	0.8
	SP 150 pmol/SP 50 pmol	0.7	(0.1, 4.2)	0.3
	SP 500 pmol/SP 150 pmol	0.8	(0.1, 4.2)	0.4

AUC, area under the curve; CrI, credible interval; SD, standard deviation; SP, Substance P.
**Posterior probability that the ratio is >1.*

Supplementary Table 3 Summary of wheal responses following skin challenges

Skin Challenge	Visit	n	Mean (SD)	Median (min-max)	n	Mean (SD)	Median (min-max)
		Part 1			Part 2		
Maximum (mm²)*							
Saline	1	9	15.2 (8.98)	15.2 (5.2–30.9)	20	16.6 (11.4)	14.0 (3.7–44.3)
	2	-	-	-	20	21.8 (12.8)	17.2 (5.6–47.2)
Histamine	1	9	44.6 (16.7)	38.5 (25.5–69.2)	20	53.2 (26.6)	50.2 (8.2–103.8)
	2	-	-	-	20	52.9 (16.3)	57.0 (28.8–78.8)
SP 5 pmol	1	9	42.4 (20.3)	40.7 (13.3– 67.9)	20	85.8 (23.5)	87.5 (27.3–122.3)
	2	-	-	-	20	92.2 (24.5)	89.7 (48.5–164.0)
SP 15 pmol	1	9	82.8 (41.8)	66.9 (37.1–139.9)	20	113.0 (30.8)	123.2 (43.4–148.7)
	2	-	-	-	20	113.1 (26.9)	110.6 (65.4–172.1)
SP 50 pmol	1	4	99.8 (48.1)	93.9 (58.4–153.3)	20	134.6 (39.4)	141.1 (41.0–215.5)
	2	-	-	-	20	151.1 (39.3)	137.32 (115.20–282.94)
SP 150 pmol	1	9	126.1 (55.3)	126.3 (20.9–203.1)	20	148.9 (47.7)	145.7 (50.4–289.9)
	2	-	-	-	20	153.0 (39.8)	153.1 (91.7–238.6)
SP 500 pmol	1	5	194.1 (178.9)	125.7 (24.6–461.8)	-	-	-
	2	-	-	-	-	-	-
Time to maximum (minutes)*							
Saline	1	9	6.8 (2.7)	5.0 (5–11)	20	5.9 (2.0)	5.0 (4–10)
	2	-	-	-	20	5.5 (1.6)	5.0 (4–10)
Histamine	1	9	22.6 (10.2)	20.0 (15–42)	20	31.2 (15.5)	30.0 (9–62)
	2	-	-	-	20	27.7 (11.5)	24.5 (14–60)
SP 5 pmol	1	9	23.9 (18.5)	20.0 (5–60)	20	20.4 (7.6)	18.5 (9–39)
	2	-	-	-	20	20.9 (7.8)	19.0 (9–39)
SP 15 pmol	1	9	22.0 (10.5)	20.0 (10–40)	20	25.3 (17.7)	19.5 (8–90)
	2	-	-	-	20	23.1 (16.7)	18.5 (11–89)

Continuation Supplementary Table 3

Skin Challenge	Visit	n	Mean (SD)	Median (min-max)	n	Mean (SD)	Median (min-max)
		Part 1			Part 2		
SP 50 pmol	1	4	16.5 (5.1)	17.5 (10–21)	20	25.3 (12.6)	23.5 (4–60)
	2	-	-	-	20	27.1 (10.9)	25.0 (15–59)
SP 150 pmol	1	9	25.3 (17.2)	20.0 (10–60)	20	31.7 (23.1)	28.0 (5–90)
	2	-	-	-	20	28.3 (10.0)	27.5 (15–41)
SP 500 pmol	1	5	16.0 (6.5)	20.0 (5–20)	-	-	-
	2	-	-	-	-	-	-
Time to complete disappearance (minutes)†							
Saline	1	9	34.1 (12.8)	39.0 (15–55)	20	17.9 (5.2)	16.0 (11–30)
	2	-	-	-	20	18.7 (3.8)	20.0 (11–27)
Histamine	1	9	79.9 (16.0)	90.0 (56–93)	20	78.5 (25.6)	90.5 (6–120)
	2	-	-	-	19	77.7 (20.9)	90.0 (40–120)
SP 5 pmol	1	7	83.0 (35.4)	62.0 (40–120)	20	82.6 (27.0)	89.0 (38–121)
	2	-	-	-	19	73.7 (18.6)	61.0 (58–121)
SP 15 pmol	1	7	96.3 (33.1)	120.0 (42–121)	18	85.3 (27.3)	90.0 (38–121)
	2	-	-	-	19	80.9 (24.5)	88.0 (40–123)
SP 50 pmol	1	2	74.5 (21.9)	74.5 (59–90)	16	91.7 (20.7)	90.0 (58–121)
	2	-	-	-	19	89.6 (22.4)	90.0 (60–122)
SP 150 pmol	1	6	81.8 (33.6)	75.5 (40–120)	16	102.6 (19.3)	104.5 (59–121)
	2	-	-	-	19	91.6 (20.9)	90.0 (60–121)
SP 500 pmol	1	4	97.3 (28.5)	104.5 (60–120)	-	-	-
	2	-	-	-	-	-	-

*SD, standard deviation; SP, Substance P. *During the 2h post challenge period. †Complete disappearance was defined as a value of 0 for wheal area, longest diameter or orthogonal diameter. Participants who did not have a disappearance within the 2h post challenge period were excluded.*

CHAPTER V

THE ORAL IRAK4 INHIBITORS ZABEDOSERTIB AND BAY1830839 SUPPRESS LOCAL AND SYSTEMIC IMMUNE RESPONSES IN A RANDOMIZED TRIAL IN HEALTHY MALE VOLUNTEERS

Published in the Journal of Clinical and Translational Science, 2024

Wouter ten Voorde[2,3], Stefan J Jodl[1], Stefan Klein[1], Andrea Wagenfeld[1], Frank S Zollmann[4], Maximilian Feldmüller[1], Naomi B Klarenbeek[2], Digna T de Bruin[2], Manon A A Jansen[2], Robert Rissmann[2,5], Beate Rohde[1], Matthijs Moerland[2,3]

1 Bayer AG, Berlin, Germany.
2 Centre for Human Drug Research, Leiden, NL
3 Leiden University Medical Center, Leiden, NL
4 Pharma Consult, Berlin, Germany.
5 Leiden Academic Centre for Drug Research, Leiden, NL

ABSTRACT

This study evaluated and characterized the pharmacological activity of the orally administered interleukin-1 receptor-associated kinase 4 (IRAK4) inhibitors BAY1834845 (zabedosertib) and BAY1830839 in healthy male volunteers. Participants received one of either IRAK4 inhibitors or a control treatment (prednisolone 20 mg or placebo) twice daily for 7 days. Localized skin inflammation was induced by topical application of imiquimod (IMQ) cream for 3 days, starting at Day 3 of treatment. The inflammatory response was evaluated by laser speckle contrast imaging (skin perfusion) and multispectral imaging (erythema). At Day 7, participants received 1 ng/kg intravenous lipopolysaccharide (LPS). Circulating inflammatory proteins, leukocyte differentiation, acute phase proteins, and clinical parameters were evaluated before and after the systemic LPS challenge. Treatment with BAY1834845 significantly reduced the mean IMQ-induced skin perfusion response (geometric mean ratio [GMR] vs. placebo: 0.69 for BAY1834845, 0.70 for prednisolone; both $p < 0.05$). Treatment with BAY1834845 and BAY1830839 significantly reduced IMQ-induced erythema (GMR vs. placebo: 0.75 and 0.83, respectively, both $p < 0.05$; 0.86 for prednisolone, not significant). Both IRAK4 inhibitors significantly suppressed the serum TNF-α and IL-6 responses (≥80% suppression vs. placebo, $p < 0.05$) and inhibited C-reactive protein, procalcitonin, and IL-8 responses to intravenous LPS. This study demonstrated the pharmacological effectiveness of BAY1834845 and BAY1830839 in suppressing systemically and locally induced inflammatory responses in the same range as prednisolone, underlining the potential value of these IRAK4 inhibitors as future therapies for dermatological or other immune-mediated inflammatory diseases.

INTRODUCTION

Interleukin-1 receptor-associated kinase 4 (IRAK4) is a serine/threonine kinase that is a key intracellular signaling component downstream of myeloid differentiation primary response protein 88-associated toll-like receptors (TLRs) and the interleukin (IL)-1 receptor (IL-1R) family that are key mediators of human innate immune responses. Inhibition of IRAK4 activity blocks the production of inflammatory cytokines, such as IL-6, tumor necrosis factor (TNF)-α, IL-12, IL-1, and type I interferons (IFNs), which are key drivers in the pathogenesis of multiple autoimmune inflammatory diseases. In mouse models, IRAK4 inhibition was shown to suppress lipopolysaccharide (LPS)-induced TNF-α activation, alleviate collagen-induced arthritis, and block gout formation.[1,2] IRAK4 has thus emerged as an attractive therapeutic target for diseases associated with dysregulated inflammation, such as chronic inflammatory skin conditions, systemic and cutaneous lupus erythematosus, and rheumatoid arthritis. The clinical efficacy of IRAK4 inhibition in rheumatoid arthritis has been demonstrated by a selective, small molecule IRAK4 inhibitor,[3] and studies of other IRAK4-targeting compounds in other indications are ongoing.[4-6]

BAY1834845 (zabedosertib) and BAY1830839 are two oral IRAK4 inhibitors with high potency and selectivity, and good oral availability across preclinical species. Synthesized by Bayer AG, Berlin, Germany,[7] both compounds are drug candidates in development for the treatment of immune-mediated inflammatory diseases. In mice with imiquimod (IMQ)-induced psoriasis, treatment with BAY1834845 or BAY1830839 significantly reduced the severity of psoriasis-like lesions and reduced the extent of erythema, skin thickening, and scaling compared with vehicle. Both compounds dose-dependently blocked IL-1β-induced inflammation in mice.[7] BAY1834845 also strongly inhibited the secretion of TNF-α in isolated murine and rat splenic cells stimulated for 24 h with LPS 1 and 0.1 µg/mL, with half-maximal inhibitory concentration (IC50) values of 385 and 1270 nM, respectively (data on file at Bayer). As part of the initial clinical phase I studies, the *ex vivo* activity of both compounds was evaluated by whole blood LPS challenges (LPS concentration 0.1 ng/mL, 6 h incubation) in healthy male volunteers. BAY1834845 (daily doses up to 240 mg for 10 days) and BAY1830839 (daily doses up to 400 mg for 10 days) suppressed TNF-α release in a dose-dependent manner, with a mean inhibition of 50% and 70%, respectively (data on file at Bayer).

The purpose of this clinical study was to evaluate and characterize the pharmacological activity of orally administered BAY1834845 and BAY1830839 in the inhibition of IRAK4 pathway-mediated reactions in healthy male volunteers. A conventional immunosuppressive agent (prednisolone) and placebo were

used as active and non-active controls, respectively. The study design allowed discrimination between systemic and peripheral inflammation, and between TLR4- and TLR7-mediated responses; *in vivo* drug activity in a peripheral tissue (skin) was evaluated based on a topical IMQ challenge driving TLR7 activation, while *in vivo* drug activity in systemic inflammation was investigated by an intravenous (I.V.) LPS challenge driving TLR4 activation. *Ex vivo* drug activity in circulating immune cells was monitored by whole blood challenges driving TLR4, TLR7/8, and IL-1R. Both the topical IMQ challenge and intravenous LPS challenge are clinically well-characterized models which have been used to demonstrate the pharmacological activity of candidate drugs.[8-11] TLR4, TLR7/8, and IL-1R are all receptors upstream of IRAK4 signalling and, therefore, serve as relevant targets for providing proof of clinical pharmacological activity and exploring the therapeutic potential of BAY1834845 and BAY1830839.

MATERIALS AND METHODS

GENERAL STUDY DESIGN

This was a randomized, partial-blind, four-arm study. Healthy male volunteers (12 per study arm) received oral treatment with one of the two study drugs (BAY1834845 or BAY1830839), matching placebo, or prednisolone as an active control, each twice daily (B.i.d.) for 7 days (Figure 1). The effects of these oral treatments on local and systemic IRAK4-driven responses, which were triggered by a topical inflammatory skin challenge conducted from Day 3 to Day 5 after start of treatment and a systemic immune challenge conducted on Day 7, were evaluated over time, while safety/tolerability was monitored closely.

This study (ClinicalTrials.gov identifier: NCT05003089) was conducted in accordance with the Declaration of Helsinki, the Council for International Organizations of Medical Sciences International Ethical Guidelines, and the International Conference of Harmonisation Good Clinical Practice Guidelines. The independent Medical Review and Ethics Committee 'Medisch Ethische Toetsingscommissie van de Stichting Beoordeling Ethiek Biomedisch Onderzoek' (Assen, The Netherlands) reviewed and approved the study prior to clinical study activities. All subjects received oral and written information and provided written informed consent before participation. The study was conducted at the Centre for Human Drug Research, Leiden, The Netherlands, between June 2021 and December 2021.

STUDY PARTICIPANTS

The study included men aged 18–55 years at the time of screening (within 42 days prior to the study treatment period). All provided informed consent and were healthy as determined by medical evaluation based on medical history, physical examination, laboratory tests, electrocardiogram (ECG), and vital signs. Individuals were excluded from the study if they had specified medical conditions, medication or drugs, or evidence of any other clinically relevant findings. Subjects with active infections, who had recently used immune-modulating drugs, or with skin disorders were excluded. Further information regarding the inclusion and exclusion criteria are provided in Data S1.

Figure 1 Study design. B.i.d., twice daily; BL, baseline; CEA, Clinician Erythema Assessment; CRP, C-reactive protein; IMQ, imiquimod; LCSI, laser speckle contrast imaging; LPS, lipopolysaccharide; PCT, procalcitonin; PK, pharmacokinetics; WB, whole blood.

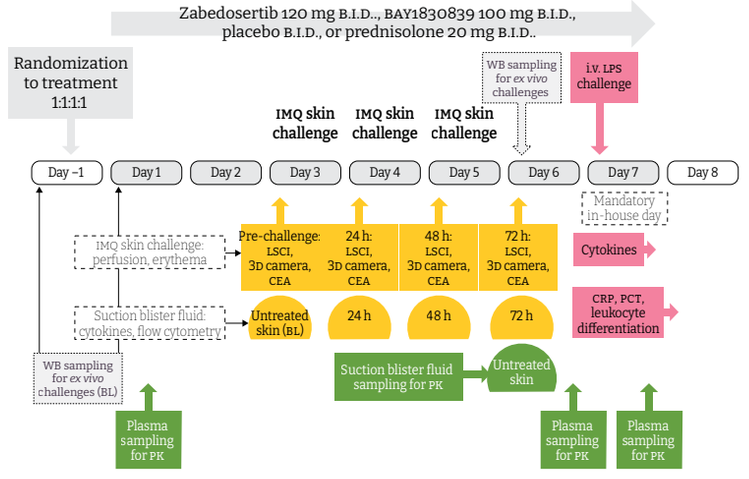

DOSE SELECTION

The selected doses of BAY1834845 (120 mg B.i.d.) and BAY1830839 (100 mg B.i.d.) were based on the drug concentrations and exposures found to exert pharmacological activity in preceding preclinical experiments, which used IL-1β-induced systemic inflammation in mice[7] and mouse collagen antibody-induced arthritis (data on file at Bayer), after taking into account species differences in potency, as well as evidence from initial clinical studies.[12,13,14,15] In these clinical studies, BAY1834845 was well tolerated in healthy male volunteers at single oral doses of up to 480 mg and at multiple oral doses of up to 200 mg B.i.d. for 10 days; in male and female patients with plaque psoriasis, a similar safety profile was also reported at 120 mg B.i.d. for 8 weeks (data on file at Bayer). In addition, single oral doses of BAY1830839 of up to 800 mg as well as multiple oral doses

of up to 200 mg B.i.d. and 100 mg T.i.d. for 10 days were generally well tolerated (data on file at Bayer). Prednisolone was administered as an active control at a supratherapeutic clinical dose (40 mg daily) for long-term use.

TREATMENTS

Study participants were randomized 1:1:1:1 to receive BAY1834845 120 mg B.i.d. (masked), BAY1830839 100 mg B.i.d. (masked), matching placebo B.i.d. (masked), or 20 mg prednisolone B.i.d. (open label). Study treatments were administered for 7 consecutive days (Days 1–7). Further information regarding the randomization and blinding procedures are provided in Data S1. Prednisolone was administered at 20 mg B.i.d. to mimic the dosing regimen of the two investigational drugs. Treatment compliance during in-house visits and on Day 6 (full day in-house) was monitored at the study site. In the ambulatory phases of the study, direct supervision of drug intake was undertaken by study personnel via a live video call. Clinical evaluations were done by treatment-blinded investigators.

IMMUNE CHALLENGES

IMQ SKIN CHALLENGE

For the IMQ skin challenge, commercially available IMQ-containing cream (Aldara™ 5% cream, Meda AB, Solna, Sweden) was used, starting after 2 days of treatment with the study drugs. IMQ cream was applied for 3 days to induce skin inflammation as previously described.[8] IMQ cream 5% (100 mg) was applied daily to tape-stripped skin treatment areas on the back under occlusion by a standard 12-mm Finn chamber (Smart Practice, Phoenix, AZ, USA). The Finn chamber was replaced with a new dose of IMQ after 24 h (treatment areas 2 and 3) and again after 48 h (treatment area 3). This resulted in the following treatment durations and doses – area 1: 24 h IMQ exposure, cumulative dose 5 mg; area 2: 48 h IMQ exposure, cumulative dose 10 mg; area 3: 72 h IMQ exposure, cumulative dose 15 mg; and area 4: no IMQ exposure (untreated control).

At baseline and 24, 48, and 72 h after the start of the IMQ skin challenge, skin reactions were evaluated using three-dimensional (3D) optical skin image capture and analysis (Antera 3D® camera, Miravex, Dublin, Ireland) for erythema and a laser speckle contrast imager (LSCI; Perimed AB, Järfälla, Sweden) for perfusion. Both procedures were performed according to the manufacturer's instructions.[8] In addition, visual assessments of the skin reaction were graded using the Clinician Erythema Assessment (CEA) score.[16]

At baseline and 24, 48, and 72 h after the start of the IMQ skin challenge, suction blisters were generated on the inflamed skin areas using a negative pressure device (NP-4; Electric Diversities, Finksburg, MD, USA).[17] Blister fluid was harvested and used to analyze immune cell subsets via flow cytometry (using Flowlogic 7.3, Inivai Technologies) as well as cytokines and chemokines via multiplex immunoassays (Meso Scale Discovery; Meso Scale Diagnostics, Rockville, MD, USA); see Data S1 for further details.

SYSTEMIC LPS CHALLENGE

After participants had undergone the IMQ skin challenge, an I.V. LPS challenge was performed on Day 7 after the start of treatment. All participants received 1 ng/kg purified Escherichia coli O113 LPS (List Labs, US, Lot #94332B4) reconstituted in 0.5 mL glucose 2.5%–sodium chloride (NACL) 0.45% and administered as a 2-min infusion. To ensure that participants stayed adequately hydrated, glucose 2.5%–NACL 0.45% was infused, starting 2 h prior to LPS administration and continuing until 6 h afterwards.[18] Circulating inflammatory proteins (acute phase proteins, cytokines), leukocyte differentiation, and clinical parameters (pulse rate, blood pressure, and temperature) were evaluated over time, starting 0.5 h after the end of the infusion and ending up to 24 h after infusion.

Ex vivo whole blood challenges Before treatment, two baseline (Day −1 and Day 1) and on Day 6 (Figure 1), *ex vivo* peripheral blood samples were drawn into TruCulture tubes (Myriad RBM, Austin, TX, USA) according to the manufacturer's instructions. Tubes contained LPS (TLR4 agonist, 0.1 ng/mL) or R848 (TLR7/8 agonist, 0.35 µg/mL). In addition, a third blood sample was incubated with IL-1β (IL-1R agonist, 125 ng/mL) in 4 mL sodium heparin tubes. Blood samples were incubated in duplicate for each challenge agent at 37°C for 24 h. After incubation, cytokine release in culture supernatants was evaluated using multiplex immunoassays; see Data S1 for further details.

PK SAMPLE COLLECTION (PLASMA AND SKIN SUCTION BLISTER FLUID)

Sample collection for pharmacokinetic (PK) analyses is described in Data S1.

SAFETY MONITORING

Adverse events (AEs) were recorded and assessed for intensity, cause, and potential relationship to study treatments or procedures at each study visit. Assessment of clinical signs and symptoms was particularly thorough during the 48 h after the I.V. LPS challenge on Day 7 to ensure participant safety. For these AEs, their potential relationship to the LPS infusion was specifically documented by the investigator as "infusion-related reactions" (as part of the AE description text) and subsequently rated as "procedure-related" AEs. This approach enabled the evaluation of the effects of the active treatments on LPS-induced adverse reactions.

STUDY ENDPOINTS

The co-primary endpoints of the study were the average change from baseline of skin perfusion/basal flow and erythema over 72 h after the start of the IMQ challenge, and the average change in systemic TNF-α and IL-6 levels over 6 h after the systemic LPS challenge. Secondary endpoints included: skin perfusion/basal flow and erythema at the individual time points (24, 48, and 72 h after the start of the IMQ challenge), CEA scores (24, 48, and 72 h after the start of the IMQ challenge), molecular responses (cytokines and immune cells in skin suction blisters) driven by IMQ; as well as immune responses in blood (e.g., immune cells, C-reactive protein [CRP], cytokines) and clinical responses (body temperature, pulse rate, systolic and diastolic blood pressure) driven by the systemic LPS challenge. Other prespecified endpoints included concentrations of total and unbound BAY1834845 and BAY1830839 in plasma and suction blister fluid, cytokine release in the *ex vivo* whole blood challenge assays, and treatment-emergent AEs (TEAEs).

STATISTICAL APPROACH AND ANALYSES

Evidence of the pharmacological activity of each treatment was evaluated using a two-step hierarchical decision: step 1 to establish assay sensitivity, and step 2 to establish superiority of the treatments versus placebo. To satisfy step 1 (IMQ skin challenge assay sensitivity), the prednisolone arm was required to show superiority in at least one of the outcome variables (erythema or perfusion) with >95% posterior probability. A sample size of 12 evaluable participants per arm was deemed sufficient to achieve >95% power for success in step 1, assuming a mean reduction versus placebo of 73% (conservative estimate based on available data, with a coefficient of variation [CV] of 15%) in erythema and a mean reduction versus placebo of 71% (with a CV of 25%) in perfusion. Proof of assay sensitivity with an effective anti-inflammatory drug was deemed important due to the limited available data for the challenges. Step 2 (main analysis) required that the active treatments demonstrated superiority versus placebo with >90% posterior probability for erythema as well as perfusion. Twelve participants were calculated as sufficient to achieve >90% power for demonstrating superiority versus placebo if the treatment effect was at least 70% of the effect of prednisolone. A Bayesian repeated measures analysis of covariance model was fitted to the original log-transformed values for change from baseline (or change from pre-challenge value, if applicable) adjusted for treatment–timepoint interaction and a random subject effect. All statistical analyses were performed using SAS software, release 9.4 or higher (SAS Institute Inc., Cary, NC, USA), R version 3.61 or higher, or JAGS version 4.3 or higher. One-sided p-values <0.05 were considered statistically significant.

RESULTS

Fifty-one eligible participants were randomly assigned to one of the four study intervention groups. Two participants were withdrawn early due to AEs (see later) and were replaced to achieve 12 evaluable participants in each treatment group (Table S1). Based on direct supervision at the study site and video call monitoring, treatment compliance was estimated to be 100% in all evaluable patients (Table S2). All randomized participants were Caucasian adult males aged between 19 and 55 years. Baseline characteristics were similar across the four participant groups (Table S1).

IMQ SKIN CHALLENGE

Based on the statistically significant difference (p = 0.02) in skin perfusion between the active control prednisolone and the placebo group, assay sensitivity was confirmed (step 1; Figure 2B,D, Table 1). Treatment with BAY1834845 and BAY1830839 reduced IMQ-driven erythema, with a GMR of treatment effect versus placebo of 0.75 and 0.83, respectively (p = 0.01 and p = 0.05, respectively; Figure 2A,C, Table 1). Treatment with BAY1834845 reduced IMQ-driven increases in skin perfusion as quantified by LSCI, with a GMR of treatment versus placebo of 0.69 (p = 0.02; Figure 2B,D, Table 1). Clinical evaluation of skin reactions indicated that participants treated with BAY1834845 and BAY1830839 had a less severe inflammatory reaction to the skin challenge than those who received placebo (Figure 2A,B, Figure S1). Overall, the effect size of BAY1834845 on IMQ-driven skin responses was comparable or better than that of prednisolone (Table 1).

SKIN SUCTION BLISTER FLUID ANALYSIS

BAY1834845, BAY1830839, and prednisolone strongly suppressed IMQ-driven IP-10 and interferon-induced myxovirus resistance protein 1 (MXA) in skin suction blister exudate (analysis on Day 6), which were the two biochemical end points showing the strongest response in this test matrix following skin challenge (Figure 3A,B). The IMQ challenge resulted in an increase in CD8+ T cells, dendritic cells, classical monocytes, and natural killer (NK) cells in suction blister fluid. The responses of CD8+ T cells and dendritic cells were suppressed by BAY1834845, BAY1830839, and prednisolone treatment at 72 h after the start of the IMQ challenge. The responses of NK cells and classical monocytes were markedly suppressed by prednisolone at 72 h post-challenge only after a preceding increase of these cell types up to 48 h post-challenge (Figure S2). No changes in systemic markers during or after the IMQ challenge were observed.

Figure 2 Changes over time in (a) skin erythema and (b) skin perfusion after start of imiquimod (IMQ) challenge, both in arbitrary units. Representative images captured 72 h after start of IMQ challenge are also shown for (c) three-dimensional (3D) camera and (d) laser speckle contrast imaging (LSCI). AU, arbitrary units; IMQ, imiquimod.

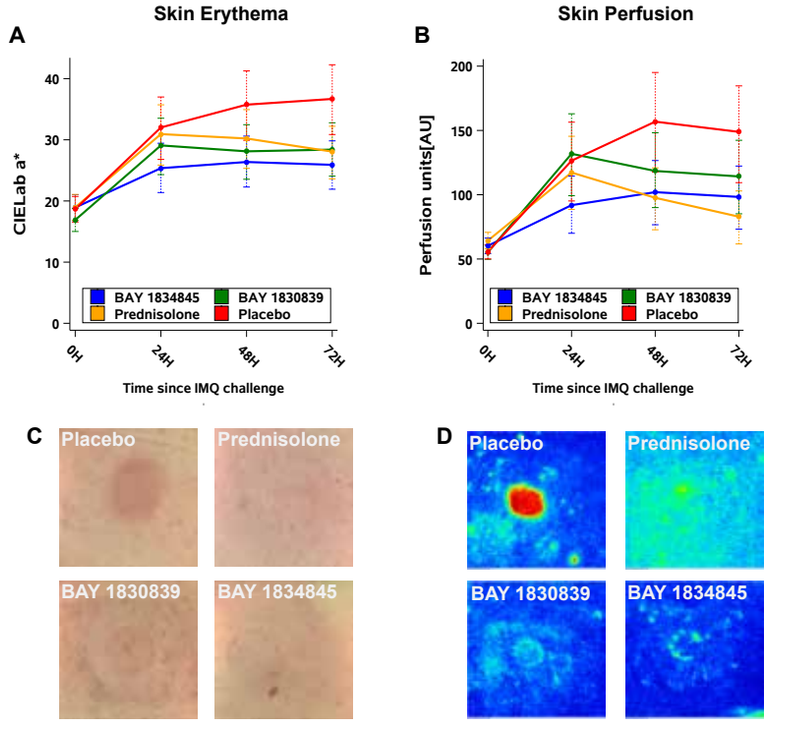

Figure 3 Changes over time in (a) IFN-γ-induced protein 10 (IP-10) and (b) myxovirus resistance protein 1 (MXA) in blister fluid after imiquimod (IMQ) challenge. LLOQ, lower limit of quantitation; LPS, lipopolysaccharide; ULOQ, upper limit of quantitation.

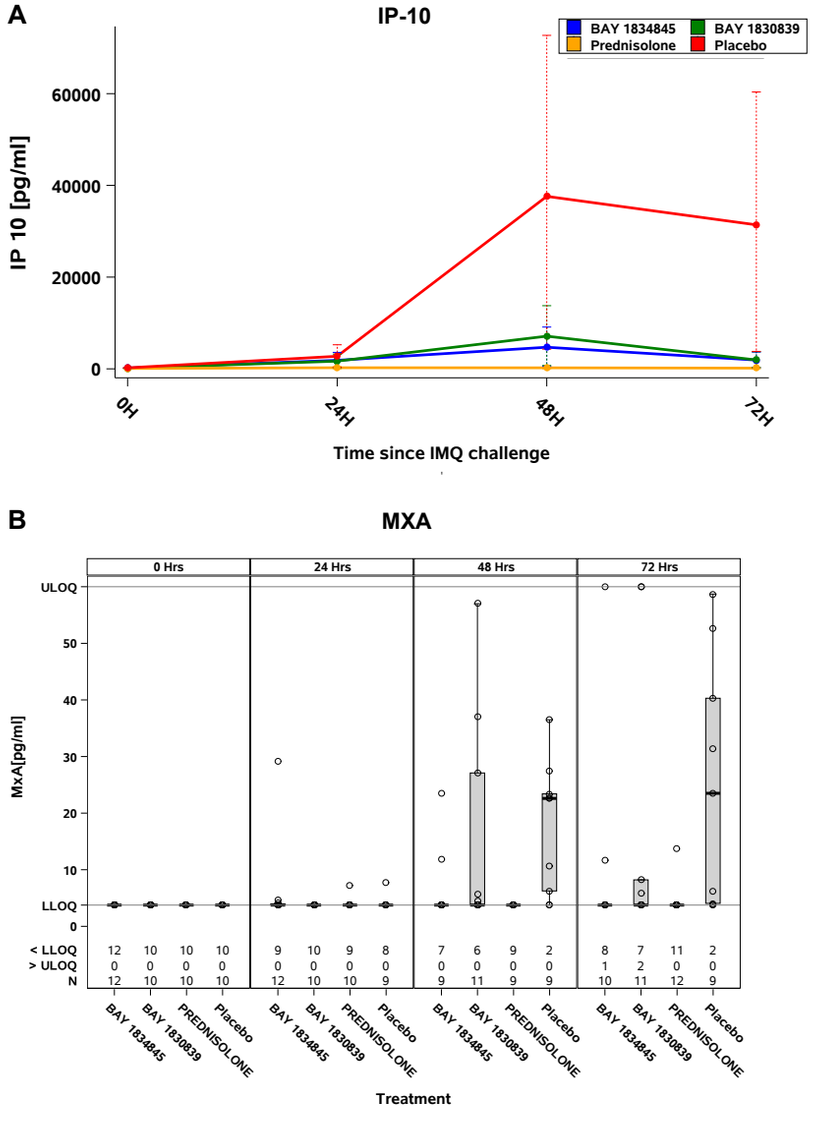

Table 1 Co-primary end point analysis: imiquimod skin challenge and systemic lipopolysaccharide challenge parameters.

	Placebo (*n* = 12)	BAY 1834845 120 mg B.I.D. (*n* = 12)	BAY 1830839 100 mg B.I.D. (*n* = 12)	Prednisolone 20 mg B.I.D. (*n* = 12)
IMQ skin challenge				
Skin perfusion/basal flow				
Geometric mean response (90% CrI) (AU)	143.02 (112.05, 172.85)	98.68 (68.65,128.58)	123.00 (85.67,158.90)	100.11 (70.08,129.15)
Geometric mean ratio of treatment effect vs. placebo (90% CrI)	1	0.69 (0.48, 0.90)	0.86 (0.60, 1.11)	0.70 (0.49, 0.90)
Posterior probability of treatment superiority to placebo	-	0.98*	0.82 (n.s.)	0.98*
Erythema				
Geometric mean response (90% CrI) (AU)	34.7 (29.9, 39.4)	26.0 (20.89, 30.92)	28.8 (23.08, 34.21)	29.8 (23.98, 35.50)
Geometric mean ratio of treatment effect vs. placebo (90% CrI)	1	0.75 (0.60, 0.89)	0.83 (0.67, 0.99)	0.86 (0.69, 1.02)
Posterior probability of treatment superiority to placebo	-	0.99*	0.95*	0.91 (n.s.)
LPS challenge				
TNF-α (blood)				
Posterior geometric mean response (90% CrI) (pg/mL)	17.25 (13.18, 21.49)	3.45 (2.28, 4.61)	2.42 (1.60, 3.26)	5.35 (3.52, 7.12)
Geometric mean ratio of treatment effect vs. placebo (90% CrI)		0.20 (0.13, 0.27)	0.14 (0.09, 0.19)	0.31 (0.20, 0.41)
Posterior probability of treatment superiority to placebo		>0.99*	>0.99*	>0.99*
IL-6 (blood)				
Posterior geometric mean response (90% CrI) (pg/mL)	18.1 (13.7, 22.3)	4.89 (3.31, 6.59)	4.71 (3.04, 6.12)	5.61 (3.71, 7.39)
Geometric mean ratio of treatment effect vs. placebo (90% CrI)		0.27 (0.18, 0.36)	0.26 (0.17, 0.34)	0.31 (0.21, 0.41)
Posterior probability of treatment superiority to placebo		>0.99*	>0.99*	>0.99*

*AU, arbitrary units; CrI, credible interval; IL, interleukin; IMQ, imiquimod; LPS, lipopolysaccharide; LSCI, laser speckle contrast imaging; TNF, tumour necrosis factor; *, statistically significant at a one-sided α of 5%; n.s., not significant.*

SYSTEMIC LPS CHALLENGE

BAY1834845 and BAY1830839 treatment significantly suppressed the marked and rapid increase in circulating TNF-α and IL-6 following I.V. LPS challenge by ≥80%, averaged over assessments from 0.5 to 6 h after the LPS challenge when compared with placebo ($p < 0.01$; Figure 4A,B). LPS-induced increases in IL-8, CRP, and procalcitonin (PCT; Figure 4C,E,F, respectively), as observed in the placebo group, were also inhibited by BAY1834845 and BAY1830839. In contrast to prednisolone, treatment with either BAY1834845 or BAY1830839 did not lead to an increase in the anti-inflammatory cytokine IL-10 compared with placebo (Figure 4D). Furthermore, BAY1834845 and BAY1830839 suppressed LPS-driven increases in systolic blood pressure and pulse rate (Figure S3) compared with placebo without suppressing the mild increase in core temperature 2–6 h after I.V. LPS challenge.

ADVERSE EVENTS RELATED TO LPS CHALLENGE

The majority of the TEAEs that occurred during the study were reported within 48 h after the start of the LPS challenge. These procedure-related TEAEs, comprising reactions related to the LPS infusion, mostly started within 1 h of beginning the LPS challenge and resolved completely after 2 h. Three of these TEAEs (tachycardia and infusion-related reactions of fever and chills) were of moderate intensity and observed in two participants in the placebo group; all other TEAEs were assessed as mild. Overall, compared with the placebo group, a clear reduction in the number of procedure-related TEAEs occurring within 48 h after the start of the LPS challenge was observed in the BAY1834845 and BAY1830839 treatment groups, in which 7 and 6 (of 12) participants, respectively, reported no procedure-related TEAEs within the assessment period (Figure 5).

EX VIVO WHOLE BLOOD CHALLENGES

Incubation of whole blood with different immune challenge agents triggered the secretion of cytokines characteristic of specific signalling pathways activated by the respective agents, thereby serving as a measure of *ex vivo* pharmacological activity. The cytokines induced by R848, LPS, and IL-1β as well as the inhibition of cytokine release per treatment arm are summarized in Table 2. Treatment with BAY1834845 and BAY1830839 resulted in an approximately 80%–95% reduction in R848-driven IL-1β, TNF-α, IL-6, and IFN-γ release; while IL-8 and IL-10, IP-10 and IFN-α responses had smaller reductions and were mildly impacted by the IRAK4 inhibition. Both IRAK4 inhibitors suppressed LPS-driven IL-1β, TNF-α, IL-6, and IL-8 release with a 50%–80% reduction. Moreover, reductions in IL-1β-driven TNF-α, IL-6, and IL-8 were observed. Overall, BAY1830839 resulted in a stronger suppression of R848-driven responses than BAY1834845. Prednisolone treatment was less effective at suppressing most R848- and IL-1β-driven cytokine responses but showed similar potency to the two IRAK4 inhibitors for the attenuation of LPS-stimulated IL-1β, IL-6, and TNF-α release.

Figure 4 Changes in estimated geometric mean response over time in (a) tumor necrosis factor (TNF)-α, (b) interleukin (IL)-6, (c) IL-8, (d) IL-10, (e) C-reactive protein (CRP), and (f) procalcitonin after intravenous lipopolysaccharide (LPS) challenge.

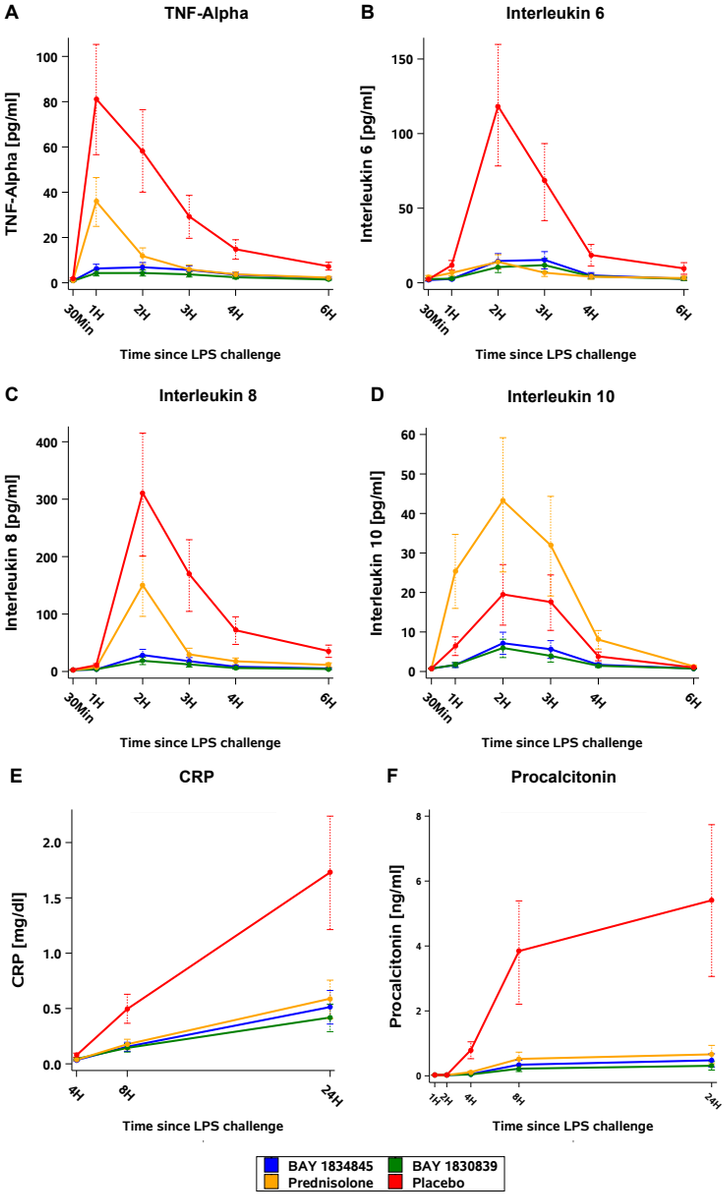

Figure 5 Subjects with procedure (lipopolysaccharide [LPS] challenge)-related treatment-emergent adverse effects within 48 h of intravenous LPS administration by treatment group (N = 12 per group). BAY1834845, BAY1830839, prednisolone, and placebo. AE, adverse effect; LPS, lipopolysaccharide.

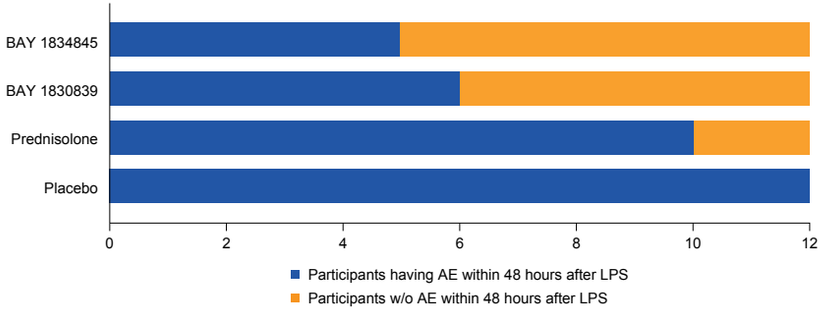

Table 2 *Ex vivo* pharmacological activity: inhibition of whole blood cytokine release triggered by R848, lipopolysaccharide, and interleukin (IL)-1β.

Challenge agent	Cytokine	BAY 1834845	BAY 1830839	Prednisolone	Placebo
R848	TNF-α	-87	-93	-32	+22
	IL-6	-77	-85	-20	+22
	IL-8	-30	-37	+133	+7
	IL-1β	-87	-92	-2	+19
	IFN-α	+11	-32	N.C.	+18
	IFN-γ	-93	-93	-67	+32
	IL-10	-69	-85	+11	+8
	IP-10	-20	-30	+10	+10
LPS	TNF-α	-51	-75	-56	+38
	IL-6	-52	-73	-71	+34
	IL-8	-60	-79	+13	+14
	IL-1β	-50	-75	-57	+30
IL-1β	TNF-α	N.C.	N.C.	+34	-1
	IL-6	-41	-81	-1	+23
	IL-8	0	-50	+30	0
	IFN-α	N.C.	N.C.	N.C.	N.C.

Data shown are the geometric mean percentage change from baseline stimulation for each cytokine; a negative change indicates a reduction of the respective marker. Some means were not calculated because too many values were below the lower limit of quantitation.
IFN, interferon; IL, interleukin; IP-10, IFN-γ-induced protein 10; LPS, lipopolysaccharide; N.C., not calculated; TNF, tumour necrosis factor.

OVERALL SAFETY AND TOLERABILITY

TEAEs were reported by 9 participants (69.2%) in the BAY1834845 group, 8 (61.5%) in the BAY1830839 group, and 12 (100%) in the prednisolone and placebo groups, respectively (Table S4). An AE leading to withdrawal from the study occurred in one participant in each of the BAY1834845 and BAY1830839 treatment groups. The two discontinuations were due to an asymptomatic and uncomplicated SARS-COV-2 infection and an upper respiratory tract infection on Day 4, respectively.

Most of the TEAEs that occurred in 36 participants were assessed as being related to study procedures and comprised reactions occurring within 48 h after the start of the I.V. LPS challenge (see Figure 5). These procedure-related AEs were reported in two participants in the BAY1834845 group, three in the BAY1830839 group, four in the prednisolone, and six in the placebo groups, respectively. In the two IRAK4 inhibitor-treated groups, these AEs included nausea, chills, asthenia, spontaneous hematoma, myalgia, headache, and oropharyngeal pain. Two participants in the placebo group reported procedure-related TEAEs of moderate intensity. All other AEs in any of the treatment groups were of mild intensity.

PK OF BAY1834845 AND BAY1830839

At 3 h post-dose on Day 6, geometric mean (CV) total plasma concentrations were 6.1 (14.9%) mg/L for BAY1834845 and 5.0 (23.6%) mg/L for BAY1830839 (Figure S4). The corresponding geometric mean (CV) total concentrations in blister fluid were 2.6 (32.3%) and 3.0 (28.3%) mg/L. The geometric mean (CV) of individual suction blister fluid versus plasma ratios were 0.43 (22.7%) for BAY1834845 and 0.59 (16.2%) for BAY1830839.

DISCUSSION

This study evaluated the pharmacological activity of the two orally administered IRAK4-specific inhibitors BAY1834845 (zabedosertib) and BAY1830839 in experimental inflammation in healthy volunteers. Pharmacological activity was investigated by *ex vivo* whole blood challenges and *in vivo* experimental models of tissue inflammation and systemic inflammation. The data-rich, proof-of-mechanism study design and selection of challenge models were chosen to (a) evaluate the translation of results obtained from investigations of BAY1834845 and BAY1830839 based on TLR-driven pharmacodynamic cell and animal models; (b) characterize the inhibitory effect of these compounds on different TLR pathways in humans, both systemically and in peripheral tissue; and (c) inform decisions regarding the potential clinical development of both compounds.

The doses of BAY1834845 and BAY1830839 used in this study were based on data from cell-based experiments, animal models, and clinical studies.[7,12,13,14,19] In multiple ascending dose phase I studies, doses of 120 mg B.I.D. BAY1834845 and 100 mg B.I.D. BAY1830839 resulted in a mean suppression of TNFα of 40% and 70% (TLR4-cytokine release in *ex vivo* whole blood assay), respectively, at corresponding systemic exposures of 5.2 (19.4%) and 4.3 (42.8%) mg/L. In the present study, average plasma concentrations (total) of 6.2 and 5.0 mg/L were observed on Day 6, 3 h after BAY1834845 and BAY1830839 intake. Drug concentrations in suction blister fluid, which acted as a proxy for dermal drug concentration, were approximately half that of systemically circulating drug concentrations. Based on the literature,[20,21,22] it is known that the ratio between systemic and interstitial fluid PK differs, and the basement membrane acting as a barrier for compound penetration might cause differences in T_{max}. Although the concentration measured at Day 6 was considerably lower than that in the suction blister fluid, the skin readouts from the IMQ skin challenge suggested efficient exposure to elicit an immunomodulatory effect.

BAY1834845 treatment significantly suppressed the IMQ-induced increase in skin perfusion as quantified by LSCI, and both IRAK4 inhibitors significantly suppressed induction of erythema as quantified by multispectral imaging. These findings were supported by visual grading of erythema and by reductions in biochemical (IP-10 and MXA) and cellular (T cells, dendritic cells, classical monocytes, NK cells) responses in suction blister fluid. The results suggest that, of the two study drugs, BAY1834845 was more effective in the topical inflammatory challenge. Overall, the effect sizes of BAY1834845 and BAY1830839 on IMQ-driven skin responses were comparable or better than that of oral prednisolone (20 mg B.I.D.), which was used as an active control. Of note, prednisolone has been shown to suppress IMQ-induced skin inflammation in mice,[23] and a recent study also demonstrated this suppressive effect in humans.[24]

In addition to the effect on the topical IMQ challenge response, the systemic pharmacological activity of BAY1834845 and BAY1830839 was evaluated by means of an I.V. LPS challenge in the same volunteers. The model is well established for the investigation of physiological mechanisms of systemic inflammation and drug candidates in clinical development. Intravenous administration of purified E. coli LPS results in flu-like signs and symptoms and increased levels of inflammatory markers, such as cytokines and acute phase reactants. The extent of the effect of LPS challenge on inflammatory markers in the current study was consistent with that seen in previous studies.[25,26] BAY1834845 and BAY1830839 strongly inhibited the responses driven by LPS; cytokine, CRP, and PCT responses were suppressed, and LPS-driven increases in systolic blood pressure and pulse rate were limited as a result of

the IRAK4 inhibition. Oral prednisolone administered at 20 mg B.I.D. had mostly comparable effects, consistent with earlier reports.[27]

Two clear differences between prednisolone and the IRAK4 inhibitors were observed. Prednisolone induced IL-10 systemically after the LPS challenge and also caused a prominent increase in classical monocytes in skin suction blisters within 48 h after the IMQ challenge, whereas BAY1834845 and BAY1830839 did not. An earlier clinical study showed that steroids upregulate constitutive IL-10 production by selectively triggering activation signals on monocytes;[27] this was not evident for BAY1834845 and BAY1830839.

The pharmacological activity of both IRAK4 inhibitors was evaluated *ex vivo* by means of whole blood challenges with specific triggers of the innate immune system. Treatment with BAY1834845 and BAY1830839 resulted in a reduction in R848-induced TLR7/8 responses, which were most prominent for NF-κB-dependent IL-1β, TNF-α, IL-6, and IFN-γ; and, to a lesser extent, for IL-8 and IL-10. Interferon regulatory factor-dependent responses (IP-10 and IFN-α) were only mildly inhibited by the two IRAK4 inhibitors, which may be explained by the potentially lower sensitivity of the assay platform for IFN-α. Both BAY1834845 and BAY1830839 suppressed LPS-induced TLR4-driven IL-1β, TNF-α, IL-6, and IL-8 release and IL-1β-induced TNF-α, IL-6, and IL-8. Overall, BAY1830839 resulted in a stronger suppression of *ex vivo* R848-driven responses and slightly higher suppression of LPS-driven responses than BAY1834845 in this assay.

BAY1834845 and BAY1830839 inhibited the IL-1β-driven IL-8 and IL-6 cytokine release by 50%–80% and 0%–40%, respectively. This contrasted with the weak effects on IL-1β-induced cytokines reported for another IRAK4 specific inhibitor (PF-06650833),[28] which even demonstrated an upregulation of these cytokines in comparison with vehicle control. These differences might be compound-dependent or could be explained by differences in experimental assay setup. Our data also suggested a similar level of pharmacological activity compared with an IRAK4 degrader, which suppressed TLR4- and TLR7/8-mediated cytokine release in peripheral blood mononuclear cells from healthy volunteers.[29]

While the clinical relevance of the differences observed between BAY1834845 (zabedosertib) and BAY1830839 in the described suppression of cytokine release remains unclear and warrants further investigation, this indirect comparison with available data from other IRAK4-targeting molecules clearly suggests a competitive profile for zabedosertib and BAY1830839.

The maximal effect size of BAY1834845 and BAY1830839 differed between experimental models. Both compounds almost completely suppressed (≥80%) TLR4-driven systemic responses of TNF-α and IL-6 release following the I.V. LPS challenge, and the observed effects were comparable or stronger than those observed for prednisolone. In the *ex vivo* whole blood challenge, inhibition of these cytokines was more pronounced by BAY1830839 (75% for TNF-α; 73% for IL-6) than by BAY1834845 (approximately 50% for both cytokines) if TLR4-driven, but similarly high (80%–90%) for both inhibitors if TLR 7/8-driven. By contrast, the inflammation induced by topical IMQ was more prominently suppressed by BAY1834845 than by BAY1830839, and the effects of both compounds on TLR7-mediated responses to the IMQ skin challenge were less pronounced compared with those in the I.V. LPS challenge. This was not surprising, given the previously reported effects of prednisolone on TLR4-driven inflammatory responses following skin inflammatory challenge with intradermal LPS; although oral prednisolone treatment significantly inhibited LPS-driven increases in skin perfusion and erythema, no full inhibition of the LPS response was observed.[30]

Based on the distinct immunomodulatory effects demonstrated by both IRAK4 inhibitors in this study, combined with favourable comparisons with prednisolone, a known strong immunosuppressant, both compounds may be clinically active and advanced further in clinical development.

Of note, the study was not designed or powered to make a quantitative comparative assessment of the two compounds in the chosen respective dose regimens, because we anticipated only marginal differences based on in vitro and *ex vivo* findings.

To investigate the effects of BAY1834845 and BAY1830839 in this study, we administered each at one dose level to obtain proof of pharmacological activity and enable decisions on the future development of these compounds. The use of additional dose levels of the two treatments could have allowed for a more extensive characterization of the respective effects in the immune challenge tests via a more detailed exposure–pharmacodynamic response evaluation.

Although the immune challenges used in this study provided clear evidence for the pharmacological activity of BAY1834845 and BAY1830839 in healthy volunteers and were comparable to preclinical data, the therapeutic effects remain to be investigated. A direct translation of the observed pharmacological activity into clinical efficacy in immune-mediated diseases is not possible by extrapolation of these findings. In addition, the immune challenges used target distinct immune mediators (TLR4 in the systemic LPS challenge and TLR7 in the IMQ skin challenge), whereas immune-mediated diseases often result from disordered activity of several interconnected and potentially dynamic signalling pathways; inhibition of one pathway does not necessarily translate into suppression of disease progression or reduction of the associated symptoms.

The combination of the observed suppression of immune responses in this study together with *ex vivo* and preclinical data served as essential steps in understanding the pharmacological responses in humans and, therefore,

contributed to the clinical development of the two tested IRAK4 inhibitors. While model limitations exist, and conclusive evidence for a direct translation into clinical efficacy could not be provided, the results of this study offer proof of pharmacological activity that are important sources to direct the scope of future development of the tested compounds. Moreover, study outcomes and efficacy data of subsequent clinical trials with patients may be hard to interpret without human pharmacology data. It is certain that a lack of evidence for the pharmacological activities of the two molecules tested in this study would have precluded further clinical development. That being said, the pharmacological effects demonstrated in this study and data from preceding phase I studies fully supported the selection of doses for phase II studies.

In addition to the beneficial immunomodulatory effects in chronic inflammatory diseases, the fast onset of action of these compounds suggests a potential application in acute conditions requiring an anti-inflammatory intervention. Notably, the observed effects in the skin challenge also underpin the potential of these compounds as future therapies for inflammatory diseases in other peripheral tissues.

Taken together, the investigations conducted in this mechanistic clinical phase I study showed that BAY1834845 (zabedosertib) 120 mg B.I.D. and BAY1830839 100 mg B.I.D. administered for 7 days achieved a rapid and distinct anti-inflammatory effect in a human skin challenge model with IMQ, as well as in a human systemic LPS challenge model. For several end points, the immunosuppressive effect of both IRAK4 inhibitors was more pronounced than the effect of prednisolone 20 mg B.I.D. The onset of action of both treatments occurred within 3 days of starting oral treatment. Both IRAK4 inhibitors achieved approximately 50% systemic exposure in suction blister fluid (as a proxy for skin exposure). No safety signals were observed during the 7 days of treatment. The human challenge methodologies used in this study (skin and systemic challenges) were well tolerated by the study participants.

The current study demonstrated proof-of-mechanism for targeted IRAK4 inhibition by BAY1834845 (zabedosertib) and BAY1830839, supporting their suitability as drug candidates for efficacy studies in appropriately selected patient populations. Results were indicative of potential immunomodulatory effects in chronic and acute inflammatory settings as well as a beneficial steroid-sparing effect for chronic autoimmune conditions (e.g., systemic and cutaneous lupus erythematosus). The outcomes of both treatments following a topical inflammatory challenge were particularly encouraging in respect of the applicability of these IRAK4 inhibitors to dermatological inflammatory diseases. In line with this, a clinical study investigating zabedosertib in patients with moderate to severe atopic dermatitis, NCT05656911, is currently ongoing.[31]

REFERENCES

1 Kelly PN, Romero DL, Yang Y, et al. Selective interleukin-1 receptor-associated kinase 4 inhibitors for the treatment of autoimmune disorders and lymphoid malignancy. J Exp Med. 2015;212(13):2189-2201.
2 Chaudhary D, Geddes B, Robinson S, et al. Identification of highly potent and selective interleukin-1 receptor-associated kinase 4 inhibitors for the treatment of rheumatic diseases. Poster presented at 76th annual meeting of the American College of Rheumatology. Arthritis Rheum. 2012;64:S459.
3 Danto S, Shojaee N, Singh R, et al. Efficacy and safety of the selective interleukin-1 receptor associated kinase 4 inhibitor, PF-06650833, in patients with active rheumatoid arthritis and inadequate response to methotrexate. Arthritis Rheum. 2019;71(Suppl. 10):2909. Accessed May 25, 2022. https://acrabstracts.org/abstract/efficacy-and-safety-of-the-selective-interleukin-1-receptor-associated-kinase-4-inhibitor-pf-06650833-in-patients-with-active-rheumatoid-arthritis-and-inadequate-response-to-methotrexate/
4 ClinicalTrials.gov NCT04772885 . A single and multiple ascending dose trial of KT-474 in healthy adult volunteers and patients with atopic dermatitis (AD) or hidradenitis suppurativa (HS). 2021. Accessed November 22, 2022. https://clinicaltrials.gov/ct2/show/NCT04772885
5 ClinicalTrials.gov NCT05178342 . Treatment of anemia in patients with very low, low or intermediate risk myelodysplastic syndromes with CA-4948 (LUCAS). 2022. Accessed November 22, 2022. https://clinicaltrials.gov/ct2/show/NCT05178342
6 ClinicalTrials.gov NCT05380934 . A clinical trial of safety and tolerance of TQH3821 tablets in adult healthy subjects. 2022. Accessed November 22, 2022. https://clinicaltrials.gov/ct2/show/NCT05380934
7 Bothe U, Günther J, Nubbemeyer R, et al. Discovery of IRAK4 inhibitors BAY1834845 (zabedosertib) and BAY1830839. J Med Chem. 2024;67(2):1225-1242.
8 van der Kolk T, Assil S, Rijneveld R, et al. Comprehensive, multimodal characterization of an imiquimod-induced human skin inflammation model for drug development. Clin Transl Sci. 2018;11(6):607-615.
9 van Poelgeest EP, Dillingh MR, de Kam M, et al. Characterization of immune cell, endothelial, and renal responses upon experimental human endotoxemia. J Pharmacol Toxicol Methods. 2018;89:39-46.
10 Niemeyer-van der Kolk T, Assil S, Buters TP, et al. Omiganan enhances imiquimod-induced inflammatory responses in skin of healthy volunteers. Clin Transl Sci. 2020;13(3):573-579.
11 Monnet E, Lapeyre G, Poelgeest EV, et al. Evidence of NI-0101 pharmacological activity, an anti-TLR4 antibody, in a randomized phase I dose escalation study in healthy volunteers receiving LPS. Clin Pharmacol Ther. 2017;101(2):200-208.
12 ClinicalTrials.gov NCT03054402 . First in human study to investigate the safety, tolerability, pharmacokinetics and to explore pharmacodynamics of BAY1834845. 2017. Accessed November 22, 2022. https://clinicaltrials.gov/ct2/show/NCT03054402
13 ClinicalTrials.gov NCT03493269 . A multiple dose study of BAY1834845 in healthy male subjects and in patients with psoriasis. 2018. Accessed November 22, 2022. https://clinicaltrials.gov/ct2/show/NCT03493269
14 ClinicalTrials.gov NCT03540615 . BAY1830839: first in man, single dose escalation, safety & tolerability and pharmacokinetics. 2018. Accessed November 22, 2022. https://clinicaltrials.gov/ct2/show/NCT03540615
15 ClinicalTrials.gov NCT03965728 . Study to investigate safety, tolerability, pharmacokinetics, and drug–drug interaction of multiple oral doses of BAY1830839 in healthy male participants. 2019. Accessed November 22, 2022. https://clinicaltrials.gov/ct2/show/NCT03965728
16 Fowler J, Jarratt M, Moore A, et al. Once-daily topical brimonidine tartrate gel 0·5% is a novel treatment for moderate to severe facial erythema of rosacea: results of two multicentre, randomized and vehicle-controlled studies. Br J Dermatol. 2012;166(3):633-641.
17 Motwani MP, Flint JD, De Maeyer RP, et al. Novel translational model of resolving inflammation triggered by UV-killed E. Coli . J Pathol Clin Res. 2016;2(3):154-165.
18 Hijma HJ, Moss LM, Gal P, et al. Challenging the challenge: a randomized controlled trial evaluating the inflammatory response and pain perception of healthy volunteers after single-dose LPS administration, as a potential model for inflammatory pain in early-phase drug development. Brain Behav Immun. 2020;88:515-528.
19 ClinicalTrials.gov NCT03244462 . Food effect, oral & intravenous pharmacokinetics and absolute bioavailability of BAY1834845 including drug–drug interaction with methotrexate. 2017. Accessed November 22, 2022. https://clinicaltrials.gov/ct2/show/NCT03244462
20 Lauharanta J, Paravicini U. Plasma and suction blister fluid levels of etretinate and its main metabolite during treatment of psoriasis. Arch Dermatol Res. 1982;272(1–2):147-149.
21 Mazzei T, Novelli A, Esposito S, Periti P. New insight into the clinical pharmacokinetics of cefaclor: tissue penetration. J Chemother. 2000;12(1):53-62.
22 Dragatin C, Polus F, Bodenlenz M, et al. Secukinumab distributes into dermal interstitial fluid of psoriasis patients as demonstrated by open flow microperfusion. Exp Dermatol. 2016;25(2):157-159.
23 Dudhgaonkar S, Ranade S, Nagar J, et al. Selective IRAK4 inhibition attenuates disease in murine lupus models and demonstrates steroid sparing activity. J Immunol. 2017;198(3):1308-1319.
24 Assil S, Buters TP, Hameeteman PW, et al. Oral prednisolone suppresses skin inflammation in a

healthy volunteer imiquimod challenge model. Front Immunol. 2023;14:1197650.
25 Dillingh MR, van Poelgeest EP, Malone KE, et al. Characterization of inflammation and immune cell modulation induced by low-dose LPS administration to healthy volunteers. J Inflamm. 2014;11:28.
26 Brooks D, Barr LC, Wiscombe S, McAuley DF, Simpson AJ, Rostron AJ. Human lipopolysaccharide models provide mechanistic and therapeutic insights into systemic and pulmonary inflammation. Eur Respir J. 2020;56(1):1901298.
27 de Kruif MD, Lemaire LC, Giebelen IA, et al. Prednisolone dose-dependently influences inflammation and coagulation during human endotoxemia. J Immunol. 2007;178(3):1845-1851.
28 Winkler A, Sun W, De S, et al. The interleukin-1 receptor-associated kinase 4 inhibitor PF-06650833 blocks inflammation in preclinical models of rheumatic disease and in humans enrolled in a randomized clinical trial. Arthritis Rheum. 2021;73(12):2206-2218.
29 Ackerman L, Acloque G, Bacchelli S, et al. IRAK4 degrader in hidradenitis suppurativa and atopic dermatitis: a phase 1 trial. Nat Med. 2023;29(12):3127-3136.
30 Buters TP, Hameeteman PW, Jansen IME, et al. Clinical, cellular, and molecular effects of corticosteroids on the response to intradermal lipopolysaccharide administration in healthy volunteers. Clin Pharmacol Ther. 2022;111(4):964-971.
31 ClinicalTrials.gov NCT05656911 . A study to learn how well the study treatment zabedosertib (BAY1834845) works and how safe it is compared to placebo in adult participants with moderate-to-severe atopic dermatitis (Damask). 2023. Accessed October 31, 2023. https://clinicaltrials.gov/study/NCT05656911

Supplementary Figure 1 Visual grading of skin reactions following IMQ challenge. IMQ, imiquimod.

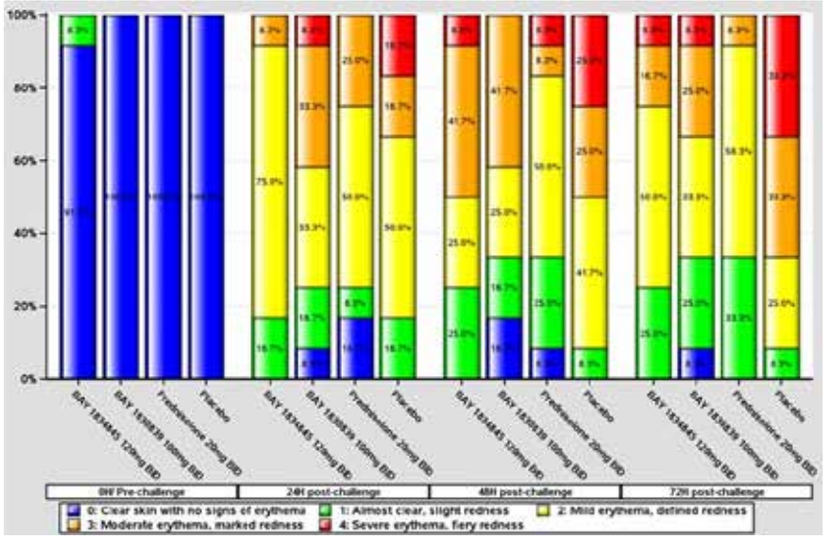

Supplementary Figure 2 Cell subsets after IMQ challenge.

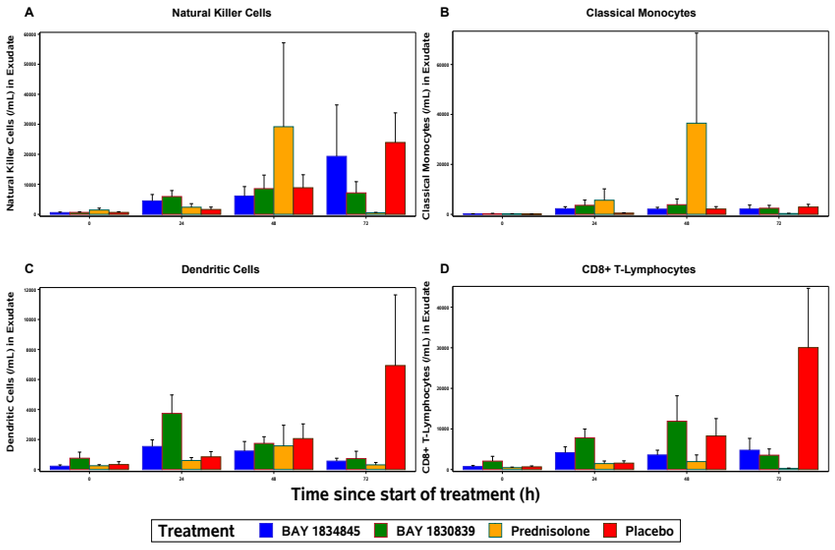

Supplementary Figure 3 Changes over time in A) systolic blood pressure, B) pulse rate, and C) core temperature. LPS, lipopolysaccharide.

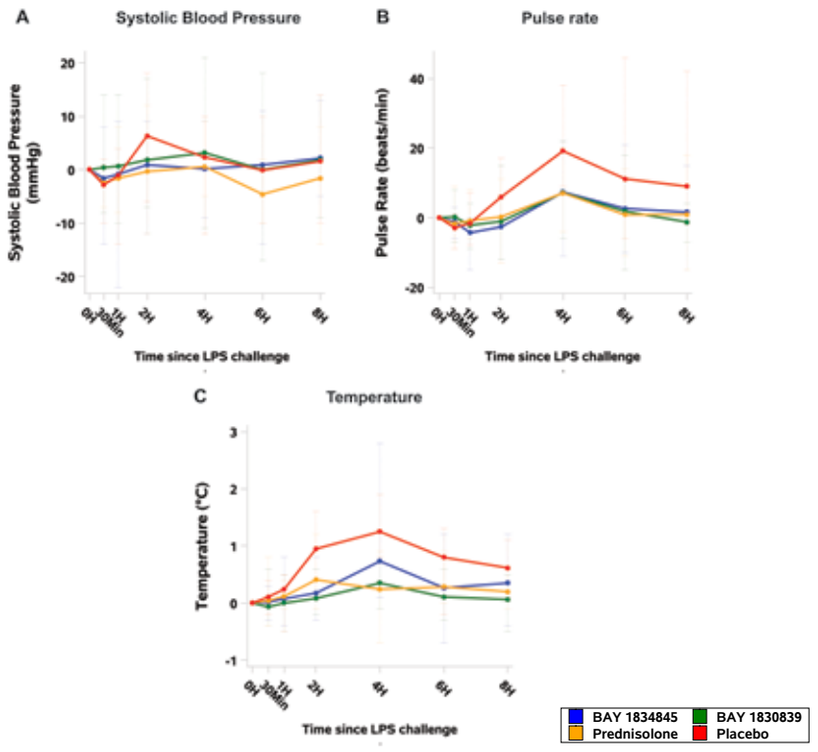

Supplementary Figure 4 Concentrations of BAY1830839 and BAY1834845 in plasma and suction blister fluid.

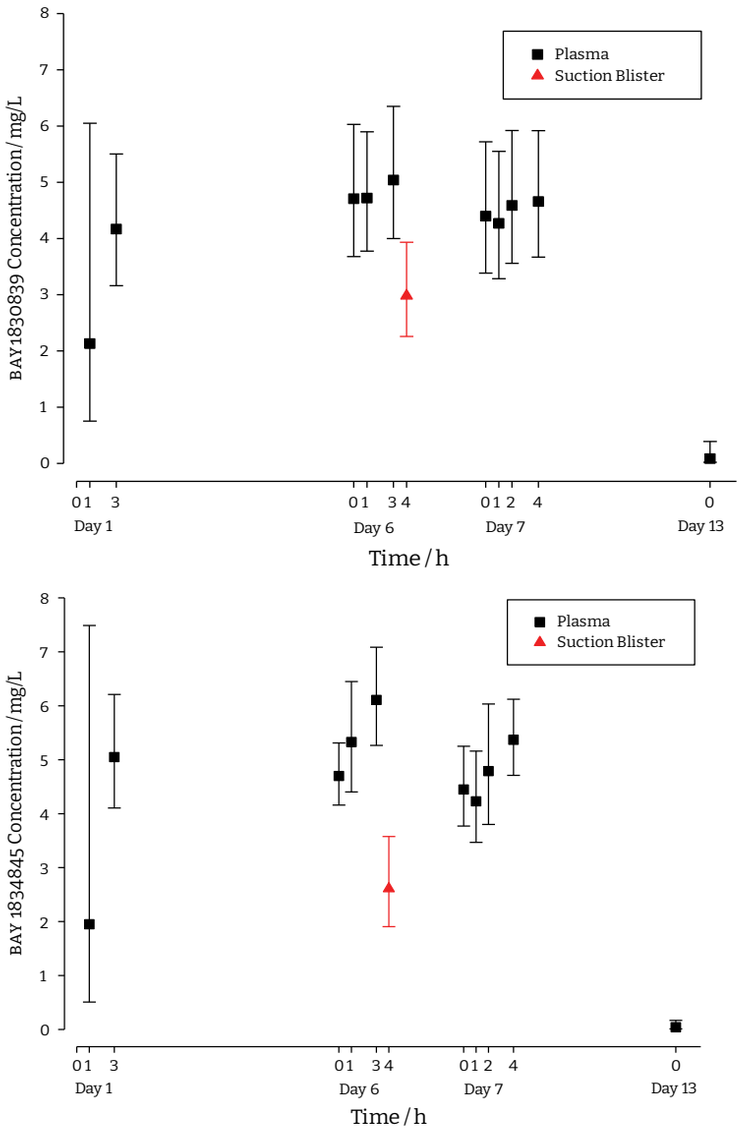

Supplementary Table 1 Clinician's Erythema Assessment (CEA) scale

Score	Skin appearance/morphological description
0	Clear skin with no signs of erythema
1	Almost clear, slight redness
2	Mild erythema, defined redness
3	Moderate erythema, marked redness
4	Severe erythema, fiery redness

Supplementary Table 2 Baseline characteristics of participants (per protocol set)

	Placebo (n = 12)	BAY1834845 120 mg B.I.D. (n = 12)	BAY1830839 100 mg B.I.D. (n = 12)	Prednisolone 20 mg B.I.D. (n = 12)	Total (n = 48)
Age, years	28.3 (10.9)	29.8 (7.8)	28.0 (10.1)	28.0 (9.2)	28.5 (9.3)
Weight, kg	78.5 (5.29)	79.2 (11.22)	78.0 (12.71)	72.0 (8.48)	76.9 (9.95)
Height, cm	185.9 (6.73)	182.1 (7.62)	181.5 (6.25)	180.0 (5.31)	182.4 (6.69)
Body mass index, kg/m²	22.8 (1.78)	23.8 (2.11)	23.6 (2.73)	22.2 (2.03)	23.1 (2.21)

Supplementary Table 3 Treatment exposures

Period of exposure, n (%)	Placebo (n = 12)	BAY1834845 120 mg B.I.D. (n = 13)	BAY1830839 100 mg B.I.D. (n = 13)	Prednisolone 20 mg B.I.D. (n = 12)
3 d	0	0	1 (7.7)	0
4 d	0	1 (7.7)	0	0
7 d	12 (100)	12 (92.3)	12 (92.3)	12 (100)
Duration, mean (SD); median [range]	7 (0); 7 [7, 7]	6.8 (0.8); 7 [4, 7]	6.7 (1.1); 7 [3, 7]	7 (0); 7 [7, 7]

Supplementary Table 4 Incidence of treatment-emergent and treatment-related adverse events in safety analysis

	Placebo (n = 12)	BAY1834845 120 mg B.I.D. (n = 13)	BAY1830839 100 mg B.I.D. (n = 13)	Prednisolone 20 mg B.I.D. (n = 12)
Any treatment-emergent AE	12 (100)	9 (69.2)	8 (61.5)	12 (100)
Mildb	10 (83.3)	9 (69.2)	8 (61.5)	12 (100)
Moderateb	2 (16.7)	0	0	0
Any treatment-related AE	6 (50)	2 (15.4)	3 (23.1)	4 (33.3)
Mildb	6 (50)	2 (15.4)	3 (23.1)	4 (33.3)
AE related to procedures required by the protocol	12 (100)	6 (46.2)	6 (46.2)	12 (100)
AE leading to discontinuation of study drug	0	1 (7.7)	1 (7.7)	0
Any SAE	0	0	0	0
Treatment-related SAE	0	0	0	0
SAE related to procedures required by the protocol	0	0	0	0
SAE leading to discontinuation of study drug	0	0	0	0
AE with the outcome of death	0	0	0	0
Any AE of special interest	0	0	0	0

SECTION III

PHARMACODYNAMICS AT THE EARLIEST PHASE OF DRUG DEVELOPMENT: RELEVANCE FOR OPTIMIZING DRUG ADMINISTRATION

CHAPTER VI

THE EFFECT OF REPEATED METHOTREXATE INJECTIONS ON THE QUALITY OF LIFE OF CHILDREN WITH RHEUMATIC DISEASES

Published in the European Journal of Pediatrics, 2019

Justin Jacobse[1,2,3], Wouter ten Voorde[2,3,4], Robert Rissmann[2,3], Jacobus Burggraaf[2,3], Rebecca Ten Cate[1], Lenneke Schrier[4]

1 Department of Pediatric Rheumatology Willem-Alexander Children's Hospital, Leiden University Medical Center, Leiden, NL
2 Centre for Human Drug Research, Leiden, NL
3 Leiden Academic Center for Drug Research, Leiden, NL
4 Leiden University Medical Center, Leiden, NL
5 Department of Pediatric Rheumatology Willem-Alexander Children's Hospital, Leiden University Medical Center, Leiden, NL

ABSTRACT

In clinical practice, the burden of repeated injections in children with rheumatic disease receiving disease-modifying anti-rheumatic drugs is significant. To investigate the nature and extent of impact on the quality of life after repeated injections, we conducted a literature review. Two relevant papers were identified, both about children with juvenile idiopathic arthritis (JIA) being administered methotrexate. The results suggest that the combination of needle fear, impact of methotrexate treatment, and procedural consequences, e.g., blood sampling, all contribute to the distress and the loss of quality of life of children with JIA. Remarkably, no studies examining fear of injections or injection pain in children with rheumatic diseases receiving biologicals were identified.

Conclusion: Strategies to optimize administration of disease modifying anti-rheumatic drugs should be systematically investigated.

INTRODUCTION

Intravenous (IV), intramuscular (IM), and subcutaneous (SC) injections are the three most frequently used procedures to administer parenteral medication, accounting for 16 billion injections worldwide on an annual basis.[29] Injections are often perceived as dolorous and pain during injections can lead to the development of needle phobia or disproportionate amounts of fear or vasovagal syncope when presented with needles.

Fear of needles or injections is a common problem in the general population[21,23,25,30] and typically begins in childhood.[2,3,22] There is an inverse correlation between age and the extent of needle pain and fear.[1,11,30] Major reasons are the increasing tolerance for pain with aging and the frequency of needle procedures during childhood.[8,19] Even the most extreme form of needle fear, blood-injury-phobia, is not uncommon; its estimated lifetime prevalence is 3.2–4.5%,[3,15] which likely is an underestimation as patients with needle phobia tend to avoid health care.[9,13,17] Needle fear is a documented barrier to immunization in children.[25]

Children and adolescents with rheumatic diseases may be particularly vulnerable to the long-term consequences of procedure-related pain like injection pain, due to their often young age at diagnosis and long duration of parenteral treatment with anti-rheumatic drugs. This medication is given intravenously or subcutaneously, every month, week or, as for children with systemic juvenile idiopathic arthritis (JIA), even every day. Children receiving treatment with injectable drugs in the home setting frequently need to be kept in position by one of their parents or caregivers while the other parent is administering the injection. These frequent painful injections are an important stress factor for many children and their families and therefore a recurrent topic during outpatient consultations. Especially for children receiving daily anakinra medical care at home can be helpful, although this comes not without added financial costs.

We were interested if the perceived high burden of treatment and development of needle phobia and its effect on long-term treatment adherence in children with rheumatic diseases had been quantified. Therefore, a literature review was performed systematically, focusing on children receiving treatment with disease- modifying anti-rheumatic drugs (DMARDS).

METHODS

A systematic search for studies on fear of needles or injection pain in children was conducted together with a librarian. The following databases were accessed: PubMed, Embase, Web of Science, and the Cochrane Library (Appendix 1 Search queries). Duplicates were removed manually. Two authors reviewed

the remaining abstracts for eligibility. Meeting abstracts were not considered for inclusion. Studies reporting on children with rheumatic diseases needing treatment with DMARDS were included. Studies regarding antibiotic prophylaxis in the context of rheumatic heart disease were excluded. As only a few abstracts were eligible, study selection was solely based on the content and no formal quality assessment was done.

RESULTS

The search resulted in 973 unique abstracts (February 20, 2018). Two relevant studies were identified, both about children with JIA taking methotrexate.[20,27] No relevant studies regarding biologicals were identified. Methotrexate is the first-choice DMARD for JIA. Common side effects of methotrexate are gastrointestinal symptoms such as nausea and vomiting, which can partially be prevented by supplying folic acid. Children who receive methotrexate frequently develop anticipatory nausea and vomiting.[5] Methotrexate can be administered orally and subcutaneously.

In the study by Mulligan and colleagues, a questionnaire was completed by a mother proxy for 171 children with JIA (mean age 9.0 years, SD 4.0 years, 72% female) taking methotrexate for at least 6 months.[20] The questions on needle-related problems were on anxiety about injections and blood tests experienced by the children during the month before, with the answers never, almost never, sometimes, often, or almost always.[20,28] Over a third of the children had fear of injections and/or blood tests often or almost always. Half of the children experienced these feelings at least sometimes. Anxiety about injections but not blood tests was more frequently observed for children with subcutaneous injections than for children receiving oral methotrexate. A younger age and a shorter treatment duration were related to anxiety about blood tests. Anxiety about blood tests was a significant independent predictor of poorer scores on a psychosocial score. Anxiety about injections was related to younger age, subcutaneous methotrexate administration, and higher disease activity. Anxiety about injections did not affect treatment adherence.

Van der Meer et al. interviewed the parents of ten children with JIA (mean age at start methotrexate 6.7 years, range 2.8–12.9 years, 90% female) receiving methotrexate who had been referred to a psychologist, and the parents of an additional 19 patients (mean age at start methotrexate 7.3 years, range 1.3–13.4 years, 76% female) with JIA also using methotrexate. Nine out of the ten children who were referred for behavioural therapy, and eight of the other group, showed panic and distress in the anticipation of methotrexate treatment. The behavioural distress was observed in the children treated with injections as well as in the children receiving oral methotrexate. The authors describe refusal of methotrexate administration by children, but do not provide quantitative data.

DISCUSSION

In the clinical setting, the focus of clinicians is often geared towards modifying and improving diseases by assessing risk and benefit. However, little is known about the impact on the quality of life of young children that are diagnosed with JIA and need to start with repeated, often long-lasting or life-long invasive therapies. While this is a very relevant topic, we identified a gap in literature which had not been appropriately addressed to date. Therefore, we systematically investigated the burden of parenteral repeated administration in children.

Pain is a common stressor in children with rheumatic diseases and is most commonly due to arthritis.[12] Clinical experience shows that young children with arthritis frequently do not show pain. Rather, their parents observe a swollen joint, e.g., knee or ankle, or limping. Older children with arthritis do more often express feeling pain. Even with stable JIA, pain remains a major problem and has a significant impact on quality of life.[4,7,16,18,24] It might seem logical to assume that children experiencing vast amounts of pain develop a higher pain threshold. However, patients with JIA have a lower threshold for experimentally induced pain than healthy controls.[10,16,26] This altered pain threshold is observed for both the affected joints as well as areas unaffected by the disease and persists after sensory neuronal input from the injured site. Perception of pain is multifactorial and it is unknown if the altered pain threshold in children with JIA has predominant physiological or psychological causes. However, it is recognized that both central and peripheral sensitization play a role in children with juvenile chronic arthritis.[14] The resulting altered pain threshold emphasizes even more the need to minimize procedural related pain.

The studies by Mulligan et al. and Van der Meer et al. show that distress associated with methotrexate administration, both orally and subcutaneous, negatively impacts the quality of life of children with JIA. The interpretation of these studies in the context of needle fear is complicated due to methotrexate associated anticipatory nausea and vomiting. The combination of needle fear, impact of methotrexate treatment, and procedural consequences, e.g., blood sampling, all contribute to the distress, and the loss of quality of life of children with JIA.

While our findings corroborate common knowledge, it is striking how little research and established evidence about scope and scale of needle fear is available. Interpretation of the literature is complicated due to the inconsistent use of terms relating to the stressors associated with therapeutic drug injections. Many questions remain to be answered regarding the perceived burden of

painful injections and needle fear in children with rheumatic diseases requiring treatment with DMARDS. First, the effect of procedural pain, i.e., injection pain, might be better studied in children receiving treatment with biologicals rather than children receiving methotrexate as the results might be confounded by anticipatory vomiting associated with methotrexate. No literature was identified which addressed this issue. Moreover, chronic therapy might affect the perceived burden over time; therefore, it could be worthwhile to longitudinally study the anxiety about injections from the start of treatment with biologicals. Also, it may be worthwhile to develop standardized, age-related tools to uniformly quantify the untoward injection-related phenomena. Future studies should use well-defined outcome parameters to systematically evaluate the different factors contributing to the decrease in quality of life due to therapeutic drug injections. Last, it might be insightful to compare procedural pain in children receiving treatment with DMARDS compared to healthy, age-matched controls, for example in the context of vaccination. Ideally, the aspects of comfort during the administration of drugs in pediatrics should be evaluated during the drug development plan. These aspects of comfort include the route of administration, frequency, and tolerance.[6]

After performing an impact analysis, new strategies might be developed to optimize administration of DMARDS to children. This aspect of health care might represent a financially less attractive target than the development of new drugs. However, ultimately, there is ample room to improve the health-related quality of life of pediatric patients with rheumatic diseases by minimalizing chronic stressors, like procedure-related pain.

ACKNOWLEDGEMENTS

We wish to thank Jan Schoones (senior medical librarian at the Walaeus library; LUMC) for his help developing the search queries.

FUNDING

This study was funded by a grant of the Dutch Arthritis Foundation to Rebecca ten Cate.

REFERENCES

1 Agras S, Sylvester D, Oliveau D. The epidemiology of common fears and phobia. Compr Psychiatry. 1969;10(2):151–156. doi: 10.1016/0010-440X(69)90022-4.

2 American Psychiatric Association (2013) Diagnostic and statistical manual of mental disorders, 5th edn. Washington, DC. 10.1176/appi.books.9780890425596

3 Bienvenu OJ, Eaton WW. The epidemiology of blood-injection-injury phobia. Psychol Med. 1998;28(5):1129–1136. doi: 10.1017/S0033291798007144.

4 Bromberg MH, Connelly M, Anthony KK, Gil KM, Schanberg LE. Self-reported pain and disease symptoms persist in juvenile idiopathic arthritis despite treatment advances: an electronic diary study. Arthritis Rheum. 2014;66(2):462–469. doi: 10.1002/art.38223.

5 Bulatović M, Heijstek MW, Verkaaik M, Van Dijkhuizen EHP, Armbrust W, Hoppenreijs EPA, et al. High prevalence of methotrexate intolerance in juvenile idiopathic arthritis: development and validation of a methotrexate intolerance severity score. Arthritis Rheum. 2011;63(7):2007–2013. doi: 10.1002/art.30367.

6 Committee for Medicinal Products for Human Use (2014) Guideline on pharmaceutical development of medicines for pediatric use. European Medicines Agency Scientific Guidelines. Accessed 15 Jul 2018

7 Dhanani S, Quenneville J, Perron M, Abdolell M, Feldman BM. Minimal difference in pain associated with change in quality of life in children with rheumatic disease. Arthritis Rheum. 2002;47(5):501–505. doi: 10.1002/art.10661.

8 Goodenough B, Thomas W, Champion DG, Perrott D, Taplin JE, von Baeyer CL, Ziegler JB. Unravelling age effects and sex differences in needle pain: ratings of sensory intensity and unpleasantness of venipuncture pain by children and their parents. Pain. 1999;80(1):179–190. doi: 10.1016/S0304-3959(98)00201-2.

9 Hamilton JG. Needle phobia: a neglected diagnosis. J Fam Pract. 1995;41(2):169–175.

10 Hogeweg JA, Kuis W, Huygen ACJ, De Jong-de Vos Van Steenwijk C, Bernards ATM, Oostendorp RAB, et al. The pain threshold in juvenile chronic arthritis. Br J Rheumatol. 1995;34:61–67. doi: 10.1093/rheumatology/34.1.61.

11 Jacobson RM, Swan A, Adegbenro A, Ludington SL, Wollan PC, Poland GA. Making vaccines more acceptable - methods to prevent and minimize pain and other common adverse events associated with vaccines. Vaccine. 2001;19:2418–2427. doi: 10.1016/S0264-410X(00)00466-7.

12 Kimura Y, Walco GA. Treatment of chronic pain in pediatric rheumatic disease. Nat Clin Pract Rheumatol. 2007;3(4):210–218. doi: 10.1038/ncprheum0458.

13 Kleinknecht RA, Lenz J. Blood/injury fear, fainting and avoidance of medically-related situations: a family correspondence study. Behav Res Ther. 1989;27(5):537–547. doi: 10.1016/0005-7967(89)90088-0.

14 Kuis W, Heijnen CJ, Hogeweg JA, Sinnema G, Helders PJM. How painful is juvenile chronic arthritis? Arch Dis Child. 1997;77(5):451–453. doi: 10.1136/adc.77.5.451.

15 LeBeau RT, Glenn D, Liao B, Wittchen HU, Beesdo-Baum K, Ollendick T, et al. Specific phobia: a review of DSM-IV specific phobia and preliminary recommendations for DSM-V. Depress Anxiety. 2010;27(2):148–167. doi: 10.1002/da.20655.

16 Leegaard A, Lomholt JJ, Thastum M, Herlin T. Decreased pain threshold in juvenile idiopathic arthritis: a cross-sectional study. J Rheumatol. 2013;40(7):1212–1217. doi: 10.3899/jrheum.120793.

17 Lilliecreutz C (2010) Blood- and injection phobia in pregnancy epidemiological, Biological and Treatment Aspects. Linköping University medical dissertations

18 Lomholt JJ, Thastum M, Herlin T. Pain experience in children with juvenile idiopathic arthritis treated with anti-TNF agents compared to non-biologic standard treatment. Pediatr Rheumatol. 2013;11(1):1–8. doi: 10.1186/1546-0096-11-21.

19 McMurtry CM, Riddell RP, Taddio A, Racine N, Asmundson GJG, Noel M, et al. Far from "just a poke": common painful needle procedures and the development of needle fear. Clin J Pain. 2015;31(10):S3–S11. doi: 10.1097/AJP.0000000000000272.

20 Mulligan K, Kassoumeri L, Etheridge A, Moncrieffe H, Wedderburn LR, Newman S. Mothers' reports of the difficulties that their children experience in taking methotrexate for juvenile idiopathic arthritis and how these impact on quality of life. Pediatr Rheumatol Online J. 2013;11(1):23. doi: 10.1186/1546-0096-11-23.

21 Nir Y, Paz A, Sabo E, Potasman I. Fear of injections in young adults: prevalence and associations. Am J Trop Med Hyg. 2003;68(3):341–344. doi: 10.4269/ajtmh.2003.68.341.

22 Öst L-G. Blood and injection phobia: background and cognitive, physiological, and behavioral variables. J Abnorm Psychol. 1992;101(1):68–74. doi: 10.1037/0021-843X.101.1.68.

23 Oswalt RM, Napoliello M. Motivations of blood donors and nondonors. J Appl Psychol. 1974;59(1):122–124. doi: 10.1037/h0035791.

24 Schanberg LE, Anthony KK, Gil KM, Maurin EC. Daily pain and symptoms in children with polyarticular arthritis. Arthritis Rheum. 2003;48(5):1390–1397. doi: 10.1002/art.10986.

25 Taddio A, Ipp M, Thivakaran S, Jamal A, Parikh C, Smart S, Sovran J, Stephens D, Katz J. Survey of the prevalence of immunization non-compliance due to needle fears in children and adults. Vaccine. 2012;30(32):4807–4812. doi: 10.1016/j.vaccine.2012.05.011.

26 Thastum M, Zachariae R, Herlin T. Pain experience and pain coping strategies in children with juvenile idiopathic arthritis. J Rheumatol. 2001;28(5):1091–1098.

27 Van der Meer A, Wulffraat NM, Prakken BJ, Gijsbers B, Rademaker CMA, Sinnema G. Psychological side

effects of MTX treatment in juvenile idiopathic arthritis: a pilot study. Clin Exp Rheumatol. 2007;25(3):480–485.
28 Varni JW, Seid M, Smith Knight T, Burwinkle T, Brown J, Szer IS. The PedsQL in pediatric rheumatology: reliability, validity, and responsiveness of the pediatric quality of life inventory generic core scales and rheumatology module. Arthritis Rheum. 2002;46(3):714–725. doi: 10.1002/art.10095.
29 WHO. WHO calls for woldwide use of "smart" syringes. http://www.who.int/mediacentre/news/releases/2015/injection-safety/en/. Accessed 1 Feb 2018
30 Wright S, Yelland M, Heathcote K, Ng S-K, Wright G. Fear of needles nature and prevalence in general practice. Aust Fam Physician. 2009;38(3):172–176.

APPENDIX 1: SEARCH QUERIES

PUBMED

(("needle phobia"[tw] OR "needle phobias"[tw] OR "needle phobic"[tw] OR "needle phobics"[tw] OR "fear of needle"[tw] OR "fear of needles"[tw] OR "needle anxiety"[tw] OR "needle pain"[tw] OR "needle fear"[tw] OR "needle fearful"[tw] OR "needle fearing"[tw] OR "needle fears"[tw] OR "fear of injection"[tw] OR "fear of injections"[tw] OR "injection fear"[tw] OR "injection fearful"[tw] OR "injection fears"[tw] OR "injection anxiety"[tw] OR "injection pain"[tw] OR "injection pains"[tw] OR (("Anxiety"[majr] OR "Fear"[majr] OR "Phobic Disorders"[majr]) AND ("Needles"[majr] OR "Injections"[majr])) OR (("Anxiety"[ti] OR "Fear"[ti] OR Phobi*[ti]) AND ("Needles"[ti] OR "Injections"[ti] OR "Needle"[ti] OR "Injection"[ti]))) AND ("Child"[mesh] OR "Infant"[mesh] OR "Adolescent"[mesh] OR "Child"[tw] OR "Infant"[tw] OR "Adolescent"[tw] OR "Children"[tw] OR "Infants"[tw] OR "Adolescents"[tw] OR "Adolescence"[tw] OR "juvenile"[tw] OR pediatr*[tw] OR paediatr*[tw] OR schoolchild*[tw] OR "girl"[tw] OR "girls"[tw] OR "boy"[tw] OR "boys"[tw]) AND english[la])

EMBASE

(("needle phobia".mp OR "needle phobias".mp OR "needle phobic".mp OR "needle phobics".mp OR "fear of needle".mp OR "fear of needles".mp OR "needle anxiety".mp OR "needle pain".mp OR "needle fear".mp OR "needle fearful".mp OR "needle fearing".mp OR "needle fears".mp OR "fear of injection".mp OR "fear of injections".mp OR "injection fear".mp OR "injection fearful".mp OR "injection fears".mp OR "injection anxiety".mp OR *"injection pain"/ OR "injection pain".ti OR "injection pains".ti OR ((exp *"Anxiety"/ OR exp *"Fear"/ OR exp *"Phobia"/) AND (exp *"Needle"/ OR exp *"Injection"/)) OR (("Anxiety".ti OR "Fear".ti OR Phobi*.ti) AND ("Needles".ti OR "Injections".ti OR "Needle".ti OR "Injection".ti))) AND (exp "Child"/ OR exp "Infant"/ OR exp "Adolescent"/ OR "Child".mp OR "Infant".mp OR "Adolescent".mp OR "Children".mp OR "Infants".mp OR "Adolescents".mp OR "Adolescence".mp OR "juvenile".mp OR pediatr*.mp OR paediatr*.mp OR schoolchild*.mp OR "girl".mp OR "girls".mp OR "boy".mp OR "boys".mp) AND english.la)

WEB OF SCIENCE

((ts=("needle phobia" OR "needle phobias" OR "needle phobic" OR "needle phobics" OR "fear of needle" OR "fear of needles" OR "needle anxiety" OR "needle pain" OR "needle fear" OR "needle fearful" OR "needle fearing" OR "needle fears" OR "fear of injection" OR "fear of injections" OR "injection fear" OR "injection fearful" OR "injection fears" OR "injection anxiety" OR "injection pain" OR "injection pains") OR ti=(("Anxiety" OR "Fear" OR "Phobia") AND ("Needle" OR "Injection")) OR ti=(("Anxiety" OR "Fear" OR Phobi*) AND ("Needles" OR "Injections" OR "Needle" OR "Injection"))) AND ts=("Child" OR "Infant" OR "Adolescent" OR "Child" OR "Infant" OR "Adolescent" OR "Children" OR "Infants" OR "Adolescents" OR "Adolescence" OR "juvenile" OR pediatr* OR paediatr* OR schoolchild* OR "girl" OR "girls" OR "boy" OR "boys") AND la=english) NOT ti=(veterinary OR rabbit OR rabbits OR animal OR animals OR mouse OR mice OR rodent OR rodents OR rat OR rats OR pig OR pigs OR porcine OR horse* OR equine OR cow OR cows OR bovine OR goat OR goats OR sheep OR ovine OR canine OR dog OR dogs OR feline OR cat OR cats))

COCHRANE

((("needle phobia" OR "needle phobias" OR "needle phobic" OR "needle phobics" OR "fear of needle" OR "fear of needles" OR "needle anxiety" OR "needle pain" OR "needle fear" OR "needle fearful" OR "needle fearing" OR "needle fears" OR "fear of injection" OR "fear of injections" OR "injection fear" OR "injection fearful" OR "injection fears" OR "injection anxiety" OR "injection pain" OR "injection pains"):ti,ab,kw OR (("Anxiety" OR "Fear" OR "Phobia") AND ("Needle" OR "Injection")):ti OR (("Anxiety" OR "Fear" OR Phobi*) AND ("Needles" OR "Injections" OR "Needle" OR "Injection")):ti) AND ("Child" OR "Infant" OR "Adolescent" OR "Child" OR "Infant" OR "Adolescent" OR "Children" OR "Infants" OR "Adolescents" OR "Adolescence" OR "juvenile" OR pediatr* OR paediatr* OR schoolchild* OR "girl" OR "girls" OR "boy" OR "boys"):ti,ab,kw)

CHAPTER VII

COMPREHENSIVE EVALUATION OF MICRONEEDLE-BASED INTRADERMAL ADALIMUMAB DELIVERY VS. SUBCUTANEOUS ADMINISTRATION: RESULTS OF A RANDOMIZED CONTROLLED CLINICAL TRIAL

Published in the British Journal of Clinical Pharmacology, 2021

Wouter ten Voorde[2,3,8,*] , Justin Jacobse[1,2,3,4,*], Anushka Tandon[2], Stefan G Romeijn[3], Hendrika W Grievink[2], Koen van der Maaden[3], Michiel J van Esdonk[2], Dirk Jan A R Moes[5], Floris Loeff[6], Karien Bloem[6], Annick de Vries[6], Theo Rispens[6], Gertjan Wolbink[6], Marieke de Kam[2], Dimitrios Ziagkos[2], Matthijs Moerland[2], Wim Jiskoot[3], Joke Bouwstra[3], Jacobus Burggraaf[2,3], Lenneke Schrier[1,7], Robert Rissmann[2,3,5,**], Rebecca Ten Cate[1,**]
** Shared first authorship, ** Shared last authorship*

1 Department of Pediatric Rheumatology Willem-Alexander Children's Hospital, Leiden University Medical Center, Leiden, NL
2 Centre for Human Drug Research, Leiden, NL
3 Division of BioTherapeutics, Leiden Academic Centre for Drug Research, Leiden University, Leiden, NL
4 Currently also affiliated with department of Pathology, Microbiology and Immunology at Vanderbilt University, Nashville, Tennessee, USA.
5 Department of Clinical Pharmacy & Toxicology, Leiden University Medical Center, Leiden, NL
6 Biologics Lab, Sanquin Diagnostic Services, Amsterdam, NL
7 Currently at Princess Maxima Centre for Pediatric Oncology, Utrecht, NL
8 Leiden University Medical Center, Leiden, NL

ABSTRACT

AIMS To evaluate feasibility of intradermal (i.d.) adalimumab administration using hollow microneedles, and to compare a single i.d. dose of adalimumab using a hollow microneedle with a single subcutaneous (s.c.) dose using a conventional needle.

METHODS In this single-centre double-blind, placebo-controlled, double-dummy clinical trial in 24 healthy adults we compared 40 mg adalimumab (0.4 mL) administered i.d. using a hollow microneedle with a s.c. dose using a conventional needle. Primary parameters were pain, acceptability and local tolerability; secondary parameters safety, pharmacokinetics and immunogenicity. We explored usability of optical coherence tomography, clinical photography, thermal imaging, and laser speckle contrast imaging to evaluate skin reaction after i.d. injections. In vitro protein analysis was performed to assess compatibility of adalimumab with the hollow microneedle device.

RESULTS While feasible and safe, injection pain of i.d. adalimumab was higher compared to s.c. adalimumab (35.4 vs. 7.9 on a 100-point visual analogue scale). Initial absorption rate and relative bioavailability were higher after i.d. adalimumab (time to maximum plasma concentration = 95 h [47–120]; F_{rel} = 129% [6.46%]) compared to s.c. adalimumab (time to maximum plasma concentration = 120 h [96–221]). Anti-adalimumab antibodies were detected in 50% and 83% of the subjects after i.d. and s.c. adalimumab, respectively. We observed statistically significantly more erythema and skin perfusion after i.d. adalimumab, compared to s.c. adalimumab and placebo injections ($P < .0001$). Cytokine secretion after whole blood lipopolysaccharide challenge was comparable between administration routes.

CONCLUSIONS Intradermal injection of adalimumab using hollowing microneedles was perceived as more painful and less accepted than s.c. administration, but yields a higher relative bioavailability with similar safety and pharmacodynamic effects.

INTRODUCTION

Biopharmaceuticals, such as monoclonal antibodies (mAbs), are used in the treatment of many chronic and life-threatening diseases.[1] Degradation and ineffective absorption of mAbs in the gastrointestinal tract, due to molecular size and conditions such as low PH and digestive enzymes, necessitates their parenteral administration. However, in clinical practice, treatments administered using subcutaneous (s.c.) injection of mAbs have been perceived as unpleasant and painful, especially during long-term use in both adults and children.[2] Thus, s.c. administration may jeopardize treatment adherence and a less invasive and less painful method to administer mAbs is warranted.

Intradermal (i.d.) administration of biopharmaceuticals through hollow microneedles is advocated as a substitute for s.c. injection, due to less pain associated with injection of drugs using microneedles,[3] and i.d. administered biopharmaceuticals may show more favourable pharmacokinetics (PK) as compared to s.c. administration.[4,5,6,7] Multiple types of microneedles exist, such as hollow and solid microneedles, and microneedles have different properties in comparison with conventional needles. For instance, the injection of pharmaceutical compounds using hollow microneedles is more superficial, i.e. into the skin (i.d.) rather than beneath the skin (s.c.). Additionally, the diameter of hollow microneedles is smaller than that of conventional hypodermic needles for s.c. injection. An unbiased and systematic approach is warranted to acquire reliable data on pain perception and patient preferences, as these are subjective concepts.[8] Therefore, it is relevant to compare pain, acceptability and local tolerability, as well as PK and pharmacodynamics (PD) between mAbs administered i.d. using a hollow microneedle with s.c. injection using a conventional hypodermic needle. Moreover, when using a new drug–device combination, chemistry, manufacturing and control aspects need consideration.

The commercially available microneedles used in the clinical trial reported in this paper have been used in various clinical studies.[9] Each device consists of 3 hollow microneedles with a length of 600 µm; this device is hereafter referred to as hollow microneedle. Although microneedle vaccine administration has been widely investigated, there are no systematic reports on MAB administration using microneedles in humans. We choose adalimumab (Humira, AbbVie) as model MAB as it is widely used for a variety of auto-immune/auto-inflammatory diseases including juvenile idiopathic arthritis. Adalimumab acts by binding to the proinflammatory cytokine tumour necrosis factor-α (TNFα), hereby preventing its interaction with the TNFα receptor.[10]

To evaluate feasibility of i.d. adalimumab administration using hollow microneedles, we performed a double-blind, double-dummy, randomized

controlled clinical trial in healthy adults, comparing a single i.d. dose of adalimumab using a hollow microneedle with a single s.c. dose using a conventional needle. Our primary aim was to systematically investigate pain, acceptability and local tolerability after i.d. adalimumab administration and to compare this with s.c. administration. Our secondary aim was to evaluate safety, PK, PD and immunogenicity of i.d. adalimumab administration and to compare this with s.c. administration. Moreover, we explored the usability of optical coherence tomography (OCT), clinical photography, thermal imaging and laser speckle contrast imaging (LSCI) in the evaluation of i.d. injections. Lastly, prior to the clinical trial we performed an elaborate in vitro protein analysis to examine whether ejection of adalimumab through a hollow microneedle bore increases particle formation or protein aggregation compared to ejection through a conventional needle. One could envision that during ejection of a protein out of a narrow microneedle, the structure of the protein might be affected. Factors contributing to the immunogenicity of mAbs include protein structure and physical degradation, such as aggregation.[11] The formation of anti-adalimumab antibodies may result in reduced treatment efficacy due to increased drug clearance (CL).[12,13]

Altogether, in this paper we provide a systematic and comprehensive approach to answer the question of whether hollow microneedles can be used safely and effectively to administer a model MAB.

MATERIALS AND METHODS

STUDY DESIGN

This was a single-centre double-blind, placebo-controlled, double-dummy clinical trial with 4 interventions: i.d. adalimumab (40 mg Humira, AbbVie, Maidenhead, Kent, UK), i.d. saline (0.9%), s.c. adalimumab, and s.c. saline. i.d. injections were given using a hollow microneedle (MicronJet600 from Nanopass Technologies Ltd., Ness Ziona, Israel), s.c. injections using a regular needle (Microlance 3 from Becton, Dickinson and Company [BD], Franklin Lakes, NJ, USA); both devices were connected to a syringe (1 mL Luer-Lok, BD). The length of the 3 needles of a MicronJet600 device is 600 µm. Injections were given according to standard operating procedures and the manufacturer's instruction. All subjects received 1 placebo injection and 1 adalimumab injection of 40 mg in 0.4 mL in the right and left upper lateral thigh by the same physician. Given the nature of the study, the physician administering the injection could not be blinded to the method of administration but was blinded to treatment, i.e., adalimumab or placebo. Therefore, this physician was not involved in the assessment of any of the predefined outcomes (evaluator-blinded). The subjects were in a prone position during and in between injections to ensure blinding (subject-blinded). Injections were spaced 5 minutes apart. Prior to administration, the sites of injection were annotated using a surgical marker (Purple Surgical, Shenley, Herts, UK). Subjects were instructed to maintain the marking while at home, and to prevent excessive sun exposure to the injection site to limit possible interference with the exploratory measurements.

PARTICIPANTS

Twenty-four healthy immunocompetent male and female subjects aged 18–45 years with Fitzpatrick skin type I-II (Caucasian) and not smoking more than 10 cigarettes per day were included in the study. The ratio male:female was 1:1. Subject health status was verified during a medical screening consisting of a medical history, physical examination, vital signs, 12-lead electrocardiogram, laboratory analysis of blood and urine, and a Mantoux and/or interferon-γ (IFN-γ) release assay. Subjects with a history of tuberculosis were excluded. Routine safety assessments were performed as described earlier.[14] Total observation time was 70 days.

SAMPLE SIZE AND RANDOMIZATION

Due to the explorative character of this trial, empirical, early clinical phase cohort sizes were used to answer the objectives of the trial. No formal power calculation was performed. A total of 24 subjects were studied (allocation s.c.: i.d. = 1:1): 12 subjects received i.d. adalimumab and s.c. placebo and 12 subjects received s.c. adalimumab and i.d. placebo. The sequence of injection, i.e., s.c. followed by i.d. injection or i.d. injection followed by s.c. injection, was counterbalanced. Randomization was done in 6 blocks of 4, each 4 arms containing 1 of each 4 sequences (adalimumab s.c. followed by placebo i.d.; placebo i.d. followed by adalimumab s.c.; placebo s.c. followed by adalimumab i.d.; adalimumab i.d. followed by placebo s.c.). The randomization code was generated using SAS 9.4 by a study-independent statistician; treatment allocation was only revealed after completion of blind data review and locking of the data. After screening and assessment for suitability, subjects were enrolled in the trial by a physician. Interventions were assigned to subjects by a study-independent statistician.

OUTCOME MEASURES

A subjective evaluation of spill was performed by visual inspection of the injection site, estimating the volume that was not injected as percentage of the intended injection volume: no spill; minor spill: 15% spillage; major spill: 15–50% spillage; critical spill: >50% spillage. Microneedles were inspected post injection for damage using bright field microscopy.

PAIN, ACCEPTABILITY AND LOCAL TOLERABILITY AFTER I.D. AND S.C. ADALIMUMAB ADMINISTRATION

To quantify pain, visual analogue scale (VAS) scores for pain using both a 10-cm VAS and the Dutch Faces Pain Scales Revised (FPSR)[15] were completed by the volunteers at screening for the Mantoux, or saline if no Mantoux was given, at the time of drug administration, and after drug administration. Pain scores were obtained separately for insertion of the needle (insertion pain) and infusion of the formulation (infusion pain). A standardized injection site examination was performed to evaluate injection sites. Pain was graded as (0) absent; (1) present; no limitations in activity of daily living (ADL); (2) present, limitations in age-appropriate instrumental ADL or requires repeated non-narcotic pain reliever; (3) present, limitations in self-care ADL or interferes with sleep or requires repeated narcotic pain reliever. Induration was scored similarly as injection site pain, but with grade (3) instead being 'limitations in self-care ADL or requires systemic treatment'. Tenderness was graded as: (0) absent; (1) mild discomfort with pressure; (2) discomfort with touch; (3) discomfort elicited by clothing or bed sheets. Pruritus was graded as (0) absent; (1) present, but minimally distracting; (2) present, distracting during routine activities; (3) interferes with sleep. Erythema, blister, ulceration, necrosis and ecchymosis were measured if present.

Subject preference for injection was examined using multiple-choice questions. Subjects were asked how they experienced the injections, how they would like to receive a potential future injection and if they feared the injection(s), using the following options: do you prefer the first injection, the second injection or do you not have a preference? Subjects were additionally asked whether they had fear or no fear. These questions were asked directly after injection, i.e. before subjects were able to see the injection, and also one day after the injections.

SAFETY, PK AND IMMUNOGENICITY OF I.D. AND S.C. ADALIMUMAB ADMINISTRATION

Adverse events were summarized by treatment group, in subsets of all treatment-emergent AEs, and separately for treatment-related AEs. Clinical laboratory and vital sign measurements were summarized by treatment and change from baseline was recorded. Summary statistics included number of subjects, mean, median, minimum and maximum values (with standard deviation). Immunogenicity, i.e. anti-adalimumab antibodies, was reported descriptively.

For PK analyses, serum adalimumab concentrations were assessed in blood collected in 4 mL plain tubes (BD) after coagulation (30–60 min) and centrifugation (2000 G for 10 min at 4°C), from day 1 (predose) to day 71 postdose. Adalimumab levels were quantified by fully automated enzyme-linked immunosorbent assay as described.[16] Briefly, TNF was indirectly coated on microtitre plates. Serum was added and incubated. Immobilized adalimumab was subsequently detected using biotinylated rabbit anti-idiotype. The lower limit of detection (LOD) for this assay is 10 ng/mL.

Anti-adalimumab antibodies were measured using a semi-quantitative radioimmunoassay as previously described.[16] Briefly, samples were incubated with sepharose-immobilized protein A (1.0 mg/TEST; Pharmacia Uppsala, Sweden) on its surface to capture IGG. After washing, radioactive-iodine labelled F(ab')2 fragments of adalimumab were added to detect drug-specific antibodies. The LOD for this assay 12 AU/mL.

Ex vivo whole blood challenge was performed to assess the effect of adalimumab on the release of cytokines by circulating immune cells and activation of these cells. Blood (6 mL) was collected in sodium heparin tubes (Becton Dickinson, NJ, USA) followed by stimulation with 2 ng/mL lipopolysaccharide (LPS; Sigma-Aldrich, Deisenhofen, Germany) and 25 µg/mL aluminium hydroxide (Alhydrogel 2%; Invivogen, Toulouse, France) for 24 hours at 37°C, 5% CO_2. Culture supernatants were assayed for release of proinflammatory cytokines TNFα, interleukin (IL)-6, IL-1β, IFNγ and IL-8 using the Mesoscale Discovery multiplex immunoassay platform.

USABILITY OF OPTICAL COHERENCE TOMOGRAPHY, CLINICAL PHOTOGRAPHY, THERMAL IMAGING AND LASER SPECKLE CONTRAST IMAGING IN THE EVALUATION OF I.D. INJECTIONS

Subjects were acclimatized in a temperature-controlled room (21°C) for 15 minutes with bare legs. The sequence of measurements was (starting with the least invasive to minimize disturbance of the subsequent measurements): (I) thermography; (II) cutaneous microcirculation; (III) 3D photography; (IV) multispectral imaging; and (v) skin morphology. Details of skin imaging methods are described below.

Skin microcirculation was quantified by LSCI (PeriCam PSI NR system, Perimed, Sweden). Laser speckle is the interference pattern returning from erythrocytes, resulting in a speckle pattern that differs under changes in blood flow.[17] Recordings of 40 seconds were taken from a distance of 15 cm with a reading frame of 7 × 7 cm. Analysis was performed using the internal software (PimSoft, Perimed, Sweden) and regions of interest were selected based on the most predominant injection site reaction. Area was calculated based on values above an arbitrary threshold of 90 PU.

Skin temperature was quantified by infrared thermography (FLIR X6540SC camera, FLIR Systems Inc., USA). After calibration for room temperature using a black body, 10 second recordings were taken from a distance of 80 cm. Recordings were averaged for analysis.

Skin morphology was assessed by OCT (D-OCT VivoSight, Michelson Diagnostics, UK). Thirty second scans were performed with a 6 mm diameter probe. Three automatically calculated parameters were used to quantify morphology (attenuation compensation, blood flow at depth and skin roughness). Qualitative analysis was performed by 2 clinical scientists with experience in analysing D-OCT images.

Erythema and swelling were quantified using a multispectral camera (Antera 3D, Miravex, Ireland), and a 3D stereophotogrammetry camera (3D LifeViz, QuantifiCare, USA). The multispectral camera was placed over the skin creating a closed environment with the lesion in the centre of the frame. Erythema was measured using the CIELab *a value. CIELab is a standardized quantitative method to discriminate colours using an XYZ-axis system. CIELab *a value is represented on the red/green axis (green colours are negative, red colours positive) and is correlated to skin erythema.[18,19] Three-dimensional images were taken from a distance of 20 cm with use of a guidance laser and analysed in imaging processing software (DermaPix Software, QuantifiCare, Valbonne, France). Volume was determined by outlining bleb circumference and height and calculated using the DermaPix (QuantifiCare, USA) algorithm for volume ($\sigma = 5$).

IN VITRO PROTEIN ANALYSIS

Adalimumab 100 mg/mL prefilled pens or syringes (depending on availability) of the same batch and expiration date were pooled. Storage containers were: (I) syringe only; (II) Verex 2 mL clear glass vial (Phenomenex, Torrance, CA, USA); and (III) syringe with a MicronJet600. For condition (I), a capped regular needle was attached during storage to prevent evaporation. Samples were measured immediately (to assess the effect of repackaging), or after storage for 4 hours at 4°C (to assess in-use stability). Directly before analysis the samples were ejected from the syringe into a glass vial and subsequently diluted to 10 or 1 mg/mL with solvent. The solvent consisted of Milli-Q water with 1.2 G per 100 mL mannitol (Sigma, St Louis, MO, USA) and 100 mg/100 mL polysorbate 80 (Sigma), and was filtered through an Anotop 10 mm, 0.1 µm syringe filter (Whatman, Maidstone, Kent, UK) before use. For nanoparticle tracking analysis (NTA) optimization, the solvent was made without polysorbate 80. Experiments were performed at room temperature, and in a dust free cabinet whenever possible. Changes in protein conformation were determined by second-derivative UV spectroscopy. The formation of adalimumab aggregates and particles was determined by dynamic light scattering (DLS), high-pressure size-exclusion chromatography (HP-SEC), micro-flow imaging (MFI) and NTA as described[20] and summarized below.

UV SPECTROSCOPY

Second-derivative UV spectroscopy was used to detect conformational changes. Measurements were performed on an Agilent 8453 UV–VIS spectrometer (Agilent Technologies, Waldbronn, Germany). Samples were measured in 2 mL half-micro quartz cuvettes (Hellma Benelux, Kruibeke, Belgium) with a path length of 10 mm in a concentration of 1 mg/mL. Absorbance was measured from 248 to 332 NM with 1 NM intervals and an integration time of 15 seconds. Background correction was performed using solvent. Second-derivative spectra were calculated with UV–Visible ChemStation software (Agilent Technologies, Walbronn, Germany) as described earlier.[20] The a/b ratio, i.e., the ratio between (I) the vertical distance between the peak minimum at 283 NM and the maximum at 287 NM and (II) the vertical distance between the minimum and maximum at 290 and 295 NM was calculated and used to determine the exposure of tyrosine residues to bulk solvent, which is sensitive to changes in the tertiary structure.[21]

DLS

DLS was used to detect aggregates in the size range from about 1 NM to 1 µm. DLS was performed on a Malvern Zetasizer Nano (Malvern, Herrenberg, Germany); 500 µL of each sample in a concentration of 10 mg/mL was analysed in plastic cuvettes at 25°C using the automatic mode (n = 3). Z-average diameter and polydispersity index were calculated using Dispersion Technology Software version 7.03 (Malvern, Herrenberg, Germany).

HP-SEC

HP-SEC was used to quantify monomers, dimers and fragments. Adalimumab samples of 1 mg/mL were injected in a volume of 50 µL onto a SRT SEC-300, 5 µm, 30 cm × 7.8 mm column (Supelco, Bellefonte, PA, USA). An Agilent 1200 chromatography system (Agilent Technologics, Palo Alto, California) combined with an Agilent 1200 UV detector and a multi-angle laser light scattering detector (DAWN HELEOS, Wyatt Technology Europe GmbH) was used. The flow rate was 0.5 mL/min. The mobile phase was composed of 50MM phosphate, 150MM arginine and 0.025% NaN_3 at pH 6.5. To quantify aggregation, UV absorption at 280 NM was recorded. From the multiangle laser light scattering signal, the root mean square diameter was calculated using the Berry Fit in the Astra software version 5.3.2.22 (Wyatt Technology Europe GmbH, Dernbach, Germany).

MFI

MFI was used to detect particles up to 70 µm. A MFI5200 (ProteinSimple, Santa Clara, AC, USA), equipped with a silane coated flow cell (1.41 × 1.76 × 0.1 mm) and controlled by the MFI View System Software version 2 was used. Prior to each

measurement the system was flushed with purified water. The background was zeroed by using solvent and performing the optimize illumination procedure. Samples of 1 mg/mL adalimumab were analysed without a predefined prerun volume because of the limited amount. Flow rate was 0.17 mL/min and camera shot rate was 22 flashes per second. Data were analysed with MFI View Analysis Suite version 1.2. For each product, stuck, edge, and slow-moving particles were removed by the software before analysis. Because no prerun volume could be used, the data were recorded throughout the entire run but processed only in the time window from 0.7 to 1.7 min where, based on the trend chart option in the software, the measurement was stable for all samples. The equivalent circular diameter was calculated as described earlier.[20]

NTA

NTA was used to detect particles between about 50 and 1000 NM. Measurements were performed with a NanoSight LM20, equipped with a sample chamber with a 635 NM laser for illumination of the particles. Samples of 10 mg/mL adalimumab were injected into the chamber by an automatic pump (Harvard Apparatus, catalogue no. 984362, Holliston, USA) using a sterile 1 mL syringe (BD Discardit II). For each sample, a 90 second video was captured with the shutter set at 29.9 ms and the gain at 680. Videos were analysed using NTA 2.0 Build 127 software. The following settings were used for tracking of the particles: background extract on; brightness 0; gain 1; blur size 3 × 3; detection threshold 10, viscosity 0.953. All other parameters were set to the automatic adjustment mode.

STATISTICS

The population analysed for pain, tolerability, preference, skin imaging and PD endpoints included all randomized subjects (n = 24 subjects). The population analysed for PK parameters and PK modelling included injections in which no spillage during treatment administration was reported (n = 43 injections). Repeated pain injection data (VAS and FPSR) were analysed with a repeated measures ANOVA with fixed factors treatment, method, time, treatment by method, treatment by time, method by time, treatment by method by time, random factor subject and repeated factor time within subject by treatment by method. The injection pain score of the Mantoux intradermal injection at screening was used as covariate. Single measured pain insertion data (VAS and FPSR) were analysed with a repeated-measures model ANOVA with fixed factors treatment, method, treatment by method, and repeated factor method within subject. The insertion pain score of the Mantoux intradermal injection at screening was used as covariate. Repeated cytokines data were analysed with a repeated-measures ANOVA with fixed factors method, time, method by time, repeated factor time within subject and the baseline as covariate. The contrasts of interest were s.c. vs. i.d. and s.c. vs. i.d. within compound. For imaging analyses, a subset of data was used as some variables were zero in some conditions or timepoints. If applicable, the factors of the mixed model were adjusted.

PK ANALYSES

PK parameters derived from serum sample concentrations were calculated using a noncompartmental analysis. The noncompartmental analysis was performed using R version 3.5.3[22] while the linear trapezoid rule was used for the calculation of areas under the plasma concentration–time curves (AUCs). Analysis of the differences between methods were based on least squares means from the ANOVA of the ln-transformed $AUC_{0\text{-}t}$,$AUC_{0\text{-}inf}$ and maximum plasma concentration (C_{max}). In addition, Wilcoxon tests were performed on time to reach C_{max} (T_{max}).

POPULATION PK MODELLING

The identification of structural differences in the PK properties of s.c. and i.d. administration, while accounting for covariates such as the presence of anti-adalimumab antibodies, was investigated using a population nonlinear mixed effects modelling approach in NONMEM (ICON plc, V7.3). Based on literature information, a 1-compartment structural model with linear absorption and linear elimination was used during model development.[23] For this structural model, the effect of anti-drug antibodies on the CL of adalimumab was tested as a time-varying covariate, increasing the CL of adalimumab at higher titre levels with the following equation: $CL = \emptyset TV_{CL} * (1 + \emptyset TV_{Titre\text{-}slope} * TITRE)$, Where individual TITRE levels proportionally increase the CL of an individual over time.

When a structural misspecification was identified in the absorption phase, modifications to the absorption part of the model were explored, in which transit models, different absorption compartments, and a model event time (MTIME) function in which the ka changes after an estimated time point, were investigated, modelled separately for each administration route.

After identification of the best structural absorption models for each route of administration, log-transformed interindividual variability was included following a forward inclusion procedure ($P < .01$) and covariates (age, weight, body mass index, gender, serum creatinine, and albumin) were explored following a forward-inclusion ($P < .01$) with backward-elimination ($P \leq .001$) procedure. Continuous covariates were tested following a power relationship centered around the median. Models were evaluated on basis of the objective function value, the parameter uncertainty (judged by the relative standard error), goodness-of-fit figures, individual model predictions vs. observations over time,

and confidence interval visual predictive checks based on 500 Monte Carlo simulations. Bootstrapping was not considered of added value as additional model evaluation tool. Data transformation was performed in R (V3.6.1[22]) and models were executed in conjunction with Perl-speaks-NONMEM (V4.8.1).[24]

STUDY APPROVAL

The study protocol was reviewed and approved by an independent medical ethics committee, the Medische Ethische Toetsingscommissie van de Stichting Beoordeling Ethiek Biomedisch Onderzoek (Assen, the Netherlands). All subjects provided informed consent prior to any study related procedures. The study was conducted at the Centre for Human Drug Research (Leiden, the Netherlands) from July 2018 until October 2018, and registered under clinical trial number NCT03607903. No interim analysis was performed.

RESULTS

Forty-seven subjects underwent medical screening. Twenty-four subjects (male:female ratio 1:1) with Fitzpatrick skin type II were administered 40 mg adalimumab (volume of 0.4 mL) i.d. or s.c. in the lateral upper thigh and placebo (volume of 0.4 mL) s.c. or i.d. in the contralateral thigh. One subject was randomized but excluded before treatment due to medical reasons and replaced (Figure 1). The mean age was 26.1 years (range 20–42). Demographic characteristics were comparable between groups (Table 1). For both s.c. and i.d. adalimumab injections, a minor spill (1–15% of intended volume not injected) occurred in 2 of 12 (17%) injections, and there was 1 (8%) major spill (15–50% of intended volume not injected) in an i.d. adalimumab injection. Both the minor spills and the major spill during i.d. injection occurred when high resistance during injection was encountered, whereas the minor spill of s.c. injection was due to backflow. Inspection of the hollow microneedles after injection using bright field microscopy did not show damaged microneedle tips (not shown).

Figure 1 CONSORT flow diagram of clinical trial. For pharmacokinetic and population pharmacokinetic analysis, subjects in whom any spillage occurred during injection were excluded. Other analyses were done with all subjects who completed the study (n = 24). i.d.: intradermal; s.c.: subcutaneous

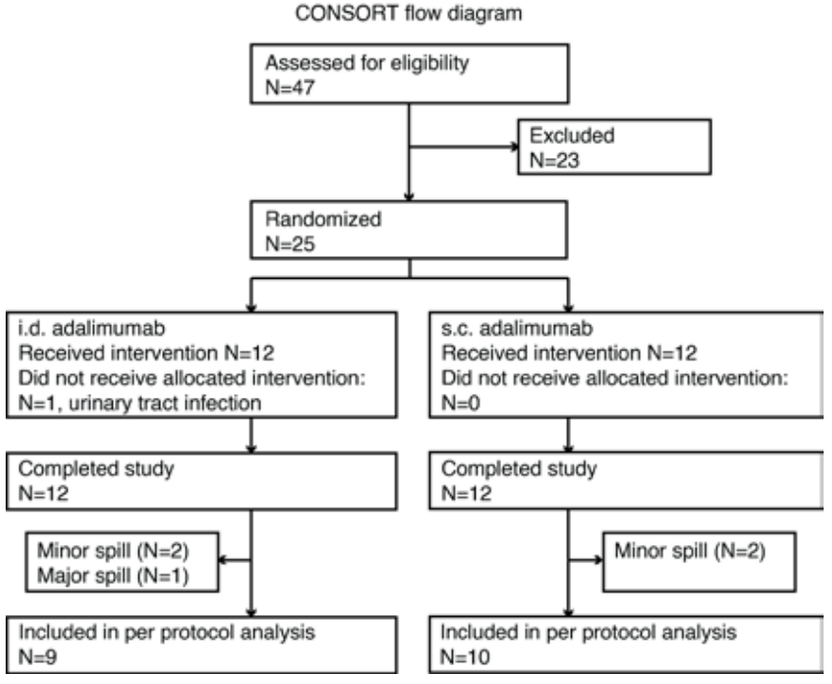

Table 1 Demographics and baseline characteristics

	All subjects n=24	
	i.d. (n=12)	s.c. (n=12)
Age (years)		
Mean (SD)	25.2 (5.3)	27.1 (7.6)
Median	23	23.5
Min-Max	20-38	20-42
Height (cm)		
Mean (SD)	177.8 (6.1)	180.1 (7.6)
Min-Max	167.3-188.5	166.5-191.1
BMI (kg/m²)		
Mean (SD)	23.8 (3.2)	23.2 (2.8)
Min-Max	19.3-29.3	20-28.8
Sex		
Female (%)	6 (25%)	6 (25%)
Male (%)	6 (25%)	6 (25%)
Race (% per group)		
Asian	0 (0%)	0 (0%)
Black or Afr. American	0 (0%)	0 (0%)
Mixed	0 (0%)	0 (0%)
Other	0 (0%)	0 (0%)
Caucasian	12 (100%)	12 (100%)

i.d.: intradermal; s.c.: subcutaneous; SD: standard deviation

PAIN, ACCEPTABILITY AND LOCAL TOLERABILITY AFTER I.D. AND S.C. ADALIMUMAB ADMINISTRATION

Pain ascribed to needle injections is often divided into insertion pain, which is pain resulting from the needle insertion, and injection pain which is pain resulting from the fluid injection. Insertion pain did not statistically significant differ between a hollow microneedle and a regular s.c. needle (Figure 2A, all p = .22). Pain associated with fluid injection was higher for i.d. vs. s.c. injections (Figure 2A, i.d. vs. s.c. estimated means 29.5 and 8.3, decrease of 72%, 95% confidence interval [CI] −83 to −53%, p < .001). Intradermal adalimumab injections were more painful (estimated mean 35.4) than s.c. adalimumab injections (estimated mean 7.9). Comparing the treatments (placebo vs. adalimumab, with both i.d. and s.c. administration methods combined) no statistically significant difference was observed (p = .55). There was no difference within the administration method between adalimumab or placebo administration (placebo vs. adalimumab within administration method p = .32 and p = .81 for i.d. and s.c., respectively). No pain was reported 24 hours after injection in any treatment group (Figure 2B). For both insertion and injection, a similar pattern in pain was reported in the Dutch FPSR15 in comparison with the VAS (data not shown). Altogether, these subject-reported outcomes indicate that there is no difference in pain between adalimumab and placebo injection, but that i.d. injection is more painful than s.c. injection.

Figure 2 Volunteer reported outcomes indicate preference for subcutaneous (s.c.) administration vs. intradermal (i.d.) administration. Healthy volunteers were injected with a single dose of adalimumab in the upper thigh and placebo in the contralateral upper thigh administered i.d. using a hollow microneedle or s.c. using a conventional needle. Insertion and injection pain were normalized to the pain score during a Mantoux which the volunteers received during screening. (A) Visual analogue scale (VAS) pain scores for insertion pain. No differences were observed between s.c. and i.d. insertion pain (p = .68). (B) VAS pain scores for injection and postinjection pain. Injection pain was significantly (p < .0001) higher for i.d. compared to s.c. injection. Postinjection pain was not present. After injection, subjects were asked multiple choice questions about their preference, for (C) how they experienced the injection, (D) how they would like to get a hypothetical future injection, (E) and for which injection they had fear. (A-E): n = 12 per group, except for Mantoux where n = 24. (A-B): mean ± standard deviation; repeated-measures ANOVA; **** P < .0001. NA: not available because not measured

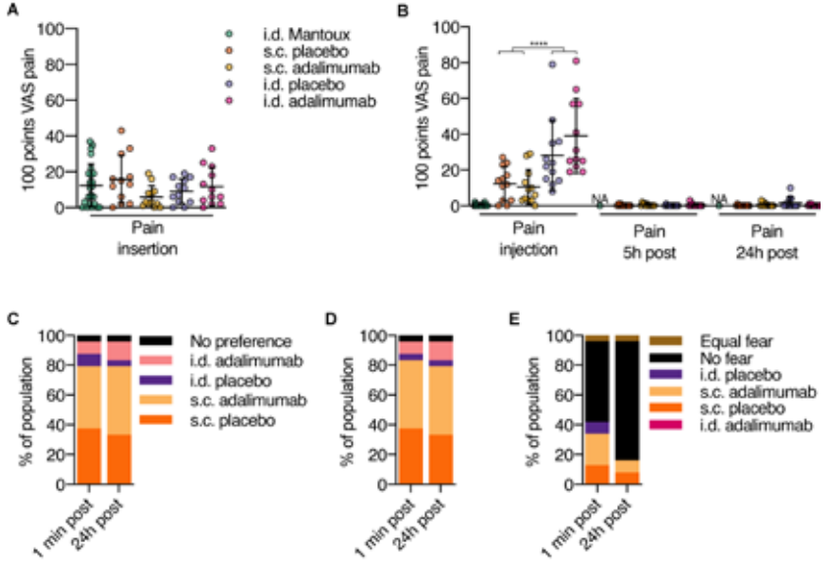

To determine which injection type was preferred, subjects were asked about their preference: immediately after the injections (i.e. before seeing the injection area) and also one day after the injections. Subject reported outcomes indicated that subjects had a preference for s.c. injection compared to i.d. injection (Figure 2C). They also preferred to receive a hypothetical next injection using s.c. rather than i.d. administration (Figure 2D). Directly after injection a majority (13 subjects, 54%) indicated no fear, while 24 hours after injection, most (19 subjects, 79%) subjects indicated no fear after injection. To summarize, we found that volunteers prefer s.c. over i.d. injection.

SAFETY

Nine treatment emergent adverse events were recorded; 5 in the s.c. group and 4 in the i.d. group. All treatment emergent adverse events were mild and self-limiting. Four subjects had fatigue, 3 had an upper respiratory tract infection, and 1 subject had a rhinitis. One subject had an injection site haematoma after i.d. adalimumab. Thus, i.d. and s.c. administration of adalimumab and saline do not raise a safety signal.

IMMUNOGENICITY

Anti-adalimumab antibodies are reported descriptively. None of the study participants had anti-adalimumab antibodies at baseline. Ten (83%, Figure 3A) and six (50%, Figure 3B) of the volunteers who received s.c. or i.d. adalimumab, respectively, treatment-emergent anti-adalimumab antibodies were detected. The median serum concentration for anti-adalimumab antibodies, for participants who developed anti-adalimumab antibodies, was 178 (range 16–864) for s.c. and 250 (range 189–940) arbitrary units for i.d. administration (Figure 3C). Presence of anti-adalimumab antibodies was associated with increased adalimumab CL. However, high variability in the $AUC_{0\text{-inf}}$ was identified due to the differences in immunogenicity, which needs to be taken into account to allow for a direct comparison of i.d. with s.c. administration.

PK OF I.D. AND S.C. ADALIMUMAB ADMINISTRATION

The adalimumab concentration time profile is displayed in Figure 3D. First, a noncompartmental analysis of PK was performed. After exclusion of subjects where any leakage occurred during injection, in the remaining subjects C_{max} was significantly higher after i.d. injection compared to s.c. injection (90% CI 0.57–0.90, p = .02). No difference was detected in $AUC_{0\text{-inf}}$ (90% CI 0.55–1.09, p = .22) or $AUC_{0\text{-last}}$ (90% CI 0.60–1.07, p = .20; per protocol subjects in Table 2, all enrolled subjects in Table S1). These data show that i.d. administration of adalimumab yields a higher maximum concentration than s.c. administered adalimumab.

Figure 3 Pharmacokinetics of adalimumab and anti-adalimumab antibodies after subcutaneous (s.c.) or intradermal (i.d.) injection. Mean anti-adalimumab levels after (A) s.c. and (B) i.d. administration (n = 12 per administration type). (C) Average anti-adalimumab levels for subjects with anti-adalimumab antibodies (n = 10 for s.c. administration and n = 6 for i.d. administration). (D) Serum adalimumab concentrations over time (D, n = 10 for s.c. administration and n = 9 for i.d. administration, noncompartmental analysis of subjects without leakage during injection). (C-D) Mean ± standard deviation. (E) Schematic depiction of population PK model. (F) Adalimumab absorption kinetics over time after adalimumab administration following microneedle i.d. or s.c. administration (typical population PK model). F: relative bioavailability; ka: absorption rate constant

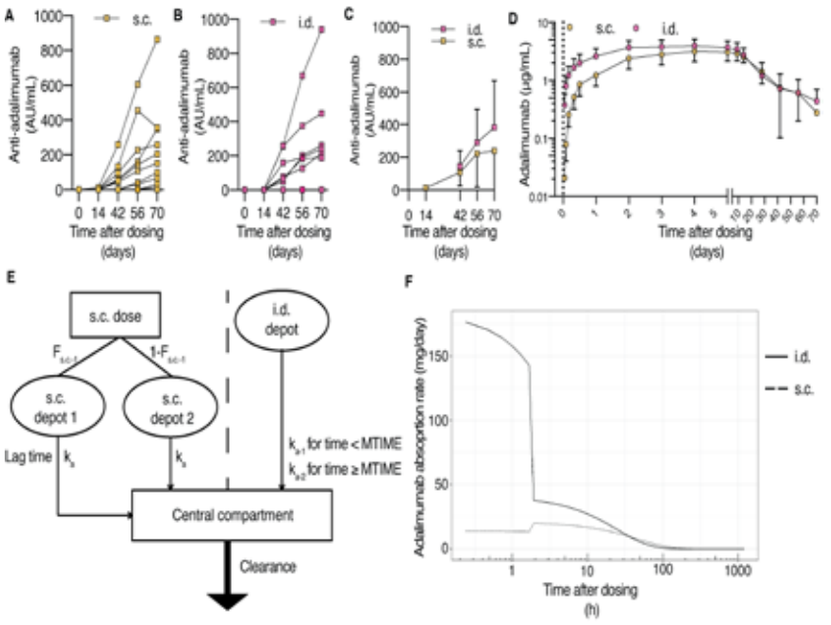

Table 2 Summary pharmacokinetic parameters for ID and SC adalimumab administration per protocol subjects, i.e. the subjects in which no leakage occurred and the intended dose of adalimumab was administered.

	s.c. (n=10)		i.d. (n=9)	
Parameter	**Mean (SD)**	**Median (range)**	**Mean (SD)**	**Median (range)**
C_{max} (µg/mL)	3.3 (1.1)	3.6 (1.5-4.8)	4.4 (0.7)	4.2 (3.6-5.5)
T_{max} (h)		120 (96-221)		95 (47-120)
$AUC_{0\text{-inf}}$ (µg*h/mL)	2359 (1167)	2048 (853-5351)	2986 (1217)	2724 (1679-4897)
$AUC_{0\text{-last}}$ (µg*h/mL)	2189 (816)	2005 (846-4019)	2688 (869)	2581 (1677-4094)

SD: standard deviation; C_{max}: maximum plasma concentration; T_{max}: time to reach C_{max}; AUC: area under the plasma concentration–time curve

To further examine PK and to be able to correct for interindividual variation in the kinetics of adalimumab and the formation of anti-adalimumab antibodies, a population PK model was developed. After exclusion of subjects in which any spill of adalimumab occurred during administration, data from 10 s.c. and 9 i.d. injections were available for model development using 275 adalimumab measurements that were above the LOD. A total of 4% of the measurements was below the LOD and therefore excluded from analysis. A significant effect between the time-varying titre levels and the CL was identified ($p < .001$), indicating that the CL of adalimumab increases in the presence of high titre levels. However, a bias in the absorption kinetics for s.c. and i.d. was identified with linear absorption kinetics. Subsequent exploration of different structural absorption models resulted in a MTIME function for the absorption rate constant (ka) after i.d. administration and 2 separate absorption compartments with equal kas and 1 with an absorption lag time for s.c. administration to be best fit for purpose (Figure 3E). In this revised structural model, significant ($p < .01$) interindividual variability on the titre-CL relationship and the central volume of distribution was identified. Additionally, a significant ($p < .01$) improvement in model fit was quantified after estimating a 29% higher relative bioavailability (F_{rel}) after i.d. administration of adalimumab compared to s.c. administered adalimumab. A negative age–CL relationship and a positive weight–CL relationship were identified. Both covariates gave $p < .001$ improvement in the model fit. The developed model showed an overall accurate description of the absorption and elimination phase of adalimumab (Figure S2). Model parameters (Table 3) were estimated with high precision and were comparable to literature values.[23] Simulations of the typical adalimumab absorption rates over time showed a clear difference between both administration routes, in which the i.d. dose had a fast initial phase which decreased after MTIME, whereas the s.c. administration had a slower initial phase and a small increase in the absorption rate, approximately 2 hours after dosing (Figure 3F).

Cytokine production was assessed by stimulating *ex vivo* whole blood with LPS and aluminium hydroxide, driving NF-κB and NLRP3 inflammasome activation. Results are shown in Figure 4. Free TNFα levels after both s.c. and i.d. administration sharply decreased from predose to postdose (mean levels predose i.d. 897 pg/mL, i.d. 48 h postdose 50 pg/mL, s.c. predose 928 pg/mL, s.c. 48 h postdose 74 pg/mL), as has been reported earlier,[16] and returned to baseline at the end of study (i.d. 70 d postdose 1149 pg/mL, s.c. 70 d postdose 850 pg/mL). No significant differences in inhibition of cytokine release were detected when i.d. adalimumab administration was compared to s.c. adalimumab administration (IFNγ $p = .61$; IL-6 $p = .31$; IL-8 $p = .81$; IL-1β $p = .61$; TNFα $p = .80$). A sex effect has been reported for LPS/aluminium hydroxide-induced IFNγ production after adalimumab administration,[14] but this was not detected in this study (IFNγ $p = .99$; IL-6 $p = .80$; IL-8 $p = .96$; IL-1β $p = .75$; TNFα $p = .08$).

Table 3 Population pharmacokinetics parameter estimates with relative standard errors.

Parameter	Estimate	RSE (%)
Absorption population parameters		
F_{ID}	1.29	6.46
Intradermal administration		
k_{a-1} (/day)	3.54	10.1
k_{a-2} (/day)	0.96	9.90
MTIME (days)	0.078	9.32
Subcutaneous administration		
k_a (/day)	0.514	9.64
F_{SC-1}	0.322	36.6
Lag time (days)	0.075	36.7
Structural model parameters		
Volume of distribution central (L)	11.5	8.02
Clearance (L/day)	0.36	4.31
Covariate relationships		
CL-age exponent[a]	-0.70	24.3
CL-weight exponent[b]	0.68	36.7
TITRE-slope (/xxx)	0.064	25.1
Inter-individual variability		
ω^2 Volume of distribution central	0.069	31.2
ω^2 TITRE-slope	0.537	37.1
Residual variability		
σ^2 Proportional residual error	0.054	13.9

CL: clearance; F: relative bioavailability; ka: absorption rate constant; MTIME, model event time; RSE: relative standard error / a) centred around 23 years / b) centred around 70 kg.

OPTICAL COHERENCE TOMOGRAPHY, CLINICAL PHOTOGRAPHY, THERMAL IMAGING AND LASER SPECKLE CONTRAST IMAGING

Three-dimensional photography was used to quantify the bleb size after i.d. injection. No bleb formation was observed after s.c. injection. After i.d. injection bleb formation was observed after both adalimumab and saline injections, which resolved in less than 1 day (Figure 5A,B). I.D. adalimumab administration but not s.c. adalimumab administration or injection of placebo caused local redness after injection (Figure 5C). OCT was used to examine breach of epidermis and fluid disposition. Penetration of the epidermis was visible for 92% of cases 10 minutes after administration of both placebo injections and s.c. adalimumab injection. All i.d. adalimumab injections showed epidermal penetration 10 minutes postdose (Figure 5D–F). Fluid disposition and vasodilatation in the dermis were visible more clearly for i.d. injections than s.c. injections.

Figure 4 Similar cytokine production after subcutaneous (s.c.) or intradermal (i.d.) adalimumab administration (A) tumour necrosis factor-α (TNFα), (B) interleukin (IL)-1β, (C) IL-8, (D) interferon (IFN)γ and (E) IL-6 release after *ex vivo* stimulation with lipopolysaccharide/aluminium hydroxide of whole blood samples. No sex effect was observed. Mean ± standard deviation. A-E: n = 12 per group, repeated measures ANOVA

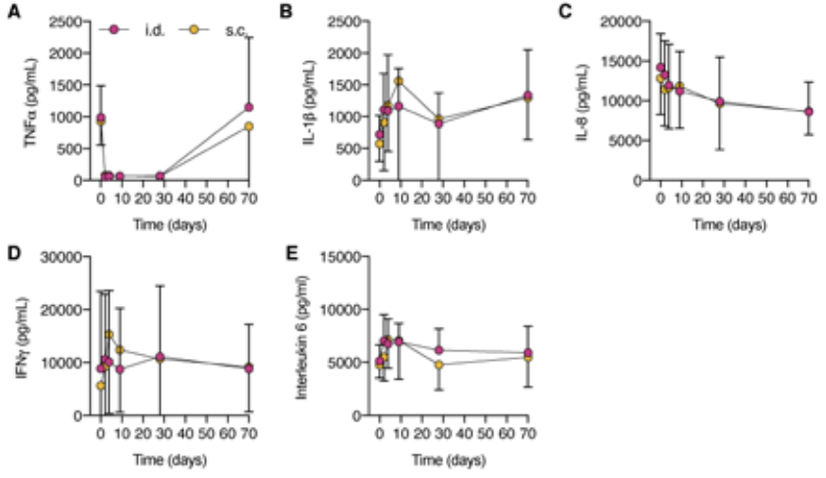

Cutaneous microcirculation of the upper legs following injections was quantified using LSCI. A significant increase in blood flow for i.d. adalimumab injections compared to i.d. placebo, s.c. adalimumab, and s.c. placebo injections was shown 10 minutes postdose ($p < .0001$, Figure 5G), followed by a decrease, reaching baseline on day 3 (data not shown). The bleb surface area was quantified using LSCI's perfused area measurements. The perfused areas were significant larger after i.d. adalimumab injections compared to i.d. placebo ($p < .0001$), and also compared to s.c. adalimumab ($p = .0012$) and placebo injections ($p < .0001$; Figure 5H,I).

Injection site temperature was measured in a temperature-controlled room using infrared thermography and corrected using standardized control areas (Figure S1).

IN VITRO PROTEIN ANALYSIS

In vitro studies were performed to investigate whether passage of adalimumab through a hollow microneedle led to protein instability, as compared to passage through a regular s.c. needle. To this end, adalimumab was subjected to the same storage conditions and ejection methods as those used in the clinical trial. Protein conformational changes were determined by second-derivative UV spectroscopy, and formation of adalimumab aggregates and particles were determined by DLS, HP-SEC, MFI and NTA. Results of the protein analysis are shown in Table 4. Second-derivative UV spectroscopy showed no change in a/b ratio between conditions and time points, indicating no protein conformational changes. With DLS, no substantial differences in Z-average diameter were found. No substantial differences in the concentration of particles ≥2 µm were detected between conditions using MFI. NTA showed nanoparticle concentrations around the lower limit of detection (10^7 ; data not shown), and mean sizes were found ranging from 188 to 414 NM. HP-SEC showed no differences in monomer content between conditions or between time points, and no evidence of aggregation or fragmentation. Molecular weights, based on multiangle laser light scattering data for the main peak, correspond to that of adalimumab reported before.[20] These data show that passage of adalimumab through a hollow microneedle before storage and after storage for 4 hours at 2–8°C does not lead to measurable protein aggregation or particle formation.

Table 4 Characterization of adalimumab after passage through a glass vial, a syringe, or a syringe with a hollow microneedle (SYR. + MN), at 0 hours and after storage at 4 °C for 4 hours. Representative data of 2 independent experiments.

	Time point	0h			4h		
	Condition	**Vial**	**Syr.**	**Syr. + MN**	**Vial**	**Syr.**	**Syr. + MN**
UV spectroscopy	a/b ratio	1.46	1.46	1.45	1.38	1.41	1.44
DLS	Z-average diameter	3.76	3.68	3.99	3.59	3.61	4.23
	in nm (SD)	(0.01)	(0.03)	(0.33)	(0.03)	(0.07)	(0.04)
	Polydispersity index	0.191	0.203	0.191	0.188	0.177	0.182
	(SD)	(0.003)	(0.039)	(0.002)	(0.001)	(0.080)	(0.009)
HP-SEC	Monomer content (%)	99.8	98.0	98.0	99.6	99.6	99.6
	Dimer content (%)	0.2	2.0	2.0	0.4	0.4	0.4
	Molecular weight monomer (10^5 Da)	1.57	1.50	1.53	1.55	1.55	1.55
NTA size estimation	Mean in nm (SD)	429 (233)	408 (180)	463 (330)	386 (182)	391 (234)	352 (179)
MFI	Particles ≥ 2 µm per mL	4581	4264	4033	3309	3631	4145

DLS: dynamic light scattering; SD: standard deviation; HP-SEC: high-pressure size-exclusion chromatography; NTA: nanoparticle tracking analysis; MFI: micro-flow imaging. UV spectroscopy, HP-SEC and MFI were measured with adalimumab samples diluted to 1 mg/mL, DLS and NTA in a concentration of 10 mg/mL.

Figure 5 Characterization of skin reaction following subcutaneous (s.c.) and intradermal (i.d.) injection. (A-C) 3D photography. (A) Typical bleb after i.d. injection. (B) Maximum height and volume of injection site. Bleb height and volume did not differ between i.d. adalimumab and i.d. placebo (height $p = .26$, volume $p = .29$). (D) Redness of the injection sites: The more positive the CIELAB *a ratio, the redder the injection site. I.D. adalimumab and placebo injections induced significantly more redness of the skin compared to s.c. adalimumab and placebo injections ($p < .0001$). Skin redness induced by adalimumab

injection was significantly higher for i.d. administration than for placebo injection ($p = .0014$; E, F) Representative OCT images of i.d. injection 10 minutes postinjection; (D, E) Cross-sectional planes of i.d. injection, and (F) top view of skin surface with 3 puncture holes. (G) Skin perfusion in arbitrary PU 10 minutes postinjection, measured with LSCI. (H) Injection site surface area 10 minutes postinjection. A significant difference in skin perfusion and surface area 10 minutes postinjection was observed for both administration methods ($p < .0001$) and treatment ($p < .0001$). (I) Representative LSCI images of both injection methods and treatments 10 minutes postinjection. LSCI: laser speckle contrast imaging; OCT: optical coherence tomography; PU: perfusion units; B, D, G, H: mean ± standard deviation, n = 12 per group, repeated measures ANOVA, **** $p < .0001$

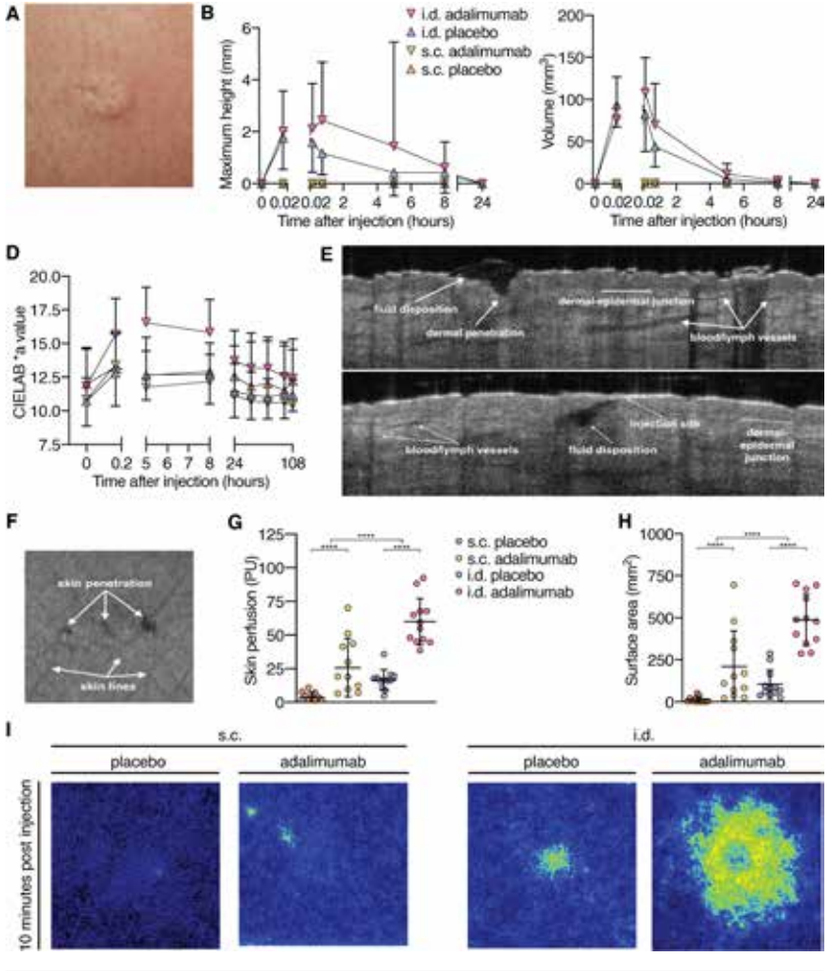

DISCUSSION

With a sophisticated and comprehensive, multimodal PK-PD safety approach we investigated a possibly minimally invasive administration method of adalimumab with a commercially available hollow microneedle. Importantly, this clinical trial shows that i.d. administration of a single dose of 40 mg adalimumab in a volume of 0.4 mL using a hollow microneedle is safe and well accepted. However, i.d. administration was associated with an increased amount of injection pain and decreased volunteer preference compared to s.c. administration. Using imaging methods, the effect of i.d. injections on the skin was thoroughly characterized. As expected, i.d. injections led to bleb formation. Notably, i.d. injection transiently increased cutaneous microcirculation as measured by LSCI. Importantly, we found that i.d. administration of adalimumab led to a higher C_{max} and a higher relative bioavailability compared to s.c. adalimumab administration. The inhibition of *ex vivo* cytokine production of whole blood stimulated with LPS/aluminium hydroxide was similar for i.d. and s.c. adalimumab administration indicating comparable PD efficacy.

Protein degradation, especially aggregation, might result in increased immunogenicity of mAbs[11] and immunogenicity of mAbs is a major reason for secondary loss of response to mAbs. Therefore, we first showed in vitro that microneedle ejection of adalimumab does not substantially alters the amount of protein fragments or aggregates compared to ejection using a regular hypodermic needle.

Hollow microneedles are frequently considered a minimally invasive device to deliver parenteral drugs.[4,25,26,27] In this study, we administered a single adalimumab dose of 40 mg in 0.4 mL or 0.4 mL placebo. We systematically studied pain associated with insertion and injection in a double-blind manner. We found that insertion pain of s.c. and i.d. administration was equal. However, injection pain of i.d. administration was significantly higher than s.c. administration. The high amount of pain is in contrast with another study, which used higher volumes but detected less pain.[27] Pain due to s.c. injection is generally attributed to different factors, i.e. volume of injection, site of injection, formulation, needle size and injection depth.[28]

The volume limit of s.c. injection is generally considered to be 1.5 mL.[29] Several studies have found higher volumes of s.c. administration to be associated with more pain.[29,30,31] Thus, the increased pain that was associated with i.d. administration in the clinical trial reported in this paper is probably due to the volume injected. The volume used in this trial was limited by a minimum volume which contains a regular dose of a MAB in adults. Future studies might investigate the volume-pain relationship for i.d. administration using hollow microneedles. We

did not detect a significant difference in pain when comparing adalimumab with placebo after i.d. and s.c. administration, which indicates that the formulation chosen in this study did not influence pain.

Although not quantified, we observed a higher injection pressure during i.d. administration compared to s.c. administration. With OCT, we detected fluid filled cavities after i.d. injection, indicating that there was no time for the compound to distribute in the skin.

We characterized the skin response to hollow microneedle administration of adalimumab using a combination of methods. The skin response following i.d. administration of adalimumab was mild and resolved within a day after injection. Using 3D photography, we showed a bleb, which is typical for i.d. administration. Furthermore, using LSCI, an increase in cutaneous microcirculation after i.d. injection of adalimumab was observed. Our observations are of interest in the context of drug absorption. The increased cutaneous microcirculation might be associated with the increased adalimumab absorption following i.d. vs. s.c. administration observed in our study. However, drugs injected s.c. may be absorbed via the lymph capillaries, or diffuse into blood capillaries, and after s.c. administration proteins with a high molecular weight, such as mAbs, are predominantly absorbed via the lymph after s.c. administration.[32,33]

Various factors influence lymph flow, one being local skin temperature. During an increase in local skin temperature, both the blood flow and the lymph flow increase.[34,35,36] We quantified local skin temperature after i.d. adalimumab administration using thermography. A limitation is that from the skin temperature measurements we cannot unequivocally conclude which type of injection (s.c. or i.d.) leads to higher skin temperature for two reasons. The temperature measurements might be confounded by difference in depth as i.d. injections are more superficial than s.c. injections. Thus, the s.c. injections might have increased the local temperature, which is not apparent from our measurements.

Initial lymphatics, the part of the lymph vessels responsible for drug uptake, are located superficially, in the dermis.[37] Under physiological conditions most of these lymph vessels are collapsed. Excess fluid (high hydrostatic pressure) and proteins (high local osmotic pressure) in the dermis cause high lymph flow. We used OCT to visualize epidermal penetration after i.d. injection. Qualitative analysis of OCT observations showed an increase in vessel diameter after i.d. injection compared to s.c. injection. Based on the OCT, no distinction can be made between blood and lymph vessels. Perhaps in the future, a new variant of OCT, Doppler OCT,[38] could be used to further characterize the physiology of MAB absorption and lymph flow.

Several studies have reported that the i.d. administration of drugs has different PK characteristics from s.c. delivery.[5,7,27,39] General observations are that T_{max} is decreased, C_{max} is increased and that relative bioavailability is either equal or increased after i.d. administration compared to s.c. administration. Most studies use insulin as model drug. For i.d. injection of insulin using hollow microneedles, it has been reported that C_{max} increases and T_{max} decreases after i.d. administration VS. s.c. administration. It has been suggested that a shift in the concentration–time profile explains why some but not all studies have reported increased relative bioavailability after i.d. injection.[5,40] Changes in PK are generally attributed to anatomical differences in the skin: the dermis has extensive vasculature and lymphatics, while the subcutis has more adipose tissue.[41] When correcting for individual differences in the covariates and the titre values, this study showed a significant difference in relative bioavailability between s.c. and i.d. administration; i.d. administration was associated with a 29% higher relative bioavailability. In our study, a clear distinction in the absorption profiles over time could be observed between s.c. and i.d. administration. Adalimumab administered by microneedle injection show a short but fast absorption, whereas s.c. dosing shows a lower absorption rate. The steep drop in absorption after a microneedle injection is caused by the distribution of sampling points and an estimated mathematical time point. In reality, this transition would probably be smoother. Altogether, the PK profile of the i.d. administration of adalimumab is favourable over s.c. administration.

The immunogenicity of mAbs is a significant clinical problem hampering the treatment of autoimmune diseases with mAbs. In this study, the number of healthy volunteers allows only for descriptive reporting of anti-adalimumab antibodies. The skin is a potent immune organ.[41] Studies have shown an increased immunogenicity of i.d. vaccines compared to s.c. vaccines and microneedles are frequently studied as a device to deliver vaccines.[42,43] By contrast, it has been suggested that i.d. administration of mAbs might lead to less immunogenicity compared to s.c. administration due to the presence of professional antigen-presenting cells in the epidermis and dermis rather than in the subcutis.[32,44] Perhaps the relatively short residence time at the i.d. injection site of the (predominantly monomeric) protein might contribute to the lack of increased immunogenicity as compared to s.c. administration. It remains to be determined whether i.d. administration of biologicals alters the incidence, degree, or time of onset of anti-drug antibody formation compared to s.c. administration.

In this study the functional effect of adalimumab administration was investigated in vitro. Whole blood was stimulated with LPS/aluminium hydroxide and secreted cytokines were measured. We found that i.d. and s.c. adalimumab reduced *ex vivo* TNFα bioavailability to a similar extent.

The increased relative bioavailability of i.d. adalimumab in our study suggests that lower doses may be used to achieve similar concentrations and subsequent

effects compared to s.c. administration. Combined with the increased elasticity of the skin of children[45] and the need for a lower (adalimumab) dose than in adults, hollow microneedles ultimately might be suitable for use in pediatric patients. However, it is of paramount importance to better understand the pain–volume relationship of i.d. injections using hollow microneedles in adults first.

In conclusion, we showed that the i.d. administration of adalimumab is feasible and leads to faster absorption and increased relative bioavailability compared to s.c. administration. The amount of pain reported in this study, higher for i.d. than for s.c. adalimumab administration, is probably explained by the injection volume of 0.4 mL. Understanding the relationship between pain and the administration of mAbs is essential before hollow microneedles can be investigated for use in the pediatric patient population.

ACKNOWLEDGEMENTS

We are indebted to our volunteers, and thankful to the team at the Centre for Human Drug Research and the pharmacy of the Leiden University Medical Center. Thanks to Karen Broekhuizen, medical writer at the Centre for Human Drug Research, who edited the manuscript for clarity. Funding: Dutch Arthritis Foundation: BP15–1-262.

REFERENCES

1 Nelson AL, Dhimolea E, Reichert JM. Development trends for human monoclonal antibody therapeutics. Nat Rev Drug Discov. 2010;9(10):767-774.
2 Jacobse J, Ten Voorde W, Rissmann R, Burggraaf J, Ten Cate R, Schrier L. The effect of repeated methotrexate injections on the quality of life of children with rheumatic diseases. Eur J Pediatr. 2019;178(1):17-20.
3 Donnelly RF, Raghu Raj Singh T, Larraneta E, McCrudden MTC. Microneedles for Drug and Vaccine Delivery and Patient Monitoring. Chichester, UK: John Wiley & Sons, Ltd; 2018.
4 Gupta J, Felner EI, Prausnitz MR. Rapid Pharmacokinetics of Intradermal Insulin Administered Using Microneedles in Type 1 Diabetes Subjects. Diabetes Technol Ther. 2011;13(4):451-456.
5 McVey E, Hirsch L, Sutter DE, et al. Pharmacokinetics and postprandial glycemic excursions following insulin lispro delivered by intradermal microneedle or subcutaneous infusion. J Diabetes Sci Technol. 2012;6(4):743-754.
6 Kochba E, Levin Y, Raz I, Cahn A. Improved Insulin Pharmacokinetics Using a Novel Microneedle Device for Intradermal Delivery in Patients with Type 2 Diabetes. Diabetes Technol Ther. 2016;18(9):525-531.
7 Milewski M, Manser K, Nissley BP, Mitra A. Analysis of the absorption kinetics of macromolecules following intradermal and subcutaneous administration. Eur J Pharm Biopharm. 2015;89:134-144.
8 Hróbjartsson A, Emanuelsson F, Thomsen ASS, Hilden J, Brorson S. Bias due to lack of patient blinding in clinical trials. A systematic review of trials randomizing patients to blind and nonblind sub-studies. Int J Epidemiology. 2014;43(4):1272-1283.
9 Levin Y, Kochba E, Kenney R. Clinical evaluation of a novel microneedle device for intradermal delivery of an influenza vaccine: Are all delivery methods the same? Vaccine. 2014;32(34):4249-4252.
10 Mahler SM, Marquis CP, Brown G, Roberts A, Hoogenboom HR. Cloning and expression of human V-genes derived from phage display libraries as fully assembled human anti-TNFα monoclonal antibodies. Immunotechnology. 1997;3(1):31-43.
11 Hermeling S, Crommelin DJA, Schellekens H, Jiskoot W. Structure-immunogenicity relationships of therapeutic proteins. Pharm Res. 2004;21(6):897-903.
12 Bartelds GM, Wijbrandts CA, Nurmohamed MT, et al. Clinical response to adalimumab: Relationship to anti-adalimumab antibodies and serum adalimumab concentrations in rheumatoid arthritis. Ann Rheum Dis. 2007;66(7):921-926.
13 Bartelds GM, Krieckaert CLM, Nurmohamed MT, et al. Development of Antidrug Antibodies Against Adalimumab and Association With Disease Activity and Treatment Failure During Long-term Follow-up. JAMA. 2011;305(14):1460-1468.
14 Dillingh MR, Reijers JAA, Malone KE, et al. Clinical evaluation of humira® biosimilar ons-3010 in healthy volunteers: Focus on pharmacokinetics and pharmacodynamics. Front Immunol. 2016;7:508.
15 Hicks CL, Von Baeyer CL, Spafford PA, Van Korlaar I, Goodenough B. The Faces Pain Scale - Revised: Toward a common metric in pediatric pain measurement. Pain. 2001;93(2):173-183.
16 Pouw MF, Krieckaert CL, Nurmohamed MT, et al. Key findings towards optimising adalimumab treatment: The concentration-effect curve. Ann Rheum Dis. 2015;74(3):513-518.
17 Briers D, Duncan DD, Hirst E, et al. Laser speckle contrast imaging: theoretical and practical limitations. J Biomed Opt. 2013;18(6):066018.
18 Everett JS, Budescu M, Sommers MS. Making Sense of Skin Color in Clinical Care. Clin Nurs Res. 2012;21(4):495-516.
19 Del Bino S, Bernerd F. Variations in skin colour and the biological consequences of ultraviolet radiation exposure. Br J Dermatol. 2013;169(SUPPL. 3):33-40.
20 Vlieland ND, Nejadnik MR, Gardarsdottir H, et al. The Impact of Inadequate Temperature Storage Conditions on Aggregate and Particle Formation in Drugs Containing Tumor Necrosis Factor-Alpha Inhibitors. Pharm Res. 2018;35(2):42.
21 Kueltzo LA, Middaugh CR. Ultravioloet absorption spectroscopy. In: Jiskoot W, Crommelin DJA, eds. Methods for structural analysis of protein pharmaceuticals. Arlington: AAPS Press; 2005.
22 R Core Team . (2017). R: A language and environment for statistical computing. R Foundation for Statistical Computing, Vienna, Austria. URL: https://www.R-project.org/
23 Berends SE, Strik AS, Van Selm JC, et al. Explaining Interpatient Variability in Adalimumab Pharmacokinetics in Patients with Crohn's Disease. Ther Drug Monit. 2018;40(2):202-211.
24 Lindbom L, Ribbing J, Jonsson EN. Perl-speaks-NONMEM (PsN) - A Perl module for NONMEM related programming. Comput Methods Programs Biomed. 2004;75(2):85-94.
25 Kim YC, Park JH, Prausnitz MR. Microneedles for drug and vaccine delivery. Adv Drug Deliv Rev. 2012;64(14):1547-1568.
26 Gill HS, Denson DD, Burris BA, Prausnitz MR. Effect of microneedle design on pain in human volunteers. Clin J Pain. 2008;24(7):585-594.
27 Gupta J, Park SS, Bondy B, Felner EI, Prausnitz MR. Infusion pressure and pain during microneedle injection into skin of human subjects. Biomaterials. 2011;32(28):6823-6831.
28 28. Usach I, Martinez R, Festini T, Peris JE. Subcutaneous Injection of Drugs: Literature Review of Factors Influencing Pain Sensation at the Injection Site. Adv Ther. 2019;36(11):2986-2996.
29 29. Mathaes R, Koulov A, Joerg S, Mahler HC. Subcutaneous Injection Volume of Biopharmaceuticals—Pushing the Boundaries. J Pharm Sci. 2016;105(8):2255-2259.
30 30. Heise T, Nosek L, Dellweg S, et al. Impact of injection speed and volume on perceived pain during subcutaneous injections into the abdomen and thigh:

a single-centre, randomized controlled trial. Diabetes Obes Metab. 2014;16(10):971-976.
31 31. Jørgensen JT, Rømsing J, Rasmussen M, Møller-Sonnergaard J, Vang L, Musæus L. Pain assessment of subcutaneous injections. Ann Pharmacother. 1996;30(7–8):729-732.
32 32. Richter WF, Bhansali SG, Morris ME. Mechanistic determinants of biotherapeutics absorption following SC administration. AAPS J. 2012;14(3):559-570.
33 33. Supersaxo A, Hein WR, Steffen H. Effect of molecular weight on the lymphatic absorption of water-soluble compounds following subcutaneous administration. Pharm Res. 1990;7(2):167-169.
34 34. O'Morchoe CCC, Jones WR, Jarosz HM. Temperature dependence of protein transport across lymphatic endothelium in vitro. J Cell Biol. 1984;98(2):629-640.
35 35. Astrup A, Bülow J, Madsen J. Skin temperature and subcutaneous adipose blood flow in man. Scand J Clin Lab Invest. 1980;40(2):135-138.
36 36. Olszewski W, Engeset A, Icger PM, Sokolowski J, Theodorsen L. Flow and Composition of Leg Lymph in Normal Men during Venous Stasis, Muscular Activity and Local Hyperthermia. Acta Physiol Scand. 1977;99(2):149-155.
37 37. Ryan TJ, Mortimer PS, Jones RL. Lymphatics of the Skin: Neglected but Important. Int J Dermatol. 1986;25(7):411-419.
38 38. Blatter C, Meijer EFJ, Nam AS, et al. *In vivo* label-free measurement of lymph flow velocity and volumetric flow rates using Doppler optical coherence tomography. Sci Rep. 2016;6:29035.
39 39. Dul M, Stefanidou M, Porta P, et al. Hydrodynamic gene delivery in human skin using a hollow microneedle device. J Control Release. 2017;265:120-131.
40 40. Rini CJ, McVey E, Sutter D, et al. Intradermal insulin infusion achieves faster insulin action than subcutaneous infusion for 3-day wear. Drug Deliv Transl Res. 2015;5(4):332-345.
41 41. Kabashima K, Honda T, Ginhoux F, Egawa G. The immunological anatomy of the skin. Nat Rev Immunol. 2019;19(1):19-30.
42 42. Lambert PH, Laurent PE. Intradermal vaccine delivery: Will new delivery systems transform vaccine administration? Vaccine. 2008;26(26):3197-3208.
43 43. Prausnitz MR, Mikszta JA, Cormier M, Andrianov AK. Microneedle-Based Vaccines. Curr Top Microbiol Immunol. 2009;333:369-393.
44 44. Büttel IC, Chamberlain P, Chowers Y, et al. Taking immunogenicity assessment of therapeutic proteins to the next level. Biologicals. 2011;39(2):100-109.
45 45. Rittié L, Fisher GJ. Natural and sun-induced aging of human skin. Cold Spring Harb Perspect Med. 2015;5(1):1-14.
46 46. Alexander SPH, Kelly E, Mathie A, et al. The Concise Guide to pharmacology 2019/20. Br J Pharmacol. 2019;176(S1) I-IV and:S1-S493.

Supplementary Table 1 Summary pharmacokinetic parameters for i.d. (A) and s.c.(B) adalimumab administration for all enrolled subjects.

A

	s.c. (n=12)		i.d. (n=12)	
Parameter	**Mean (SD)**	**Median (range)**	**Mean (SD)**	**Median (range)**
C_{max} (mug/mL)	3.3 (1.0)	3.4 (1.5-4.8)	4.0 (4.1)	4.1 (1.6-5.6)
T_{max} (h)	145 (54)	120 (96-221)	90 (23)	96 (47-120)
$AUC_{0\text{-}inf}$ (µg*h/mL)	2401 (1094)	2054 (853-5316)	2514 (1173)	2623 (619-4805)
$AUC_{0\text{-}last}$ (µg*h/mL)	2130 (690)	2005 (846-2603)	2332 (976)	2485 (619-4805)
CL (L/h)	0.02 (0.01)	0.02 (0.01-0.05)	0.02 (0.02)	0.02 (0.01-0.06)

B

	s.c. (n=10)		i.d. (n=9)	
Parameter	**Mean (SD)**	**Median (range)**	**Mean (SD)**	**Median (range)**
C_{max} (mug/mL)	3.3 (1.1)	3.6 (1.5-4.8)	4.4 (0.7)	4.2 (3.6-5.5)
T_{max} (h)	142 (120)	120 (96-221)	85 (85)	95 (47-120)
$AUC_{0\text{-}inf}$ (µg*h/mL)	2359 (1167)	2048 (853-5351)	2986 (1217)	2724 (1679-4897)
$AUC_{0\text{-}last}$ (µg*h/mL)	2180 (816)	2005 (846-4019)	2688 (869)	2581 (1677-4094)
CL (L/h)	0.02 (0.01)	0.02 (0.01-0.05)	0.02 (0.01	0.01 (0.01-0.02)

Supplementary Figure 1 Skin temperature after s.c. and i.d. injections. (A) Control thermography recordings were subtracted from injection site temperatures to calculate the difference in °C as change from baseline on a time point for the first day after injection. n = 12 per group, mean ± SD. (B) Images in the top panel are representative of reactions 1 minute postdose, and images in the bottom panel are representative of reactions 10 minutes postdose.

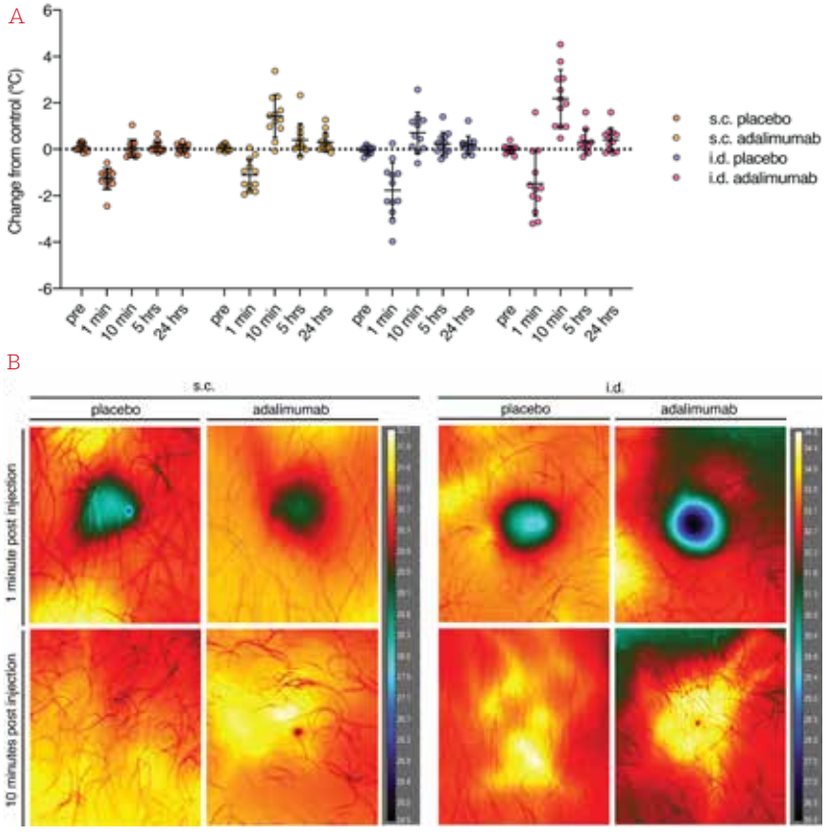

Supplementary Figure 2 Model fit of population PK model 500 Monte Carlo simulations were performed for a visual predictive check of the adalimumab population PK model after the development of a separate structural model for the absorption of microneedle (A) and s.c. (B) administration of adalimumab. The blue coloured rectangles are the 95% confidence interval around the 5 and 95% prediction interval. The orange rectangles are the 95% confidence interval around the median prediction. Data was binned per observation time. The dashed lines are the 5, 50 and 95% distribution of the data.

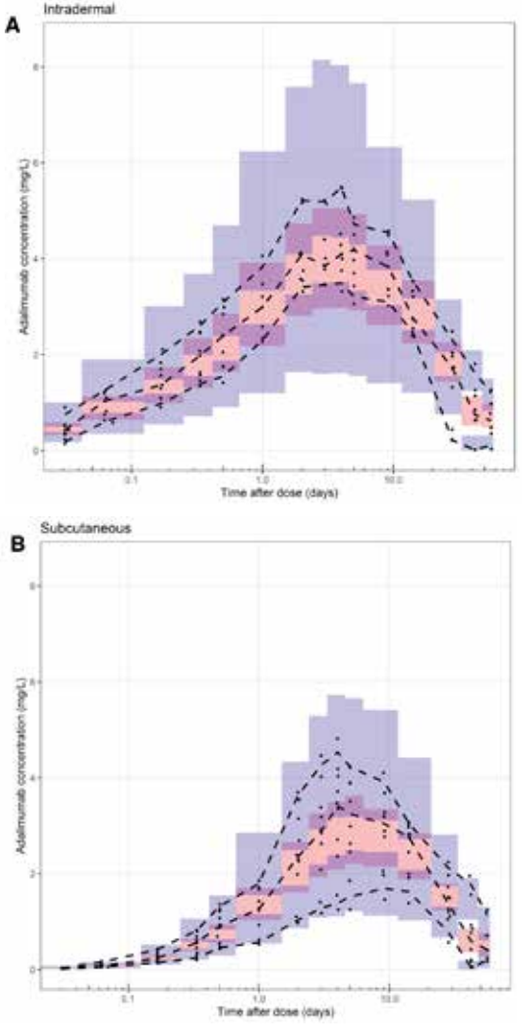

SECTION IV

SUMMARY AND APPENDICES

CHAPTER VIII

GENERAL DISCUSSION

Well-informed decisions are needed in the earliest phase of dermatological drug development. Only 6.3% of the drugs targeting immunosuppressive and anti-inflammatory processes reaches market registration. Knowledge about the pharmacodynamic properties of a dermatological agent is essential to increase the probability of success from early-phase clinical trials to market registration in dermatology. Despite the increasing amount of early-stage drug trials incorporating pharmacodynamic endpoints, there seems to be a lack of understanding how to integrate pharmacodynamic outcomes into early-stage dermatological drug trials. There are success stories from investigations employing objective pharmacodynamic endpoints in both disease and challenge models, showing that integrating such endpoints during the initial clinical stages of drug development is feasible. This thesis investigates and advocates a more objective methodology, suggesting the integration of imaging techniques and precise biomarkers as pharmacodynamic endpoints in early-stage dermatology trials. However, this advocacy for pharmacodynamic endpoints in early-stage dermatology trials raised two main questions: how to evaluate pharmacodynamic endpoints in early-stage dermatology trials and which specific pharmacodynamic endpoints should be considered for evaluation.

As the predominant focus of studies in the earlier stages of drug development remains on healthy volunteers, challenge models are being unequivocally endorsed. The present thesis outlined how pharmacological and trauma-based derma-immunological challenges are developed and how objective pharmacodynamic endpoints are evaluated in early-stage trials in clinical pharmaco-dermatology. Two types of skin challenge models were explored: trauma-based derma-immunological challenges, wherein a physical intervention was applied on skin to provoke an immunologic and inflammatory response to mimic a dermatological disease (**section I**), and pharmacological skin challenges, wherein a pharmacological agent is administered to the skin (**section II**). These challenges were applied in five early-phase dermatological trials. Additionally, one clinical trial was initiated to set an example how to evaluate pharmacodynamic endpoints in a classical phase I feasibility and dosing study but without using a skin challenge model (**section III**). After outlining the outcomes of the clinical trials, the focus of this discussion is to address the queries raised in the introduction: how to evaluate pharmacodynamic endpoints in early-stage dermatology trials and which specific pharmacodynamic endpoints should be considered for evaluation. With this we try to contribute to answering the question which objective pharmacodynamic endpoints deserve consideration in early-phase clinical pharmacology trials in dermatology.

SUMMARY OF FINDINGS

SECTION I: PHARMACODYNAMICS OF TRAUMA-BASED DERMA-IMMUNOLOGICAL CHALLENGES

In **chapter 2**, we presented a cutaneous full-thickness wound model to test novel wound healing treatments. In this chapter, three- and four-mm full thickness punch biopsies were taken from the lower back of healthy volunteers and left to heal without intervention. We aimed to characterize physiological wound healing with a multimodal test battery consisting mainly of non-invasive methodologies in a healthy volunteer challenge model. We demonstrated for the first time that a test battery of non-invasive techniques can objectively monitor quantifiable changes over time of the distinct wound healing phases, that is phase II inflammation, phase III proliferation and phase IV remodeling, while excluding the hemostasis phase. Additionally, multiple parameters were integrated and visualized in a radar chart highlighting the most important parameters and most suitable biomarkers per phase. Key findings of this study were that clinical imaging was an objective read-out for wound healing assessments, and we were able to distinguish the distinct phases of wound healing by integrated, multidimensional data visualization. The developed wound healing model shows promise to be a valuable tool for the standardized testing of novel wound healing treatments.

In **chapter 3**, we presented a trauma-based model aimed at the characterization of epidermal wound healing; this model was however based on the principle of suction blistering. In this chapter, we refined a previously developed suction blister model for analysis of suction blister fluid to monitor epidermal wound healing. This chapter illustrated for the first time that in our hands the blister method is suitable to monitor epidermal wound healing over time. We were able to induce blisters successfully and reproducibly with a clear separation of dermis and epidermis. The inflammation, proliferation, and remodeling phases were distinctly visible using objective pharmacodynamic biomarkers. We quantified several pharmacodynamic parameters, i.e., wound healing features, skin barrier function and skin perfusion via clinical imaging techniques, TEWL assessments and D-OCT. All parameters differed over time with comparable and acceptable variability. We were able to detect dermal structures with an emphasis on the separation of epidermis using D-OCT. Additionally, we could objectively measure the pharmacodynamic effects of a topical treatment alongside the blister suction model. Although the effects were limited, the techniques used to quantify the effects were sensitive enough to pick up differences over time.

SECTION II: PHARMACODYNAMICS OF PHARMACOLOGICAL CHALLENGES

Chapter 4 demonstrated a pharmacological model with substance P (SP). This chapter outlined the setup of an intradermal challenge model utilizing SP, a neuropeptide known to induce wheal and flare responses and serving as a potential challenging agent for investigating such responses mediated by the mas-related G-protein coupled receptor member X2 (MRGPRX2) receptor. Main objectives of this open-label, two-part, prospective enabling study in healthy volunteers were to assess the robustness of the SP response by evaluating the effect of varying doses of SP on wheal and flare, which are endpoints associated with MRGPRX2 receptor-mediated mast cell degranulation. Initially, a single challenge visit involving 20 healthy subjects aimed to determine the optimum dose range of SP for subsequent evaluation. Intradermal microdialysis (IDM) was employed to SP-challenged skin, involving the insertion of dialysis membranes into the dermis, which were then perfused at low rate with perfusate. This technique facilitated continuous sampling of interstitial fluid from SP-challenged skin, enabling assessment of the effect-time relationship. Subsequently, the effect of the selected dose of SP on wheal and flare responses, also assessed with IDM, was evaluated at two consecutive challenge visits. The time profile of the challenge for wheal and flare responses provided greater insight and characterization of the effect of multiple doses of SP over multiple timepoints, in addition to determining the potential carryover effect following repeated challenge. Lower doses of SP produced dose-dependent wheal and flare responses. Findings of this study support the fit-for-purpose validation for application of the challenge model in future clinical studies.

Chapter 5 described the effects of two novel, highly selective inhibitors of interleukin-1 receptor-associated kinase 4 (IRAK4), BAY1834845 (zabedosertib) and BAY1830839 or a control treatment ,i.e. prednisolone 20 mg or placebo, in human *in vivo* experimental challenge models of topical and systemic inflammation. The investigations conducted in this mechanistic clinical phase 1 study revealed that administering BAY1834845 (zabedosertib) at 120 mg B.i.d. and BAY1830839 at 100 mg B.I.D. for 7 days resulted in a rapid and distinct anti-inflammatory effect in a human skin challenge model with IMQ, as well as in a human systemic LPS challenge model. Both the topical IMQ challenge and intravenous LPS challenge are clinically well-characterized models that have been utilized to demonstrate the pharmacological activity of candidate drugs. What sets this study apart is the combination of two already established models, highlighting the potential utility of concomitant use of various novel human pharmacological models for evaluating the immunomodulatory effects of anti-inflammatory molecules in early-stage drug development.

SECTION III: PHARMACODYNAMICS AT THE EARLIEST PHASE OF CLINICAL DRUG DEVELOPMENT: RELEVANCE FOR OPTIMIZING DRUG ADMINISTRATION

Subcutaneous injections of drugs have been perceived as unpleasant and painful, especially during long-term use in both adults and children. **Chapter 6** explored the impact of repeated methotrexate injections via microneedles in children. This chapter presented the findings of a systematically performed literature review focused on children undergoing treatment with disease-modifying anti-rheumatic drugs (DMARDS). Insights from this review hold significance due to the perceived high treatment burden and the development of needle phobia among children with rheumatic diseases, which may affect long-term treatment adherence. The review identified two relevant studies involving children with juvenile idiopathic arthritis (JIA) receiving methotrexate. These studies indicated that needle fear, the effect of methotrexate treatment, and procedural consequences, such as blood sampling, all contribute to the distress and reduced quality of life among children with JIA. Notably, no studies investigating fear of injections or injection-related pain in children with rheumatic diseases receiving biologicals were found. This study emphasizes the importance of systematically exploring needle fear to optimize the administration of DMARDS, thus laying the groundwork for the setup of a prospective placebo-controlled trial outlined in the subsequent chapter of this thesis.

Chapter 7 detailed the establishment of a single-center double-blind, placebo-controlled, double-dummy clinical trial aimed at addressing the safety and efficacy of using hollow microneedles to administer a model monoclonal antibody (MAB). This chapter describes the feasibility of the intradermal administration of adalimumab via hollow microneedles versus conventional needles, evaluating their effects on pain, acceptability, local tolerability, pharmacokinetics, and immunogenicity. Conducted among 24 healthy adults, this trial compared the intradermal administration of 40 mg adalimumab (0.4 mL) using a hollow microneedle with subcutaneous administration using a conventional needle. Intradermal administration of biopharmaceuticals through hollow microneedles is suggested as an alternative for subcutaneous injection due to reduced injection-related pain and potentially more favorable pharmacokinetics compared to subcutaneous administration. Additionally, the applicability of optical coherence tomography, clinical photography, thermal imaging, and laser speckle contrast imaging in assessing skin reactions following intradermal injections was explored. In vitro protein analysis was performed to evaluate the compatibility of adalimumab with the hollow microneedle device. Intradermal injection of adalimumab via hollowing microneedles was found to be more painful and less accepted than subcutaneous administration, but

higher relative bioavailability with comparable safety and pharmacodynamic effects were found.

CHALLENGE MODELS IN EARLY-STAGE DERMATOLOGICAL DRUG DEVELOPMENT

Challenge models serve as invaluable tools for drug developers, enabling the replication of physiological and pathophysiological processes associated with inflammatory skin diseases. Initially, the focus of this thesis was on delineating two clinical trials with trauma-based challenge models: a cutaneous full-thickness wound model to test novel wound healing treatments and a model based on the principle of suction blistering. The wound healing models described and scrutinized in the clinical trials explained upon in **chapters 2** and **3** characterize pioneering research, using an explorative approach. Findings reveal that the most obvious challenge in trauma-based skin challenges lies in the uncertainty surrounding the time course of assessments. Balancing the inclusion of a comprehensive assessment scheme, which yields rich data, with the reasonable burden it places on participants, proves to be a pivotal consideration. Presently, information regarding the appropriate timing of assessments relies on preclinical studies, often conducted in animal models or in vitro models.[1] Regrettably, literature pertaining to early-phase studies incorporating trauma-based challenge models offers scant insights into the temporal aspect of assessments, typically reporting only the time to closure. Consequently, intriguing disparities observed over time, such as those between TGF-β1 and TGF-β3 discussed in **chapter 2,** present challenges in interpretation. These growth factors, integral to both inflammation and proliferation phases, are thought to activate similar intracellular signaling pathways.[2,3] Nonetheless, discrepancies in the elevations of TGF-β1 and TGF-β3 appear discordant, posing complexities in understanding their respective roles within the context of derma-immunological challenges. These complexities also relate to the interpretation of unexpected outcomes, e.g., that IL-6 would consistently yield zero values in the QPCR analysis in a normal wound healing model devoid of intervention, which again might be due to the sampling rate. The deconstruction of physiological processes into discrete components through modeling constitutes a fundamental aspect of research. Consequently, understanding the time course of events in multiple scenarios, e.g., diseased skin versus healthy skin, full-thickness versus scratch wounds, will furnish us with insights into the underlying mechanisms of wound healing.

The establishment of a suction blistering model in **chapter 3** represents an initial stride toward devising an epidermal wound model in healthy volunteers incorporating multiple non-invasive measurements. However, a remaining issue is the fidelity of the blisters generated in this model to those characteristic of epidermolysis bullosa (EB) and other bullous diseases. By introducing acute trauma, we bypass a normally longer process (days/weeks versus 1.5 hours) which might elicit an immune response different from chronic disease states.[4] Additionally, insights gathered from this challenge model confronted us with an apparent ambiguity. Notably, tissue inhibitors of metalloproteinases (TIMPS) increased directly post-wounding yet reverted to baseline levels more swiftly compared to matrix metalloproteinase-9 (MMP-9), the latter of which displayed a continued escalation until day 4. As future investigations unfold, including analogous blister suctioning models, we anticipate an increased understanding of the timing and implications of these findings as well as an integrated analysis as performed for the full-thickness wounds.

Conversely, a more extensive body of knowledge exists regarding the time course of assessments within trials including pharmacological challenge models. **Chapter 4** highlighted a pharmacological model employing substance P (SP), while **chapter 5** delineated a human skin challenge model integrating topical IMQ and systemic LPS to elucidate the effects of a candidate IRAK4-inhibitor. Notably, the combined IMQ/LPS challenge model, deployed for the first time in a clinical trial together with novel IRAK4 inhibitors, proved to be groundbreaking. This innovation enabled the differentiation of local and systemic challenge effects, affirming the feasibility of this model in healthy volunteers. **Chapter 4** provided support for the utility of the SP model. Despite the existence of dose-dependent data on SP effects, a comprehensive characterization and insights into potential carryover effects following repeated challenges were lacking. Nevertheless, data revealed the absence of a carryover effect when the challenge was repeated after a 2-week interval. This study was a testimony to the continuous development of challenge models since each new study contributes to knowledge about the model.

In summary, the selection of a specific pharmacological skin challenge in early-phase clinical trials appears contingent upon the underlying research question. Such skin challenges supply proof-of-mechanism in early-phase clinical trials, while including safety and pharmacokinetic parameters, and insights into dose escalation based on pharmacodynamic measures. Nonetheless, the presence of model limitations, such as an unknown time course of assessments, precludes the provision of conclusive evidence for a direct translation into clinical efficacy, particularly in studies including trauma-based challenge models.

PHARMACODYNAMIC ENDPOINTS IN EARLY-STAGE DERMATOLOGICAL DRUG DEVELOPMENT

This thesis advocates a more objective approach that incorporates imaging techniques and accurate as well as precise biomarkers as pharmacodynamic endpoints in early-stage dermatology trials. While outcomes reported by physicians and patients offer clinically relevant information and can be integrated into routine dermatologic practice and pivotal phase 3 dermatology trials, their applicability in early-stage trials is limited. This thesis bundles 5 randomized controlled trials wherein the most appropriate objective pharmacodynamic outcome measures were chosen, and several non-invasive (imaging) tools were successfully applied to detect biomarkers. The challenge remains in identifying biomarkers accurate enough to make critical go/no-go decisions in early-stage dermatology trials. Ideally, a parametric and accurate biomarker of the pharmacological influence of a critical pathophysiological process is available to reflect the pharmacodynamic effect of a therapeutic agent. Thorough generation of data and experience in biomarker studies are therefore warranted. This thesis highlights many imaging techniques, such as stereophotogrammetry, multispectral imaging, optical coherence tomography (OCT), laser speckle contrast imaging (LSCI) and transepidermal water loss (TEWL). Additionally, it mentions more standard techniques (e.g., QPCR and HE biopsy staining) that are not within the scope of this discussion. While providing insight into the intricate interplay of physiological processes in human skin, including inflammation, immune responses, wound healing, and angiogenesis, not all techniques are readily applicable biomarkers *yet*. In general, LSCI proved to be a highly reliable and easy to execute technique. The inter-subject variability was acceptable allowing to detect treatment and challenge effects. In our hands, OCT proved to be an especially useful qualitative tool but lacked consistency in calculating automated quantitative parameters. Despite its rapidity, simplicity, compactness, and cost-effectiveness, OCT had some limitations that became obvious in **chapter 2**. Although OCT was an objective read-out for wound healing assessments in this study, it did not have the diagnostic power and resolution needed to detect all wound healing processes and small microenvironmental changes which, currently, could only be assessed using histology. Its spatial resolution might have been troubled by the so-called resolution-penetration depth paradox, i.e., imaging deeper tissues generates visuals with poor resolution and imaging superficial cells generates visuals with relatively good resolution.[5] The resolution of OCT is between the very good spatial resolution of confocal microscopy, which only detects cells without tissue penetration, and the resolution of ultrasound that visualizes tissue lower than the dermis but is unable to detect individual cells. While OCT can detect significant structures within the dermis, it lacks the specificity required to distinguish between diseases effectively. In addition, OCT required trained operators to reduce the number of artefacts in scans. In addition, TEWL is known to be subject to numerous environmental and individual variables, such as age, gender, ethnicity, anatomical location, skin temperature, external surroundings, seasonal variations, smoking habits, and measurement tools.[6,7] Consequently, establishing a definitive 'normal' TEWL value and determining thresholds indicating pathological significance remain topics of ongoing debate.

Based on the findings presented in this thesis, it can be concluded that some techniques (TEWL, LSCI and multispectral imaging) are currently more suited for implementation as objective endpoints than others (OCT). However, ongoing advancements in imaging and detection techniques show promise in improving resolution while maintaining imaging depth. Examples include line-field optical coherence tomography and reflectance confocal microscopy.[8,9] Line-field confocal optical coherence tomography (LC-OCT) combines the principles of time-domain OCT and confocal microscopy, utilizing line illumination and detection with a broadband laser and a line-scan camera. With these developments, OCT or an advanced type of OCT could become a future biomarker in clinical drug development. In the near future, improved imaging techniques might be less-invasive alternatives for biopsies and staining that are still the gold standard in drug development and clinical practice. The challenge in developing a test battery of non-clinical imaging methodologies lies in identifying the most sensitive and representative endpoints and excluding endpoints with too much variability and noise. In exploratory research (as in this thesis), it is entirely feasible to include numerous endpoints. However, when exploratory endpoints become primary or secondary endpoints and underlie data-driven decisions, study designs should be lean and only include endpoints with sufficient sensitivity and reproducibility to be considered as reliable biomarkers.

MULTIMODAL PROFILING

Changes in parameters observed through imaging modalities or biomarker assessments are less relevant without accompanying clinical effects. Therefore, profiling the interplay of physiological processes in human skin in early-stage research should eventually incorporate multimodal parameters, including both physician-evaluated and patient-reported scores alongside imaging modalities and objective biomarkers. The blueprint of mechanistic dermatology trials using multiple readout angles as described earlier was developed to capture multimodality in early-stage clinical pharmacology studies by considering pharmacokinetic and pharmacodynamic properties of a new drug, and sensitive and objective endpoints from different domains.[10] Combining all

readouts provides a multifaceted overview of a dermatological condition, but also allows to gain insight into its pathophysiology and into the relationship between pathophysiology and clinical representation. Clinical endpoints are composed to assume a pivotal role in later-phase clinical trials. And although early-phase clinical trials are not inherently designed to directly assess clinical endpoints, insights into potential clinical efficacy are invaluable in the trajectory toward successful compound marketing. Evaluating clinical endpoints can also offer insights into the pathophysiology of dermatologic conditions, but most clinical efficacy scales show limited objectivity, inter-rater variability, and lack of sensitivity.[11–13]

A clinical composite score attempts to combine clinical parameters by averaging their individual scores (e.g., a score of erythema of 1, and oedema of 2 results in an EASI score average to 0.3 with an involvement of 1-9% of the skin).[14] Using clinical composite scores in advanced statistical modelling might not be the holy grail, as implementing composite scores into a multifaceted analysis including objective sensitive quantitative endpoints might reduce the sensitivity of the outcome. Considering that the expected effect and signal-to-noise ratio are small, clinical scores offer limited value in advanced statistical models.

The challenge lies in effectively interpreting the information from multiple endpoints to entirely profile disease progression, while ensuring attention to detail and monitoring individual parameter changes. This thesis outlines numerous (non-) invasive imaging methodologies employed to examine individual parameters. However, a shift in a single parameter does not necessarily equate to a change in clinical impact. As was illustrated in drug development, targeting a single protein or receptor believed to be responsible for disease symptoms does not always indicate clinical impact, which also accounts for imaging modalities and biomarkers that phenotype challenge effects. By integrating all parameters into domains and/or paradigms, and using this comprehensive approach to detect treatment effects, we may be better equipped to describe diseases and drug impacts in a more realistic manner. It should be noted however that incorporating multiple endpoints in a multifaceted analysis will result in small pieces of information on many parameters. Decisions about the relevance of each finding requires thoughtful interpretation of the results of preselection of the most relevant parameters to be included in a statistical model.

FUTURE DIRECTIONS

This thesis is built upon the assumption that assessing the pharmacodynamic properties of a dermatological agent could increase the probability of success from early phases to market registration in the field of pharmacological dermatology. Only 6.3% of the drugs targeting immunosuppressive and anti-inflammatory processes, reaches market registration. The results presented in this thesis point towards a more nuanced future perspective on how early-phase clinical trials with skin challenge models and with objective outcomes assessments could improve marketing success.

OPTIMIZING EARLY GO/NO-GO DECISIONS

As new compounds compete with standard of care and regulatory bodies demand greater evidence prior to market approval, drug development grows increasingly complex.[15] Combined with a more reluctant investment climate, there is a need for early indicators of efficacy to enhance the chances of success. Integrating objective and quantitative endpoints in derma-immunological trials provides crucial insights into a compound's performance at an early stage, aiding in making go/no-go decisions. While this does not necessarily translate to an increase in the 6.3% of drugs reaching the market, it could help to allocate less resources on ineffective compounds. Moreover, better dose rationale within patient populations, based on a pharmacodynamic approach to dose escalation, could potentially lead to increased approvals.

REDESIGNING EARLY-STAGE TRIALS

The IRAK4 study in **chapter 5** clearly illustrated how insights gained from biomarker assessments at an early stage could inform the redesign of subsequent clinical trials. This mechanistic clinical phase 1 study delineated a human skin challenge model integrating topical IMQ and systemic LPS to elucidate the effects of a candidate IRAK4 inhibitor. The results of this study helped drug developers differentiate a target indication and proceed to a subsequent phase 2 study with more knowledge about their compounds. Currently, a study is underway in atopic dermatitis with the candidate IRAK4 inhibitor tested in **chapter 5**. By utilizing these biomarker-heavy and mechanistic question-based development strategies, the indicated 6.3% market approval rate for all new compounds in immunological dermatology might be lifted to 13.8%.

EVOLVING TECHNOLOGY

Imaging techniques are continuously evolving. For instance, accurate erythema measurements with smartphones (ScarletRed)[16] are increasingly common, replacing the exclusive reliance on clinical scores. Imaging modalities employing non-visible light are also advancing, enhancing skin penetration while maintaining resolution.[9] Moreover, analysing capabilities of digital images are rapidly improving. Previously, algorithms were used to classify and annotate certain skin structures beneath the surface, but with the aid of artificial

intelligence and enhanced algorithms, this can be achieved without human intervention, leading to even higher specificity. These advancements promise to enhance image quality and quantitative analysis, thereby facilitating a better understanding of diseases and improving success rates.

THE IDEAL EARLY-STAGE CLINICAL TRIAL

Ideally, early-stage clinical trials in healthy volunteers should consistently incorporate relevant biomarkers. The era of exclusively focusing on safety and tolerability has passed and investors now demand more information regarding proof of concept as well.[17] This shift necessitates drug developers to prioritize target engagement from the outset, prompting drug testers to consider appropriate biomarkers to test new therapeutics. The selection of these biomarkers should be based on the most important question to answer for a compound. For instance, if literature and preclinical work indicate that dermal penetration of a compound is a challenge, dermal PK assessment becomes a valuable tool for evaluation. Similarly, if a novel technique like microneedles is used for compound delivery into the dermis, OCT or ultrasound are useful to detect fluid disposition in the dermal layer. Although quantitative readouts are crucial for comprehending the underlying mechanism, totally discarding clinical scores is unwarranted. The combination of objective readouts with subjective clinical scores facilitates understanding the correlation between the two and aids in translating proximal biomarkers (e.g., cytokine analysis) into clinical effects (e.g., itch or erythema).

OVERALL CONCLUSIONS

This thesis explored various skin challenge models that provoke immunologic and inflammatory responses and simulate dermatological diseases. Objective pharmacodynamic endpoints in clinical pharmaco-dermatology were evaluated across several early-stage dermatology trials, with some biomarkers proving useful and others not. The findings underscore the necessity of thorough validation and feasibility assessments for biomarkers before including them as primary or secondary endpoints in clinical trials. The 'trial and error' paradigm remains crucial for testing devices in clinical settings and identifying useful parameters. By examining diseases using these pharmacodynamic imaging tools, both with and without treatment, valuable insights are gained into disease pathology and drug effects. While the ideal of measuring effect with a single well-validated biomarker remains elusive in dermatology trials, combining multiple aspects of disease pathophysiology will be the focus for future dermatology research.

REFERENCES

1 Saeed S, Martins-Green M. Animal models for the study of acute cutaneous wound healing. Wound Repair Regen. 2023;31(1):6-16. doi:10.1111/WRR.13051
2 Roberts AB, Sporn MB. Differential expression of the TGF-beta isoforms in embryogenesis suggests specific roles in developing and adult tissues. Mol Reprod Dev. 1992;32(2):91-98. doi:10.1002/MRD.1080320203
3 Werner S, Grose R. Regulation of Wound Healing by Growth Factors and Cytokines. Physiol Rev. 2003;83(3):835-870. doi:10.1152/physrev.2003.83.3.835
4 Paller AS, Pope E, Rudin D, et al. A prospective short-term study to evaluate methodologies for the assessment of disease extent, impact, and wound evolution in patients with dystrophic epidermolysis bullosa. Orphanet J Rare Dis. 2022;17(1):1-16. doi:10.1186/S13023-022-02461-Z/TABLES/5
5 Brand S, Poneros JM, Bouma BE, Tearney GJ, Compton CC, Nishioka NS. Optical coherence tomography in the gastrointestinal tract. Endoscopy. 2000;32(10):796-803. doi:10.1055/S-2000-7714
6 Alexander H, Brown S, Danby S, Flohr C. Research Techniques Made Simple: Transepidermal Water Loss Measurement as a Research Tool. J Invest Dermatol. 2018;138(11):2295-2300.e1. doi:10.1016/J.JID.2018.09.001
7 Peer RP, Burli A, Maibach HI. Experimental Variability in TEWL Data. Dermal Absorpt Decontam A Compr Guid. Published online January 1, 2022:259-294. doi:10.1007/978-3-031-09222-0_15
8 Levine A, Markowitz O. Introduction to reflectance confocal microscopy and its use in clinical practice. JAAD Case Reports. 2018;4(10):1014. doi:10.1016/J.JDCR.2018.09.019
9 Latriglia F, Ogien J, Tavernier C, et al. Line-Field Confocal Optical Coherence Tomography (LC-OCT) for Skin Imaging in Dermatology. Life (Basel, Switzerland). 2023;13(12):2268. doi:10.3390/LIFE13122268
10 Rissmann R, Moerland M, van Doorn MBA. Blueprint for mechanistic, data-rich early phase clinical pharmacology studies in dermatology. Br J Clin Pharmacol. 2020;86(6):1011-1014. doi:10.1111/bcp.14293
11 Silman A, Harrison M, Brennan P. Is it possible to reduce observer variability in skin score assessment of scleroderma? The ad hoc International Group on the Assessment of Disease Outcome in Scleroderma. J Rheumatol. 1995;22(7):1277-1280. Accessed May 18, 2024. https://europepmc.org/article/med/7562758
12 Clements P, Lachenbruch P, Siebold J, et al. Inter and intraobserver variability of total skin thickness score (modified Rodnan TSS) in systemic sclerosis. J Rheumatol. 1995;22(7):1281-1285. Accessed May 18, 2024. https://europepmc.org/article/med/7562759
13 Pope JE, Baron M, Bellamy N, et al. Variability of skin scores and clinical measurements in scleroderma. J Rheumatol. 1995;22(7):1271-1276. Accessed May 18, 2024. https://europepmc.org/article/med/7562757
14 Hanifin JM, Baghoomian W, Grinich E, Leshem YA, Jacobson M, Simpson EL. The Eczema Area and Severity Index—A Practical Guide. Dermatitis. 2022;33(3):187. doi:10.1097/DER.0000000000000895
15 Kola I, Landis J. Can the pharmaceutical industry reduce attrition rates? Nat Rev Drug Discov. 2004;3(8):711-715. doi:10.1038/NRD1470
16 Partl R, Jonko B, Schnidar S, et al. 128 SHADES OF RED: Objective Remote Assessment of Radiation Dermatitis by Augmented Digital Skin Imaging. Stud Health Technol Inform. 2017;236:363-374. doi:10.3233/978-1-61499-759-7-363
17 Pharma R&D return on investment falls in post-pandemic market | Deloitte UK. Accessed May 18, 2024. https://www2.deloitte.com/uk/en/pages/press-releases/articles/pharma-r-d-return-on-investment-falls-in-post-pandemic-market.html

APPENDICES

NEDERLANDSE SAMENVATTING

Vroege fase geneesmiddelenontwikkeling op het gebied van dermatologie kent verschillende uitdagingen. De menselijke huid is het grootste orgaan van het lichaam en is betrokken bij het in evenwicht houden van complexe processen zoals ontsteking, reacties van het afweersysteem, wondgenezing en nieuwvorming van vaten. Dit subtiele evenwicht wordt verstoord bij veel inflammatoire huidaandoeningen, en de ontwikkeling van nieuwe dermatologische middelen richt zich voornamelijk op medicijnen die dit evenwicht kunnen herstellen. In vroege fase geneesmiddelenonderzoek worden studies uitgevoerd zonder informatie over het middel na toediening aan de mens. Hierdoor is soms nog onduidelijk wat de juiste (effectieve) dosering is, wat het beste doseringsschema is en wat de precieze farmacologische werking is. Dit draagt bij aan een lage kans op succes, 13,8% van alle geneesmiddelen die ontwikkeld worden halen uiteindelijk marktregistratie. Voor geneesmiddelen in de dermatologie die gericht zijn op immunosuppressie en het remmen van ontsteking ligt deze kans nog lager, op slechts 6,3%.

Om de kans op succes van vroege fase onderzoek tot marktregistratie te vergroten is een alternatief, rationeler ontwikkelmodel voorgesteld, waarin farmacodynamische eigenschappen zoals binding aan de juiste target al in het vroegste klinische stadium van geneesmiddelenontwikkeling kunnen worden geëvalueerd. Deze paradigmaverschuiving roept echter vragen op voor de vroege fase van geneesmiddelenontwikkeling binnen de dermatologie, namelijk: hoe kunnen farmacodynamische eindpunten in vroege klinische dermatologische onderzoeken worden geëvalueerd en welke specifieke farmacodynamische eindpunten moeten hierbij in overweging worden genomen?

Het gebruik van farmacodynamische eindpunten in vroege fase klinisch geneesmiddelenonderzoek is niet nieuw. Door de complexiteit van medicijnen en eerder genoemde lage slagingspercentages wordt nu meer nadruk gelegd op vroeg inzicht in het werkingsmechanisme. In de immuno-oncologie is 74% van de fase I-studies verrijkt met farmacodynamische markers, waarvan 94% van de markers in het bloed zijn te meten. Deze trend zien we ook bij onderzoeken naar immunologische indicaties door de beschikbaarheid van bloedtesten en ervaring uit de oncologie.

Het onderzoeken en evalueren van farmacodynamische eigenschappen van nieuwe dermatologische middelen in vroege klinische onderzoeken bij gezonde vrijwilligers is uitdagend door het ontbreken van de specifieke aandoening die bestudeerd wordt. Om dit probleem te verhelpen, worden *skin challenge* modellen ingezet om ontstekings- en afweerreacties na te bootsen bij gezonde mensen.

Daarnaast zijn er wondgenezingsmodellen, zoals tape-stripping en blaarinductie, die ook worden gebruikt om immuun- en ontstekingsreacties te bestuderen. Deze modellen zijn waardevol in zowel preklinisch als klinisch onderzoek en helpen bij het begrijpen van de genezingsprocessen. Daarnaast bieden deze modellen mogelijkheden om de farmacodynamiek beter te doorgronden en inzicht te krijgen in menselijke (patho)fysiologie.

In 2020 presenteerden we een blauwdruk voor het uitvoeren van vroege dermatologische onderzoeken, waarbij vijf pijlers centraal staan (Rissmann *et al.* (2020), 10.1111/bcp.14293). Deze omvatten het verkennen van farmacokinetische en farmacodynamische eigenschappen van nieuwe geneesmiddelen, het opnemen van gevoelige en objectieve eindpunten, en het integreren van multidisciplinaire data. Door de principes van deze vijf pijlers te volgen, kan de kans op vroegtijdige identificatie van ongewenste geneesmiddelkenmerken, bijvoorbeeld gerelateerd aan veiligheid, farmacokinetiek of farmacodynamiek, worden vergroot, waardoor het risico op falen in latere klinische fases kan worden verminderd.

Hoewel er in de dermatologie steeds meer nieuwe technieken beschikbaar zijn om de farmacodynamische eigenschappen van dermatologische middelen te beoordelen, klinische scores foor de arts, zoals de *Eczema Area and Severity Index* (EASI) en de *Psoriasis Area and Severity Index* (PASI), de norm in klinische onderzoeken. Deze schalen zijn vaak laag sensitief en erg subjectief wat leidt tot variabiliteit.

Om de farmacodynamische effecten van nieuwe middelen beter te begrijpen, zijn dus objectief-kwantificeerbare meetmethoden nodig. Het monitoren van microcirculatie en het gebruik van biomarkers kunnen waardevolle inzichten in huidziekten en genezingsprocessen bieden. De identificatie van nauwkeurige en meetbare biomarkers blijft echter een uitdaging.

Recente ontwikkelingen in digitale tools en beeldvormende technieken hebben geleid tot verbeterde objectieve meetmethoden. Het 'DermaToolbox'-concept biedt richtlijnen voor het integreren van sensitieve en objectieve eindpunten. Innovaties zoals digitale versies van traditionele schalen en technieken zoals stereofotogrammetrie en *optical coherence tomography* (OCT) verbeteren de evaluatie van dermatologische geneesmiddelen aanzienlijk.

Ondanks de vele vroege onderzoeken die farmacodynamische eindpunten gebruiken, ontbreekt het vaak aan inzicht in hoe deze resultaten effectief kunnen worden gecombineerd en geïntegreerd in dermatologische onderzoeken. Succesverhalen met objectieve farmacodynamische eindpunten in ziekte- en challenge modellen tonen de haalbaarheid aan van integratie in de vroege klinische stadia.

Huidige studies richten zich voornamelijk op gezonde vrijwilligers, waarbij *skin challenge* modellen de voorkeur hebben. Nieuwe trauma-gebaseerde *skin challenge* modellen, zoals gedeeltelijke en volledige wondmodellen, bieden mogelijkheden om de fysiologische processen in de dermatologie beter te begrijpen. Vanwege de beperkingen van klinische scores pleiten we voor een objectievere aanpak door beeldvormende technieken en nauwkeurige biomarkers te gebruiken als farmacodynamische eindpunten in vroege onderzoeken.

Dit proefschrift beschrijft de ontwikkeling van farmacologische en trauma-gebaseerde *skin challenge* modellen en de evaluatie van objectieve farmacodynamische eindpunten in vroege fase geneesmiddelenonderzoek binnen de dermatologie. Sectie I behandelt de ontwikkeling van deze trauma-gebaseerde modellen en hun rol in het karakteriseren van immunologische processen. Sectie II bespreekt de evaluatie van farmacodynamische activiteit bij verschillende farmacologische modellen, terwijl sectie III laat zien hoe deze eindpunten kunnen worden geïntegreerd in klassieke fase I-onderzoeken.

SECTIE I: FARMACODYNAMICA VAN TRAUMA-GEBASEERDE DERMA-IMMUNOLOGISCHE CHALLENGES

In hoofdstuk 2 wordt een cutaan wondmodel geïntroduceerd, waarbij drie- en vier-mm punchbiopten van de onderrug van gezonde vrijwilligers worden genomen en zonder interventie worden gelaten om te genezen. Met een multimodale testbatterij, voornamelijk bestaande uit niet-invasieve methoden, is aangetoond dat objectieve monitoring van de verschillende fasen van wondgenezing mogelijk is. De belangrijkste bevindingen waren dat klinische beeldvorming een objectieve meting biedt voor wondgenezing en dat we de verschillende fasen —ontsteking, proliferatie en remodeling— effectief konden onderscheiden door middel van geïntegreerde multidimensionale datavisualisatie.

Hoofdstuk 3 introduceert een blaarmodel om epidermale wondgenezing te karakteriseren. Dit hoofdstuk toont aan dat het blaarmodel effectief is in het monitoren van epidermale wondgenezing over de tijd. We konden blaren succesvol en reproduceerbaar induceren, met een duidelijke scheiding van dermis en epidermis. Het model maakt het mogelijk om de fasen van ontsteking, proliferatie en remodeling te visualiseren met behulp van farmacodynamische biomarkers. De resultaten tonen aan dat de technieken gevoelig genoeg zijn om significante veranderingen in de huidstructuren en genezingsprocessen over tijd te detecteren, wat de toepasbaarheid van dit model in toekomstige studies ondersteunt.

SECTIE II: FARMACODYNAMICA VAN FARMACOLOGISCHE CHALLENGES

Hoofdstuk 4 beschrijft de opzet van een intradermaal challenge model met substance P (SP), een neuropeptide dat *wheal*- en *flare*-reacties induceert. De studie heeft als doel de robuustheid van de SP-reactie te beoordelen door de effecten van verschillende doses SP op *wheal* en *flare* te evalueren. De bevindingen bevestigen dat lagere doses SP dosisafhankelijke reacties oproepen, wat inzicht biedt in de farmacodynamiek van SP en de rol van de *Mas-related G-protein coupled receptor member X2* (MRGPRX2) bij het mediëren van mestcel degranulatie.

In hoofdstuk 5 worden de effecten van twee nieuwe, selectieve *interleukin-1 receptor-associated kinase 4* (IRAK4) remmers (BAY1834845 en BAY1830839) besproken, die in vivo zijn getest in modellen van lokale en systemische ontsteking. De resultaten tonen aan dat deze remmers een snelle en significante ontstekingsremmende werking vertonen in zowel de lokale IMQ-challenge als de systemische LPS-challenge. Dit benadrukt de toegevoegde waarde van deze modellen in het evalueren van de immunomodulerende effecten van geneesmiddelen en accentueert de waarde van de combinatie van verschillende farmacologische modellen voor het begrijpen van de mechanismen van nieuwe therapieën in de vroege stadia van geneesmiddelenontwikkeling.

SECTIE III: FARMACODYNAMICA IN DE VROEGSTE FASE VAN KLINISCHE GENEESMIDDELENONTWIKKELING

Hoofdstuk 6 verkent de impact van herhaalde methotrexaatinjecties via micronaalden bij kinderen met reumatische aandoeningen. De literatuurstudie benadrukt de hoge behandelbelasting en de ontwikkeling van naaldangst, wat de therapietrouwheid op lange termijn kan beïnvloeden. De studie identificeert dat factoren zoals angst voor injecties en de gevolgen van de behandeling bijdragen aan de stress en verminderde kwaliteit van leven bij kinderen. Dit hoofdstuk legt de basis voor het belang van het systematisch onderzoeken van naaldangst, met als doel de toediening van *disease-modifying antirheumatic drugs* (DMARD) te optimaliseren.

Hoofdstuk 7 bespreekt een gerandomiseerde, placebo-gecontroleerde studie die de veiligheid en effectiviteit van intradermale toediening van adalimumab via holle micronaalden evalueert. De bevindingen suggereren dat hoewel de intradermale toediening meer pijn en een lagere acceptatie met zich meebrengt in vergelijking met subcutane injecties, het ook een hogere biologische beschikbaarheid vertoont. Daarnaast werden verschillende beeldvormingstechnieken, zoals optische coherentie tomografie en thermale beeldvorming, toegepast om huidreacties na intradermale injecties te beoordelen. Dit hoofdstuk concludeert dat intradermale toediening via holle micronaalden een veelbelovende alternatieve toedieningswijze biedt, met potentieel voor verbeterde farmacokinetiek en vergelijkbare farmacodynamische effecten, wat de weg vrijmaakt voor verdere studies en toepassingen in de klinische praktijk.

CHALLENGE MODELLEN IN DE VROEGSTE FASE VAN ONTWIKKELING VAN DERMATOLOGISCHE GENEESMIDDELEN

Challenge modellen zijn belangrijke hulpmiddelen voor geneesmiddelenontwikkelaars, omdat ze fysiologische en pathofysiologische processen die gepaard gaan met inflammatoire huidaandoeningen kunnen repliceren in gezonde mensen. Dit proefschrift richt zich op twee klinische onderzoeken met trauma-gebaseerde challenge modellen: een cutaan wondmodel voor het testen van nieuwe wondgenezingstherapieën en een model gebaseerd op het principe van blaarwonden. De bevindingen in hoofdstukken 2 en 3 benadrukken dat een grote

uitdaging bij trauma-gebaseerde huidmodellen de onzekerheid over de tijdsduur van de evaluaties is. Het balanceren van een uitgebreid beoordelingsschema met de belasting voor deelnemers is cruciaal. Huidige informatie over de timing van beoordelingen is vaak afhankelijk van preklinische studies, maar er is weinig literatuur over de tijdsaspecten van vroege fase-studies met deze modellen.

De discrepanties in de hoeveelheid van groeifactoren zoals TGF-β1 en TGF-β3, en onverwachte uitkomsten zoals nulwaarden van IL-6 in normale wondgenezing, compliceren de interpretatie. Het begrijpen van het tijdsverloop van fysiologische processen is fundamenteel voor verder onderzoek, zoals het vergelijken van zieke en gezonde huid of volledige dikte versus krab en snijwonden.

Bij het gebruik van een challenge model rijst de vraag in hoeverre het model relevant en representatief is voor de echte ziekte. De blaren die in hoofdstuk 3 zijn ontstaan, hebben anatomisch dezelfde diepte, maar het is onduidelijk of het genezingsproces vergelijkbaar verloopt met dat van bijvoorbeeld epidermolysis bullosa.

In hoofdstuk 5 hebben we gebruik gemaakt van twee challenge-modellen binnen dezelfde gezonde vrijwilliger. Het combineren van twee farmacologische modellen (IMQ en LPS) is een innovatieve benadering die ons in staat stelt om zowel lokale als systemische effecten te onderscheiden binnen één proefpersoon. Door deze opzet wordt de variabiliteit tussen proefpersonen uitgesloten, wat de gevoeligheid voor het detecteren van geneesmiddeleffecten aanzienlijk vergroot.

Het onderscheid tussen de modellen gaat echter verder dan alleen het verschil tussen lokale en systemische effecten. De downstream uitleesparameters en compensatiemechanismen verschillen sterk tussen beide modellen, en het is van belang om deze verschillen goed te begrijpen voordat een vertaling naar een ziektebeeld kan worden gemaakt.

Samenvattend blijft de keuze van een specifiek farmacologische *skin challenge* model in vroege klinische studies afhankelijk van de onderliggende onderzoeksvraag. Deze challenges maken bewijs van geneesmiddelmechanismen en inzicht in veiligheid en farmacokinetische parameters mogelijk in een vroeg stadium van ontwikkeling. Desondanks zijn er beperkingen aan de modellen, zoals een onbekende tijdsduur van de evaluaties, en de vergelijking met een ziektebeeld, wat het bieden van sluitend bewijs voor klinische werkzaamheid bemoeilijkt.

FARMACODYNAMISCHE EINDPUNTEN IN VROEGE FASE DERMATOLOGISCHE GENEESMIDDELENONTWIKKELING

Dit proefschrift pleit voor een meer objectieve benadering die beeldvormingstechnieken en nauwkeurige biomarkers als farmacodynamische eindpunten in vroege dermatologie studies integreert. Hoewel uitkomsten van klinische scores waardevolle informatie bieden, is hun toepasbaarheid in vroege fase-studies beperkt. Het proefschrift bundelt vijf gerandomiseerde gecontroleerde proeven waarin de meest geschikte objectieve farmacodynamische uitkomstmaten zijn gekozen.

De uitdaging ligt in het identificeren van nauwkeurige biomarkers voor kritische beslissingen in vroege dermatologie onderzoeken. Verschillende beeldvormingstechnieken zoals stereofotogrammetrie, multispectrale beeldvorming, en optische coherentie tomografie worden genoemd. Hoewel LSCI als betrouwbaar wordt beschouwd, vertoont optische coherentie tomografie beperkingen in diagnostische kracht en specificiteit.

De resultaten suggereren dat sommige technieken momenteel geschikter zijn als objectieve eindpunten dan andere. Ontwikkelingen in beeldvormingstechnieken bieden hoop voor betere resolutie en minder invasieve alternatieven voor biopsieën.

TOEKOMSTIGE RICHTINGEN

Het meten van veranderingen in parameters zonder bijbehorende klinische effecten is minder relevant. Voor een effectieve profilering van de interactie tussen fysiologische processen in de menselijke huid is het essentieel om multimodale parameters te hanteren. Dit proefschrift benadrukt de noodzaak om verschillende benaderingen te combineren om een beter inzicht te krijgen in de pathofysiologie en klinische presentatie van huidaandoeningen. Daarnaast pleit het proefschrift voor het integreren van farmacodynamische eigenschappen in vroege fase klinische proeven om de kans op succes te vergroten. Gezien de behoefte aan vroegtijdige indicatoren van werkzaamheid in de steeds complexere omgeving van geneesmiddelenontwikkeling, kunnen objectieve en kwantitatieve eindpunten waardevolle inzichten opleveren.

ALGEMENE CONCLUSIES

Dit proefschrift onderzoekt verschillende *skin challenge* modellen die immunologische en inflammatoire reacties uitlokken. De bevindingen benadrukken de noodzaak van grondige validatie van biomarkers voordat ze als primaire of secundaire eindpunten worden opgenomen in klinische studies. Door de ziekte en geneesmiddeleffecten te bestuderen met behulp van farmacodynamische beeldvormingstools, worden waardevolle inzichten verkregen. Gezien de complexe pathofysiologie van dermatologische aandoeningen is het combineren van deze farmacodynamische tools van essentieel belang voor een diepgaand begrip van de ziekteprocessen, de zogenoemde multimodale aanpak. Dit vergroot niet alleen ons inzicht in de ziekte, maar draagt bij aan een grotere kans op succes bij de ontwikkeling van nieuwe geneesmiddelen.

CURRICULUM VITAE

Wouter ten Voorde was born on January 20, 1995, in Leiderdorp and raised in Langeraar. He graduated from Scala College Alphen aan den Rijn in 2014 and then pursued a bachelor's degree in Bio-Pharmaceutical Sciences at Leiden University. In his final undergraduate year, he completed an internship focused on brain-derived exosome isolation in the Systems Pharmacology division under Prof. Dr. E.C.M. de Lange. After earning his bachelor's degree, Wouter continued with a master's program in Bio-Pharmaceutical Sciences and Business Studies. During his master's, he completed two internships: one at the Centre for Human Drug Research (CHDR) and another at DDCD consulting, a company founded by former CHDR CEO, Prof. Dr. A.F. Cohen. After finishing his master's degree with honors, Wouter began his PhD as a clinical scientist at CHDR, under the supervision of Prof. Dr. J. Burggraaf and Prof. Dr. R. Rissmann. During his PhD, he was trained as a clinical pharmacologist. After completing his PhD, Wouter took on the role of Business Development Manager at CHDR.

LIST OF PUBLICATIONS

2024

Ten Voorde W, Jodl SJ, Klein S, Wagenfeld A, Zollmann FS, Feldmüller M, Klarenbeek NB, de Bruin DT, Jansen MAA, Rissmann R, Rohde B, Moerland M. The oral IRAK4 inhibitors zabedosertib and BAY1830839 suppress local and systemic immune responses in a randomized trial in healthy male voluntewers. *Clin Transl Sci. 2024 Mar;17(3):e13771. doi: 10.1111/cts.13771.*

Ten Voorde W, Wind S, Abdisalaam I, Mancini A, Linders F, Jansen MAA, Niemeyer-van der Kolk T, Burggraaf J, Rissmann R. A suction blister model to characterize epidermal wound healing and evaluate the efficacy of the topical wound healing agent INM-755 in healthy volunteers. *Eur J Pharm Sci. 2024 Jul 29:106867. doi: 10.1016/j.ejps.2024.106867.*

Bekkers VZ, Zdunczyk KM, Bik L, **Ten Voorde W**, Aarts P, Oerlemans F, Bohoslavsky R, Haedersdal M, Prens EP, Rissmann R, van Doorn MBA. Needle-free jet injector treatment with bleomycin is efficacious in patients with severe keloids: a randomized, double-blind, placebo-controlled trial. *Clin Exp Dermatol. 2024 Jul. doi: 10.1093/ced/llae254.*

2023

Huisman BW, Pagan L, Naafs RGC, **Ten Voorde W**, Rissmann R, Piek JMJ, Damman J, Juachon MJ, Osse M, Niemeyer-van der Kolk T, van Hees CLM, van Poelgeest MIE. Dermatoscopy and Optical Coherence Tomography in Vulvar High-Grade Squamous Intraepithelial Lesions and Lichen Sclerosus: A Prospective Observational Trial. *J Low Genit Tract Dis. 2023 Jul 1;27(3):255-261. doi: 10.1097/LGT.0000000000000731.*

Ten Voorde W, Saghari M, Boltjes J, de Kam ML, Zhuparris A, Feiss G, Buters TP, Prens EP, Damman J, Niemeyer-van der Kolk T, Moerland M, Burggraaf J, van Doorn MBA, Rissmann R. A multimodal, comprehensive characterization of a cutaneous wound model in healthy volunteers. *Exp Dermatol. 2023 Jul;32(7):1028-1041. doi: 10.1111/exd.14808.*

Ten Voorde W, Akinseye C, Abdisalaam I, Wind S, Klarenbeek N, Bergmans M, van Doorn M, Rissmann R, Kaur R, Hotee S, Foster K, Nair A, Fortunato L, Macphee C, Mole S, Baumann K, Brigandi R. Intradermal substance P as a challenge agent in healthy individuals. *Clin Transl Sci. 2023 Oct;16(10):1856-1865. doi: 10.1111/cts.13592.*

2022

Buters TP, Hameeteman PW, Jansen IME, van Hindevoort FC, **Ten Voorde W**, Grievink HW, Schoonakker M, de Kam ML, Gilroy DW, Feiss G, Rissmann R, Jansen MAA, Burggraaf J, Moerland M. Clinical, Cellular, and Molecular Effects of Corticosteroids on the Response to Intradermal Lipopolysaccharide Administration in Healthy Volunteers. *Clin Pharmacol Ther. 2022 Apr;111(4):964-971. doi: 10.1002/cpt.2516.*

2021

Ten Voorde W, Jacobse J, Tandon A, Romeijn SG, Grievink HW, van der Maaden K, van Esdonk MJ, Moes DJAR, Loeff F, Bloem K, de Vries A, Rispens T, Wolbink G, de Kam M, Ziagkos D, Moerland M, Jiskoot W, Bouwstra J, Burggraaf J, Schrier L, Rissmann R, Ten Cate R. Comprehensive evaluation of microneedle-based intradermal adalimumab delivery vs. subcutaneous administration: results of a randomized controlled clinical trial. Br J Clin Pharmacol. 2021 Aug;87(8):3162-3176. doi: 10.1111/bcp.14729.

Buters TP, Hameeteman PW, Jansen IME, van Hindevoort FC, **Ten Voorde W**, Florencia E, Osse M, de Kam ML, Grievink HW, Schoonakker M, Patel AA, Yona S, Gilroy DW, Lubberts E, Damman J, Feiss G, Rissmann R, Jansen MAA, Burggraaf J, Moerland M. Intradermal lipopolysaccharide challenge as an acute in vivo inflammatory model in healthy volunteers. *Br J Clin Pharmacol. 2022 Feb;88(2):680-690. doi: 10.1111/bcp.14999.*

2019

Jacobse J, **Ten Voorde W**, Rissmann R, Burggraaf J, Ten Cate R, Schrier L. The effect of repeated methotrexate injections on the quality of life of children with rheumatic diseases. *Eur J Pediatr. 2019 Jan;178(1):17-20. doi: 10.1007/s00431-018-3286-8.*